NGT-A1-002-080
NGT-80001

A MANNED MISSION TO MARS

PRELIMINARY DESIGN REVIEW 2

MAY 12, 1986

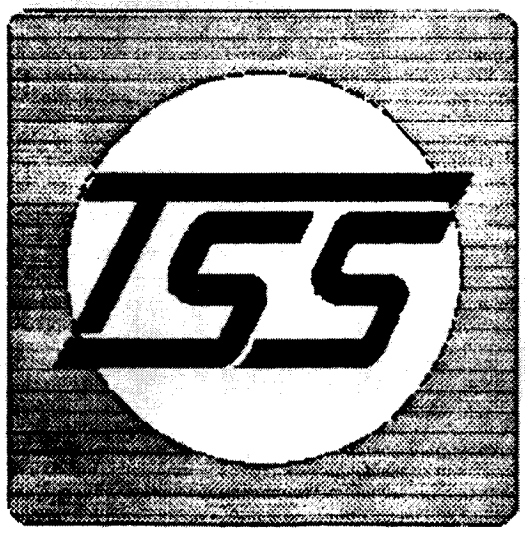

TEXAS
SPACE
SERVICES

THE UNIVERSITY OF TEXAS AT AUSTIN

EXECUTIVE OVERVIEW

A prominent item on NASA's agenda of future space exploration activities is a manned mission to Mars. In response to this, design groups at the University of Texas, Texas A&M University, and several other institutions are conducting studies in conjunction with NASA's Johnson Space Center. The goal of this work is to provide alternative viewpoints on important aspects of such a mission. Texas Space Services has been working on two such aspects, a two stage ascent/descent vehicle, and a reconnaissance of the Martian moons. Described in this final report is the work done by TSS during this design period. Areas investigated by the Ascent/Descent group included aerodynamic analysis, descent analysis, ascent analysis, propellant selection, in-situ propellant production, main engine sizing, and preliminary vehicle configuration and scenario development. Areas of Moon Reconnaissance Group investigation included the science of Phobos and Deimos, transfer trajectory analysis, landing sites on the Martian moons, precursor mission definition, preliminary vehicle configuration for a manned mission to Phobos, definition of an unmanned probe mission to Deimos, and development of exploration scenarios.

TABLE OF CONTENTS

LIST OF FIGURES

LIST OF TABLES

1.0 GENERAL SUMMARY

Texas Space Services has developed two areas of a manned Mars mission for preliminary design: a two stage ascent/descent vehicle and a reconnaissance of the Martian moons. A primary goal of this design effort has been to establish a permanant presence in the Martian system.

Considerable work on a single stage ascent/descent vehicle has been conducted by a previous contractor. TSS has developed a two stage vehicle as a comparison study. A two stage vehicle offers several advantages over a one stage vehicle, including a lighter ascent weight and greater cargo capacity. The lower stage of the vehicle, which will be left on the surface at departure, will be used for surface operations including habitation and in-situ propellant production. The lower stage will also provide a space for cargo which will be brought to the surface and not returned with the ascent vehicle, including a surface rover.

Unlike the ascent/descent vehicle, little work had been done previously on a reconnassiance mission to the moons, Phobos and Deimos. TSS considers this exploration a primary objective in a mission to the Martian system. The origins and compositions of the moons are unknown, and there surface features are unexplained. A manned mission to one or both of the moons would return significant amounts of scientific data. If the moons are indeed captured asteroids, as some scientists theorize, then operations developed from exploration of the moons could be used in future missions to the asteroid belt. Work done by TSS in this area has included outlining of requirements of a precursor mission to Phobos and Deimos, the preliminary design of a Transfer Reconnassiance Vehicle (TRV) to travel to Phobos, the development of a scenario for the exploration of Phobos, and the outlining of the requirements for an unmanned probe to Deimos.

The Manned Mars Mission Program at TSS is divided into three groups. The Ascent/Descent Vehicle Group has been responsible for the preliminary design of a two stage ascent/descent vehicle. Research of delta-v requirements for deorbit and descent, and for ascent have been conducted. Also, studies on in-situ propellant production and aerodynamics have been conducted. A vehicle configuration has been selected, and studies have focused on determining the mass and volume requirements of this configuration.

The Mars Moon Reconnaissance Group has been responsible for a preliminary study of a reconnaissance mission to the Martian moons. The trajectory analysis has involved delta-v trade studies for several mission scenarios. The moon science research has involved the study of the geology and topography of Phobos and Deimos. These studies have led to the development of a plan for the exploration of these two moons. First, a precursor mission to the moons was defined to obtain information about them. Next, a mission scenario was developed for a manned exploration of Phobos, and a vehicle was designed to accomplish this. In addition, the requirements for an unmanned probe to Deimos were developed.

The Management Group is composed of the project manager, the managers of the two technical groups, and the contract monitor. This group has been responsible for assigning tasks, developing timelines, and assisting the project manager.

2.0 ASCENT/DESCENT GROUP

The results of the GOTC study of the bent biconic design in the Fall of 1985 showed that the biconic ballistic coefficient is much too high to effectively slow the vehicle without extremely large drag devices, such as rotofoils and parachutes. Thus, TSS chose to focus its attention on two possible vehicles, an Apollo-type capsule, and a flying saucer type vehicle. The latter proved to be most effective in terms of atmospheric entry, realizing a total of only 9,000 kg of fuel to place a total of 157,000 kg on the planet's surface.

2.1 VEHICLE CONFIGURATION

Three two-stage vehicle configurations were initially studied. The criteria for vehicle selection included the capability to leave the descent stage behind for later reuse and the abililty to completely reuse the ascent stage. This would be accomplished by having additional descent stages on the barge (in orbit) and having a single set of reusable engines on the ascent vehicle. The following requirements and assumptions were defined for the vehicle sizing analysis:

- A one-way manned descent capable of carrying 500 kilograms of payload.
- Only single pass entry trajectories are considered.
- Six g_{Earth} is the maximum loading to be experienced by the vehicle and crew.
- The pullout altitude for the equilibrium glide phase of flight will be at least four kilometers.
- The vehicle will be capable of flying at least 200 kilometers in crossrange.

- The vehicle will have at least a 5 kilometer crossrange capability in hover.
- The internal volume of the vehicle must satisfy permanent habitat as well as cargo requirements.
- The T/W_{Mars} of the deceleration configuration is assumed to be four.
- Design constraints due to atmospheric heating must be considered.

The first design studied was a lifting body (Figure 2.1.1) that was basically a two-stage version of the bent biconic studied by GOTC. It was realized that the bent biconic did not offer a significant volume and mass-carrying capability for cargo as well as habitation. Additionally, a two stage version of the vehicle would be difficult to enter and exit due to the excessive height of the manned section of the vehicle when it is on the ground. Although the bent biconic had very good aerodynamic characteristics, the control of the vehicle during the actual landing portion of the flight as well as the stability of the vehicle on the Martian surface were questionable.

The second configuration studied was a lifting ballistic body similar to the Apollo descent vehicle (Figure 2.1.2). Like the bent biconic, the Apollo-type vehicle did not offer significant mass and volume carrying capabilities. It would, however, provide for simpler access to the surface as well as greater stability on landing.

The third vehicle studied was a variation of the lifting ballistic body of the Apollo. It was essentially a flattened-out Apollo and resembles a flying saucer (Figure 2.1.3). The flying saucer shape, while having aerodynamic coefficients no better than the Apollo, would have a much

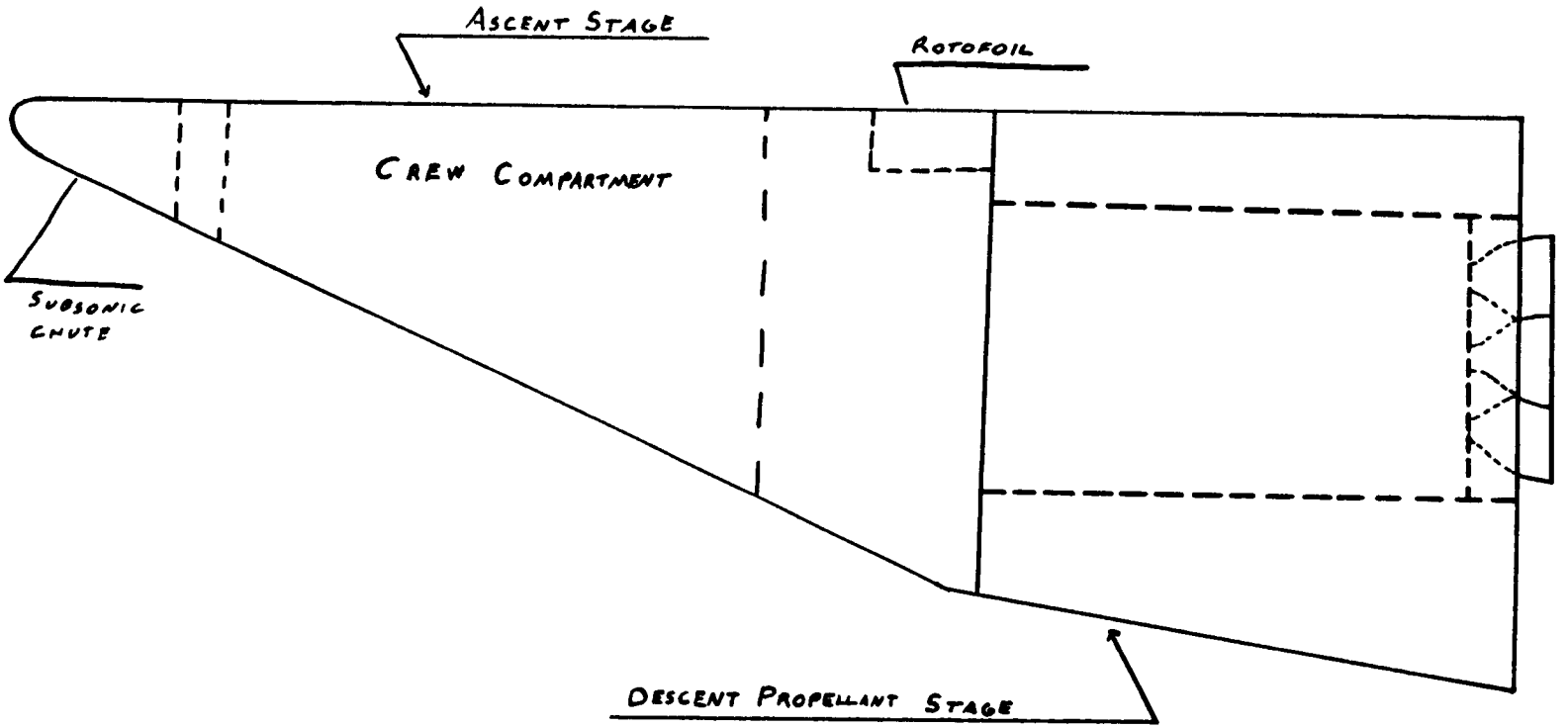

Figure 2.1.1 Bent Biconic Ascent/Descent Vehicle

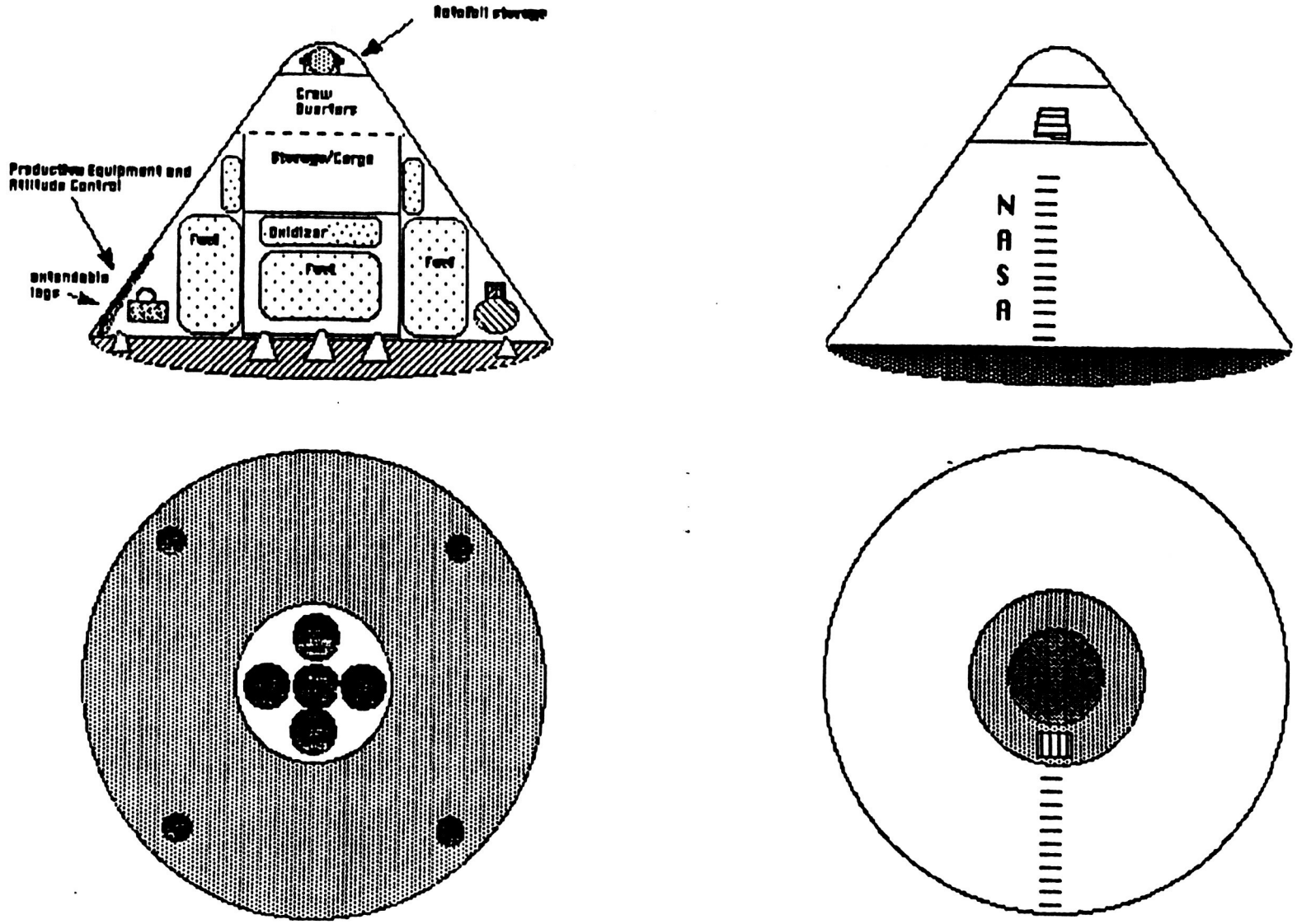

Figure 2.1.2 Apollo Type Ascent/Descent Vehicle

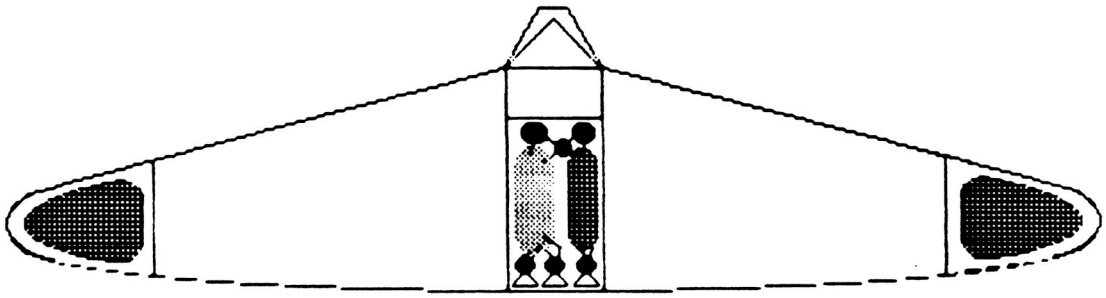

Figure 2.1.3 Flattened Apollo, Flying Saucer Ascent Descent Vehicle

larger planform area per unit mass, thus providing greater total lift and drag during the descent portion of the flight. Additionally, while the descent stage would be an extremely high-drag vehicle, the ascent stage would be streamlined. This shape would also offer significant volume for cargo carrying as well as habitation in its descent stage. Finally, the flying saucer would provide easy access to the surface as well as be very stable while on the Martian surface, even in the occasionally fierce Martian wind storms. For these reasons, the flying saucer shape was chosen as the prototype vehicle for this study.

Previous scenarios for a manned mission to Mars have included a separate cargo-descent vehicle (CDV) in addition to the ascent/descent vehicle (ADV) for transferring equipment to the surface of Mars. The ADV was assumed to have a single stage bent bicomic configuration. The CDV was going to be used to carry down the unassembled permanent habitat as well as the rover vehicle and all necessary scientific equipment. Due to possible construction difficulties with the assembly of the permanent habitat as well as the possibility for a significant savings in mass, TSS chose to investigate the use of a two-stage ADV which will not require a separate CDV. The descent stage will be completely reusable for other purposes and will become the permanent or semi-permanent habitat. Additionally, separate descent stages could be linked together in a modular fashion, thus extending the usefulness of the design. It is felt that this design will provide significant cost savings as well as simplify the overall mission scenario for a first-time visit to Mars.

LANDING GEAR

Although extensive research was not done on the landing system of the ADV, certain system requirements were defined. It was determined that six pads spaced 60 degrees apart would be arranged around the bottom of the descent portion of the ADV. The pads must be capable of fulfilling the following criteria:

1. Support the vehicle during soft landing (gross weight: 200,000 kg)
2. Have the capacity for extension (height of the bottom of the ship above the ground at least 3 m.)
3. Have the capacity to lower and support the vehicle to a height of 1 m (kneeling capability)
4. Redundancy: a total of six separate pads for redundancy and stability. Any three non-adjacent pads should be capable of supporting the ship.
5. Power system used (hydraulic, mechanical, or electrical) must remain effective after long-term exposure to space enviornment.

2.2 MASS AND VOLUME SIZING

The mass of the vehicle was essentially sized by the atmospheric entry. The figure realized was 200 metric tons. Mass and volume estimates of the main components of the descent portion of the ascent/descent vehicle (ADV) were made based on the assumptions of a five-man crew and a 60 day stay time. Values used for life support and support equipment masses and volumes were based on shuttle orbiter data. Total vehicle weight upon atmospheric entry was determined to be 165,444.4 kg. The detailed mass and volume estimates for the entire ship are listed in Tables 2.2.1 and 2.2.2. These are also illustrated graphically in Figures 2.2.1 and 2.2.2.

TK! Solver programs were used to size the fuel and propellant tanks used for the deorbit burn and for hover above the planet's surface. The deorbit burn was defined to be the burn required to transfer the vehicle from the parking orbit to 100 km above the planet's surface, where it was assumed that the Martian atmosphere begins. Hover took place about four meters above the planet's surface and lasted for three minutes. Program listings and results of the sizing are shown in are shown in Appendix A.

While the mass was sized by the atmospheric study, the volume was sized by system requirements. A TK! program was developed to determine the volume of a vehicle given radius and height information. The vehicle is essentially a right circular cone on a spherical base. The volume requirements for the entire ship was 1556.7 m^3, and the ship was sized at 2000 m^3 to allow for a safety margin. The descent portion of the vehicle has a radius of 18 m and a height of 7.7 m. See Figure 2.2.3

In Table 2.2.1 are mass and volume estimates for the ascent and descent stages of the ADV. These are also illustrated graphically in Figures

Table 2.2.1 Ascent and Descent Mass and Volumes- Breakdown

Assumptions:
5 man crew
60 day stay
180 sec hover time

Component	Descent ship---------- Mass (kg)	Volume (m3)	Ascent Vehicle---------- Mass (kg)	Volume (m3)
Life and Support				
food	351	4.2	48.21	0.58
Air Revitalizaion	462.66	1.6	63.55	0.22
Water Recovery	1,113.56	5.09	152.96	0.70
N2 storage (leakage)	725.74	0.5	99.69	0.07
Furnishings	75	4	10.30	0.55
Storage Lockers	3	1	0.70	0.23
Living Space	0	61.2	0.00	14.30
Personal Items	40	5	40.00	5.00
Tools	10	0.01	10.00	0.01
Crew	419	0	419.00	0.00
EVA suits	225	7	225	7.00
Subtotoal	3,424.96	89.6	1,069.42	28.66
Support Equipment				
Communications	55	0.15	55	0.15
Navigations	45	0.1	45	0.1
Data Acquisition	270	0.85	40	0.32
Displays	90	0.28	90	0.28
Airlock	225	1.25	225	1.25
Subtotoal	685	2.63	455	2.1
ROVER:				
Lunar	226.8	4.25	0	0
Enclosed	11,000	90	0	0
SHIP				
Structure	30,000	436.8	6,780	12
Fuel Tank (dry)	1,200	1.6	400	0.5
Oxidizer Tank (dry)	3,300	4.4	700	1
Engines and Pumps	6,200	6.5	1,200	0.5
Fuel Cells	1,553.55	4.3	200	1
Subtotoal	42,253.55	453.6	9,280	15
PAYLOAD				
Scientific Payload	9,000	300	500	2
ISPP Equipment*	10,000	500	0	0
Subtotoal	19,000	800	500	2
FUEL and Ox				
Fuel	21,410.5	57.66	8,974.9	24.17
Oxidizer	67,443.6	58.99	28,271.2	24.73
Subtotoal	88,854.1	116.66	37,246.1	48.9
Grand Total	165,444.4	1,556.74	48,550.52	96.656721
Target	200,000	2,000	48,995	100

sources JSC 16277, space operations center, nasa, 1979
PDR1, fall 85
Lunar Bases and Space Activities of the 21st Century

Table 2.2.2 Ascent and Descent Mass and Volumes- Overview

Summary	Descent Vehicle		Ascent Vehicle	
	Mass (kg)	Volume (m3)	Mass (kg)	Volume (m3)
Life and Support	3,424.96	89.6	1,069.42	28.66
Computers & Equipment	685	2.63	455	2.1
Payload	30,226.8	894.25	500	2
Structure	42,253.55	453.6	9,280	15
Total Fuel & Ox	88,854.1	116.66	37,246.1	48.9
Unused	34,555.59	443.26	444.48	3.34
total wet mass	165,444.4	1,556.74	48,550.52	96.66
Unused	34,555.59	443.26	444.48	3.34
total wet mass	200,000	2,000	48,995	100

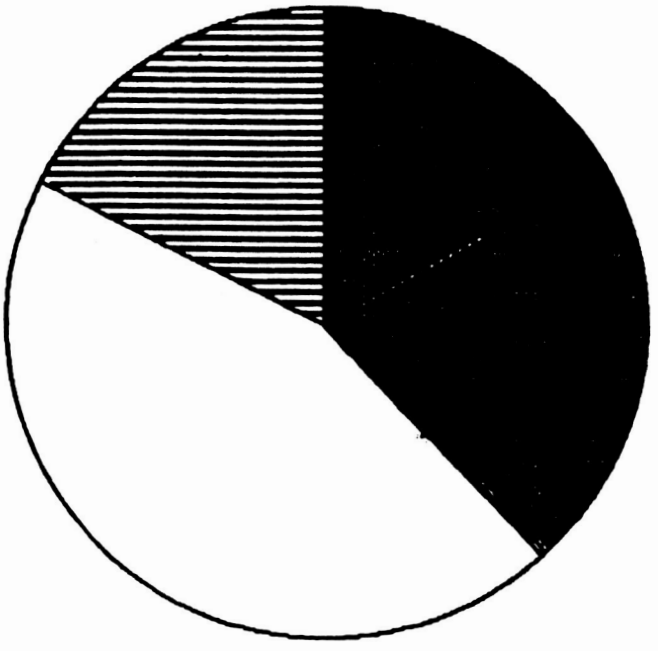

Figure 2.2.1 Descent Vehicle Mass Ratios

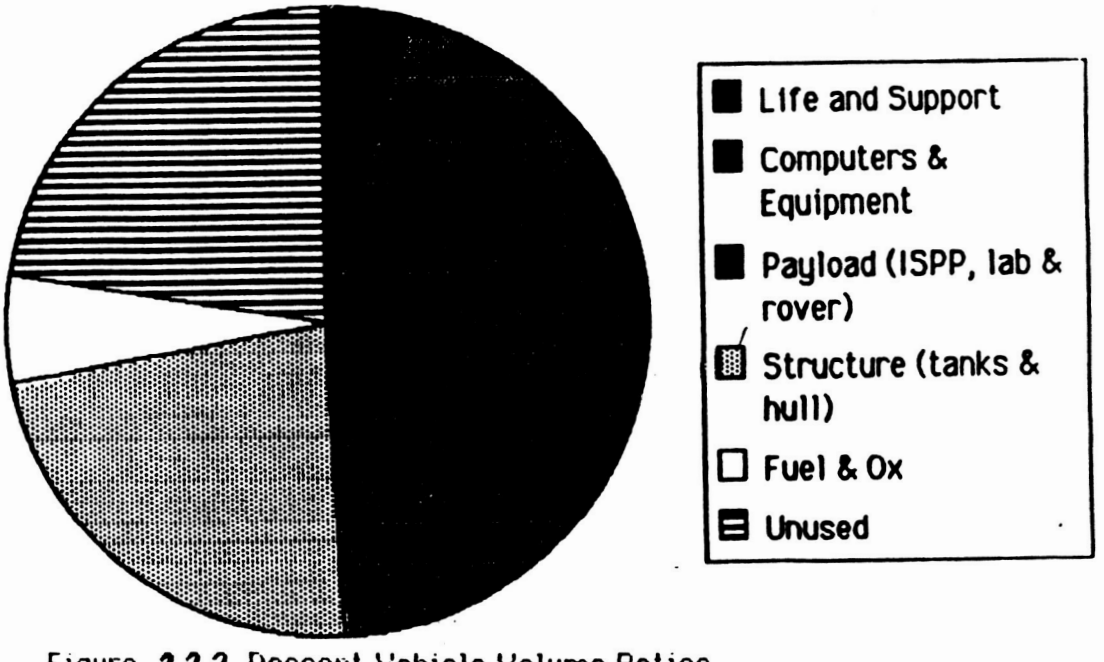

Figure 2.2.2 Descent Vehicle Volume Ratios

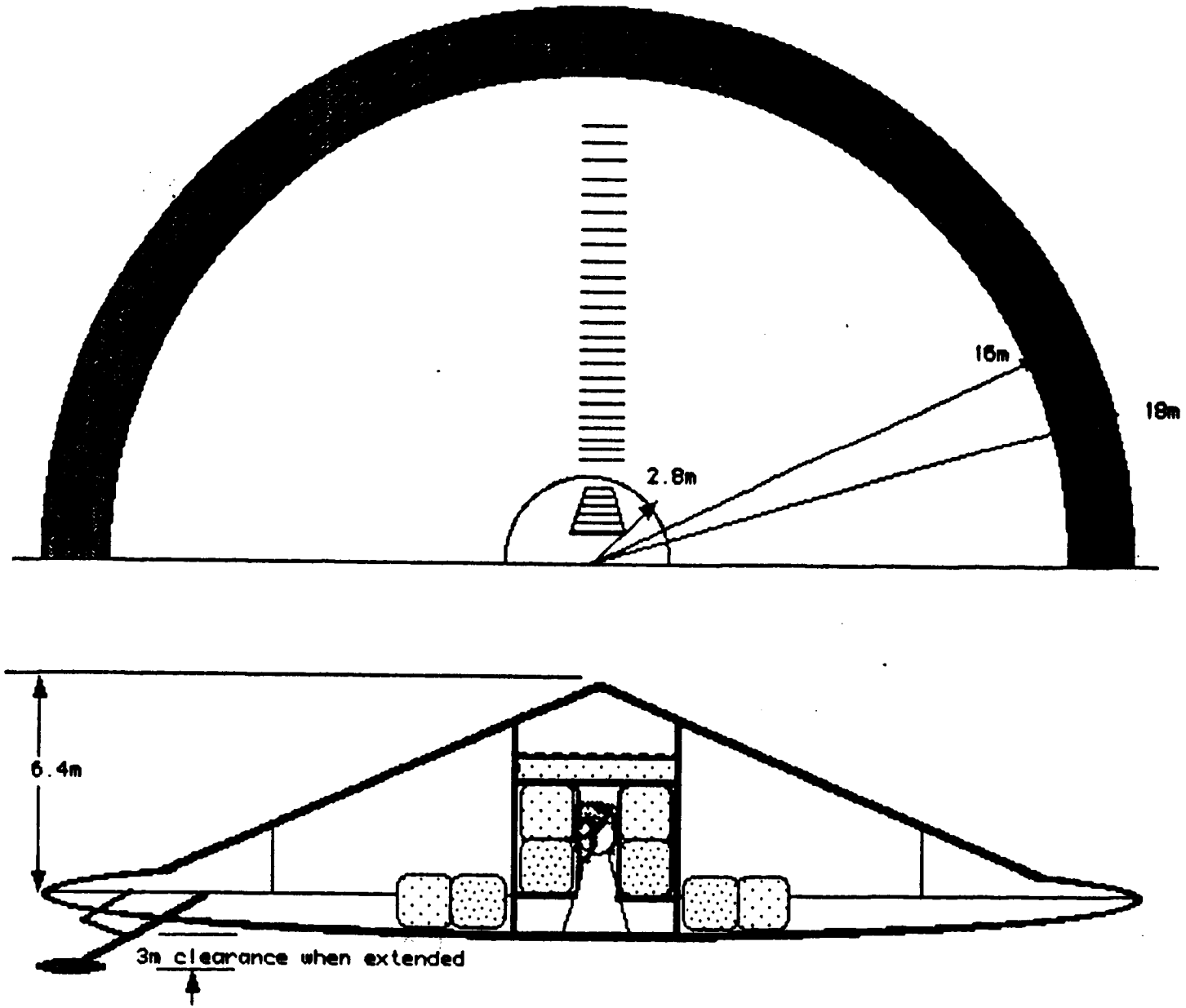

Figure 2.2.3 The Descent Vehicle

2.2.4 and 2.2.5. The total mass of the ascent portion of the vehicle was estmated at 48,995 kg. The ascent portion was sized for a five-man crew and a 14 day contingency mission. Essentially a cylinder, it is 6 m in diameter and 7 m in height (including 2.75 m for the engine nozzle), with a volume of 100 m^3. Note that it is nearly as wide as tall, and thus stability problems are anticipated. A more stable configuration is illustrated in Figure 2.2.6a.

PROPELLANT REQUIREMENTS

The propellant needs of the vehicle were determined by four factors: deorbit burn, powered deceleration, hover and ascent. It was determined that strap-on tanks would be used for the deorbit section of the flight (Figure 2.2.6b). The maximum mass of the deorbit fuel is 45,000 kg. This allows us to obtain a mass ratio of 1.225 for the deorbit burn.

The powered deceleration portion of the flight requires 9000 kg of propellant. Assuming a hover time of three minutes, 42,600 kg of propellant is required. The ascent portion of the flight requires 37,200 kg. Thus the total onboard propellant required at atmospheric entry is 88,800 kg.

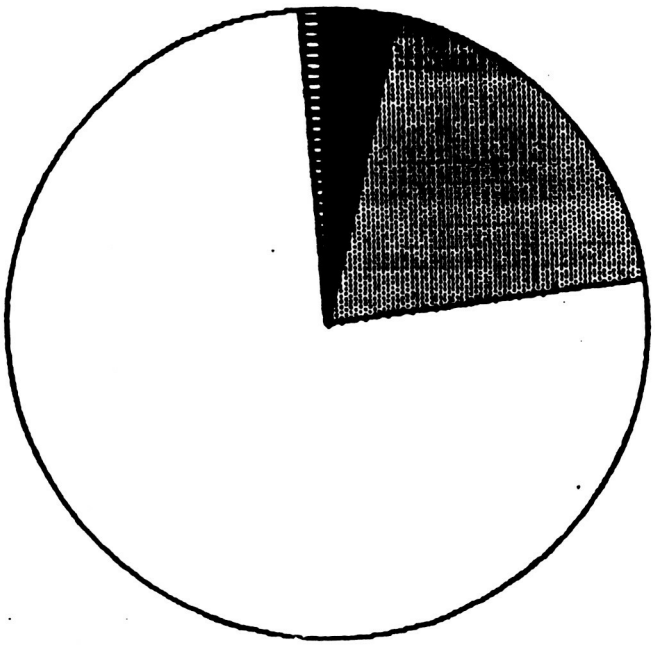

Figure 2.2.4 Ascent Vehicle Mass Ratios

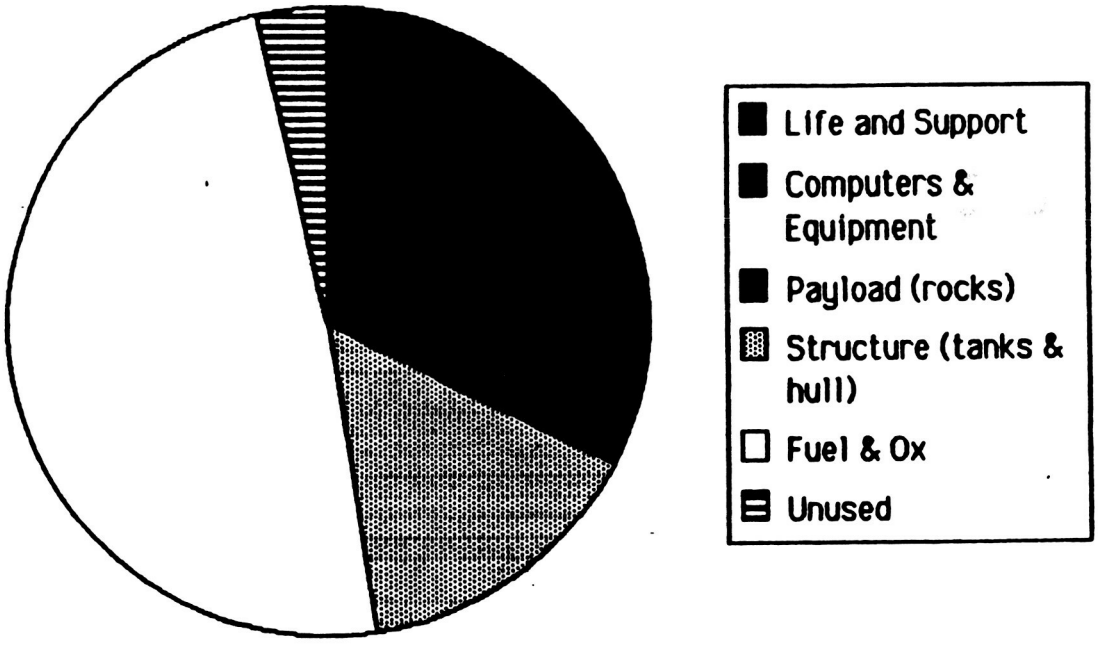

Figure 2.2.5 Ascent Vehicle Volume Ratios

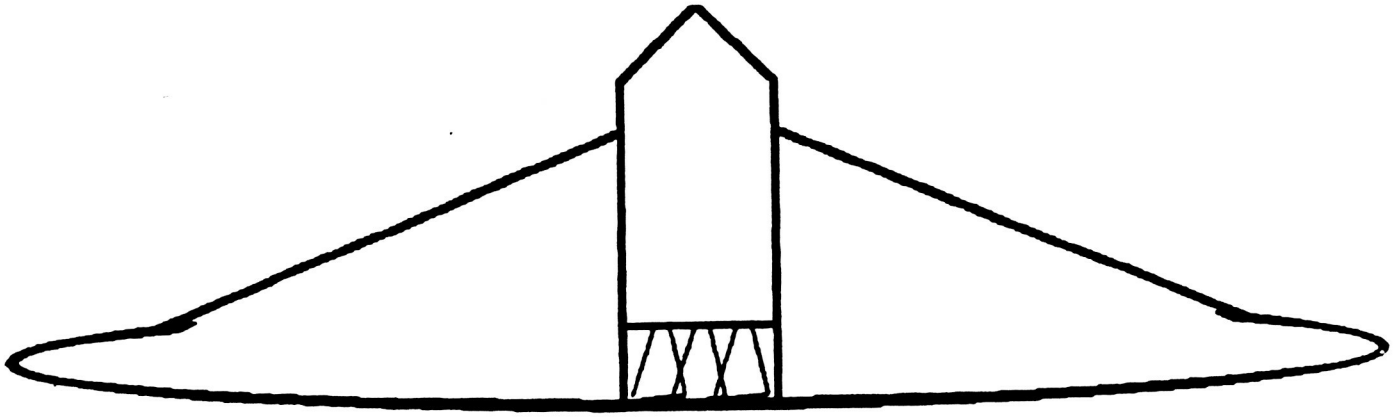

Figure 2.2.6a **Improved Stability Ascent Module**

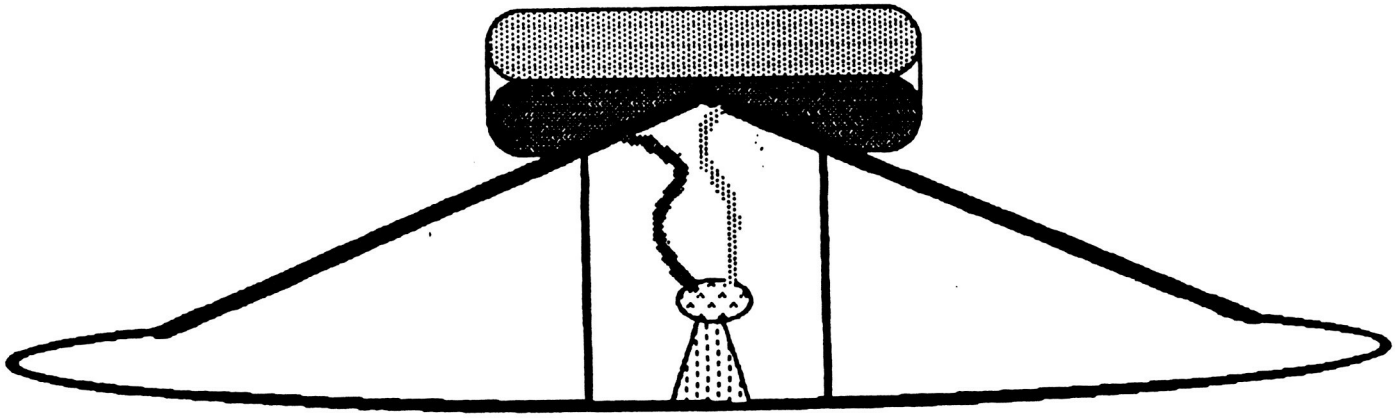

Figure 2.2.6b **Deorbit Scenario, Strap-on Throw-Away Tanks**

2.3. DEORBIT SCENARIO

Although deorbit delta-v is of importance, the design parameters for the entry vehicle require that it arrive at the planet's atmosphere with tanks full. With this consideration, TSS recommends that provision be made for an external throw-away tank be used for the deorbit burn. Alternatively, a small strap-on solid or liquid motor could be used for this purpose.

TSS pursued the study of the descent scenario in two phases conducted independently. Phase one involved developing a program to be used to calculate initial conditions for atmospheric entry, deorbit delta-v, transfer orbit parameters, etc. The phase two study was concerned with the atmospheric descent. A FORTRAN program has been developed to simulate this descent.

2.3.1 DEORBIT DELTA-V

The simplest transfer from an elliptical parking orbit to the Martian surface is a Hohman transfer with the deorbit burn at the apoapsis of the parking orbit. The target point for this type of transfer is 180° from the burn point, or directly below the periapsis of the parking orbit. This case requires the minimum deorbit delta-v but gives the maximum entry velocity. Another possibility with the Hohman transfer is to make the deorbit burn at periapsis. In this case, the target point is directly below the apopsis of the parking orbit.

In order to obtain a compromise between delta-v requirements and entry velocity, transfer trajectories initiated at intermediate points in the parking orbit were studied. This was done using a Lambert targeting program (DODV) with TKI Solver. An advantage of choosing an intermediate

point on the parking orbit for the deorbit burn is it increases the range of possible target locations. Given a specific entry flight path angle, transfer orbits initialized at apoapsis or periapsis require mid-course corrections for specific landing sites. Deorbit burns at other points along the transfer orbit allow more flexibility in landing site selection.

The program has been modified to include the additional delta-v requirements of a plane change. The final deorbit burn was sized for a plane change of 10°, since most of the planet is accessible in the present parking orbit (inclined at an angle of 63°). Additional modifications allow for circularization at any point in the orbit, and account for delta-v due to planet rotation. The rotation of Mars grants the deorbit scenario an additional 250 m/s or so, depending on latitiude and inclination.

The program developed is a TKI Solver model using Lambert Targeting. The user is able to specify any combination of parameters for calculation. For example, by specifying an entry velocity, the user can vary the true anomaly at the initial burn and study the delta-v required. In addition, TKI solver allows the user to generate tables and plots of the data, studying results for deorbit from the entire parking orbit.

DODV (Deorbit Delta-V, see Appendix B) calculates the following parameters in the MKS system, any of which may be specified for analysis:

* Delta-v from parking orbit
* Transfer orbit parameters
* Flight path angle at burn
* Atmospheric entry velocity
* Flight path angle at atmos entry
* Mass ratio for deorbit burn

* Circularization delta-v

with the following assumptions:

* Two body problem
* Spherical, rotating Mars
* μ of Mars = 42828.28 km^3/s^2
* Radius of Mars = 3395.0 km
* Single burn to tranfer orbit
* Negligible burn time
* Atmosphere of Mars begins at 100 km over planet surface

2.3.2. RESULTS OF DODV STUDY

The DODV program is designed to provide entry velocity, height above planet surface and flight path angle upon atmospheric entry. By varying parameters of the transfer orbit and true anomaly of the parking orbit at burn, the delta-v required can be minimized.

Specific, independent results of the DODV study:

1. Delta-v window: The delta-v required for a single burn is minimized for fire at apoapsis, and is maximized for fire at periapsis. This results in: 752.65 > delta-v > 78.25 m/s.

2. The entry velocity is dependent only on two parameters, specifically, semi-major axis and periapsis of the transfer orbit. Thus, by specifying any two parameters, (entry velocity and periapsis), the delta-v for deorbit from any point on the parking orbit can be studied to find the most effective deorbit scenario. (see Table 2.3.1)

3. Entry velocity window: Since the entry velocity (Ve) is dependent on only two parameters of the transfer orbit, a vacuum periapsis equivalent

Table 2.3.1 Table shows constant entry velocity for constant transfer orbit characteristics (at = 6500, vacuum periapsis height = 0) Note minimum delta-v occurs at minimum delta gamma (flight path angle) change at deorbit burn.

	f (deg)	Ve (m/s)	Deltav (m/s)	Dgamma (deg)
	360	4233.11	1129.40325	-16.483109
	352.5	4233.11	986.123961	-14.404823
	345	4233.11	859.04286	-12.607064
	337.5	4233.11	748.27463	-11.074028
	330	4233.11	652.775933	-9.7784633
	322.5	4233.11	570.865552	-8.6879955
	315	4233.11	500.656874	-7.7701509
	307.5	4233.11	440.335582	-6.9953752
	300	4233.11	388.297399	-6.3383138
	292.5	4233.11	343.191681	-5.7779727
	285	4233.11	303.913805	-5.2973032
	277.5	4233.11	269.575461	-4.8825649
	270	4233.11	239.469156	-4.5226497
	262.5	4233.11	213.034776	-4.2084382
	255	4233.11	189.831325	-3.9322031
	247.5	4233.11	169.514756	-3.6870457
	240	4233.11	151.822023	-3.4663692
	232.5	4233.11	136.561774	-3.2634636
	225	4233.11	123.613619	-3.0715155
	217.5	4233.11	112.942909	-2.8849884
	210	4233.11	104.655665	-2.705036
	202.5	4233.11	99.194494	-2.5567325
*	195	4233.11	98.1951653	-2.5460855
	187.5	4233.11	109.631367	-3.1001194
	180	4233.11	180.593446	-6.0720743

to the planet surface (periapsis altitude = 0) was chosen for the initial study based on results of the GOTC study for the flight path angle window. This results in: 4270 > Ve > 3570 m/s. (see Table 2.3.1) The rotation rate of Mars further reduces the entry velocity, depending on inclination (currently 64 deg.) and lattitude of initial entry.

4. The minimum delta-v occurs when the change in flight path angle is minimized at burn (dgama = 0). Thus, after the tranfer orbit parameters have been determined, the true anomaly for deorbit burn is also determined by this parameter. (see Table 2.3.2)

5. As suspected, circularization near periapsis did not add appreciably to the deorbit delta-v. This is illustrated in Figure 2.3.1.

6. Combining circularization with inclination changes, it is better to take out some of the incination upon circularization. The amount taken out depends on where the deorbit burn takes place in the parking orbit, and the amount of inclination desired. (see Figures 2.3.1 and 2.3.2)

7. A change in inclination is most efficient when done between 190 and 260° true anomaly in the orbit. (see Figure 2.3.2)

The final deorbit program and parameters are illustrated in Table 2.3.4. In summary, the deorbit delta-v allowed for was 988.7 m/s. This results in an entry velocity of 3300 m/s, a 10° plane change with mass ratio of 1.304, or approximately 60 metric tons of fuel for the deorbit. This figure is quite high, but may be significantly reduced by allowing for a slightly greater atmospheric entry velocity. Future considerations of the descent scenario should be concerned with burn time and three dimensional lambert targeting (not feasable with TKI Solver).

Table 2.3.2 Table shows effect of changing tranfer orbit parameters on entry velocity (f = periapsis).

at (km)	Ve (m/s)	Deltav (m/s)
3800	3638.36	773.727619
3937.5	3692.05	794.916563
4075	3741.42	816.892316
4212.5	3786.99	839.130197
4350	3829.18	861.269885
4487.5	3868.37	883.068242
4625	3904.87	904.365157
4762.5	3938.96	925.059113
4900	3970.86	945.089809
5037.5	4000.79	964.425808
5175	4028.92	983.055772
5312.5	4055.42	1000.98223
5450	4080.42	1018.21713
5587.5	4104.05	1034.77869
5725	4126.41	1050.68914
5862.5	4147.62	1065.97312
6000	4167.75	1080.65651
6137.5	4186.89	1094.76569
6275	4205.11	1108.32693
6412.5	4222.48	1121.36601
6550	4239.05	1133.908
6687.5	4254.88	1145.97703
6825	4270.01	1157.59625
6962.5	4284.5	1168.78775
7100	4298.38	1179.57253

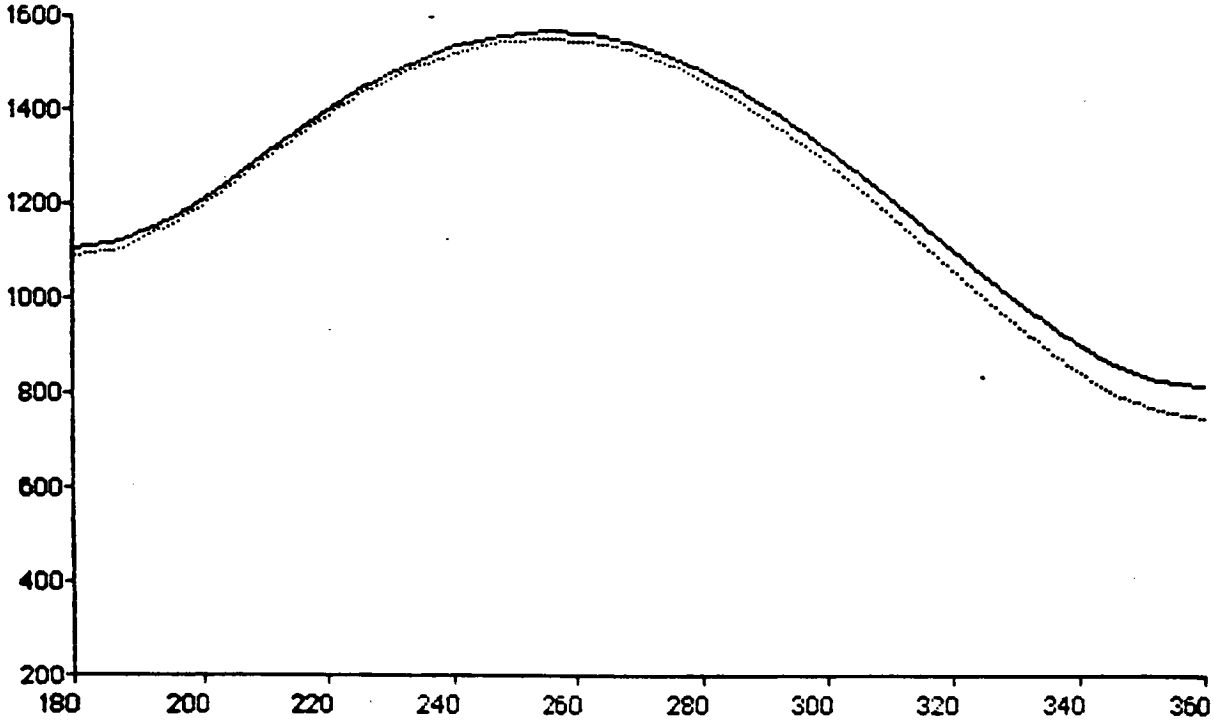

Figure 2.3.1 DU vs F, i=5°, Dotted line = no pl. chg.

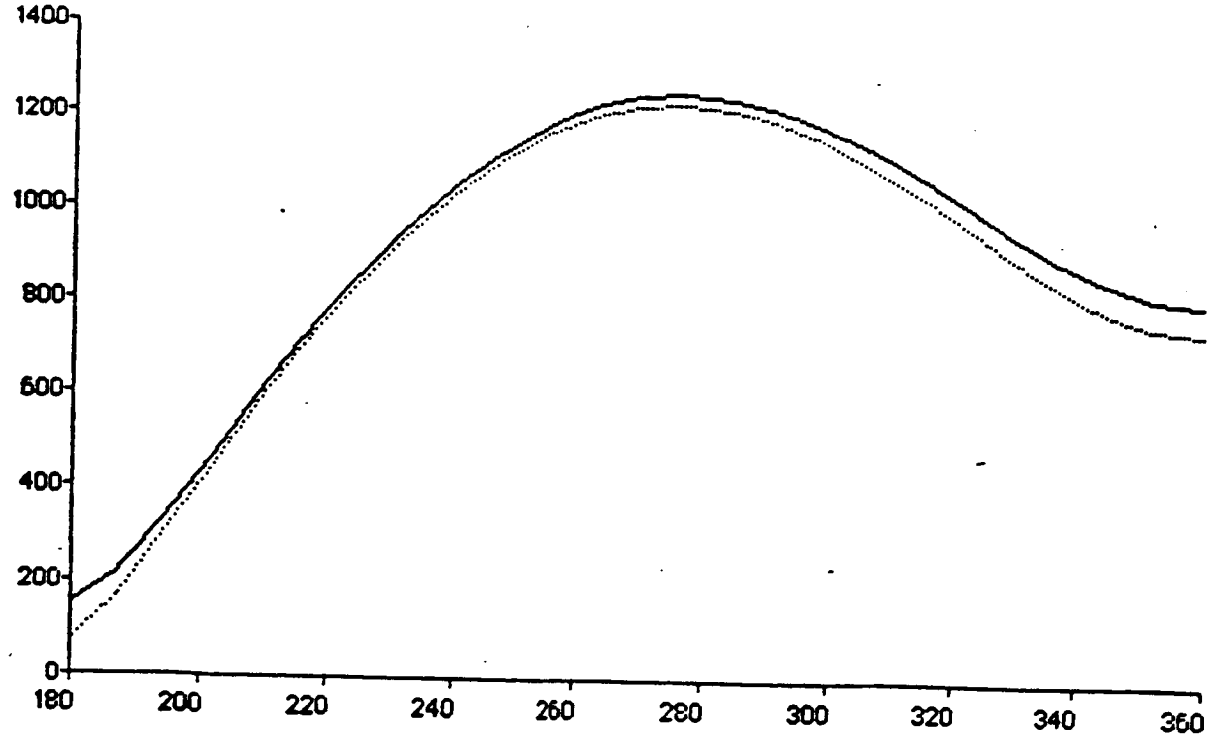

Figure 2.3.2 DU, dotted line = no pl. chg, solid line w/pl. chg.

2.4 AERODYNAMICS

2.4.1 AERODYNAMIC DESCENT ANALYSIS

The vehicle parameters addressed in this study are:

- vehicle mass fully loaded with fuel and payload, (Mo)
- ballistic coefficient, ($M/S*C_L$)
- L/D
- pullout altitude
- propulsive deceleration delta V
- T/W_{Mars} for Hover
- hover time

The analysis for sizing the vehicle was broken into four major areas:

1) Entry corridor and entry velocity
2) Aerodynamic deceleration
3) Aerodynamic heating
4) Propulsive deceleration
5) Hover

A three degree of freedom trajectory simulation was developed to analyze the aerodynamic and propulsive phases as well as the aeroheating of the entry trajectory. A listing of the program (Reference 2.4.1) can be found in Appendix C. A listing of the descent profile can be found in Appendix D. All simulations were initialized at an altitude of 100 km.

The relationship between L/D ratios and crossrange capability, as well as the ballistic coefficient for the vehicle, were obtained using this trajectory simulation. It should be noted that the flying saucer ADV vehicle chosen for study by TSS will have a much higher ballistic coefficient and a

much lower lift-to-drag ratio than the bent biconic ADV of previous reports; thus, the flying saucer will be better able to effectively use drag as a delta-V device while, at the same time, it will have a reduced crossrange capability.

The aerodynamic entry trajectory is illustrated in Figure 2.4.1. When the ADV enters the atmosphere at an altitude of 100 km. the lift and drag vectors will help to slow the vehicle. At the pullout altitude of 70 km. the vehicle rotates its angle of attack to allow for a more shallow flight path angle. During this phase, the flight path angle actually becomes slightly positive at an altitude of approximately 45 km. The ADV then undergoes the equilibrium glide phase in which very little altitude is lost as the vehicle decelerates further. In other words, the lift vector is continually rotated to maintain a somewhat constant value for lift as the dynamic pressure steadily decreases. This phase also serves to slow down the vehicle in a region of constant density, thus reducing the g-loading considerably during this phase.

The equilibrium glide phase comes to an end when the available lift can no longer maintain the vehicle in level flight. Even though equilibrium glide is no longer possible, the vehicle will continue to decelerate, and its flight path angle will gradually turn downward as its velocity decreases.

At an altitude of 10 km and a flight time of 20 minutes the protective engine shield covering is slid into the main body on a sliding track. At this altitude the stagnation temperature is sufficiently low (523 K) that the engines will be safe. This altitude will also allow sufficient time (50 seconds) for the shield to be moved. This system will allow for the use of the main engines for the deorbit burn.

Figure 2.4.1 DESCENT PROFILE

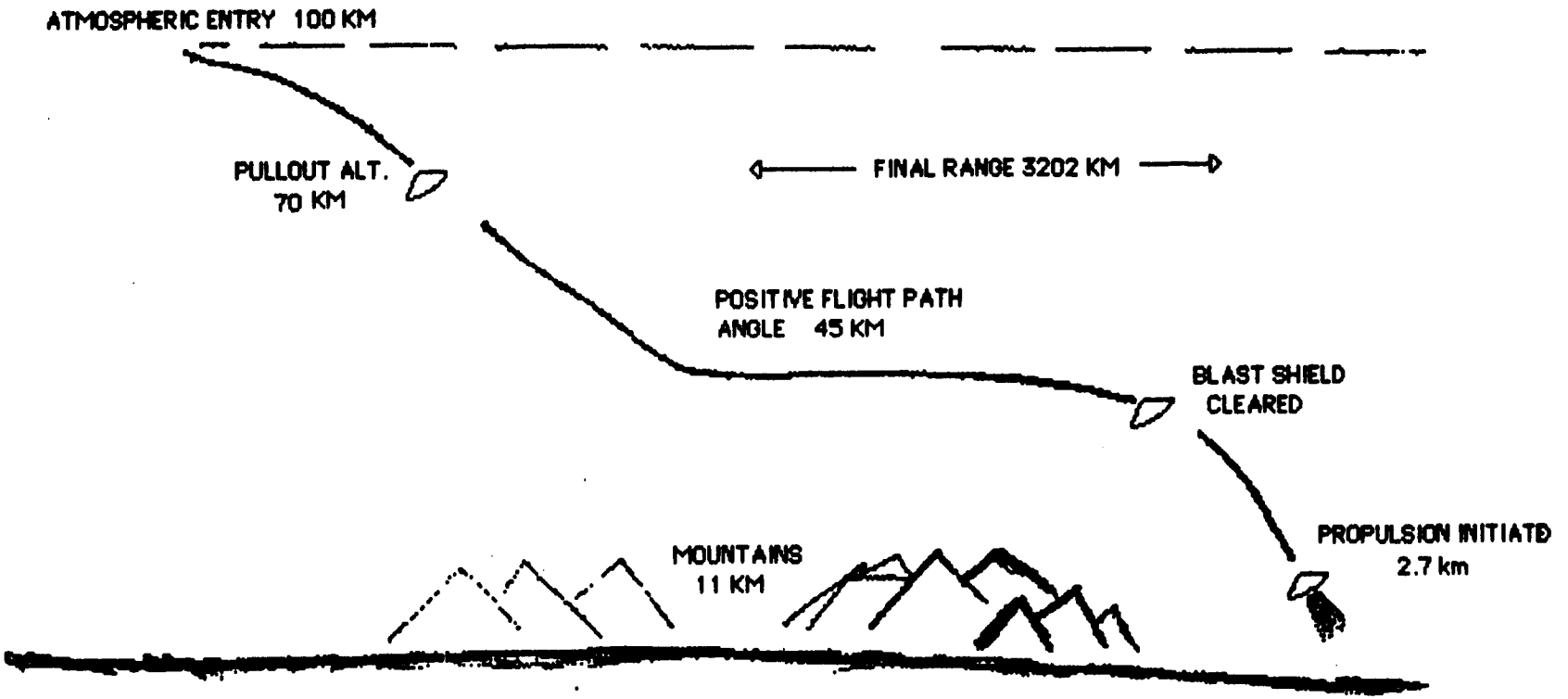

At an altitude of 2.69 km and a flight time of 20 minutes 53 seconds the engines are ignited and the propulsive deceleration begins. The remaining velocity of 207 m/s will now be removed. Notice that the flight path angle begins to rapidly approach -90°.

After firing the engines for 33 seconds the vehicle is brought to zero velocity at an altitude of 415 meters and the hover phase of the flight is initiated. The hover will allow a crossrange of 5 km and will last for approximately 4 minutes.

In addition to the actual descent profile (Appendix D), a detailed summary of the descent can be found in Fig. 2.4.2. Note that the vehicle undergoes a g-load maximum of 3.89 and a maximum stagnation temperature of 1 143 K. The total flight time is 21 minutes 27 seconds, and the final range is 3 202 km. The descent fuel mass is 9 804 kg and the hover fuel mass is 48 647 kg for a T/W_{mars} of 1.1.

It was found that the aerodynamic descent for the flying saucer vehicle was much more efficient than that of the bent biconic vehicle studied in previous semesters. This efficiency appears in the large reduction of fuel mass as well as a reduction in the total mass of the vehicle. The bent biconic had an initial wet mass of 360 000 kg (Reference 2.4.2) and a total fuel mass of 310 471 kg with a total payload mass of 7 000 kg. The descent fuel required by the flying saucer was only 9 804 kg. and the total wet mass of the flying saucer was 200 000 kg. The significant fuel savings occurs from the much smaller mass required of the flying saucer at hover initiation (190 197 kg versus 361 000 kg) as well as the two-stage configuration of the flying saucer; i.e. the ascent fuel required by

Figure 2.4.2 DESCENT PROFILE

INITIAL MASS OF VEHICLE	200 000.	KG
INITIAL FLIGHT PATH ANGLE	-.5	DEGREES
COEFFICIENT OF LIFT	.5	
LIFT/DRAG	.5	
VEHICLE RADIUS	18.	METERS
BALLISTIC NUMBER	393.	KG/M^2
PULLOUT ALTITUDE	70	KM
ATM. ENTRY ALT.	100	KM

PROPULSION PROFILE

THRUST	800 000	N
PROPULSION ACTIVATION ALT.	2.2	KM
FUEL MASS FLOW RATE	387.	KG/S
PROPULSION DELTA-V	207.	M/S
PROPULSION TIME	27.	S

FINAL AND MAXIMUM DESCENT CHARACTERISTICS

LANDING TIME	1 289.	S
LANDING ALT.	3.8	M
MAXIMUM STAGNATION TEMPERATURE	1 145.8	K
MAXIMUM G-EARTH DECELERATION	3.8	
MASS OF DESCENT FUEL	9 804.	KG
MASS OF 4 MIN. HOVER FUEL	48 647.	KG
TOTAL DESCENT FUEL	58 451.	KG

the flying saucer ascent vehicle was only 38 000 kg. since the ascent vehicle's wet mass was only 48 000 kg (versus an ascent fuel mass of 154 985 kg and a wet vehicle mass of 205 000 kg for the bent biconic).

Another factor favoring the flying saucer is the simplified descent profile. While both vehicles were analyzed using a similar method, the bent biconic vehicle used a more complicated trajectory which includes the use of rotofoils and a radical attitude change. The flying saucer, on the other hand, maintains a fairly constant descent attitude and requires no special aerobraking devices. Additionally, during the propulsion and hover phase of the flight, the bent biconic would be flown as a very tall vehicle supported by rear mounted engines. The flying saucer, however, would present a low, flat configuration which would be much more stable and not as critically dependent on a low center-of-gravity as the bent biconic.

It is felt by TSS that the two-stage flying saucer is a worthy alternative to the one stage bent biconic on the basis of the results of the aerodynamic entry and the fact that a separate cargo descent vehicle will not be needed; therefore, the flying saucer should be the vehicle of choice for the manned mars mission.

2.4.2 HEATING

The ascent/descent vehicle will be entering the martain atmosphere at hypersonic speeds and will require heat shielding. This semesters heat analysis was performed in three phases. First, a study of the possible types of thermal protection systems was conducted. Second, an estimate of the maximum temperature was calculated. Third, thermal protection for the A/D

vehicle was decided.

2.4.2.1 SYSTEMS

There were four types of thermal protection systems looked into by the study. These were ceramic tiles, ablative shielding, titanium shields, and advanced carbon-carbon. All are considered state of the art (Reference 2.4.2).

FIBROUS REFACTORY COMPOSITE INSULATION (FRCI)

This is an insulative/reradiative system. FRCI is a derivative of the Shuttle ceramic tiles, but much lighter and stronger: it reduces weight by approximately fifty per cent. FRCI is made of a blend of silica and aluminum borosilicate fibers. The tiles have a low coefficient of thermal expansion. The following table lists some properties for FRCI tiles:

TABLE 2.4.1

Temp Limit	Ther Conduct.	Thickness
1260 C	.017-.052 W/mK	1.3-8.9 cm

Density will vary according to use. Normal tile density will be 5-9lb/ft^3. Heavy tiles for use around hatches or doors will have a density of 12 lb/ft^3.

Advantages: Ceramic tiles are a proven technology. They are lightweight, reuseable, and efficient.

Disadvantages: FRCI is not as damage resistant as metal alloys or carbon-carbon.

ADVANCED CARBON-CARBON (ACC)

ACC is a reradiative hot structure. This TPS material is a derivative of the reinforced carbon-carbon material used on the space shuttle. ACC consists of a carbon matrix reinforced with graphite fibers, coated with silicon carbide and impregnated with silica. The following table lists some properties of ACC.

TABLE 2.4.2

Density	Temp. limit	Thickness
12 lb/ft3	1600 °C	4.8 cm

Advantages: Carbon-carbon is a proven technology and it is damage resistant.

Disadvantages: ACC requires additional insulation and more complicated fabrification.

TITANIUM TILES

Titanium tiles are a reradiative hot structure. They have a temperature limit of 720 K. Tiles are attached mechanically.

Advantages: Titanium tiles are damage resistant and have a mechanical attachment to the spacecraft struture.

Disadvantages: These tiles are slightly heavier than ceramic tiles. The tiles must provide for expansion and contraction without buckling, without distortion fo the aerodynamic surface, and without plasma ingestion.

THROWAWAY ABLATOR

This system has been used numerious times in the past. Ablative material can take very high temperatures by varing their thichness.

Advantages: Ablative materials have the highest temperature limit and are proven.

Disadvantages: Ablative are 4 to 8 times as heavy as the tile system.

2.4.2.2 Temperature Estimate

In order to properly select a good TPS it is necessary that one determines the max temperature generated by the craft upon re-entry. Two methods were used to estimate what the max temperature would be.

The first method :

It was found that for design purposes the heat transfer rate could be assumed to equal (Reference 2.4.3):

$$dq/dt = 0.5\ r\ V^3 \cos i$$

where

r = density in front of the shock

V = velocity of the vehicle

i = angle between the surface and stream velocity; the ratio of a unit flow area to a corresponding surface area

i was assumed to be 90 degrees to insure maximum conditions. This reduces equation to:

$$dq/dt = 0.5\, r\, V^3$$

It was found that T max could be expressed as (Reference 2.4.4):

$$T_{max} = (q/sig\ e)^{.25}$$

substituting equation gives:

$$T_{max} = 0.5\ \ V^3/sig\ e)^{0.25}$$

where:

sig =emissivity of the shield

e = stephan boltzmann constant,

This equation was incorporated into the aerodynamics program and the stagnation temperature was found at each point. Using this method a maximum temperature 1140 K was generated .

Normal Shock Method:

The second method calculated the stagnation point temperature generated across a normal shock and estimated what the temperature at the vehicle. The equations govering the properties across a bow shock are given by:

Continuity:

$$r_1 V_1 = r_2 V_2$$

Momentum:

$$P_1 + r_1V_1^2 = P_2 + r_2V_2^2$$

Energy:

$$H_1 + 0.5V_1^2 = H_2 + 0.5V_2^2$$

Perfect Gas:

$$\frac{P_1}{r_1 T_1} \qquad \frac{P_2}{r_2 T_2}$$

A program was obtained from Dr. John Bertin which substituted for the perfect gas equation a subroutine called Molliere. Molliere solved the real gas case for air. Using air in place of carbon dioxide should not produce significant error. The program guessed a solution for two variables and iterated within a certain tolerance to obtain solutions for the stagnation point temperature across the shock. This program was run for several points of descent and the results are printed in Table 2.4.3.

TABLE 2.4.3

Alt (Km)	Velocity(m/sec)	Temp(K)
100	3500	2716
94.7	3493	2710
87.7	3484	2702
80.3	3413	2691
76.0	3465	2667
71.3	3453	2692
63.3	3422	2772
58.4	3384	2820
49.5	3210	2812
46.1	2988	2731
30.0	1514	1236

It can be seen from Table 2.4.3 that the maximum stagnation point temperature is 2820 K. To estimate the tempertature that would be generated on the craft Dr. Bertin was consulted. He estimated that for the given conditions the surface temperature would be 1000 K.

2.4.2.3 SELECTION OF THERMAL PROTECTION SYSTEM

FRCI tiles were chosen for protecting the bottom half of the A/D vehicle. The tiles 1400 K tempertature limit provides adequate protection for the 1000 k temperatures expected upon entry. The tiles weight savings over the other candidates was a key to its selection. FRCI tiles are also proven state of the art technology. There will need to be a circular shield on the bottom of the vehicle. This shield to protect the engines during entry will be slid out of the way when propulsion begins.

Titanium tiles were selected as the surface material for the upper half of the A/D vehicle. During entry the temperature on the upper half of the vehicle is insignificant, but the titanium must be able to withstand the temperatures generated by the exhaust during takeoff. Assuming isentropic conditions the maximum exit temperature will reach 1430 K. The exhaust will only be on the upper surface for a few seconds during takeoff so the surface should not reach a temperature higher than titaniums 720 K limit. An added advantage of titanium is that ot offers some protection from Martian storms and in space flight the titanium tiles could face out and help to protect the more vulnerable FRCI tiles underneath. In addition, the titanium improves the structure of the vehicle, due to the strength of the titanium.

2.4.3. HOVER PROGRAM

The TKI Solver program HOVER was used to determine fuel and oxidizer needs for the ADV during hover. Given an initial vehicle weight and desired hover time, the program calculates the required mass of the fuel and oxidizer, the required volume of the fuel and oxidizer, and total propellant mass and volume. The mass of the tanks were determined using a structural factor of 0.15. Values for initial wet mass of the vs. burn time are shown in figure 2.4. Note the sharp increase in wet mass as the burn time approaches 500 seconds.

2.4.4 RECOMMENDATIONS

Overall the work done on heating this semester we feel was good. The estimates of the heating seem resonable for a preliminary study. The

2.5 ASCENT / PROPULSION ANALYSIS

In proceeding with the ascent analysis, it was found that the propulsion system could not be considered independently if an optimum ascent or propulsion sizing was to be performed. To perform the analysis, a TK! Solver model was created which contained the equations governing ascent, and those for engine performance. In the sections which follow, the analysis is described in more detail.

2.5.1 ASCENT ANALYSIS

The primary goal of the ascent analysis has been to optimize the mass ratio of initial to final ascent vehicle weight to the minimum required to get the vehicle from the Martian surface to a desired parking orbit. The first step in analysis was to model the ascent. The ascent model chosen is depicted in Figure 2.5.1. The ascent is divided into four flight segments. The first is a powered gravity turn to a low elliptical transfer orbit. The second segment is an unpowered elliptical coast trajectory to an intermediate circular orbit. The third is a circular orbit with radius equal to the radius of perigee of the parking orbit, and the fourth is the parking orbit. In modelling each flight segment, worst case assumptions were made to add a safety factor to the calculations. A description of the modelling of each segment follows.

A diagram of the first segment is found in Figure 2.5.2. In modeling this segment, several worst case assumptions were made. First, a "flat", non-rotating Mars model was chosen. Although this is not a true representation of ascent, it offers advantages over a rotating, spherical Mars model in addition to its simplification of the analysis. The advantage

selecton of our thermal protection system should provide for protecting the ship. There was little work done on radiation shielding and a study of this is recommended. There does not seem to be a need for a more in depth study of heating due to the design of this course.

REFERENCES

2.4.1 Carter, Preston, Mars Cargo Descent Vehicle Sizing Analysis, Universities Space Research Association, NASA Johnson Space Center, August 7, 1985.

2.4.2 GOTC Corporation, Preliminary Design Review 2, Fall, 1985.

2.4.3 Wolverton, Raymond W., Flight Performance Handbook for Orbital Operations, John Wiley and Sons, Inc., New York, 1963.

2.4.4 Fowler, Wallace T., and Garcia, Frank T. Jr., Thermal Protection Optimization for the Space Shuttle, University of Texas.

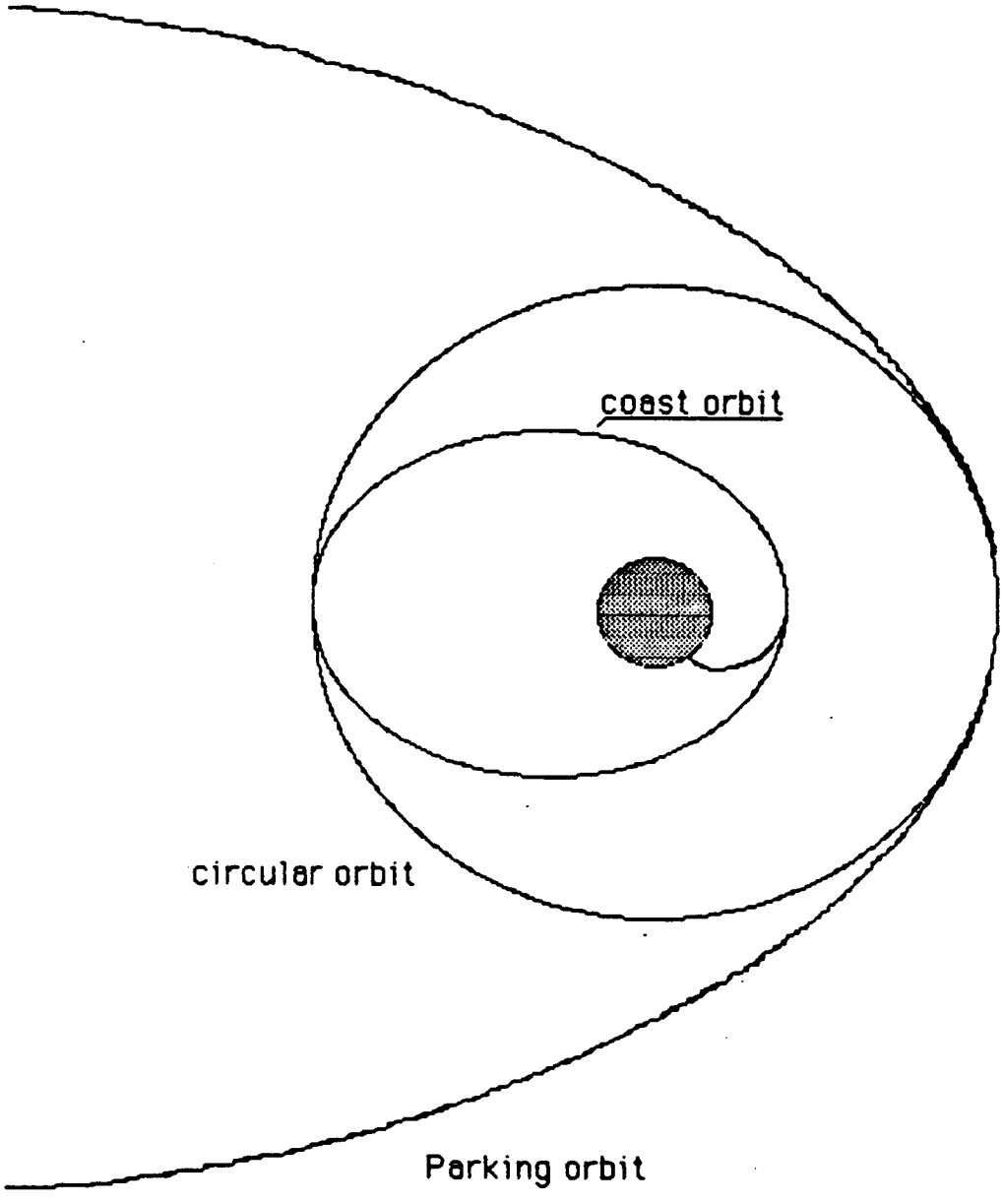

Figure 2.5.1 Ascent Trajectory Profile

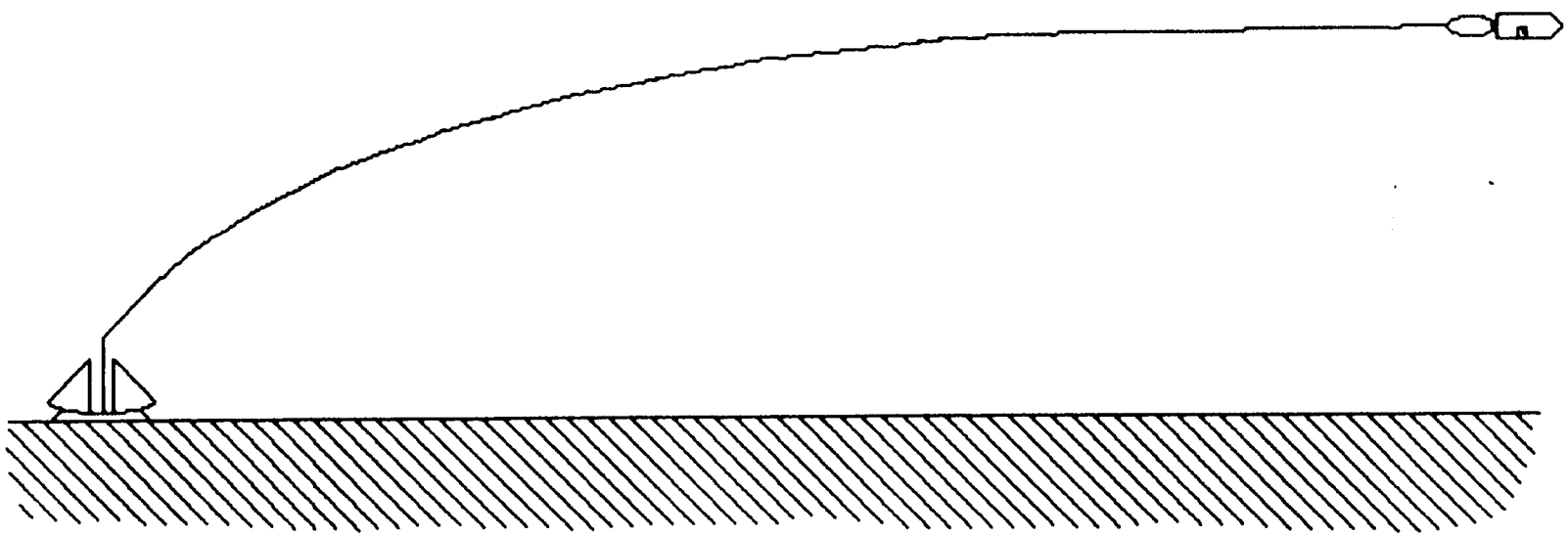

Figure 2.5.2 Gravity Turn Trajectory

is that in a rotating planet model, the ascent vehicle, if launched eastward, gains a velocity component from the planet's rotation, while in the flat model, this component is not added. This is desirable in that it builds an additional velocity capability into the vehicle over that actually required. A second simplification was that the atmospheric drag in the Martian atmosphere was negligible. A justification for this assumption is that the atmosphere of Mars has a very low density and pressure. Drag depends on both of these factors. In addition, the vehicle will be traveling at a lower velocity in the denser lower atmosphere as it ascends, also resulting in lower drag. Therefore the drag term will be much lower than the other forces acting on the vehicle. The equations governing this segment of flight are found in References 2.5.1 and 2.5.2.

During the first portion of this project period, a FORTRAN code utilizing a Runge-Kutta fourth order integrator was written to integrate the equations of motion governing the gravity turn. To make this first analysis independent of mass, dimensionless masses were used. This involved using a mass of one mass unit at the end of the gravity turn, and determining a mass ratio for the flight. Two approaches were used in this first analysis. First, a single time of flight was considered, and integrations were conducted for mass ratios from two to ten in increments of 0.1 mass units. In the second approach, a single mass ratio was selected and integrated for a number of times of flight. The problem a two point boundary value problem with the final conditions being the velocity and altitude for orbit insertion with a flight path angle of zero and the initial conditions being some low altitude with a small velocity and a flight path angle of between 80 and 90 degrees. Good results were difficult to obtain, due to problems in

matching the boundary conditions initially. However, mass ratios on the order of three to four were encountered. A printout of the two programs used and output is found in Appendix E.

Due to the difficulty in matching boundary conditions, a different method was selected to analyze the ascent. This involved using the ideal delta-v equations and gravity losses as described in Reference 2.5.2. The governing equations are as follows:

$$\text{Delta-v} = I_{SP} \ln(M_0/M_f)$$

$$\text{TW ratio} = \text{Thrust}/ W_0$$

$$\dot{m} = \text{Thrust}/ I_{SP}$$

These equations were incorporated into the overall ascent/propulsion sizing model developed, which is described later in section 2.5.3, along with other equations defining the time of flight. It should be pointed out here, that from this program, a mass ratio of 3.7 was obtained for this portion of the flight, which is the same range found in the FORTRAN analysis.

In segments two, three, and four, analysis was simple in that it involved only conic section orbits and their governing equations (Reference 2.5.3). For first analysis, a TK! Solver model was created to determine the effect of changing the periapsis of the coast orbit on the delta-v required for parking orbit insertion and the mass ratio. The model varied the altitude of perigee and determined the delta-v required to place the vehicle in the 500 km circular orbit using the ideal delta-v formula. A print out of the model is found in Appendix E. A print out of the results is found in Table 2.5.1. As can be seen, the range in values of delta-v is large and decreases with increasing coast orbit perigee. However, the magnitudes of the mass

Table 2.5.1. ASCENT COAST SEGMENT FROM Hp TO 500 Km PARKING ORBIT

Hp (Km)	Rp (Km)	a (Km)	Vp (Km/sec)	Va (Km/sec)	DELTAVa (Km/sec)	M. Ratio
20	3407.5	3647.5	3.653232934	3.202158514	.1108499445	1.031807
40	3427.5	3657.5	3.637575763	3.207148792	.1058596663	1.030354
60	3447.5	3667.5	3.622060899	3.212104167	.1009042911	1.028913
80	3467.5	3677.5	3.606686308	3.217025022	.09598343646	1.027483
100	3487.5	3687.5	3.591449996	3.221911732	.09109672584	1.026066
120	3507.5	3697.5	3.576350008	3.22676467	.08624378837	1.024660
140	3527.5	3707.5	3.56138443	3.231584199	.08142425882	1.023266
160	3547.5	3717.5	3.54655138	3.236370681	.07663777744	1.021884
180	3567.5	3727.5	3.531849018	3.241124468	.07188398993	1.020513
200	3587.5	3737.5	3.517275534	3.245845911	.06716254724	1.019153
220	3607.5	3747.5	3.502829157	3.250535353	.06247310551	1.017803
240	3627.5	3757.5	3.488508147	3.255193132	.05781532599	1.016465
260	3647.5	3767.5	3.474310797	3.259819583	.05318887492	1.015138
280	3667.5	3777.5	3.460235432	3.264415035	.04859342342	1.013821
300	3687.5	3787.5	3.446280411	3.268979811	.04402864743	1.012514
320	3707.5	3797.5	3.432444119	3.273514231	.03949422755	1.011218
340	3727.5	3807.5	3.418724975	3.278018609	.03498984908	1.009933
360	3747.5	3817.5	3.405121424	3.282493257	.03051520179	1.008657
380	3767.5	3827.5	3.39163194	3.286938478	.02606997992	1.007391
400	3787.5	3837.5	3.378255027	3.291354576	.02165388207	1.006135
420	3807.5	3847.5	3.364989214	3.295741847	.01726661117	1.004889
440	3827.5	3857.5	3.351833056	3.300100584	.01290787425	1.003653
460	3847.5	3867.5	3.338785135	3.304431076	.00857738258	1.002426
480	3867.5	3877.5	3.325844059	3.308733607	.00427485141	1.001208
500	3887.5	3887.5	3.313008458	3.313008458	0	1

ratio are on the same order of magnitude, with small changes. It was decided from this fact, and an assumption that most atmospheric effects could be ignored past an altitude of 150 kilometers, that the choice for perigee of the coast orbit should be 150 kilometers.

2.5.2 PROPULSION SYSTEM ANALYSIS

2.5.2.1 PROPELLANT SELECTION

The first step in the propulsion system analysis was choosing a fuel oxidizer combination for the ascent/descent vehicle. The following criteria were set in determining the fuel chosen:

1) Crew safety
2) Ease of storage
3) Specific impulse
4) Insitu Propellant Production Possibilities
5) Engine components

The fuels considered were found in a Pratt and Whitney Vestpocket Handbook, and the a can be found in Tables 2.5.2 and 2.5.3. Based on these criteria, the choices were narrowed to the following two combinations, hydrogen/liquid oxygen and methane/liquid oxygen. In comparing these two choices, methane was chosen as the fuel for the following reasons based on information found in Reference 2.5.4.

1) Methane has a greater density than hydrogen, allowing for smaller, lighter storage tanks, and thus a lighter vehicle structurally with more space for other cargo is possible.
2) Less pump horsepower is required for a given thrust. Also,

Table 2.5.2

Liquid Rocket Oxidizer Properties

Oxidizer	Chemical Formula	B.P. °F	F.P. °F	δ @ 77°F Sp. Grav	Sp. Heat BTU/lb °F @ 77°F	Crit. Temp. °F	Crit. Press. psia	Vapor Press. @ 77°F, psia	Vapor Press. @ 160°F, psia	Viscosity Centi-poise @ 77°F	Cost $/lb	Toxicity
Oxygen	O_2	−297.4	−361.1	1.143(3)	0.406(3)	−182	731	(1)	(1)	0.190(3)	0.03	Nontoxic
Fluorine	F_2	−306.6	−363.3	1.510(3)	0.367(3)	−200	808	(1)	(1)	0.24(3)	3.50	High
Ozone	O_3	−169.6	−315.0	1.46(3)	0.354(3)	10.2	802	(2)	(2)	1.55(3)		High
Oxygen Difluoride	OF_2	−228.6	−371	1.521(3)		−72	719	(2)	(2)	0.283(3)	5.50	High
100% Hydrogen Peroxide	H_2O_2	302.4	31.2	1.443	0.63	835	3145	0.038	0.58	1.156	1.00	Low
90% Hydrogen Peroxide	90% H_2O_2 10% H_2O	285.5	11.3	1.387	0.66			0.852	0.76	1.156	0.50	Low
Nitrogen Tetroxide	N_2O_4	70.1	11.8	1.433	0.374	316.4	1470	17.2	111	0.393	0.075	High
Inhibited Red Fuming Nitric Acid	83% HNO_3 2% H_2O 15% N_2O_4	150	−63.4	1.555	0.419	520		2.57	19	1.29	0.055	Medium
Chlorine Trifluoride	ClF_3	53.2	−105.4	1.809	0.309	308	837.7	24.9	118	0.41	2.40	High
Perchloryl Fluoride	ClO_3F	−52.2	−230.8	1.412	0.263	203.3	778.9	172	501	0.384(3)	0.50	Medium
Bromine Pentafluoride	BrF_5	105.4	−76.9	2.46		387		8.38	43.0		4.50	High
Tetranitro-methane	$C(NO_2)_4$	258.8	56.8	1.63	0.297			0.213	2.28	1.76		Medium

Liquid Rocket Fuel Properties

Fuel	Chemical Formula	B.P. °F	F.P. °F	δ @ 77°F Sp. Grav	Sp. Heat BTU/lb °F @ 77°F	Crit. Temp. °F	Crit. Press. psia	Vapor Press. @ 77°F, psia	Vapor Press. @ 160°F, psia	Viscosity Centi-poise @ 77°F	Cost $/lb	Toxicity
Hydrogen	H_2	−423	−434.4	0.071(3)	2.22(3)	−399.8	188.1	(1)	(1)	0.0139(3)	0.50	Nontoxic
Diborane	B_2H_6	−134.5	−265.9	0.437(3)	0.669(3)	62.1	581	(1)	(1)	0.133(3)	40.00	High
Pentaborane	B_5H_9	140	−52	0.618	0.573	456	557	4.0	21	0.3	10.00	High
Methane	CH_4	−258.7	−296.5	0.424(3)	0.822(3)	−117	673	(1)	(1)	0.115(3)	0.20	Low
Ethane	C_2H_6	−127.5	−277.6	0.546(3)	0.581(3)	89.8	708	600	(1)	0.162(3)	0.006	Low
Propane	C_3H_8	−43.7	−305.8	0.585(3)	0.534(3)	206	617	130	368	0.205(3)	0.006	Low
Ethylene	C_2H_4	−154.7	−272.5	0.566(3)		49.3	742	(1)	(1)	0.26(3)	0.05	Low
Acetylene	C_2H_2	−119.2	−115.2	0.612(3)	0.35(3)	96.8	911		(1)			Medium
RP-1	$(CH_{1.95})_n$	10% Evap @ 390°F	−76.0	0.81	0.48	758	315		0.7	2.0	0.02	Low
Hydrazine	N_2H_4	236.3	34.7	1.004	0.737	716	2135	0.28	2.85	0.90	1.60	Medium
Monomethyl-hydrazine	CN_2H_6	189.5	−62.3	0.874	0.70	609	1195	1.0	9.0	0.781	2.05	Medium
Unsymmetrical Dimethylhydrazine (UDMH)	$C_2N_2H_8$	146	−71.0	0.786	0.653	482	786	3.03	18.5	0.509	0.85	Medium
50% Hydrazine & 50% UDMH	50% N_2H_4 50% $C_2N_2H_8$	158	18.8	0.898	0.694	634	1696	2.75	15.1	0.817	1.225	Medium
Anhydrous Ammonia	NH_3	−28.0	−107.9	0.604	1.09	270	1639	130	516	0.135	0.045	Medium
Triethyl-aluminum	$(C_2H_5)_3Al$	367.9	−50	0.832	0.52	603	550	Nil	0.15	2.58		

(1) Above critical point.
(2) Value taken at the normal B.P. rather than 77°F.
(3) Value taken at −297.5°F.

Table 2.5.3

Theoretical Rocket Engine Propellant Summary [1]

Oxidizer	Fuel	$P_c = 1000$ psia, Optimum Sea Level Expansion Shifting Equilibrium					$P_c = 100$ psia, $\epsilon_c = 40$, Shifting Equilibrium				
		r	δ_p	T_c (°R)	c^* (ft/sec)	I_s (sec)	r	δ_p	T_c (°R)	c^* (ft/sec)	I_{sea} (sec)
O_2	H_2	4.0	0.284	5330	7950	388	4.5	0.325	5610	7840	454
	CH_4	3.15	0.811	6350	6120	310	3.25	0.817	5840	5960	365
	C_2H_6	2.95	0.896	6480	6050	307	2.95	0.896	5930	5880	362
	C_3H_8	2.75	0.911	6500	6020	305	2.82	0.912	5960	5860	359
	C_2H_2	1.6	0.857	7460	6590	330	1.65	0.867	6690	6390	384
	C_2H_4	2.45	0.885	6850	6100	312	2.5	0.887	6170	5945	365
	RP-1	2.55	1.00	6590	5900	299	2.6	1.01	6030	5730	351
	N_2H_4	0.90	1.065	6120	6220	313	0.95	1.066	5680	6060	367
	UDMH	1.67	0.975	6490	6120	310	1.67	0.975	5940	5960	364
	NH_3	1.41	0.833	5580	5880	295	1.41	0.833	5260	5790	347
F_2	H_2	8.0	0.468	7120	8370	410	10.2	0.538	6820	8050	475
	B_2H_6	5.45	1.09	8980	7370	371	5.5	1.12	7920	7110	431
	B_5H_9	4.6	1.20	9120	7130	360	4.6	1.2	8000	6860	417
	CH_4	4.35	1.021	7620	6770	345	4.45	1.027	7050	6680	408
	N_2H_4	2.25	1.31	8420	7290	364	2.25	1.33	7580	7070	422
	CN_2H_6	2.38	1.24	8200	6840	347	2.43	1.246	7400	6650	408
	UDMH	2.45	1.192	7770	6610	339	2.45	1.192	7030	6440	408
	N_2H_4–UDMH [2]	2.50	1.26	8150	6940	349	2.50	1.264	7330	6740	409
	NH_3	3.3	1.18	8240	7210	360	3.3	1.18	7450	7000	417
O_3	H_2	3.8	0.284	5830	8580	423	4.1	0.298	5650	8390	493
OF_2	H_2	5.75	0.374	6300	8390	411	6.0	0.384	6000	8180	474
	CH_4	5.0	1.06	7960	7080	356	5.1	1.07	7200	6880	414
	C_2H_6	4.4	1.15	8180	7100	355	4.6	1.15	7380	6870	413
	C_2H_4	4.35	1.17	8250	7050	354	4.4	1.18	7450	6860	412
OF_2	B_2H_6	3.67	0.993	8350	7350	372	3.67	0.993	7410	7130	434
	N_2H_4	1.62	1.272	7340	6850	345	1.62	1.272	6610	6650	403
	CN_2H_6	2.4	1.25	7850	6950	350	2.4	1.25	7050	6730	407
	N_2H_4–UDMH [2]	2.1	1.24	7700	6940	350	2.18	1.24	6970	6730	407
H_2O_2 (100%)	B_2H_6	1.84	0.795	4880	6460	333	1.86	0.807	4610	6260	391
	N_2H_4	2.27	1.27	5270	5770	288	2.32	1.276	5010	5700	338
N_2O_4	N_2H_4	1.33	1.21	5870	5860	292	1.36	1.23	5500	5740	342
	CN_2H_6	2.17	1.20	6110	5730	288	2.26	1.21	5660	5570	338
	UDMH	2.6	1.166	6190	5680	287	2.7	1.17	5720	5520	336
	N_2H_4–UDMH [2]	2.0	1.20	6050	5560	287	2.0	1.2	5620	5570	339
HNO_3 15% N_2O_4	RP-1	5.0	1.329	5670	5180	263	5.1	1.33	5300	5070	309
	UDMH	3.1	1.255	5680	5410	272	3.2	1.26	5320	5290	330
CLF_3	N_2H_4	2.80	1.495	7010	5970	293	2.85	1.498	6460	5840	339
	UDMH	3.0	1.365	6430	5550	278	3.05	1.369	6060	5460	325
CLO_3F	N_2H_4	1.45	1.2115	6220	5910	295	1.5	1.215	5760	5770	345

(1) Specific impulse is at mixture ratio for maximum I_s. (2) Equal parts by weight of Hydrazine and UDMH. Ammonia, chlorine trifluoride, and perchloryl fluoride are taken to be liquids at 77°F. All other propellants are taken to be liquids at 77°F or at the normal B.P. whichever is lower.

there is a smaller pressure loss incured due to the fact that the denser fuel increases the thrust per unit throat area.

3) Methane can be produced easily on the Martian surface from Carbon Dioxide in the Martian atmosphere.

In determining engine performance parameters, a combusion chamber pressure of 3000 psia was decided on based on the fact that the current state of the art in propulsion systems, the Space Shuttle Main Engines, uses this combustion chamber pressure. From data on next generation advanced engines to be used in the Orbital Transfer Vehicle (Reference 2.5.4), the chamber pressures that have been proposed have been on the order of 1,500 to 2,000 psia (Table 2.5.4).

Advanced OTV propulsion system concepts

Parameter	Aerojet	Rocketdyne	Pratt & Whitney
Thrust, lbf	3,000	15,000	15,000
Cycle	Expander H_2-O_2	Expander H_2	Expander H_2
Chamber pressure, psia	2,000	2,000	1,500
Nozzle area ratio	1,200:1	1,300:1	6,40:1
Specific impulse, lbf-sec/lbm	482	492	486
Turbomachinery speeds, rpm			
H_2	200,000	178,000	150,000
O_2	75,000	56,200	67,390
Control	Closed loop	Closed loop	Closed loop
Throttlability	30:1	30:1	30:1
Range	2 steps	3 steps	3 steps
Mode	(15:1 continuous)	Discrete	Discrete
Key technologies	Gaseous oxygen drive turbine Annular thrust chamber Multiple engine control	Hydrogen pump critical speed Multivariable closed loop controls High area ratio nozzle	High speed hydrogen cooled gears Advanced thrust chamber material High area ratio nozzle

The performance of the engine is given by the specific impulse of the engine obtained from the following equation from Reference 2.5.5:

$$I_{sp} = \frac{1}{g}\sqrt{\frac{2\gamma g}{\gamma-1}\frac{R_u T}{m}\left[1-\left(\frac{P_2}{P_1}\right)^{\frac{\gamma-1}{\gamma}}\right]}$$

2.5.2.2 ENGINE SIZING

The first step in engine sizing was to determine the combustion chamber size. Based on in Reference 2.5.7, the following equations were

used to size the combustion chamber:

$V_c = L^* A_t$

$L_c = V_c / A_c$

where

V_c = the combustion chamber volume

L_c = Combustion chamber length

A_t = Throat area

L^* = the chamber characteristic length

A_c = chamber area

From present engines, the value for L^* is about 43 inches or 1.0922 meters. For A_c, a typical value of the contraction ratio, A_c/A_t is 1.75.

To size the engine nozzle and obtain a near-optimum bell shaped contour, it was decided to use the parabolic approximation suggested by G.V.R. Rao in Reference 2.5.8 and depicted in Figure 2.5.3. As seen in the figure, in the converging section of the nozzle, upstream of the throat, is an arc of a circle with radius of curvature 1.5 R_t. Imediately past the throat, another circular arc is used, with a radius of 0.382 R_t. Just past this, the parabolic section begins. The required data for this sizing is as follows:

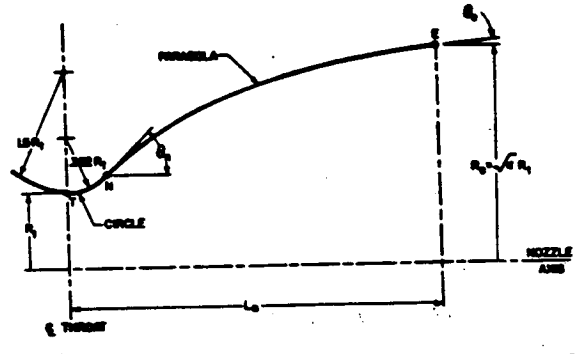

Fig.2.5.3–***Parabolic approximation of bell nozzle contour.***

1) Nozzle throat radius

2) Axial length of the nozzle from throat to exit plane

3) The expansion ratio of the nozzle

4) The initial wall angle of the parabola

To obtain the nozzle throat radius and expansion ratio of the nozzle, the assumption was made that there was an isentropic expansion through the engine nozzle. From this assumption, the following equations govern the flow (Reference 2.5.6):

$$M_e = \sqrt{\frac{2}{\gamma-1}\left[\left(\frac{P_c}{P_e}\right)^{\gamma-1/\gamma} - 1\right]}$$

$$A_e/A_t = \sqrt{\frac{1}{M_e^2}\left[\frac{2}{\gamma+1}\left(1 + \frac{\gamma-1}{2} M_e^2\right)\right]^{\gamma+1/\gamma-1}}$$

$$\dot{M} = \frac{A_t P_c}{\sqrt{T_c}} \sqrt{\frac{\gamma}{R}\left(\frac{2}{\gamma+1}\right)^{\gamma+1/\gamma-1}}$$

where

M_e = exit mach number

P_c = Combustion chamber pressure

P_e = exit pressure

γ = Specific heat ratio

$\dot{M}$ = Mass flow rate of propellant

A_e = Nozzle exit area

A_t = Throat area of nozzle

From these equations, the throat area, exit area, and exit Mach number are calculated from the known propellant flow rate, chamber and exit pressures, and exhaust gas specific heat.

Next, to obtain the axial length of the nozzle, a 15 degree half angle conical nozzle was used as a reference. By taking what is known as a

fractional nozzle length, the bell nozzle length can be calculated. For the 15 degree nozzle:

$$L_n = \frac{R_t\left(\sqrt{A_e/A_t} - 1\right) + R\left(\sec\alpha - 1\right)}{\tan\alpha}$$

where

L_n = the nozzle length

R_t = the throat radius

A_e/A_t = the expansion ratio

R = the radius of curvature of the converging section of the nozzle

α = half angle of the conical nozzle

From G.V.R. Rao's approximation, the value for R is approximated as 1.5 R_t, as mentioned above.

To obtain the initial wall angle of the parabolic section, Reference 2.5.6 has a chart of curves for various nozzle expansion ratios and fractional lengths. This figure is shown in Figure 2.5.4. However, for the needed expansion ratios for a Mars ascent, no data was shown, and no equation was given defining the curves, so research was conducted to find some means to determine the initial parabolic angle of the section, which is also the maximum wall angle. Reference 2.5.6 contained a section on the method of

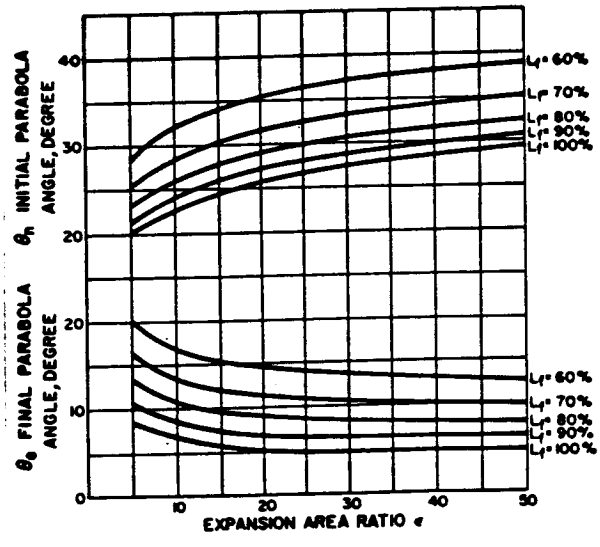

Fig.2.5.4.–θ_n and θ_e as function of expansion area ratio ϵ.

characteristics. As a result, a value was given for the maximum angle of a minimum length nozzle. This value was given to be one half of the Prandtl-Meyer function, which is given by the equation:

$$\nu(M) = \sqrt{\frac{\gamma+1}{\gamma-1}}\ \tan^{-1}\sqrt{\frac{\gamma-1}{\gamma+1}(M^2-1)} - \tan^{-1}\sqrt{M^2-1}$$

By comparing several values of one half of the Prandtl-Meyer function and the corresponding expansion ratios with Figure 2.5.4, the fractional length which most closely corresponded to these points was a L_f of 60%, giving a nozzle length of .6 L_n.

With an equation for the initial parabola angle and the throat radius, point N on Figure 2.5.3 could be located. With respect to the throat and nozzle axis, the location is:

N_t = distance out from axis = 0.382 R_t sin θ_n

N_a = axial distance from throat = R_t + 0.382 R_t (1 - cos θ_n)

Next, with this point known, the initial angle known, and the point at the exit plane known, the equation for the parabola can be determined. Assuming the parabolic equation to be of the form:

$x = a(r + b)^2 + c$

$dx/dr = 2\ a\ (r + b) = \tan \theta_n$

where

x = length along the axis of the nozzle

r = radius outward of nozzle

a, b, and c are constants to be determined from the three boundary conditions

Boundary conditions

at $r = N_t$, $x = N_a$ therefore $N_t = a(N_a + b)^2 + c$

at $r = r_e$, $x = .6\ L_n$, therefore $r_e = a(L_n + b)^2 + c$

at $r = N_t$, $\theta_n = \gamma_e/2$

These equations can be solved for a, b, and c, and then the exit angle of the nozzle calculated as:

$\theta_e = \text{atan}(2\ a\ (r + b))$

As with the equations for ascent, these equations were added to the ascent/propulsion model.

2.5.3 ASCENT/PROPULSION SIZING PROGRAM

Based on the equations for ascent and propulsion mentioned throughout this section, an overall sizing model was created with TK! Solver. A printout of the final model used is found in Appendix D. From this model, the mass, weight, maximum g-loading at burn out, ascent propellant volume, and nozzle sizing are determined. To obtain output, a final mass after parking orbit insertion was determined from data in Reference 2.5.7. The value was 6162 Kilograms. Based on this value and the other inputs, the ascent vehicle was sized. The results of this sizing are found in Table 2.5.5. At this point, it should be pointed out the difficulties in obtaining a good mass for the vehicle. One constraint the that affected the results was that the maximum g-loading must not exceed 6. It was found that by increasing the thrust to weight ratio, the g-loading went up, but the initial mass went down. The exit pressure had a similar affect on the model, in that as the

Table 2.5.5

St	Input	Name	Output	Unit	Comment
		a	2.7408347		
		b	.02548669		
		c	-.0138930		
		ACO	3712.5	Km	Semi-major axis of coast orbit
		Ae	3.0156941	m^2	Exit area of nozzle
	15	alpha		degrees	Conical nozzle half angle
	6624.2	APO		Km	Semi-major axis of parking orbit
		Aratio	146.33894		Exit to throat area ratio
		At	.02060760	m^2	Throat area
		DensF	424	Kg/m^3	Density of the fuel
	1000	DensH2O		Kg/m^3	Density of Water
		DensO	1143	Kg/m^3	Density of the oxidizer
		DVCIRC	.07902663	Km/sec	Delta v from to circular orbit
		DVCOI	3.7075595	Km/sec	Delta v of coast orbit insertion
		DVGRAV	.53138105	km/sec	delta v loss due to gravity
		DVPOI	.62534227	Km/sec	Delta-v of parking orbit insertion
		DVT	4.9433094	Km/sec	Total delta v
		g	3.7183807	m/sec^2	Mars surface gravity
	6.673E-11	G		m^3/kg se	Universal gravitational constant
	1.16	gamma			Ratio of specific heats
		Gmax	5.9344689		Max g'loading
	500	HCOA		Km	Alt. of coast orbit at apogee
	150	HCOP		Km	Alt. of coast orbit at perigee
		HICIRC	500	Km	Alt. of intermediate circular orbit
		HPOA	5973.4	Km	Alt. of parking orbit at apogee
		HPOP	500	Km	Alt. of parking orbit at perigee
		ISP	3461.8049	m/sec	Specific impulse of vehicle
	.6	Lf			Fractional length of nozzle based on 15 degree half angle conical nozzle
		Ln	2.7557654	m	Nozzle length, based on % of 15 degree half angle conical nozzle
	6.3943E23	MASSmar		kg	Mass of Mars
L		Mdot	242.08095	Kg/sec	Propellant mass flow rate
L		MdotO	183.74819	Kg/sec	Oxidizer mass flow rate
L		MdotF	58.332760	Kg/sec	Fuel mass flow rate
L		MDRY	11748.909	kg	Final dry vehicle mass
		Me	4.8128519		Nozzle exit mach number
L		MF	8974.9549	Kg	Mass of Fuel
L		MO	48994.973	kg	Initial wet vehicle mass
L		MOx	28271.108	Kg	Mass of Oxidizer
		MRCIRC	1.0230907		Mass ratio for Circularization delta-v
L	6162	MPAY		kg	Mass of payload
		MRCOI	2.9182681		Mass ratio of coast orbit insertion
		MRGRAV	1.1659058		Mass ratio due to gravity delta-v loss
		MRPOI	1.1979845		Mass ratio for parking orbit insertion
L		MPROP	37246.063	kg	Mass of propellant at lift off
		MRTOTAL	4.1701719		Total mass ratio

St	Input	Name	Output	Unit	Comment
	4.2669E13	MUmars		m^3/sec	Mars Gravitational parameter
		Na	.02582332		distance along centerline to end of expansion section
		Nt	.09489014	m	Radius from centerline to end of expansion section
		nu	113.16107	degrees	Prandtl-Meyer function
		OFRV	1.1685039		Oxidizer to fuel volume ratio
	3.15	OFRW			Oxidizer fuel ratio by weight
	3000	Pc		psia	Chamber pressure
	1.5	Pe		psia	Nozzle exit pressure
		phi1	33.419463	degrees	
		phi2	79.714219	degrees	
	311.88644	R		m^2/Ks^2	Ideal gas constant
		RCOA	3887.5	Km	radius of coast orbit at apogee
		RCOP	3537.5	Km	Radius of coast orbit at perigee
		Re	.97975775	m	Nozzle exit radius
		RICIRC	3887.5	Km	Radius of intermediate circular orbit
	3387.5	Rmars		Km	Radius of Mars
		RPOA	9360.9	Km	Radius of parking orbit at apogee
		RPOP	3887.5	Km	Radius of parking orbit at perigee
		Rt	.08099137	m	Throat radius
		R1	.12148706	m	Radius of curvature of convergent inle
		R2	.03093870	m	Radius of curvature of divergent sect.
		SOS	719.28347	m/s	Speed of sound at nozzle exit
	.424	SpGrF			Specific gravity of the fuel
	1.143	SpGrO			Specific gravity of the oxidizer
	.15	STFACT			Structural factor
		TB	142.90657	sec	Burn time from surface to coast orbit
	4080	Tc		K	Chamber temperature
		Te	1430.0318	K	Temperature at nozzle exit
		theta1	56.580537	degrees	Initial angle of parabolic nozzle sect
		theta2	10.285781	degrees	
L		THRUST	838037.03	N	Thrust of vehicle
		thrust	838037.03	N	Thrust calculated from Isp
	4.6	TWRATIO			Thrust to weight ratio
		VCOA	3.2339703	Km/sec	Vel. of coast orbit at apogee
		VCOP	3.5539391	Km/sec	Vel. of coast orbit at perigee
		VPOP	3.9383392	Km/sec	Vel. of parking orbit at perigee
L		Vdot	.29833684	m^3/sec	Total volume flow rate of propellant
L		VdotF	.13757726	m^3/sec	Volume flow rate of fuel
L		VdotO	.16075958	m^3/sec	Volume flow rate of oxidizer
		VICIRC	3.3129969	Km/sec	Vel. of intermediate circular orbit
L		VolO	24.734128	m^3	Volume of Oxidizer
L		VolProp	45.901474	m^3	Volume of Propellant
L		VolF	21.167347	m^3	Volume of Fuel
		Ue	3461.8049	m/s	Nozzle exit velocity
L		WEIGHT	182181.96	N	Weight of vehicle on surface of Mars

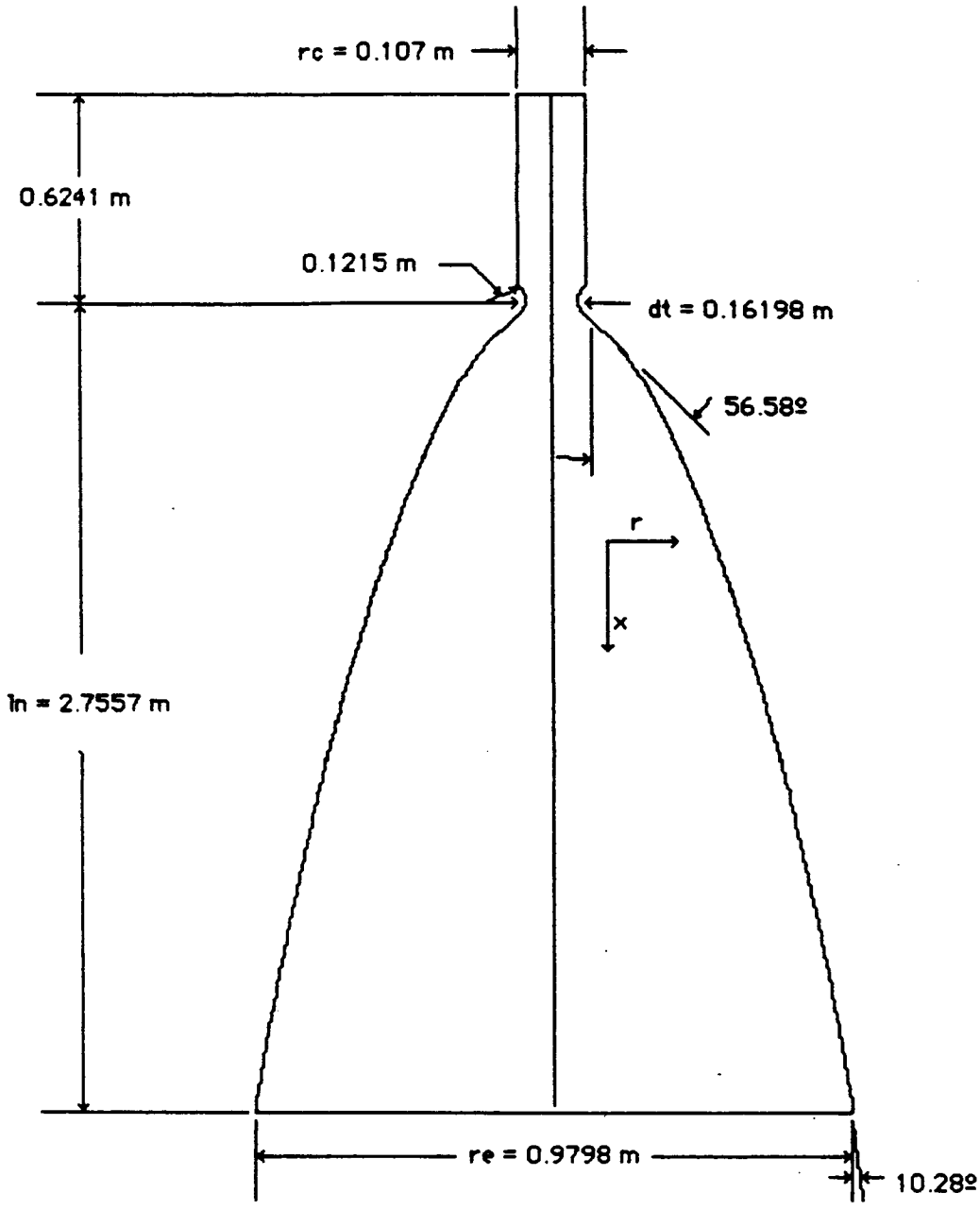

Area ratio	146.34	Chamber pressure	3000 psia
Throat area	0.0206 sq m	Chamber temperature	4080 K
Exit area	3.0157 sq m	Mass flow rate	242.08 kg/sec
Exit pressure	1.5 psia	Propellants	CH4, O2
Isp	353 seconds	O/F Ratio (weight)	3.15
Thrust	838037. N 188399. lb	O/F Ratio (volume)	1.168

equation for parabola $x = 2.74 (r + 0.02548)^2 - 0.013093$

FIGURE 2.5.5 Main Engine

exit pressure was lowered, the g-loading went up. In addition, as the exit pressure was lowered, the nozzle exit length went up as well as the exit area, producing a nozzle which was too large to be practical. As seen from the output, the vehicle mass on the ground before ascent was about 49,000 kilograms, with approximately 37,000 kilograms of propellant.

From the output, a diagram of the engine was made. This is depicted in Figure 2.5.5.

REFERENCES SECTION 2.5

2.5.1 Ashley, Holt, Engineering Analysis of Flight Vehicles, Addison-Wesley Publishing Company, Reading, Massachusetts, 1974, pages 265-299.

2.5.2 Stagnaro, Michael J., *An Approach to Preliminary Launch Vehicle Sizing*, NASA-Johnson Space Center, Advanced Programs Office, December, 1985.

2.5.3 Bate, Roger R., Mueller, Donald D., and White, Jerry E., Fundamentals of Astrodynamics, Dover Publications, Inc., New York, 1971.

2.5.4 Gorland, Sol, "Integration Becomes the Name of the OTV Game", *Aerospace America*, Vol. 22, No. 8, August, 1984, pages 70-73.

2.5.5 Sutton, George P., Rocket Propulsion Elements, John Wiley and Sons, Inc., New York, 1963.

2.5.6 Anderson, John D., Modern Compressible Flow with Historical Perspective, McGraw-Hill Book Company, New York, 1982.

2.5.7 GOTC Corporation, Preliminary Design Review 2, The University of Texas, Fall, 1985.

2.5.8 Huzel, Dieter K., and Huang, David H., Design of Liquid Propellant Rocket Engines, National Aeronautics and Space Administration, Washington, D.C., 1971.

2.6 IN-SITU PRODUCTION

A voyage to Mars can not be accomplished without the use of immense stores of energy and material. For a manned crew to make this trip, the necessity for safety and reliability, as well as redundancy in life support systems, is obvious. Given these necessities, a mission scenario to Mars becomes a massive endeavor.

One way to reduce the immense payload is to make use of the indigenous materials of the planet. Such items as oxygen, water, and fuels can be produced from known Martian resources. This process, known as 'in-situ' production, is the only logical way of conducting a cost-effective trip to Mars.

2.6.1 WATER PRODUCTION

2.6.1.1 WATER AVAILABILITY

Water is the most important resource for a manned mission to Mars. Water in the form of solids, liquids, or solid hydrates potentially can be found in quantity on Mars and its moons.

Mars' distance from the Sun and its thin carbon dioxide atmosphere create a frigid environment ranging from 15° Celsius at midday in the middle latitudes to -125° Celsius at high latitudes in the winter. Under these conditions water is unstable anywhere on the surface, and during the winter it will rapidly freeze; at lower latitudes even water-ice is unstable and will slowly evaporate into the Martian atmosphere.

These conditions pose many questions when viewed from the standpoint of Martian topography. There is ample evidence of substantial errosion by running water - channels, flood patterns, and networks of

dried-up tributaries and riverbeds are just the beginning. So where has all the water on Mars gone?

One explanation is that the water is trapped in the polar ice caps, but since the ice caps are composed mainly of frozen carbon dioxide, this theory can not account for the large amounts of water necessary to create the features we see.

Recent interpretations of Martian geography suggest that large quantities of water may exist in natural reservoirs, frozen underground. High-resolution Viking photographs have proven very important in these recent findings. After viewing thousands of Viking photos, astrogeologist Mike Carr and geophysicist Steven Squyres of NASA's Ames Research Center have been able to identify and document a phenomenon called 'terrain softening'. In the higher latitudes of both the northern and southern hemispheres, above 30° north and below 30° south, the topography appears muted and softened; crater rims in these regions are often rounded and clusters of craters are blurred. Carr and Squyres believe that "this is a direct result of ice in the ground – that the materials creep." In the equatorial regions the warmer temperatures have caused the water to sublimate or become diffused in the soil. But, in the higher latitudes the water has become locked in permafrost layers beneath the surface. In the areas where 'terrain softening' has been discovered, the ice-laden ground is believed to extend for "hundreds of meters if not kilometers downward."

A small group of meteorites, called the Shergottite, Nakhlite, and Chassignite (SNC), believed to be impact debris that escaped from the Martian surface, offer more evidence for water on Mars. If these meteorites are of Martian origin, their chemical compositions reveal a

history of water indicative of vast flooding and deep reservoirs of subsurface ice.

With all this evidence for the existence of water, our ability to utilize indigenous Martian water no longer becomes a problem of availability, but one of procurement.

2.6.1.2 WATER EXTRACTION

The Martian atmosphere is thin, but it is often saturated with water, and there are numerous ways of extracting it from the environment.

Water can be extracted directly from the atmosphere by compressing the atmospheric gases and condensing the water out. Since the proportion of water to carbon dioxide in the Martian atmosphere is roughly .0002, a tonne of carbon dioxide will yield about 0.2 kilograms of water. Solar-powered dehumidification of the atmosphere could produce over one kilogram of water for every 100,000 cubic meters of atmosphere injested.

If ice exists on the surface, water can be obtained directly through melting. This technique will work best near the polar regions on Mars where ice is thought to exist in abundance beneath the carbon dioxide ice caps. In the higher latitudes, water is assumed to be trapped as subsurface permafrost. This permafrost could be collected using robotic scoops and heated at the excavation site to evaporate the water. The steam would then be piped back to the base camp, condensed and stored, or used in fuel production.

Hydrated minerals, believed to be common on Mars, offer other sources of water on Mars. These minerals could be heated to temperatures

exceeding 120°C to dehydrate them and extract their water. The dehydrated minerals could then be used for shielding or construction of the Martian base camp.

The moons of Mars offer further sources of water in the form of hydrated minerals. The contents of the Martian moons are believed to be carbonaceous chondrite. The most common types of carbonaceous chondrites have water in the following amounts: Type I, 20.8%; Type II, 13.35%; Type III, 1.0%. There is evidence that the moons of Mars are of the Type I variety, which offers the most water of any of the carbonaceous chondrites.

Two systems for collecting and processing water-saturated top soil have been proposed. The systems consist of robotic scooper vehicles with on-board processing facilities. The soil collection procedure would be essentially the same for both configurations. First, the upper layers of the sand-like Martian topsoil are collected by the scoop and deposited in the collection bin. Any large rocks are sorted out and the remaining soil is crushed using a cone crusher and the processed soil is heated to evaporate the water. The collected water is stored until the vehicle arrives back at camp, at which time it is processed by the in-situ production facilities.

A conventional scoop, similar to those used by bulldozers, will not work well on Mars, because the low Martian gravity and the light weight of the vehicle (a must, given weight considerations) do not produce enough frictional force to withstand the force exerted by the hydraulics of the scoop. Instead, a 'clamshell' scoop which is hinged in the middle will be used to collect the soil. This scoop will exert less force on the vehicle, making the likelihood of tipping or sinking an unbalanced vehicle much less.

The first design, Figures 2.6.1, proposes a vehicle which moves forward on tracked wheels, and collects soil using a back and forth pattern similar to that used by farmers when harvesting; it tows a water tank which is detachable, so that the vehicle can tow other payloads. Problems arise for this configuration during the scoop phase, when the vehicle is resting on the just-excavated soil. During this phase, an unbalanced vehicle can topple due to weight loading, shifting soil, or large rocks under the wheels. For this reason, the wheels are set wide to counteract this tipover tendency. The water tank can be replaced with an onboard tank, Figure 2.6.2. This gives the vehicle the versatility of towing other payloads or an extra water tank for an extended mission.

The 'crab' configuration, Figure 2.6.3 was proposed to alleviate the problems inherent in the first design. This vehicle can move sideways or diagonally on tracked wheels, following a zigzag pattern as it collect soil. The weight of the scoop on the front side is counterbalanced by the weight of the water tank on the back side of the vehicle. This configuration is also wider to counteract tipover tendencies caused by large rocks under the wheels or inbalances in the scoop load, which when coupled together caused a problem for the first design. It is unable to tow an extra water tank while performing its soil selection task, which will limit its mission duration capabilities.

2.6.2 PROPELLANT PRODUCTION

In-situ propellant production (ISPP) is of obvious importance to the Manned Mars Mission. The fuel and oxidizer produced could be used to provide propellant for the descent craft, as well as electrical, thermal, and

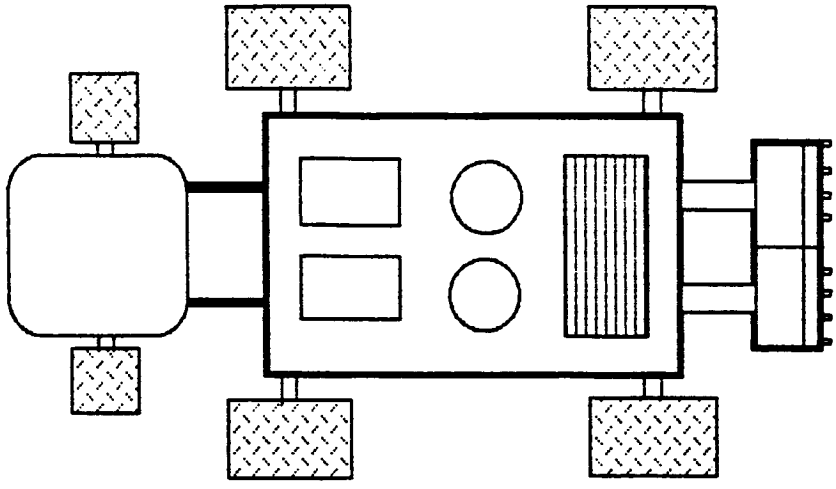

TOP VIEW

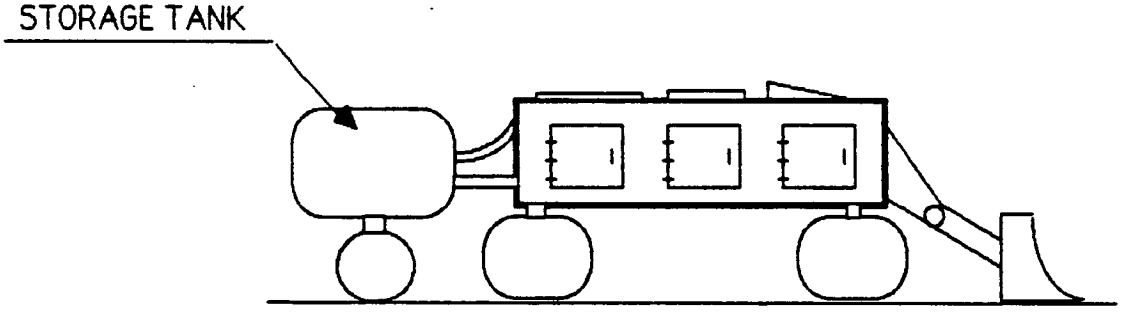

SIDE VIEW

Figure 2.6.1 Conventional Configuration

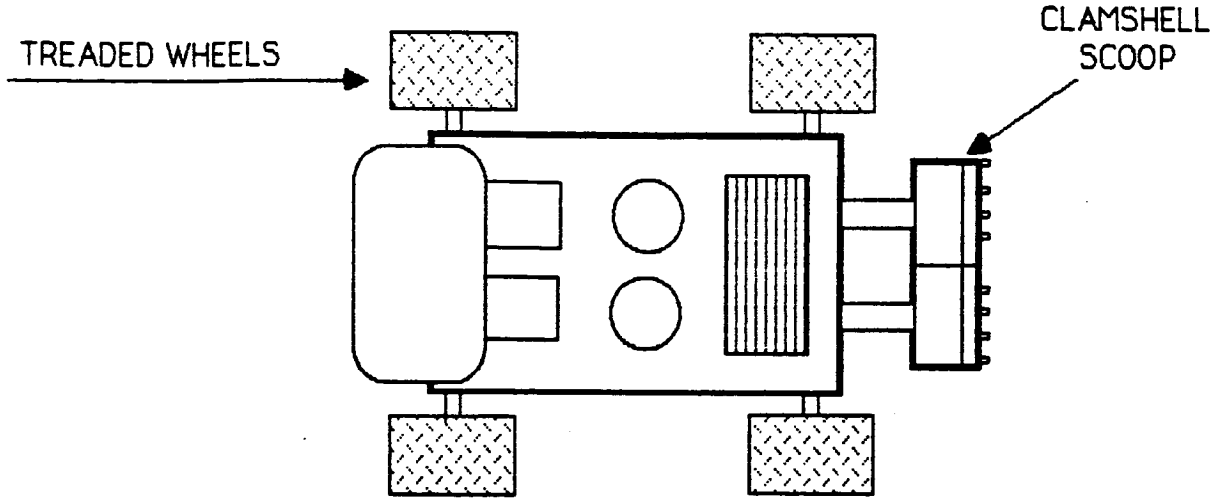

TOP VIEW

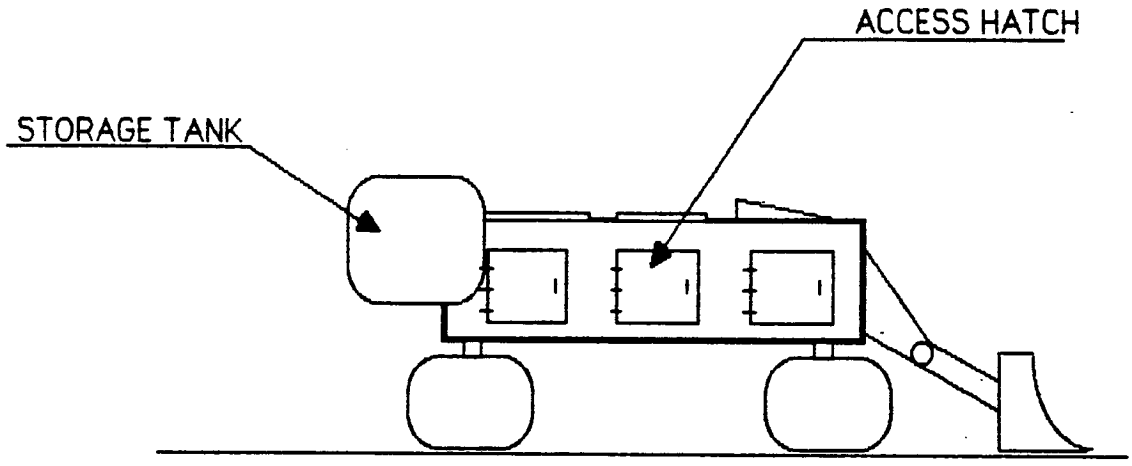

SIDE VIEW

Figure 2.6.2 Conventional Configuration With External Tank

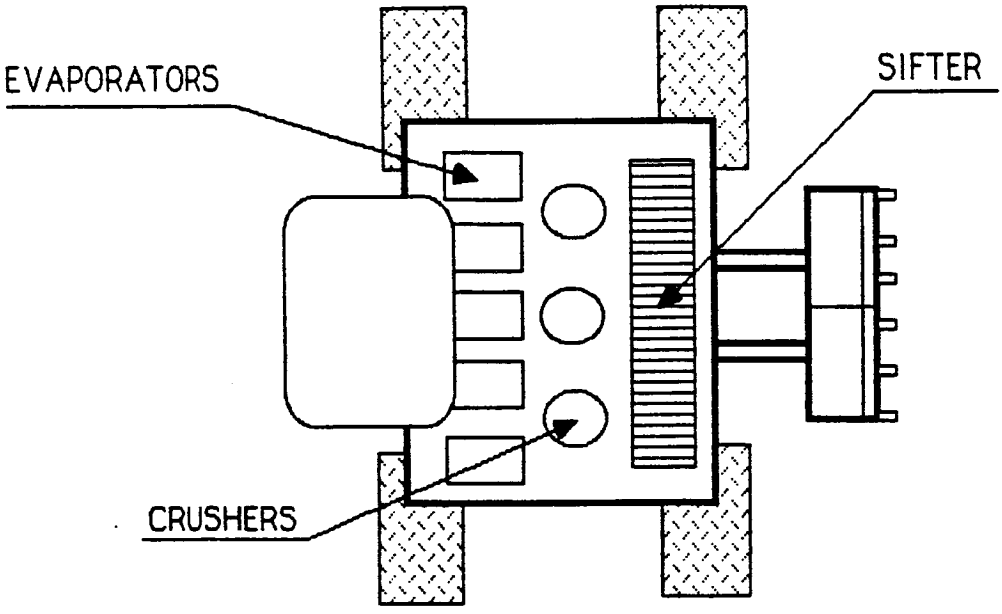

TOP VIEW

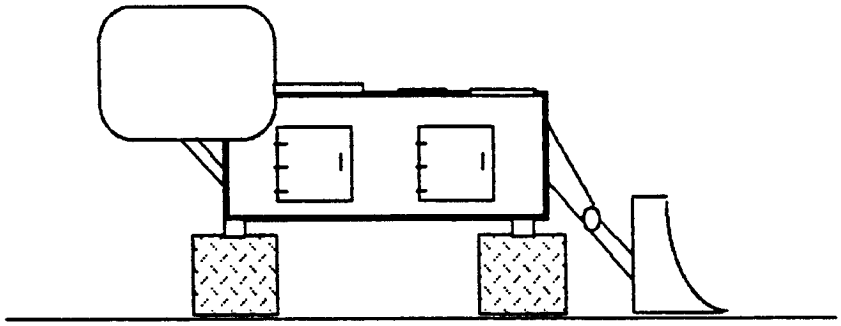

SIDE VIEW

Figure 2.6.3 Crab Configuration

chemical energies. Thermal energy rejected during the ISPP cycle could be recycled to heat a habitat or for some other worthwhile purpose. In addition to its use on the ascent/descent vehicle, the fuel and oxidizer produced by the ISPP process could also be used to power robotic surveyors, manned rovers and other surface vehicle, as well as fuel cells.

Many fuel/oxidizer combinations are possible for a Martian ascent/descent vehicle, but because the atmosphere is made up largely of carbon dioxide, nitrogen, and argon, Table 2.6.1, fuel/oxidizer combinations are limited. The most feasible fuels are hydrocarbons, while oxygen appears to be the most abundant and easily attainable oxidizer. The necessary elements in these compunds are carbon, hydrogen, and oxygen. Hydrogen and oxygen are attainable by splitting water, and carbon and oxygen can be produced by splitting carbon dioxide. The carbon and hydrogen can then be combined to form any number of hydrocarbon fuels, with the oxygen as the oxydizer.

2.6.2.1 THERMOCHEMICAL HYDROGEN FORMATION

At the present time electrolysis is the only technically feasible way of obtaining hydrogen and oxygen from water, without using energy rich substances such as methane or coal. Typical electrolysis efficiencies are about 65%, and present-day electrical generation technology can achieve efficiencies of close to 50%. This means the entire process of converting heat to hydrogen through electrolysis can be carried out with about 30% efficiency, with future technologies increasing this number to 40% at the most.

TABLE 2.6.1. COMPOSITION OF LOWER ATMOSPHERE

Carbon Dioxide	95.32	
Nitrogen	2.70	
Argon	1.60	
Oxygen	0.13	
Carbon Monoxide	0.07	
Water Vapor	0.03	
Neon	2.50	ppm
Krypton	0.30	ppm
Xenon	0.08	ppm
Ozone	0.03	ppm

Using thermochemical generation, better efficiencies can be achieved. The concept of thermochemical hydrogen generation involves the formation of chemical potential energy directly from heat energy, without the intermediate production of electricity. An easy way of doing this is to heat water sufficiently to dissociate it into hydrogen and oxygen.

$$H_2O \rightarrow H_2 + O_2$$

However, this would require temperatures exceeding 3000°K, and on Mars, heat sources at this temperature are not easily accessible, which makes this method costly in terms of energy and therefore undesirable.

The desired thermochemical process consists of multi-step reactions producing hydrogen and oxygen at separate stages and regenerating all reagents except the dissociated water. A generalized representation of the process is given below:

$$2AB + 2H_2O \rightarrow 2AH + 2BOH \qquad (1)$$

$$2BOH \rightarrow 2B + H_2O + {}^{m}O_2 \qquad (2)$$

$$2AH \rightarrow 2A + H_2 \qquad (3)$$

$$2A + 2B \rightarrow 2AB \qquad (4)$$

This water splitting process has at least four distinguishable steps, but a real cycle will frequently require more, with the reagents A and B representing simple or complex mixtures of substances. The thermochemical

reaction would use heat at 1000°-1100°K, which could be delivered by a high temperature gas-cooled nuclear reactor.

The thermochemical process has many advantages over the electricity/electrolysis system, the main one being its increased efficiency due to its higher acceptance heat. The thermochemical plant is also more cost effective than the electricity/electrolysis system. Electrolysis tends to be a modular operation which shows little economic improvement as the installations grow, but a thermochemical plant can be expected to show considerable improvement as operations expand. This leaves thermochemical hydrogen formation as the necessary choice for the Manned Mars Mission.

An extensive feasibility study needs to be done on the use of thermochemical fuel formation reactions. This includes: the best mixtures of reagents which can be used in the thermochemical process, and chemical analysis as well as testing of the final chemical configuration used in the reaction; the design of a special reactor to provide the high temperatures needed for the process.

2.6.2.2 OXIDIZER ANALYSIS

The oxidizers considered for analysis were: ozone, hydrogen peroxide, and oxygen. The positive and negative qualities of each will be discussed more fully in the following paragraphs.

Ozone

This oxidizer gives an excellent specific thrust of 493 seconds when combined with hydrogen, by far the best of any fuel/oxidizer combination considered; see Table 2.6.2. Ozone is present in the Martian atmosphere and

TABLE 2.6.2. SPECIFIC IMPULSE(SECONDS)*

FUEL	OXIDIZER	I_{SP}(VACUUM)	I_{SP}(SEA LEVEL)
H_2	O_3	493	423
H_2	O_2	454	388
C_2H_2	"	384	330
N_2H_4	"	367	313
CH_4	"	365	310
C_2H_4	"	365	312
$C_2N_2H_8$	"	364	310
C_2H_6	"	362	307
C_3H_8	"	359	305
CO	"		209
N_2H_4	H_2O_2	338	288

* THESE VALUES ARE FOR A SHIFTING EQUILIBRIUM REACTION AND A COMBUSTION PRESSURE OF 1000 PSIA.

TABLE 2.6.3. BOILING AND FREEZING POINTS

FUEL/OXIDIZER		BOILING(°F)	FREEZING(°F)	SPEC.GRAV.
CH_4	METHANE	-258.7	-296.5	.822
C_2H_2	ACETYLENE	-119.2	-115.2	.612
C_2H_4	ETHYLENE	-154.7	-272.5	.566
C_2H_6	ETHANE	-127.5	-277.6	.546
C_3H_8	PROPANE	-43.7	-305.8	.585
$C_2N_2H_8$	UDMH	146.0	-71.0	.786
H_2	HYDROGEN	-423.0	-434.4	.071
H_2O_2	PEROXIDE	302.4	31.2	1.443
NH_3	AMMONIA	-28.0	-107.9	.604
N_2H_4	HYDRAZINE	236.3	34.7	1.004
O_2	OXYGEN	-297.4	-361.1	1.143
O_3	OZONE	-169.6	-315.0	1.460

could be produced on the surface. It has a relatively low boiling point, Table 2.6.3, and would need a refrigeration unit if it were to be stored on the surface, but since its boiling point is close to the average Martian temperature, its bleed-off rate would be minimal. Another drawback is that it is difficult to work with. NASA does not use ozone as an oxidizer, so the technology for utilizing it is not very advanced.

Hydrogen Peroxide

This oxidizer is non-toxic if handled correctly and because of its high boiling point, it can be stored for long periods of time with no substantial bleed-off. Hydrogen peroxide is hypergolic with hydrazine, producing a specific thrust of about 338 seconds on the surface of Mars. Storage tanks and lines must be clean when hydrogen peroxide is used, or it will decompose rapidly and may result in an explosion.

Oxygen

Of all the oxidizers considered oxygen appears to be the best choice. It is non-toxic as well as non-corrosive, and can be combined with a number of hydrocarbon fuels to produce specific impulses ranging from 359 to 454 seconds on the Martian surface. It has a very low boiling point and would require an extensive refrigeration unit for storage, and insulation of its tanks and lines. Even with these precautions oxygen could not be stored for long periods of time and a large bleed-off rate should be expected. NASA has dealt with oxygen on many prior occasions, so the necessary technology need only be adapted to be used in the Manned Mars Mission.

2.6.2.3 Fuel Analysis

The fuels considered were mainly hydrocarbons because of the availability of their base elements in abundance on Mars. In addition, since nitrogen can be found in quantity, a couple of nitrogen based fuels will also be considered.

Hydrogen

Like oxygen, hydrogen is non-toxic, non-corrosive, but has a boiling point close to absolute zero. Therefore, it also requires a very bulky refrigeration unit and insulated lines, and bleed-off rates over time will be substantial. In addition, before hydrogen can be introduced into its tanks and lines, they must be flushed with helium. When used with oxygen or ozone it produces excellent specific impulses, but because of its low molecular weight and low density, Table 2.6.4, it requires large tank volumes.

Carbon Monoxide

Carbon Monoxide is toxic and requires bulky tanks and extensive insulation. Combined with oxygen it has a relatively poor specific impulse when compared to the hydrocarbon fuels, but because of the abundance of carbon dioxide in the Martian atmosphere, it can be produced in large quantities.

Methane

Methane is the leading fuel candidate for the Manned Mars Mission. It is non-toxic, and can be stored in all common metals and insulations (asbestos, neoprene, epoxies etc). It is easily producible on Mars if enough water can be collected, but would require refrigeration because of its low

TABLE 2.6.4. MOLECULAR WEIGHTS(KG/KG-MOLE)

CH_4	16.042
C_2H_2	26.020
C_2H_4	28.052
C_2H_6	30.068
CO	28.010
CO_2	44.010
H_2	2.016
H_2O	18.016
H_2O_2	34.016
O_2	32.000
O_3	48.000

boiling point. When combined with oxygen, it produces a good specific impulse, and does not require excessive tank volumes.

Acetylene, Ethylene, Ethane, Propane

These hydrocarbons are similar to methane in most respects, but in general have lower specific impulses. In all cases they are easier to store due to their higher boiling points, but still would require refrigeration. Due to their more complex chemical structures, they will be more difficult to produce on Mars, and would require larger amounts of hydrogen and carbon to produce.

Hydrazine

Hydrazine is hypergolic with hydrogen peroxide and gives good performance, but it is toxic, and decomposes when in contact with metal oxides. It also reacts chemically with carbon dioxide, which is very undesireable on Mars.

Unsymmetrical-Dimethyl Hydrazine

UDMH is stable because of its high boiling point and can be stored for long periods of time with no noticeable bleed-off. It is hypergolic with hydrogen peroxide, but like hydrazine it is toxic and will react with carbon dioxide.

2.6.2.4 Propellant Formations

Taking into account the pros and cons of the fuel/oxidizer combinations so far considered, the following paragraphs will attempt to offer production techniques utilizing the known strengths of some of the more promising combinations.

Carbon Monoxide/Oxygen

The first system to be discussed produces oxygen and carbon monoxide from carbon dioxide. Carbon dioxide is drawn into the system and heated to the temperature at which the oxygen and carbon dioxide dissociate. The oxygen is separated from the carbon monoxide, cooled to cryogenic temperatures, and stored as a liquid. The carbon monoxide is also stored for later use.

$$CO_2 \rightarrow CO + {}^{m}O_2$$

Because of the low atmospheric pressures on Mars, a vacuum system to draw in the carbon dioxide will be difficult to operate; therefore, sublimation of the carbon dioxide into frost using a cryogenic fluid is recommended. The solid carbon dioxide can then be collected and processed.

Hydrogen/Oxygen

The second system requires the presence of substantial amounts of water on Mars, and produces hydrogen and oxygen. First, the water is split into hydrogen and oxygen using thermochemical techniques, then the gases are cooled and stored in liquid form.

$$H_2O \rightarrow 2H_2 + {}^{m}O_2$$

Methane/Oxygen

The third system requires the availability of water and carbon dioxide on Mars. Using a system devised by Ash, Dowler, and Varsi (Ash, et al. 1978), both methane and oxygen could be produced. The first step is to gather the water and carbon dioxide from the local environment. The water would then be separated into oxygen and hydrogen, with the oxygen being cooled and stored. The hydrogen could then be combined with carbon dioxide using a nickel catalyst to produce methane and water, with the excess water being channeled back into the system for reprocessing.

$$CO_2 + 2H_2O \rightarrow CH_4 + 2O_2$$

Based on specific impulse, volume, and energy requirements, the methane/oxygen system has been chosen for the TSS Manned Mars Mission.

2.6.3 MATERIALS PRODUCTION

Mars, like the Earth is rich in natural resources. The Martian atmosphere alone can provide a plethora of valuable elements in addition to ample supplies of water and carbon dioxide. The Martian soil can also provide valuable minerals necessary for an extended stay on the surface; iron and many other elements are quite abundant.

REFERENCES

2.6.1 Cordell, Bruce, *Mars...*, L5 News, November, 1985.

2.6.2 Duke, Michael B., Mars Resources, NASA Johnson Space Center, Houston, Texas.

2.6.3 Hoffmann, Stephen J., A Review of In-Situ Propellant Production Techniques for Solar System Exploration, Report No. 1-120-340-515, April, 1983.

2.6.4 Ryason, P. R., *Solar Photochemical Fuel Formation*, Survey of Progress in Chemistry, JPL, Vol. 9, 1980, pp. 89-120.

2.6.5 Schreiner, Felix and Appelman, Evan H., *The Thermochemical Generation of Hydrogen from Water*, Survey of Progress in Chemistry, Vol. 8, 1977, pp. 171-194.

2.6.6 Spangenburg, Ray and Moser, Diane, *The Secret Ice of Mars*, Space World, February 1986, pp. 14-19.

3.0 MOON RECONNAISSANCE GROUP

3.1 AN INTRODUCTION TO PHOBOS AND DEIMOS

The moons of Mars, Phobos and Deimos, are a very interesting and mysterious pair. They were discovered by Asaph Hall in 1877 at the U.S. Naval Observatory. Using a 26-inch refracting telescope, he sighted the two moons as Mars was making its closest approach to Earth since 1845. However, scientists had been predicting the existence of Phobos and Deimos hundreds of years before Asaph Hall's siting. Johannes Kepler and Bernard Fontenelle both believed that Mars had moons. In 1726, Johnathan Swift even predicted the moons' existence in his book Gulliver's Travels. Swift wrote of the scientists of Lupta discovering the two Martian moons and calculating their orbit radii and periods. Many, including Voltaire, agreed with Swift's prediction and pursued it vigorously. Based upon complex and intensive mathematical studies, astronomers drew the conclusion that the aberrations of Mars might be produced by one or more small satellites orbiting the planet (Reference 1).

After Hall's discovery, little else was learned about Phobos and Deimos. Because of their small size, closeness to Mars and peculiar motions, many theories about the Martian moons were proposed. I.S. Shklovsky, a Russian physicist, put forth probably the most bizarre theory on Phobos and Deimos. He believed the moons of Mars were actually artificial satellites of a mysterious, long-vanished race of super beings. He further believed that Phobos was hollow inside and possibly contained artifacts from the doomed civilization of Mars (Reference 2).

As ludicrous as these theories sound, some scientists were defending them until the Mariner missions. Thanks to Mariner missions 6,7 and 9, and the two Viking missions, we now know conclusively that the moons, Phobos

and Deimos, are natural bodies.

There are still many unexplained mysteries about Phobos and Deimos.Their origin, formation, and ages are all unknown. They may be captured asteroids, and if they are, were they captured separately or are they remnants of a single larger captured asteroid? They may have formed in place, and if they did , did they form as long as four billion years ago or did they form more recently? Were they once one body? What are their ages? When did they join Mars? How did they join Mars? What information do they shed on the origin and history of the planets and satellites of the Solar System? These are all questions that could be answered by a mission to the moons of Mars (Reference 3). This is why we believe a manned reconnaissance of Phobos and Deimos should be considered as a desirable, if not primary, operation of any manned mission to Mars.

REFERENCES

1. Caidin, Martin, Destination Mars, Doubleday and Company, Inc., Garden City, N.Y.,1972, p.39.

2. Caiden, p.178.

3. Singer, S. Fred, "The Ph-D Proposal: A Manned Mission to Phobos and Deimos," The Case for Mars, Univelt, Inc., San Diego, CA., 1984, p. 45.

3.2 SCIENTIFIC DATA ON PHOBOS AND DEIMOS

Phobos and Deimos are small, very dark, heavily cratered, asteroid-like moons. Photographs of the two moons appear in figure 3.2.1. Phobos is the larger of the two moons and has the innermost orbit. Its mean orbit radius of approximately 9378 km has a period of 7 hours 39 minutes. This means that Phobos' revolution about Mars is faster than the rotation of Mars itself- a rare if not unique phenomenon in our Solar System. Phobos, already inside the "Roche Limit" where internal gravity alone is too weak to hold it together, could conceivably become a ring plane about Mars within the next 50 million years (Reference 2). Deimos is about half as big as Phobos and is the outermost satellite of Mars. Its mean orbit radius is approximately 23,459 km and the period of Deimos is 30 hours 17 minutes. Since Deimos is close to a synchronous altitude above Mars, it remains within line-of-sight of surface points on Mars for up to forty hours at a stretch (Reference 3). Both orbits have very low eccentricities and inclinations and can be characterized as circular and equatorial for first-cut analyses. Table 3.2.1 summarizes the above information.

Both satellites are irregular in shape, but can be approximated as triaxial ellipsoids. Phobos is about 13.5 x 10.7 x 9.6 km across, and Deimos is about 7.5 x 6.0 x5.5 km across. The approximated shapes and cross-sections of the two moons appear in figure 3.2.2. Both satellites have spin periods synchronous with their orbital periods, and are moving in such a way that the longest axis of each always points towards Mars (Reference 6). As mentioned earlier, Phobos and Deimos are very dark satellites with

a) Phobos

b) Deimos

Figure 3.2.1 The Martian Moons (Reference 1)

	Phobos	Deimos
Orbital Elements		
Semi-major axis	9378 km 2.76 R_{Mars}	23459 km 6.90 R_{Mars}
Eccentricity	0.015	0.00052
Inclination (deg)	1.02	1.82
Sidereal period	$7^h39^m13.85^s$	$30^h17^m54.87^s$
Physical Parameters		
Longest axis	13.5 km	7.5 km
Intermediate axis	10.7 km	6.0 km
Shortest axis	9.6 km	5.5 km
Rotation	synchronous	synchronous
Density	2.0 g cm^{-3}	1.9 g cm^{-3}
Mass	9.8×10^{18} g.	2.0×10^{18} g
Albedo	0.05	0.06
Surface gravity	1 cm sec^{-2}	0.5 cm sec^{-2}

Table 3.2.1 Characteristics of Phobos and Deimos

(Reference 4)

very low reflective properties. Their albedos are 0.05 and 0.06 respectively, about the darkest among satellites in our Solar System. The low masses and low densities, along with their reflective properties, suggests that Phobos and Deimos are of carbonaceous chondrite composition. The surface gravity on both moons is almost negligible. The above information is also summarized in table 3.2.1.

Photometric, polarimetric and radiometric data all indicate that the surfaces of both satellites are covered with a fine-grained regolith derived, most probably, from the comminution of the surfaces by impacts (Reference 7). The intricate texture and microstructure of the regoliths seems to be lunar-like. Phobos' regolith cohesion ($\sim 10^4$ dyne/cm^2) is apparently lower than that of Phobos as a whole ($\sim 10^6$ dyne/cm^2) indicating that a substantial regolith covers a more solid interior (Reference 8). Deimos seems to have similar characteristics. In comparison, the material on the surfaces of Phobos and Deimos is most likely far less dense and cohesive than that of the earth's moon. Unfortunately, it is impossible to determine the depth of a regolith by photometric techniques (Reference 9). However, by observing crater walls and crater fill, an approximate regolith can be estimated. Several craters on Phobos reveal a layering in their walls. Measurements of these layers suggests a possible regolith layer 200 m deep. Many craters on Deimos are filled with 10-20 m of sediment, providing an estimate of the minimum average depth of regolith on this satellite (Reference 10). Several scientists believe the depth could be as deep as 100 m. So, despite their low surface gravities, Phobos and Deimos seem to have accumulated significant layers of regolith.

The compositions of the moons is unknown. However, as previously

stated, the low masses, low densities and low albedos suggests a composition similar to type 1 carbonaceous chondrites. A composition of this type would agree with the captured asteroid theory of the moons' origin because it is widely believed that carbonaceous chondrites had to form in the outer half of the Solar System. Table 3.2.2 illustrates the average composition of type 1 carbonaceous chondrites. Examples of carbonaceous chondrite meteorites appear in table 3.2.3. Since both the densities of Phobos and Deimos are smaller than the three meteorite examples, it may be that the moons have an even higher percentage of water and clays in them. These tables show that Phobos and Deimos are ideal candidates as sources of raw materials for conversion into water, air and even hydrocarbon fuels (Reference 13). Also, the high amounts of clays provides a ready source of building materials.

While there are many similarities in the two moons of Mars, each moon has its own unique surface features, making Phobos and Deimos strikingly different in appearance.

The most interesting feature on Phobos is the large number of grooves, long linear depressions formed in the regolith, on the surface. Typically, grooves are 100-200 m wide, 10-20 m deep, and have smooth concave-up cross profiles (Reference 14). A map of Phobos appears in figure 3.2.3. The large crater centered at 50° W and 0° N is Stickney crater. It is the largest crater on Phobos and is approximately 10 km across. The grooves are largest and most numerous near the large crater Stickney, and are absent from the area opposite Stickney (Reference 16). The grooves are believed to have formed at the same time or at a time quickly after the formation of Stickney. According to this theory, the impact that caused Stickney fractured Phobos along already existing weak zones. The impact

Oxides	wt%
SiO_2	44.3
TiO_2	0.18
Al_2O_3	4.24
Cr_2O_3	0.42
FeO	9.25
MnO	0.14
MgO	38.2
CaO	2.89
Na_2O	0.60
K_2O	0.05
Ni	0.32
S	0.42

Table 3.2.2 Average Composition of a Type I Carbonaceous Chondrite (Reference 11)

CARBONACEOUS CHONDRITES

Type*	Example	$\bar{\rho}$ (g/cm^3)	Weight %			
			$H_2O^\dagger$	Organics	Clays**	Magnetite
C 1	Orgueil	**2.2**	20	3.6	60-80	10-15
C 2	Murchison	**2.7**	13	2.5	50-70	5
C 3	Allende	**3.4**	1	0.5	<10	<5

After: MASON (1973) Handbook of Elemental Abundance in Meteorites

* Wood - van Schmus

† Mostly in clay minerals

** "hydrated silicates"

Table 3.2.3 Carbonaceous Chondrite Meteorites (Reference 12)

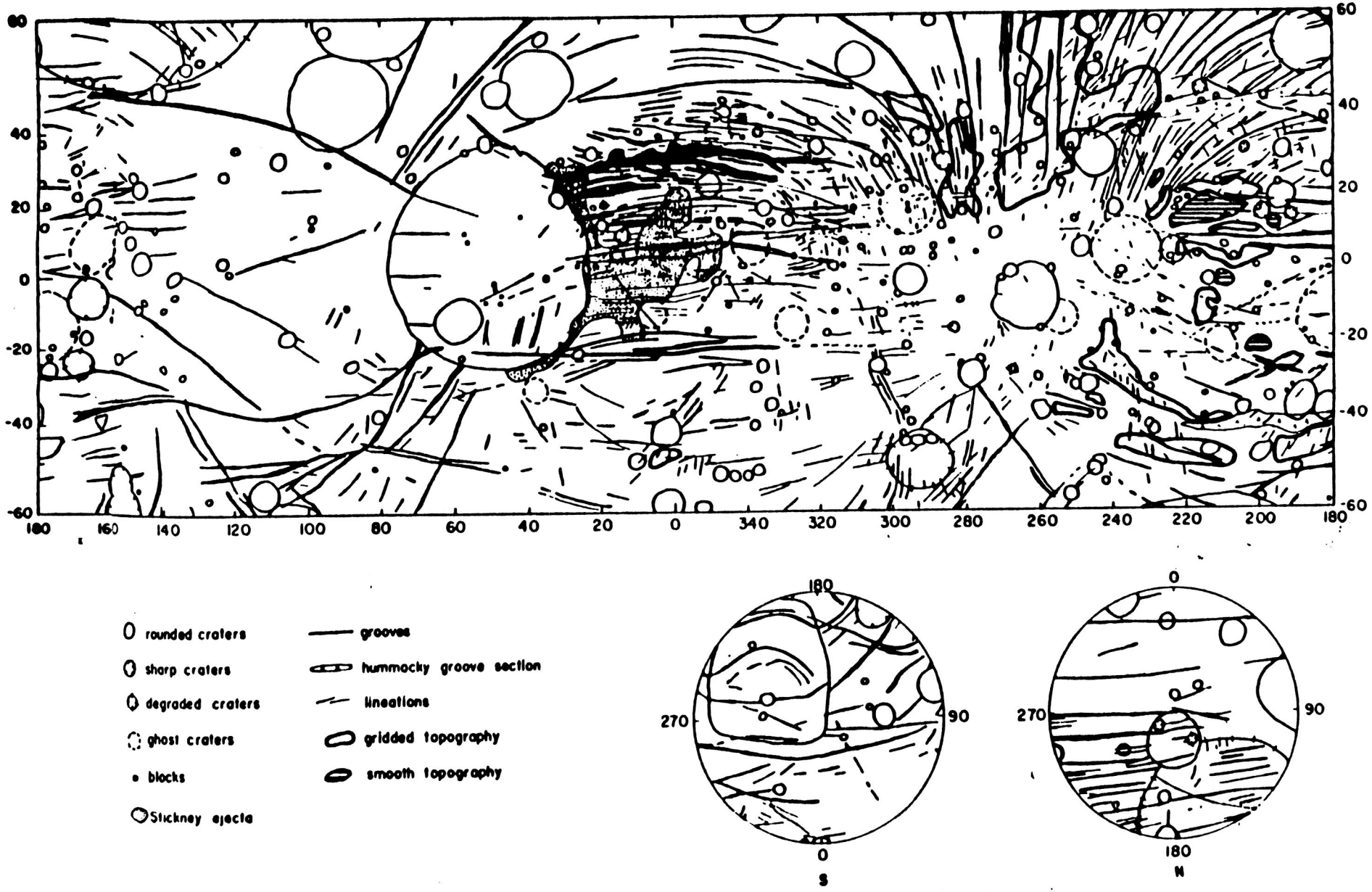

Figure 3.2.3 Map of Phobos (Reference 15)

heated the general area to a level where vaporization of the volatiles in Phobos occurred. The volatiles escaped through the fractures, expelling regolith in the process. As the cohesive strength of the regolith decreased, due to the vaporization of the bonding materials, the regolith slumped toward the central fracture. Volatile outgassing and regolith slumping continued until Phobos cooled down, and the grooves took their final form. This process is illustrated in Figure 3.2.4. The suggested carbonaceous chondrite composition of Phobos would explain why Phobos might tend to fracture during a severe impact, since low density carbonaceous material is known to be mechanically very weak. Such a composition also explains the possible release of volatiles along some of the fractures leading to the formation of pits and possible raised rims (Reference 18).

There are several other interesting surface features on Phobos. The ejecta blocks associated with the crater Stickney might be consolidated ejecta or boulders thrown out on the formation of the crater. These blocks could be samples of the interior of Phobos or fragments of the meteorite that created Stickney. The area east of Stickney, commonly referred to as the Stickney ejecta, may be blocks mantled with finer debris, all emplaced ballistically, or it may be some form of base-surge deposit (Reference 19). The area opposite of Stickney is interesting simply because this is where the grooves disappear. The ridges in the Southern hemisphere of Phobos may be outcrops of material different from the regolith. Finally, there are the smooth areas on Phobos which are of unkown origin.

Deimos is just as interesting as Phobos, if not more puzzling. In contrast to Phobos' grooved surface, Deimos appears smooth. This smooth appearance is a result of many of the impact craters on Deimos being filled with sediment. This fill appears to be ejecta, a view supported by the

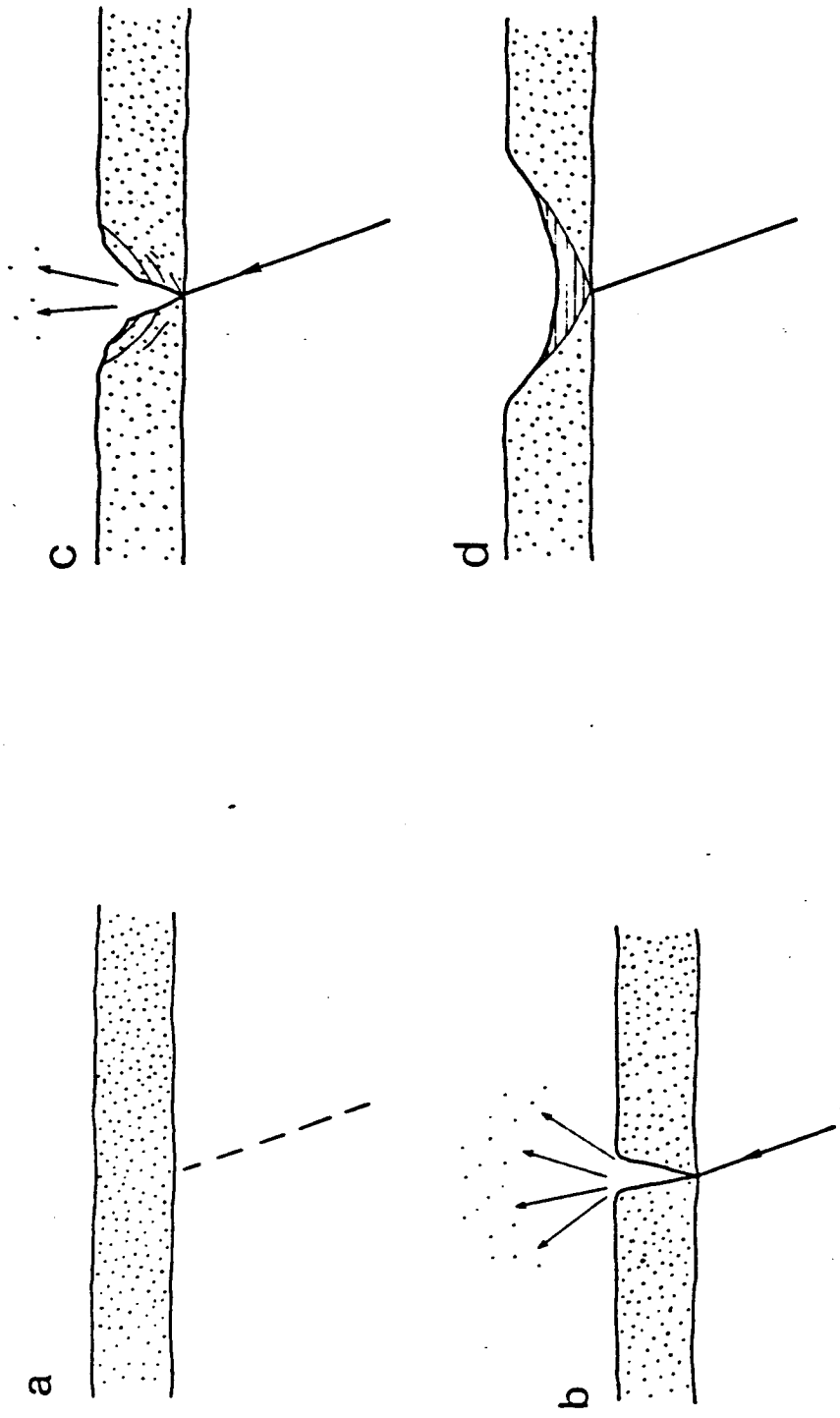

Figure 3.2.4 Groove Formation on Phobos (Reference 17)

ubiquitos presence on Deimos of numerous blocks and patches of higher albedo material (Reference 20). The blocks are roughly half as high as they are wide, and are greater in number than those found on Phobos. Whether these blocks are fragments of meteorites or Deimos itself is unclear. The bright albedo markings on Deimos are also unexplained. Though there is no significant color difference between the bright areas and the rest of Deimos, the normal albedo of the bright patches is 30% greater than surrounding areas. There are also bright patches that are linear or tapered streamline forms. These particular markings are associated with small craters. The albedo features show no relief, and if they are deposits of some material, they are undoubtedly very thin since many are formed adjacent to craters less than 10 m across which must have rim heights of only centimeters (Reference 21). This brings up another interesting point. There is considerable evidence on Deimos of downslope movement, whereas Phobos had little or no evidence. This downslope movement is evident in the albedo streamers, as they tend to be downslope from the ridges of craters.

It is believed that there are no grooves on Deimos because there is no crater large enough to indicate an impact severe enough to fracture the small moon. However, there are theories that Deimos may consist of a mechanically stronger material than Phobos.

Whatever Deimos' composition is, there are still some unanswered questions as to its smooth surface. Deimos, with roughly half the surface gravity and escape velocity of Phobos, has retained significantly more debris and is blanketed much more, as evidenced by the large number of blocks and large amounts of fill. The reason for this remains unclear.

REFERENCES

1. Thomas, P. and J. Veverka, "Grooves on Asteroids: A Prediction," Icarus, Vol. 40, Number 3, December 1979, p. 395.

2. Spitzer, Cary R., editor, Viking Orbiter Views of Mars, NASA Scientific and Technical Information Branch, Washington, D.C., 1980, p. 95.

3. Oberg, James, Mission to Mars, The New American Library, Inc., New York, 1982, p. 150.

4. Boston, Penelope J., editor, The Case for Mars, Univelt, Inc., San Diego, CA, 1984, p. 306.

5. Veverka, J., "The Surfaces of Phobos and Deimos," Vistas in Astronomy, Vol. 22, 1978, p. 167.

   Veverka, J., and P. Thomas, "Phobos and Deimos: A Preview of What Asteroids are Like?", Asteroids, The University of Arizona Press, Tucson, AZ, 1979, p. 633.

6. Veverka, Vistas, p. 163.

7. Ibid., p. 164.

8. Thomas, P., "Surface Features of Phobos and Deimos," Icarus, Vol. 40, Number 2, 1979, p. 266.

9. Veverka, Vistas, p. 164.

10. Ververka, Asteroids, p. 642.

11. McSween, Harry Y., Jr., A. Ken Fronabarger and Steven G. Driese, "Ferromagnesian Chondrules in Carbonaceous Chondrites," Chondrules and their Origins, Lunar and Planetary Institute, Houston, TX, 1983, p. 199.

12. Veverka, Vistas, p. 171.

13. Oberg, Mission, p. 152.

14. Thomas, P., J. Veverka, A. Bloom, and T. Duxbury, "Grooves on Phobos: Their Distribution, Morphology and Possible Origin," Journal of Geophysical Research, Vol. 84, No. B14, December 30, 1979, p. 8457.

15. Thomas, Icarus, p. 225.

16. Ibid, p. 231.

17. Thomas, Journal, p. 8474.

18. Veverka, Vistas, p. 175.

19. Thomas, Icarus, p. 230.

20. Veverka, Vistas, p. 180.

21. Thomas, Icarus, p. 235.

3.3 PRECURSORY MISSION TO PHOBOS AND DEIMOS

The results of the science study on the moons indicate that not enough information is known about Phobos and Deimos to land a manned vehicle on the moons with a reasonable degree of safety. Therefore, an unmanned precursory mission to the moons of Mars is necessary to provide vital information needed for a successful manned mission.

This mission should include both an orbiter and a lander, with Viking technology and systems providing the basis for these vehicles. Several different scenarios could be used for a mission of this type. One of them might include one lander and one orbiter, with the lander landing on Phobos and the orbiter rendezvousing with Phobos first, then traveling on to Deimos after its Phobos operations are completed. These vehicles could arrive at the Martian system as one package,as Viking did.

There are several primary science objectives that this precursory mission must meet. They are:

- provide complete, high resolution imagery of the moons
- refine current astronomical data
- determine the gravity fields
- determine regolith's compactibility and bearing strength
- determine mineralogy, petrology, and elemental composition of the regolith
- determine water content and availability
- determine radiation and micrometeorite exposure
- provide a basis for the selection of future landing sites
- provide a basis for the determination of the moons' origin and history
- provide a transponder for navigational and tracking purposes

Some of the possible experimental techniques that could be used are:

- visible and IR spectrometry (mineralogy)
- x-ray fluorescence (elemental composition)
- gamma-ray spectrometry (radioactive elements)
- television or CCD imagery

The information provided by this precursory mission could prove invaluable for mission planners designing a manned mission to Phobos and Deimos.

3.4 TRAJECTORY SCENARIOS

The Trajectory Division has completed several studies to determine the minimal energy trajectory to reach the moons. Most of the trajectories under consideration start from the parking orbit. The studies completed compute delta-v as a function of inclination and of radius. Delta-v as a function of inclination was determined for two orientations of the parking orbit. In the first orientation, Figure 3.4.1, the line of apsides lies in the plane of the moon's orbit, ie., periarian and apoarian are both in the orbital plane. Although this orientation is not realistic due to the geometry and apsidal rotation rate of the parking orbit, this analysis was done to determine if substantial delta-v savings could be gained by changing the orientation of the parking orbit. The second orientation assumes the line of apsides perpendicular to the line of nodes, Figure 3.4.2.

For both these orientations, a Hohmann transfer with a plane change was utilized to optimize the trajectory. In the first orientation, the first burn was made at the periarian of the parking orbit and the second burn at the orbital radius of the moon in question. Using a TK! Solver model, it was determined that it was optimal to take out part of the plane change at the first burn rather than take it all out at the second burn. For a minimal delta-v of 2.88 km/s, 1.8 degrees of the 64.12 degree plane change should be taken out at the first burn to reach Phobos. To reach Deimos, 2.9 degrees of the plane change should be taken out at the first burn to achieve a minimal delta-v of 2.80 km/sec. Figures 3.4.3 and 3.4.4 show total delta-v versus lower inclination for trajectories to Phobos and Deimos. The equations and variables to solve the TK! Solver model appear as Figure 3.4.5. For the second orientation, the first burn is made at the semi-latus rectum

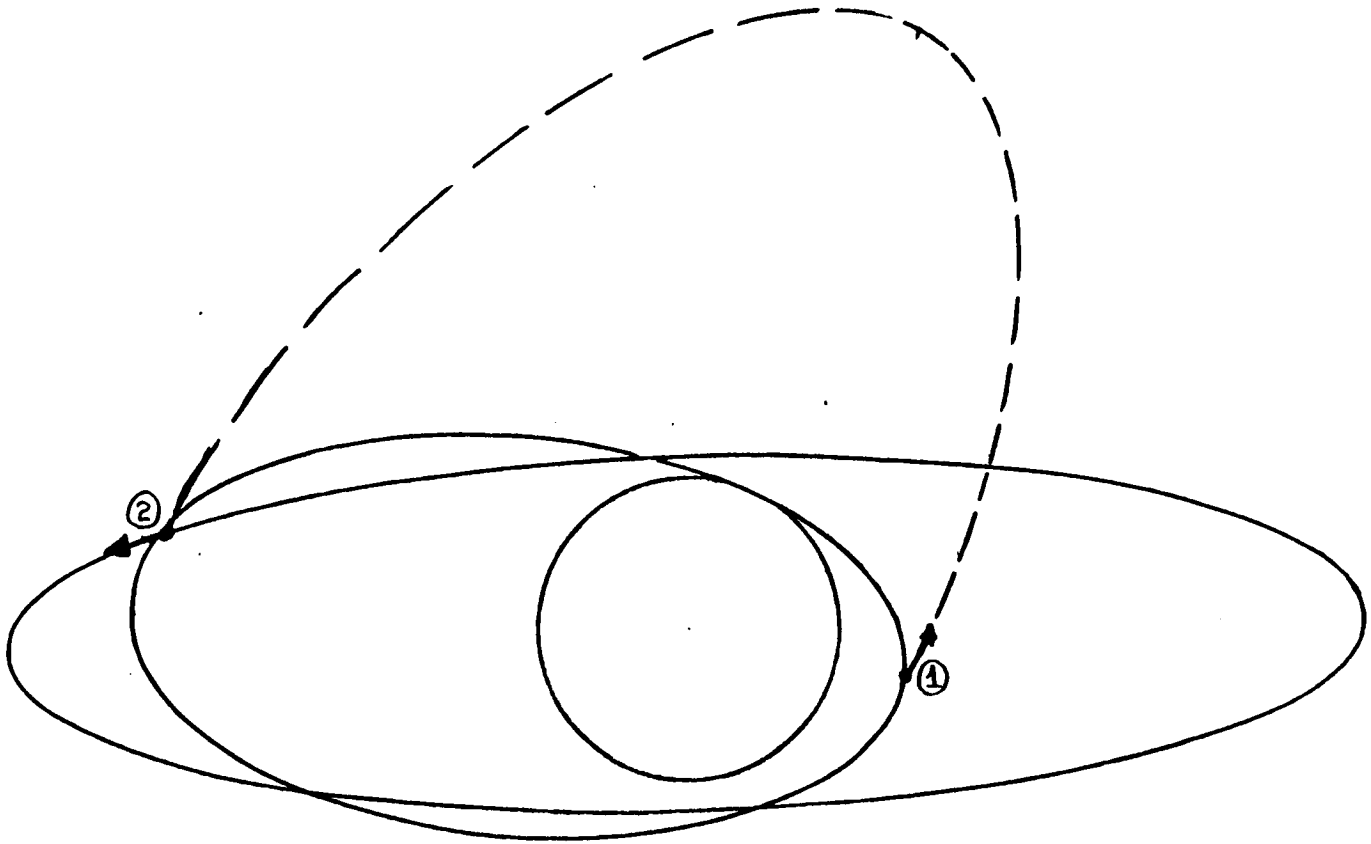

Figure 3.4.1 Line of Apsides in the Plane of the Moon's Orbit

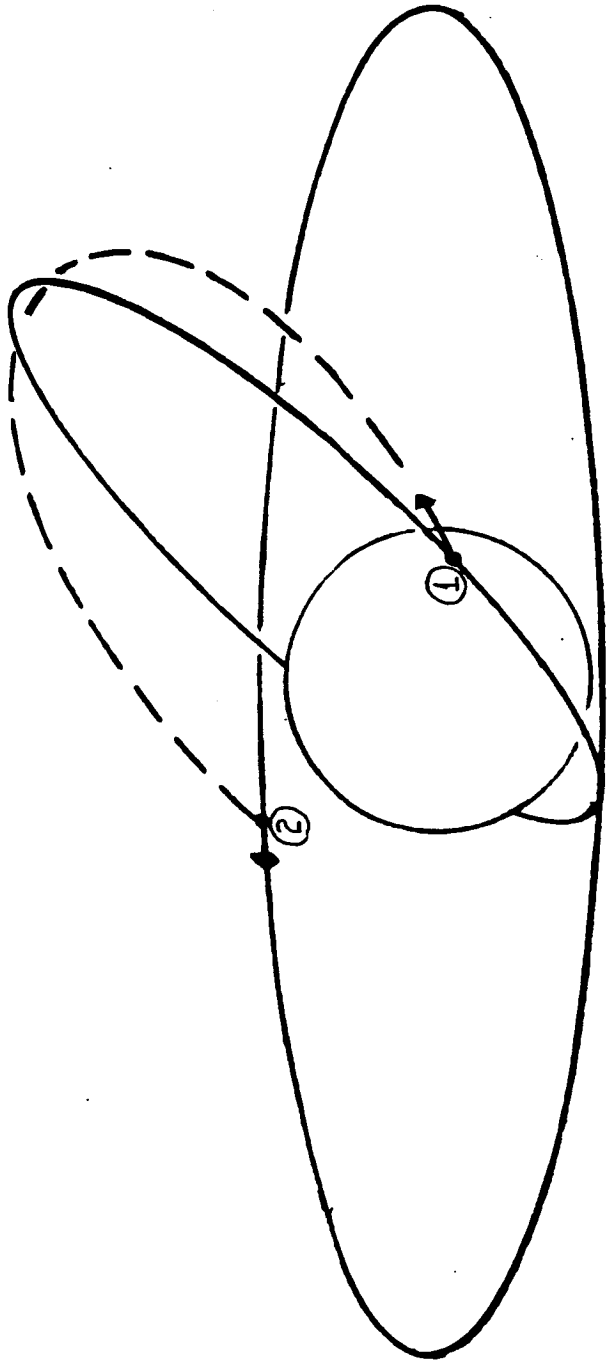

Figure 3.4.2 Line of Apsides Perpendicular to the Line of Nodes

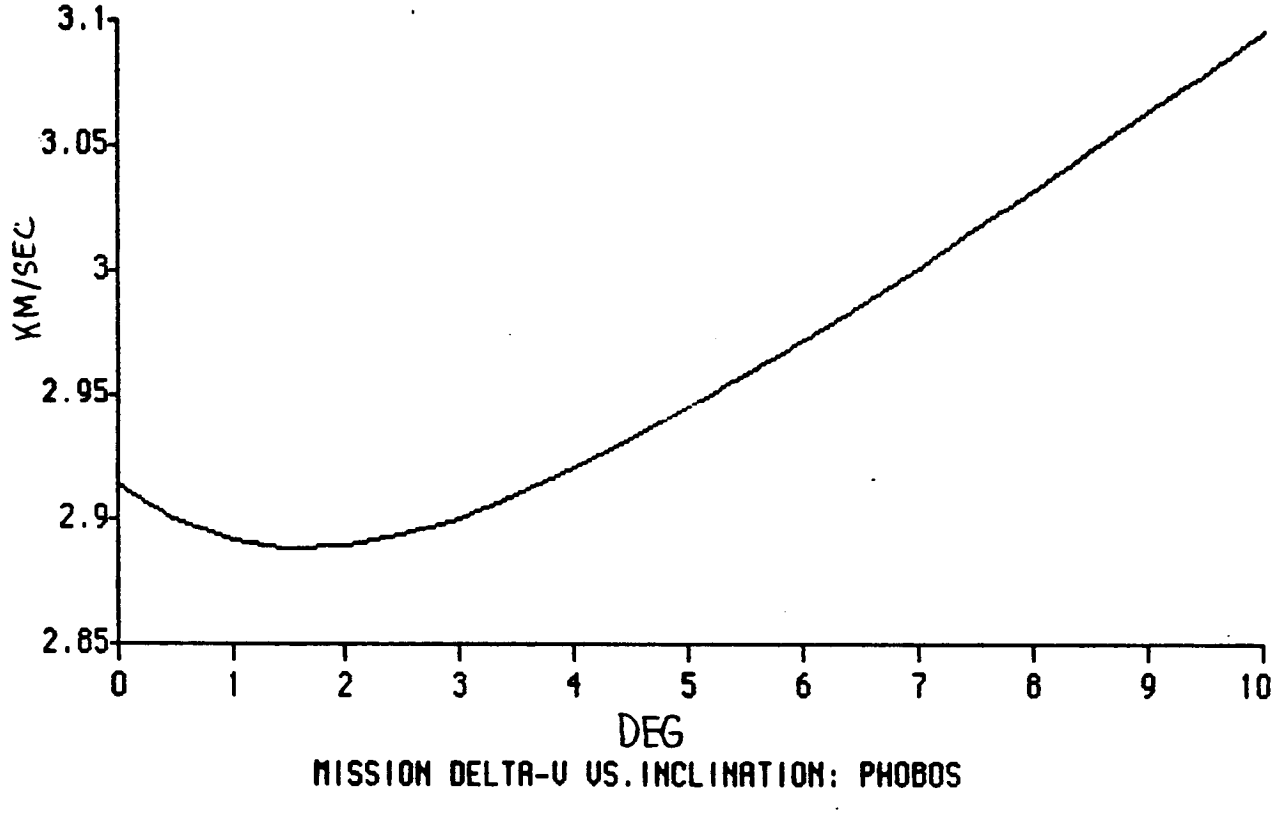

Figure 3.4.3 Total Delta Vee vs Lower Inclination: Phobos
(Apsides in Plane)

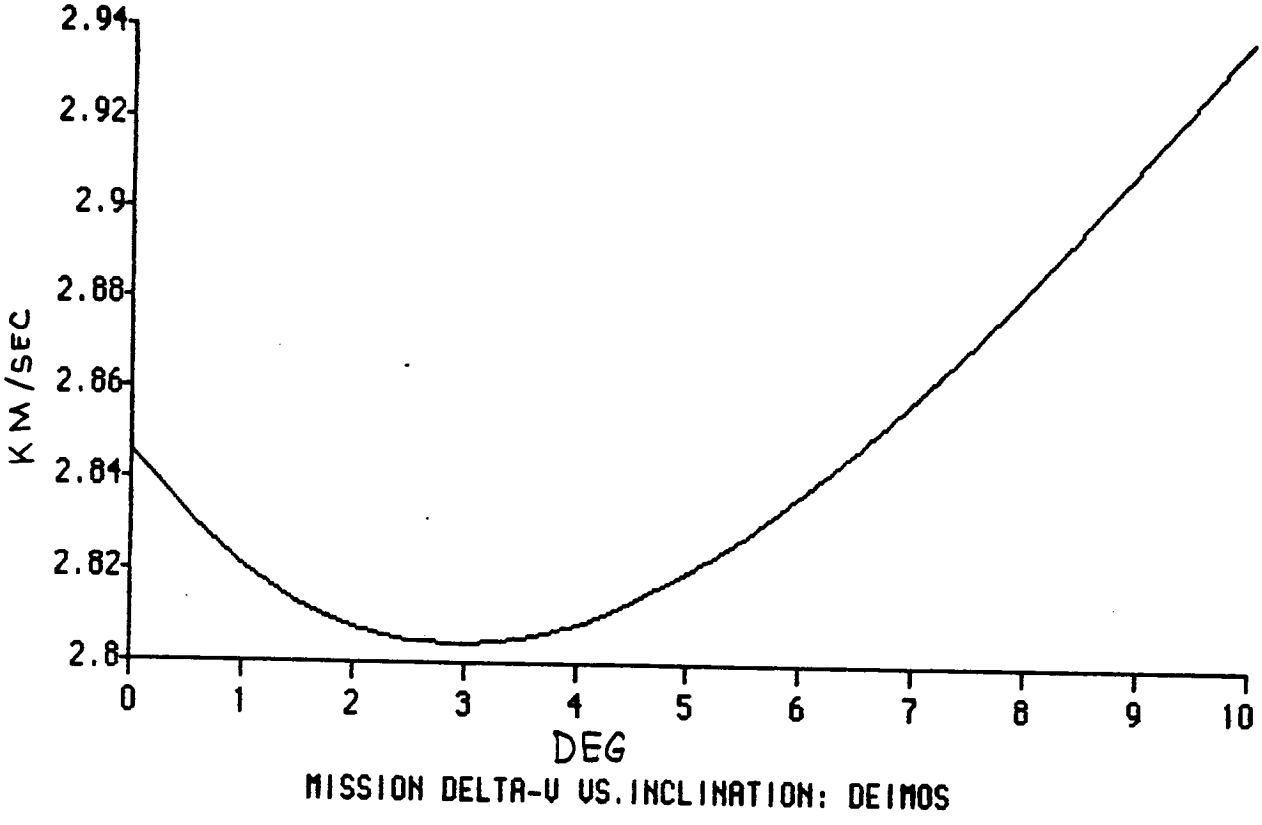

Figure 3.4.4 Total Delta Vee vs Lower Inclination: Deimos
(Apsides in Plane)

of the parking orbit and the second burn at the radius of the moon in question. For this orientation a TK! Solver model was also used to determine how much of the plane change should be taken out at the first burn. For a minimal delta-v of 1.742 km/sec, 2.4 degrees should be taken out at the first burn to reach Deimos and 1.25 degrees should be taken out for a minimal delta-v of 2.20 km/sec to reach Phobos. Figures 3.4.6 and 3.4.7 show total delta-v versus lower inclination for trajectories to Phobos and Deimos for this orientation. The equations and variables to solve this TK! Solver model appear as Figure 3.4.8.

The next scenario considered was a four-burn transfer, see Figure 3.4.9. This scenario is an extension of the previous model, however, in this case delta-v is considered as a function of transfer orbit radius. Here, again, a Hohmann transfer with a plane change is used to optimize the trajectory. The first burn is again made at the semi-latus rectum of the parking orbit. At this burn, the optimum lower inclination previously solved for is taken out. The second burn is made at the transfer radius, which is being optimized, and the rest of the plane change is taken out. After a transfer orbit is established, the third burn can be made. At the third burn, another Hohmann transfer is made to match moon orbit. At the fourth burn, the Hohmann transfer is completed and the moon velocity is matched. The results of this TK! Solver model appear as delta-v versus transfer orbit radius in Figure 3.4.10. This figure indicates that the optimum transfer radius is very nearly the orbital radius of the moon in question. This would imply that the four-burn transfer would collapse down to a two-burn transfer. The equations and variables used to solve this model appear as Figures 3.4.11 and 3.4.12.

```
S Rule
  vp1 = sqrt(mu*(2/rp1-1/ap1))
  vtp = sqrt(mu*(2/rp1-1/(rp1+r2)))
  dv1 = sqrt(vtp^2+vp1^2-2*vtp*vp1*cos(dil))
  vta = sqrt(mu*(2/r2 -1/(rp1+r2)))
  vc2 = sqrt(mu/r2)
  dv2 = sqrt(vta^2+vc2^2-2*vta*vc2*cos(dih))
  dvt = dv1 + dv2
  dit = dil + dih
```

St	Input	Name	Output	Unit	Comment
	42828	mu		km^3/s^2	Gravitational Parameter
		vtp	4.4072622	km/s	Perigee Transfer velocity
	23500	r2		km	Outer orbit radius
		dv1	.85878208	km/s	Delta v #1
		vta	2.5328917	km/s	Apogee transfer Velocity
		vc2	1.8237336	km/s	Higher Orbit Velocity
		dv2	2.080114	km/s	Delta v #2
	64.12	dit		deg	Inclination between orbits
L		dvt	3.2335723	km/s	Total Delta v
L	0	dil		deg	Lower Delta Inclination
		dih	54.12	deg	Higher Delta Inclination
		vp1	3.9506875	km/sec	Vel. at Periapsis
	3897.5	rp1		km	Parking Orbit Periapsis
	6724.2	ap1		km	Parking Orbit Semi-Major Axi
	9550.5	ra1		km	Radius at Apoapsis of P.O.

Figure 3.4.5 TK! Solver Model: Total Delta Vee vs Lower Inclination (Apsides in Plane)

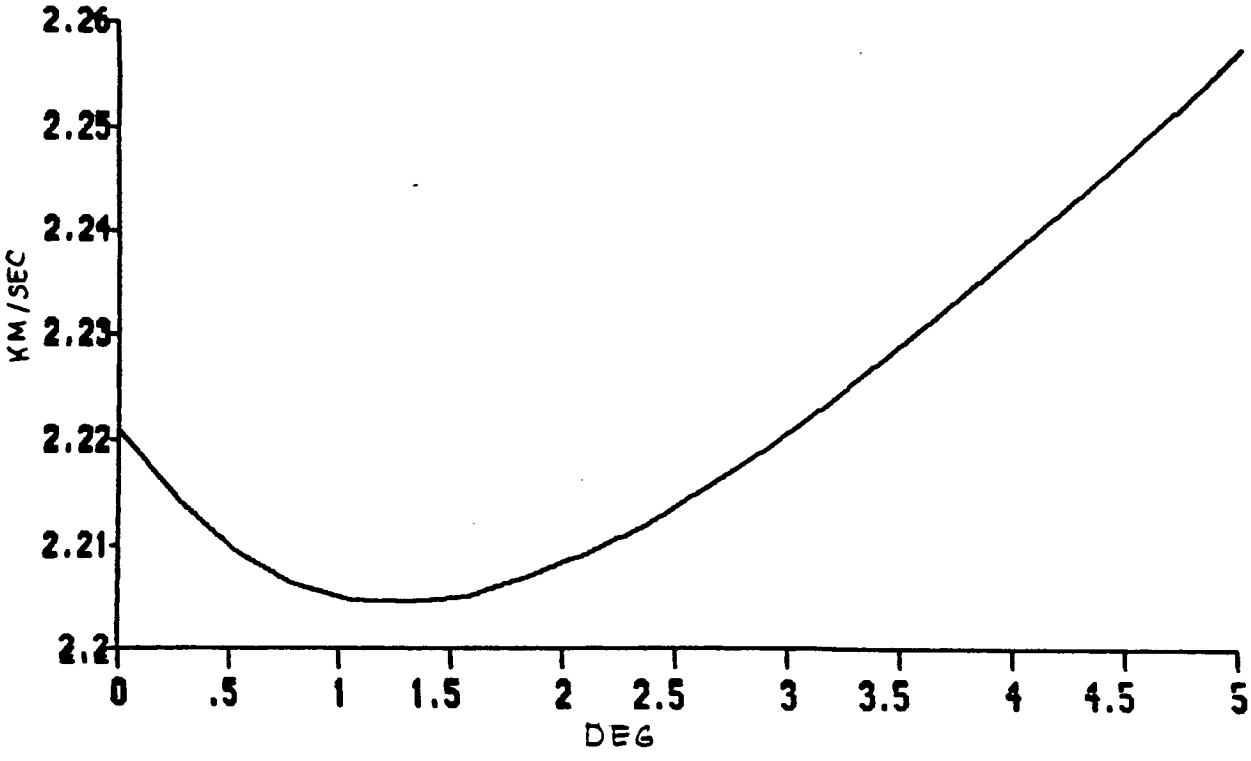

Figure 3.4.6 Total Delta Vee vs Lower Inclination: Phobos
(Apsides Perpendicular)

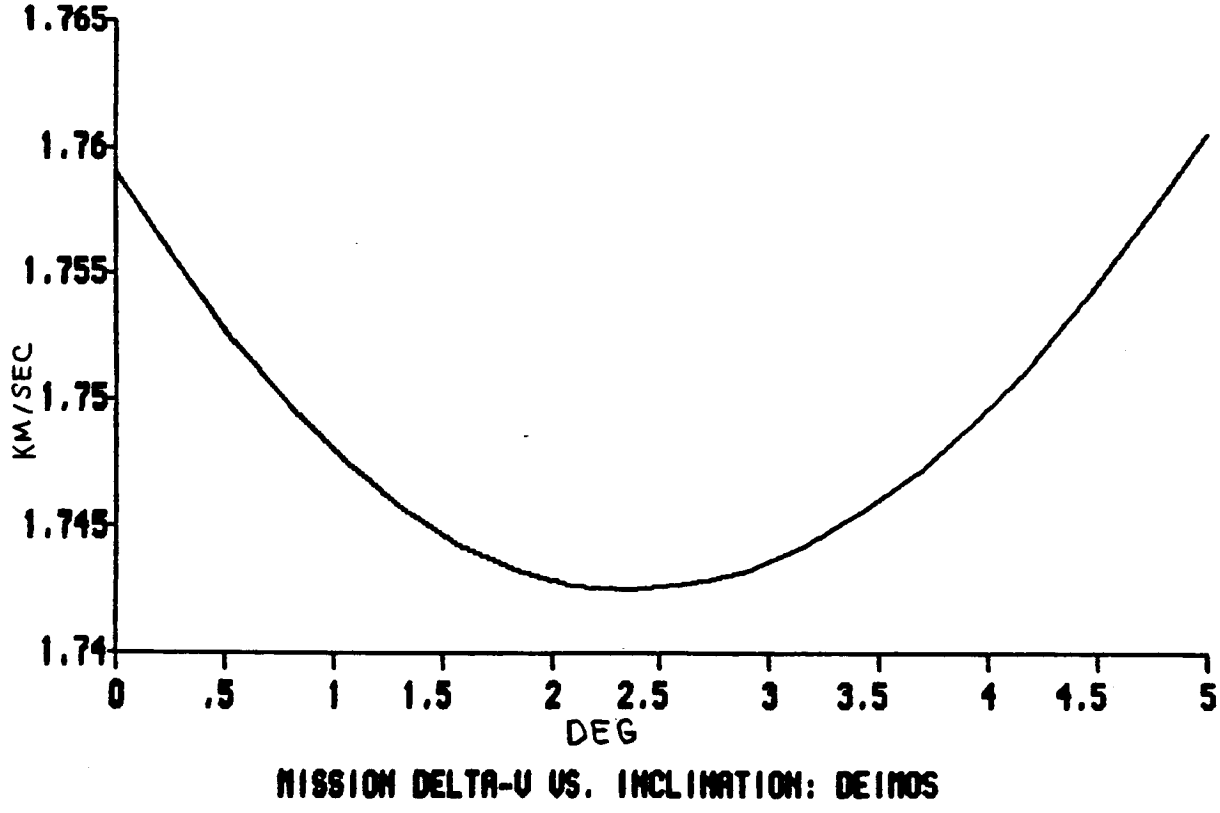

Figure 3.4.7 Total Delta Vee vs Lower Inclination: Deimos
(Apsides Perpendicular)

```
vp1 = sqrt(mu*(2/r1-1/ap))
vtp = sqrt(2*mu*(1/r1-1/(r1+r2)))
dv1 = sqrt(vtp^2+vp1^2-2*vtp*vp1*cos(dil))
vta = sqrt(2*mu*(1/r2-1/(r1+r2)))
vc2 = sqrt(mu/r2)
dv2 = sqrt(vta^2+vc2^2-2*vta*vc2*cos(dih))
dvt = dv1 + dv2
dit = dil + dih
r1  = ap*(1-e^2)
```

St	Input	Name	Output	Unit	Comment
		vc1		km/s	Lower orbit Velocity
	42828	mu		km^3/s^2	Graviational Parameter
		r1	5521.0456	km	Lower Orbit Radius
		vtp	3.1293783	km/s	Perigee Transfer velocity
	9450	r2		km	Outer orbit radius
		dv1	.13254451	km/s	Delta v #1
		vta	1.8283006	km/s	Apogee transfer Velocity
		vc2	2.1288644	km/s	Higher Orbit Velocity
		dv2	2.0723842	km/s	Delta v #2
	64.12	dit		deg	Inclination between orbits
L		dvt	2.2211519	km/s	Total Delta v
L	0	dil		deg	Lower Delta Inclination
		dih	62.62	deg	Higher Delta Inclination
		vp1	3.0241063	km/s	velocity of park.orb.@ peria
	6724.2	ap		km	semi-major axis of park orb.
	.423	e			

Figure 3.4.8 TK! Solver Model: Total Delta Vee vs Lower Inclination (Apsides Perpendicular)

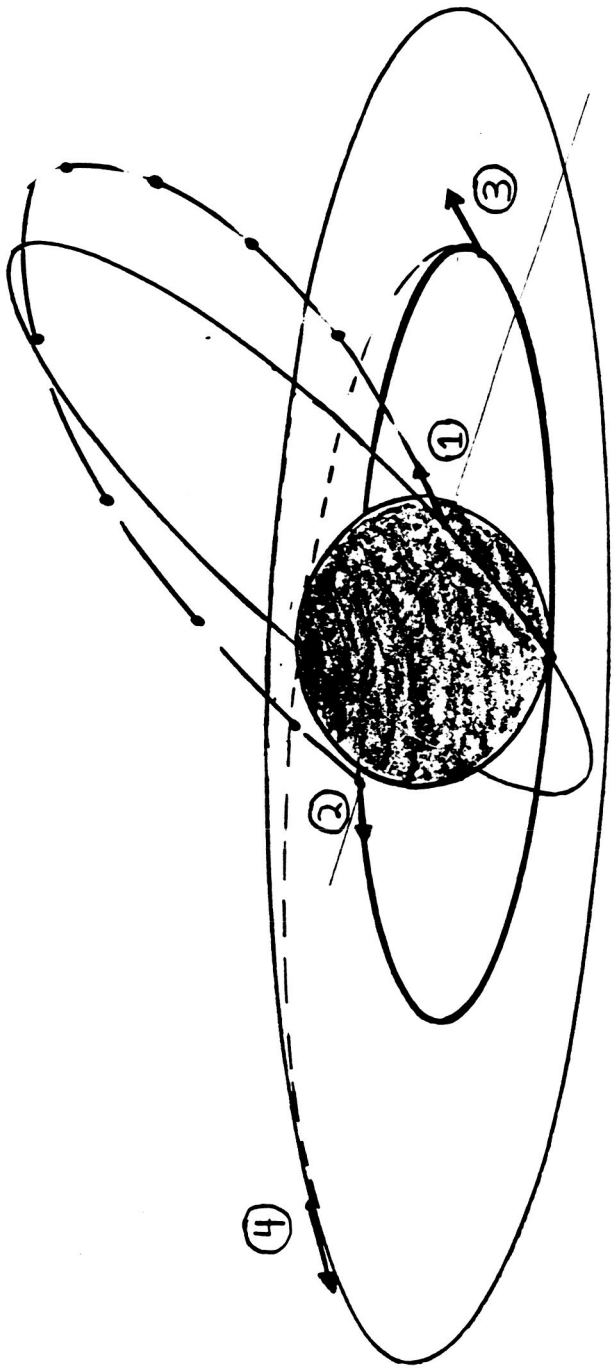

Figure 3.4.9 Four-Burn Transfer

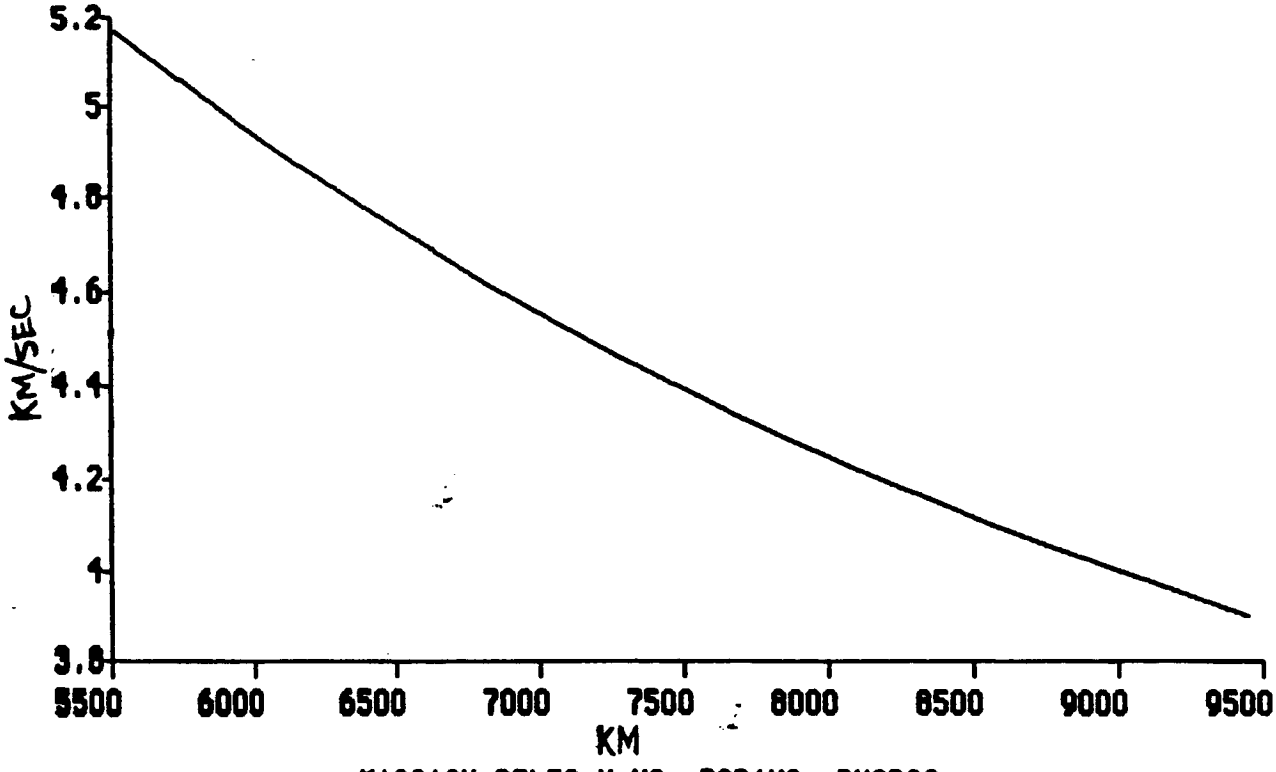

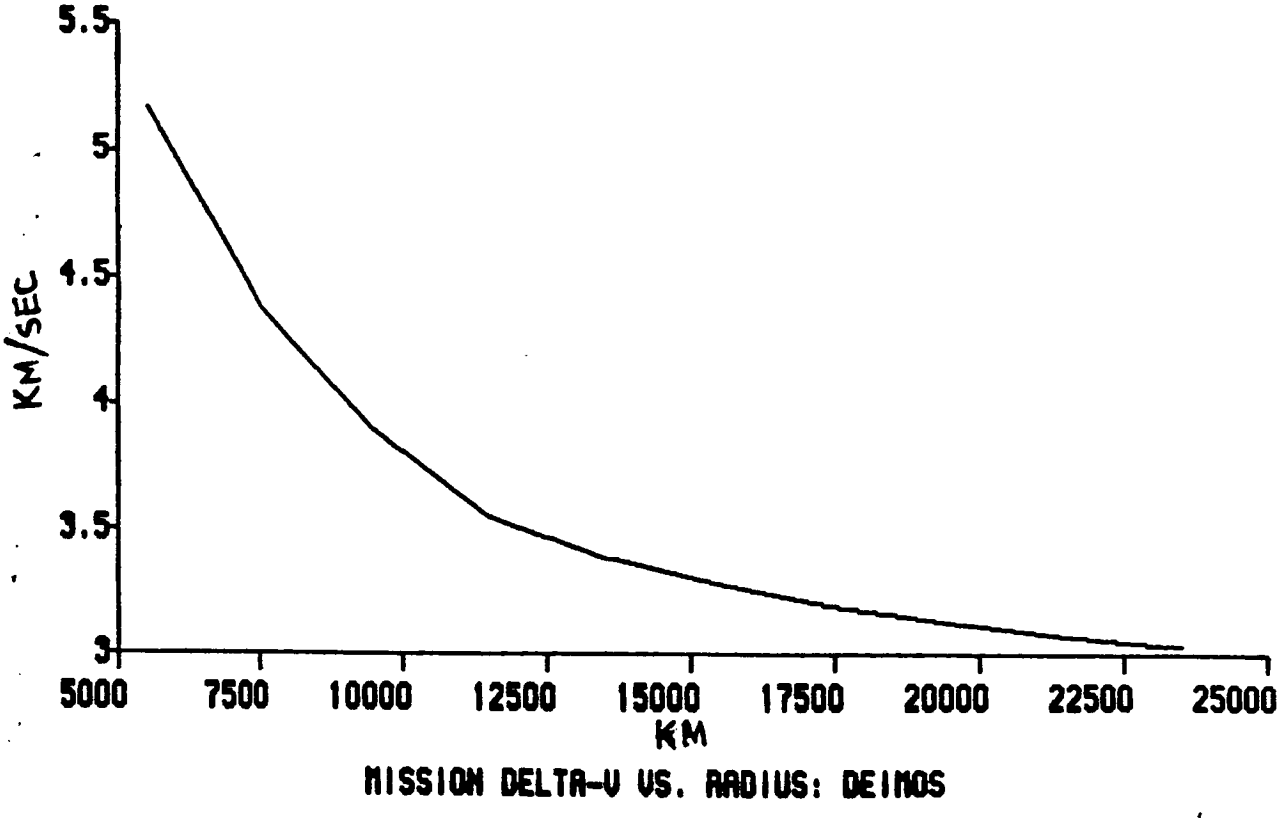

Figure 3.4.10 Total Delta Vee vs Transfer Orbit Radius

```
rpark = ap*(1-e^2)/(1 +e*cos(f))
-mu/(2*ap) = vp^2/2 - mu/rp
h=rp*vp
-mu/(2*ap) = (vpark^2)/2 - mu/rpark
h = rpark*vpark*cos(phi)
vparkt = vpark*cos(phi)
vparkr = vpark*sin(phi)
ato = (rpark + r)/2
vlto = sqrt(mu*(2/rpark - 1/ato))
dvlt = vlto - vparkt
dvlto = sqrt(dvlt^2 + vparkr^2)
dvlpc = sqrt(2*vlto^2 -2*vlto^2*cos(dil))
dvt1^2 = dvlpc^2 + dvlto^2
v2c  = sqrt(mu/r)
v2t  = sqrt(mu*(2/r - 1/ato))
dv2to= sqrt(v2c^2+v2t^2-2*v2c*v2t*cos(dih))
at   = r+rmoo/2
v3c  = v2c
v3t  = sqrt(mu*(2/r - 1/at))
dv3to= abs(v3t - v3c)
v4c  = sqrt(mu/rmoo)
v4t  = sqrt(mu*(2/rmoo - 1/at))
dv4to= abs(v4t - v4c)
TOTDV= dv4to+dv3to+dv2to+dvt1
```

Figure 3.4.11 TK! Solver Model: Four-Burn Transfer (Equations)

Ot	Input	Name	Output	Unit	Comment
	42828	mu		km^3/s^2	GRAVITATIONAL PARAMETER
	6724.2	ap		km	P.O. SEMI-MAJOR AXIS
		vp	3.9506875	km/sec	VEL. AT P.O. PERIAPSIS
	3897.5	rp		km	P.O. RADIUS OF PERIAPSIS
		h	15397.804	km^2/sec	P.O. ANG. MOMENTUM
		vpark	3.0238421	km/sec	VEL. AT FIRST BURN
		rpark	5521.6144	km	A(1-e^2)
		phi	22.74747	deg	FLIGHT PATH ANGLE
		vparkt	2.7886417	km/sec	TANGENTIAL COMP. OF VPARK
		vparkr	1.1692297	km/sec	RADIAL COMP. OF VPARK
		ato	14510.807	km	SEMI-MAJ. AXIS:TRANS. ORBIT
L	5521.04	r		km	VARIABLE RADIUS
		v1to	3.5442064	km/sec	VEL. TO REACH MOON ORBIT
		dv1t	.75556467	km/sec	DEL-VEE TO MATCH ORBIT
		dv1to	1.3921121	km/sec	TOTAL DEL-VEE TO MATCH ORBIT
		dv1r		km/sec	DEL-VEE TO LOSE RAD. COMP.
		dv1pc	.07732106	km/sec	DEL-VEE TO PLANE CHANGE
	1.25	di1		deg	LOWER INCLINATION
		dvt1	1.3942577	km/sec	TOT. DEL-V OF INTER. ORBIT
		v2c	1.3499882	km/sec	CIRC. VEL. AT R
		v2t	.83275494	km/sec	CIRC. VEL. OF TRANSFER ORBIT
		dv2to	1.2209199	km/sec	TOTAL DEL-V TO CIRC. INTER.
	62.87	dih		deg	REST OF INCLINATION
		at	35250	km	SEMI-MAJ.AXIS:AFTER 3RD BURN
	23500	rmoo		km	ORBIT RADIUS OF MOON
		v3c	1.3499882	km/sec	CIRC. VEL. AFTER 3RD BURN
		v3t	1.5588321	km/sec	VEL. AFTER 3RD BURN
		dv3to	.2088439	km/sec	TOTAL DEL-V TO LEAVE INTER.
		v4c	1.3499882	km/sec	CIRC. VEL. AT MOON ORBIT
		v4t	1.5588321	km/sec	TRANS. VEL. AT MOON ORBIT
		dv4to	.2088439	km/sec	TOTAL DEL-V TO GAIN MOON ORB
L		TOTDV	4.7386142	km/sec	TOTAL DELTA-VEE
	.4229	e			
	90	f		deg	

Figure 3.4.12 TK! Solver Model: Four-Burn Transfer (Variables)

Also considered was a three-burn transfer to Phobos, see Fig. 3.4.13. In this maneuver, the first burn is made at apoarian of the parking orbit. At this burn, a circular orbit having a radius of the parking orbit apoarian is established. However, only 90% of the circular velocity is attained at this burn. This to allow a transfer orbit just inside Phobos orbit to be established. At the second burn, all of the plane change is taken out. The transfer orbit is now just inside the orbit of Phobos and intersects the orbit of Phobos at the point where the second burn was made. This walking orbit makes it possible to properly phase a rendezvous with Phobos. Walking orbit is maintained until the fourth burn is made. This burn is made at the intersection of Phobos orbit and walking orbit to match the orbit of Phobos. This maneuver required a delta-v of 2.6 km/sec. The equations and variables used in this model appear as Figure 3.4.14.

The last possibilty investigated was a transfer from the interplanetary trajectory to Deimos; before parking orbit is established. This maneuver was considered specifically for the unmanned probe to Deimos. To effect this transfer, Lambert targeting was used, see Figure 3.4.15. This involved using the subroutine SLMBRT in the Mission Subroutine Library, the programs and samples of the output appear as Figs. 3.4.16-.18. The initial and final position vectors relative to Mars are the required inputs to the subroutine. The initial position vector was found given the right ascension and declination of the v-infinity vector relative to the center of Mars. Given these two parameters, the v-infinity vector was decomposed into rectangular components. To find a radius vector, the velocity vector was multiplied by a unit of time. Here, the unit of time was days. The time was varied from one to seven days to determine what the

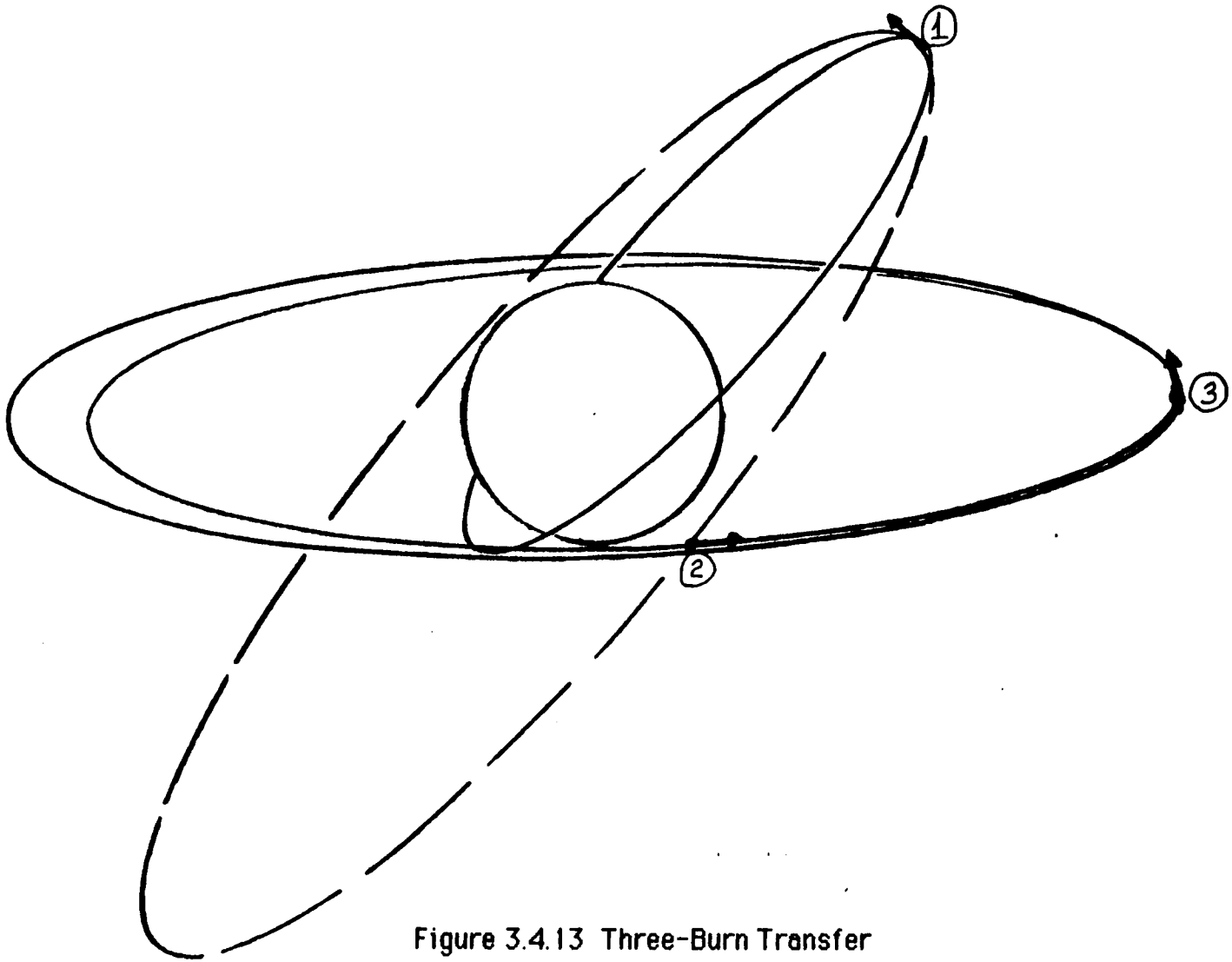

Figure 3.4.13 Three-Burn Transfer

```
pi      = acos(-1.0)
-mu/(2*a) = (vap^2)/2-(mu/rap)
vcap    = sqrt(mu/rap)*.9
delv1   = vcap-vap
vmoon   = sqrt(mu/rmoon)
delv2    = sqrt(vcap^2+vmoon^2-2*vcap*vmoon*cos(i))

 delv3   = sqrt(mu/rap)*.1
 dvt     = delv1+delv2+delv3
```

St	Input	Name	Output	Unit	Comment
	42828	mu		km^3/s^2	gravitational parameter
	6724.2	a		km	semi-major axis p.o.
		vap	1.6121836	km/s	vel. at apoapsis
	9550.9	rap		km	radius at apoapsis
		vcap	1.9058304	km/s	vel. to circ. @ apoapsis
		dvcir		km/s	delta-vee to circ.
		vmoon	2.1288644	km/s	vel. of the moon
	9450	rmoon		km	radius of moon
		delv		km/s	delta-v of plane change
	64.12	i		deg	plane inclination
	8595.81	aor		km	semi-maj. axis of new orbit
	23500	amoon		km	semi-maj. axis of moon orbit
		pi	3.1415927		
		delv1	.29364683	km/s	
		delv2	2.149968	km/s	
		delv3	.21175894	km/s	
		dvt	2.6553738	km/s	

Figure 3.4.14 TK! Solver Model: Three-Burn Transfer

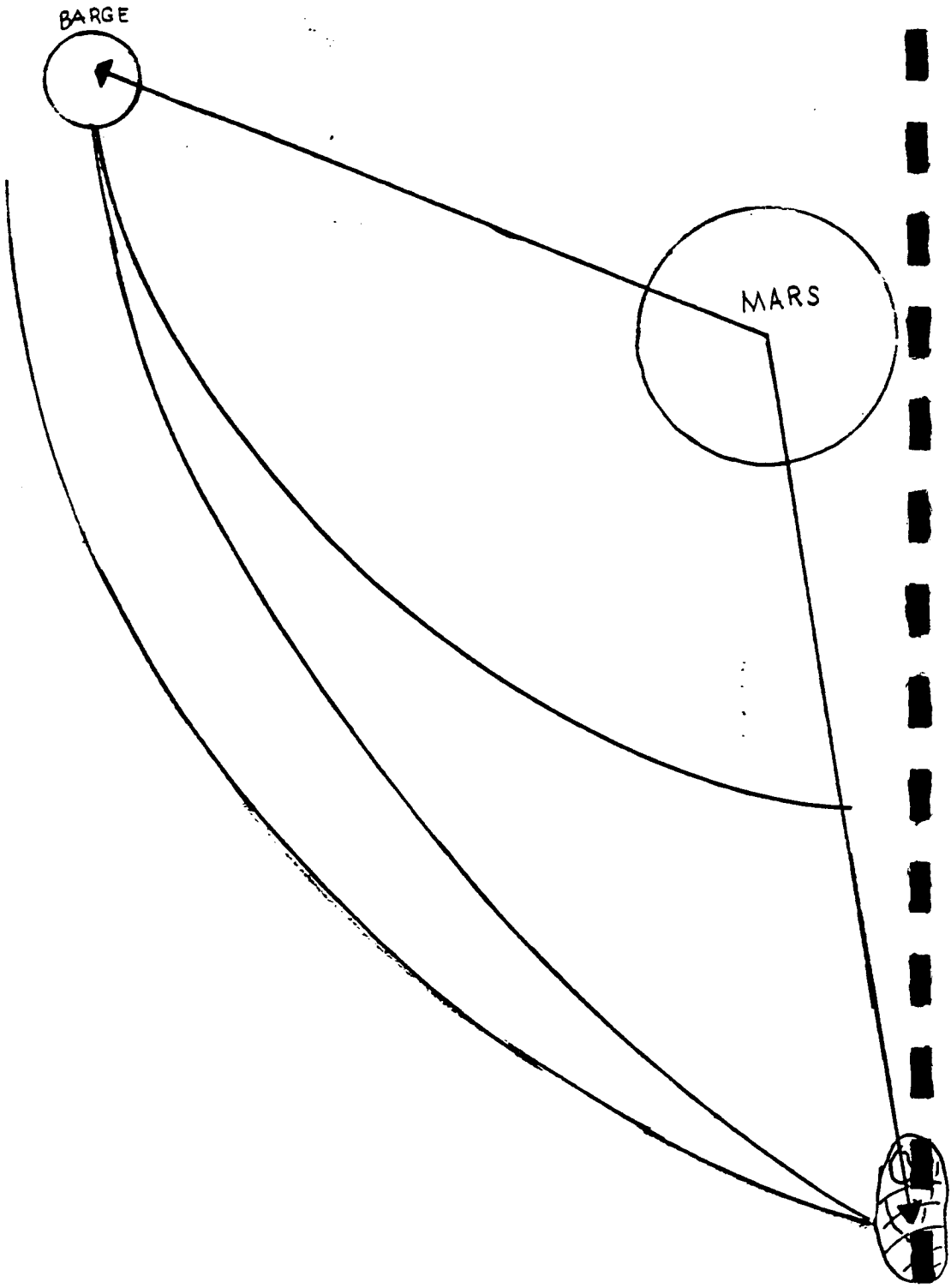

Figure 3.4.15 Lambert Targeting

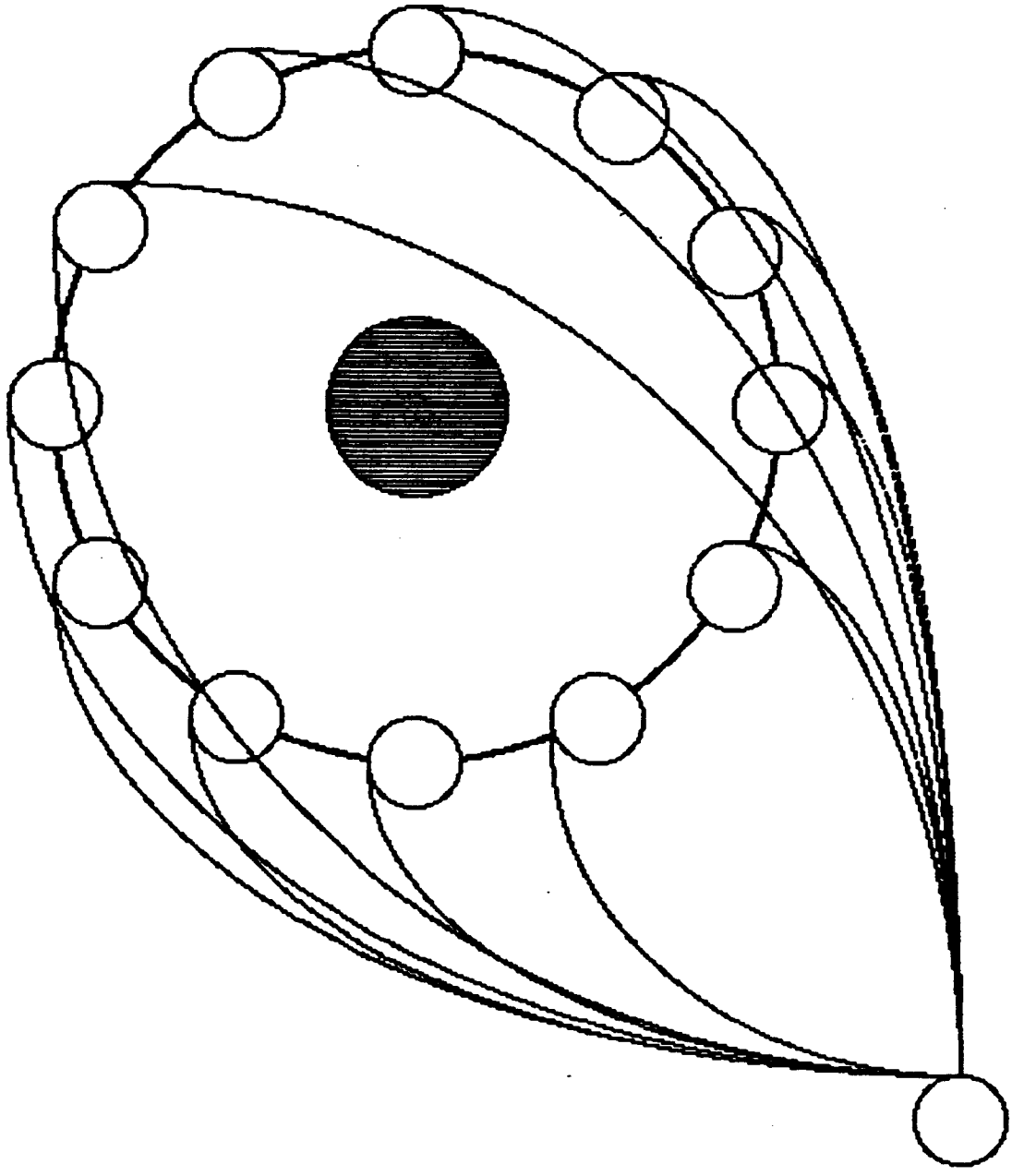

Figure 3.4.16 Lambert Targeting of the Orbit of Deimos

```
      PROGRAM OOPS(INPUT,OUTPUT,TAPE5=INPUT,TAPE6=OUTPUT)
      DIMENSION RI(3),RT(3),VI(3),VT(3),ESETC(8),P(7),X(3),XDOT(3)
      DIMENSION VCIR(3),DV1(3),DV2(3),VINFI(3)
      PI=ACOS(-1.0)
C     DETERMINE RECTANGULAR, MARS-CENTERED POSITION VECTOR OF BARGE
C     V-INFINITY OF THE BARGE IN THE INTERPLANETARY TRAJECTORY
      VIN=17793.0
C     CHANGE V-INFINITY FROM FEET PER SEC TO KM/DAY
      VINF=VIN*3600.0*24.0*12.0*2.54/1E05
C     INITIALIZE TIME PARAMETER FROM 1 TO 7 DAYS
      DO 10 I=1,7
C     CALCULATE POSITION VECTOR MAGNITUDE GIVEN V-INFINITY
C     AND TIME
      RIMAG=I*VINF
C     CALCULATE THE Z-COMPONENT OF THE POSITION VECTOR
C     GIVEN THE DECLINATION OF THE V-INFINITY VECTOR
C     AND ITS MAGNITUDE
      RI(3)=SIN(.3281)*RIMAG
C     BY GEOMETRY, CALCULATE THE X- AND Y-COMPONENTS OF THE
C     POSITION VECTOR GIVEN THE RIGHT ASCENSION OF
C     THE V-INFINITY VECTOR AND THE MAGNITUDE OF ITS
C     PROJECTION IN THE PLANE
      RPROJ=SQRT(RIMAG**2-RI(3)**2)
      RI(1)=SIN(.311)*RPROJ
      RI(2)=COS(.311)*RPROJ
C     COMPENSATE THE Z-COMPONENT FOR THE RADIUS OF MARS
      RI(3)=RI(3)+4000.0
C     DETERMINE COMPONENTS OF THE V-INFINITY VECTOR
C     OF THE BARGE IN KM/SEC
      VINFI(1) = (RI(1)/(I*24.0*3600.0))
      VINFI(2) = (RI(2)/(I*24.0*3600.0))
      VINFI(3) = ((RI(3)-4000.0)/(I*24.0*3600.0))
      WRITE(6,15) I
   15 FORMAT(//,'THIS IS FOR',I2, 'DAY(S)')
      WRITE(6,20) RI
   20 FORMAT(//,'RI(1)=',E12.7,/,'RI(2)=',E12.7,/,'RI(3)=',E12.7)

C     DETERMINE THE MARS-CENTERED POSITION VECTOR OF DEIMOS
C     AT 30 DEGREE INCREMENTS AROUND ITS ORBIT
      DO 5 J=30,360,30
      Y=J
C     THE ORBITAL RADIUS OF DEIMOS IS :
      R=23500.0
C     ASSUME THE Z-COMPONENT OF DEIMOS' MARS-CENTERED POSITION
C     VECTOR IS ZERO BECAUSE THE ANGLE BETWEEN THE ECLIPTIC AND
C     THE EQUATORIAL IS APPROXIMATELY ONE DEGREE
      RT(3)=0.0
C     CONVERT FROM DEGREES TO RADIANS
      XX=DETORAD(Y)
C     DECOMPOSE THE ORBITAL RADIUS INTO X- AND Y-COMPONENTS
C     OF THE POSITION VECTOR
      RT(1)=R*COS(XX)
      RT(2)=R*SIN(XX)
      WRITE(6,25) RT
   25 FORMAT(//,'RT(1)=',E12.7,/,'RT(2)=',E12.7,/,'RT(3)=',E12.7)
C     COMPUTE THE COMPONENTS OF THE VELOCITY VECTOR OF DEIMOS
C     AGAIN ASSUMING THE Z-COMPONENT OF VELOCITY IS NEGLIGIBLE
C     USE THE CIRCULAR VELOCITY OF DEIMOS
      GRAVP = 42828.0
      VCIRC=SQRT(GRAVP/R)
      VCIR(3)=0.0
```

Figure 3.4.17 Lambert Code: Orbital Element Method

```
      VCIR(1)= VCIRC*COS(XX)
      VCIR(2)= VCIRC*SIN(XX)
C     INPUT INTO SLMBRT TRANSFER TIME, TRANSFER ANGLE,(GREATER OR
C     LESS THAN PI),AND THE GRAVITATIONAL PARAMETER OF MARS
      P(1)=I
      P(2)=PI/3.0
      P(7)=3.214E14
C     GIVEN THE INITIAL POSITION VECTOR FROM MARS TO THE BARGE
C     IN THE INTERPLANETARY TRAJECTORY AND THE FINAL POSITION VECTO
C     VECTOR FROM MARS TO DEIMOS, SLMBRT RETURNS THE RESPECTIVE
C     INITIAL AND FINAL VELOCITY VECTORS
      CALL SLMBRT(P,RI,RT,VI,VT,IERR)
C     CONVERT THE VELOCITY VALUES FROM KM/DAY TO KM/SEC
      VI(1)=VI(1)/(24.0*3600.0)
      VI(2)=VI(2)/(24.0*3600.0)
      VI(3)=VI(3)/(24.0*3600.0)
      VT(1)=VT(1)/(24.0*3600.0)
      VT(2)=VT(2)/(24.0*3600.0)
      VT(3)=VT(3)/(24.0*3600.0)
      WRITE(6,35) VI,VT
   35 FORMAT(//,'VI(1)=',E12.7,/,'VI(2)=',E12.7,/,'VI(3)=',E12.7
     +/,'VT(1)=',E12.7,/,'VT(2)=',E12.7,/,'VT(3)=',E12.7)
C     COMPUTE THE DELTA-VEE AT DEPARTURE BETWEEN V-INFINITY OF
C     THE BARGE AND VI, LAMBERT VELOCITY
      DV1(1) = VINFI(1)-VI(1)
      DV1(2) = VINFI(2)-VI(2)
      DV1(3) = VINFI(3)-VI(3)
      WRITE(6,*) DV1
      DVTOT1 = SQRT(DV1(1)**2 + DV1(2)**2 + DV1(3)**2)
C     COMPUTE THE DELTA-VEE AT ARRIVAL BETWEEN MOON VELOCITY
C     AND VT, LAMBERT VELOCITY
      DV2(1) = VCIR(1)-VT(1)
      DV2(2) = VCIR(2)-VT(2)
      DV2(3) = VCIR(3)-VT(3)
      WRITE(6,*) DV2
      DVTOT2 = SQRT( DV2(1)**2 + DV2(2)**2 + DV2(3)**2)
      DVTOT  = DVTOT1 + DVTOT2
      WRITE(6,86) DVTOT
   86 FORMAT(//,'THE TOTAL DELTA-VEE IS',F12.7,'KM/SEC')
    5 CONTINUE
   10 CONTINUE
      STOP
      END
      FUNCTION DETORAD(X)
      PI=ACOS(-1.0)
      DETORAD=(PI/180.0)*X
      RETURN
      END
```

(Fig. 3.4.17 Continued)

```
      PROGRAM SPIT(INPUT,OUTPUT,TAPE5=INPUT,TAPE6=OUTPUT)
      DIMENSION RI(3),RT(3),VI(3),VT(3),ESETC(8),P(7),X(3),XDOT(3)
      DIMENSION VINFI(3),DV1(3),DV2(3)
      PI=ACOS(-1.0)
C     DETERMINE RECTANGULAR, MARS-CENTERED POSITION AND VELOCITY
C     VECTOR OF BARGE GIVEN V-INFINITY OF THE BARGE
      VIN=17793.0
C     CONVERT V-INFINITY FROM FEET PER SEC TO KM/DAY
      VINF=VIN*3600.0*24.0*12.0*2.54/1E05
C     INITIALIZE TIME PARAMETER FROM ONE TO SEVEN DAYS
      DO 10 I=1,7
C     DETERMINE MAGNITUDE OF POSITION VECTOR, RIMAG,
C     GIVEN V-INFINITY AND AN INTERVAL OF TIME IN DAYS
      RIMAG=I*VINF
C     DETERMINE Z-COMPONENT GIVEN RIMAG AND THE DECLINATION
C     OF THE V-INFINITY VECTOR
      RI(3)=SIN(.3281)*RIMAG
C     DETERMINE THE X- AND Y-COMPONENTS OF THE POSITION
C     VECTOR GIVEN RIMAG AND THE RIGHT ASCENSION OF V-INFINITY
      RPROJ=SQRT(RIMAG**2-RI(3)**2)
      RI(1)=SIN(.311)*RPROJ
      RI(2)=COS(.311)*RPROJ
      RI(3)=RI(3)+4000.0
C     COMPENSATE Z-COMPONENT FOR RADIUS OF MARS
      WRITE(6,15) I
C     DETERMINE COMPONENTS OF THE V-INFINITY VECTOR
C     OF THE BARGE IN KM/SEC
      VINFI(1) = (RI(1)/(I*24.0*3600.0))
      VINFI(2) = (RI(2)/(I*24.0*3600.0))
      VINFI(3) = ((RI(3)-4000.0)/(I*24.0*3600.0))
   15 FORMAT(//,'THIS IS FOR ',I2,'DAY(S)')
      WRITE(6,20) RI
   20 FORMAT(//,'RI(1)=',E12.7,/,'RI(2)=',E12.7,/,'RI(3)=',E12.7)

C     THE ORBITAL ELEMENTS OF DEIMOS ARE
      ESETC(1)= 47000.0
      ESETC(2)= 0.0028
      ESETC(3)= .03142
      ESETC(4)= 2.356
      ESETC(5)= 1.571
      ESETC(6)= 1.0
      ESETC(7)= 3.214E14
      ESETC(8)= 1.26
C     GIVEN THE ORBITAL ELEMENTS OF DEIMOS,
C     OETORC RETURNS THE RECTANGULAR, MARS-CENTERED
C     COMPONENTS OF DEIMOS' POSITION AND VELOCITY VECTORS
      CALL OETORC(ESETC,X,XDOT)
      RT(1)=X(1)
      RT(2)=X(2)
      RT(3)=X(3)
      WRITE(6,25) RT
   25 FORMAT(//,'RT(1)=',E12.7,/,'RT(2)=',E12.7,/,'RT(3)=',E12.7)

C     CHANGE THE UNITS OF XDOT, THE MOON VELOCITY, FROM
C     KM/DAY TO KM/SEC
      XDOT(1)=XDOT(1)/(24.0*3600.0)
      XDOT(2)=XDOT(2)/(24.0*3600.0)
      XDOT(3)=XDOT(3)/(24.0*3600.0)

C     GIVEN INPUTS OF TRANSFER TIME, (HERE IN DAYS), TRANSFER
C     ANGLE, (GREATER OR LESS THAN PI), AND THE GRAVITATIONAL
```

Figure 3.4.18 Lambert Code: Geometric Method

```
C     PARAMETER OF MARS IN KM/DAY AS WELL AS THE INITIAL
C     AND FINAL POSITION VECTORS; SLMBRT RETURNS THE INITIAL
C     AND FINAL VELOCITY VECTORS
C     THE INITIAL POSITION VECTOR IS MEASURED FROM MARS
C     TO THE BARGE IN THE INTERPLANETARY TRAJECTORY AND
C     THE FINAL POSITION VECTOR IS MEASURED FROM MARS TO DEIMOS
C     THE POSIITON VECTOR TO DEIMOS IS FOUND AT TEN EQUAL
C     INTERVALS OF DEIMOS PERIOD TO YIELD A LOCI OF VELOCITY
C     VECTORS AT EVERY ONE-TENTH OF THE ORBIT PERIOD
      P(1)=1
      P(2)=PI/3.0
      P(7)=3.214E14

      CALL SLMBRT(P,RI,RT,VI,VT,IERR)
C     CHANGE THE UNITS OF THE VELOCITY VECTORS FROM
C     KM/DAY TO KM/SEC

      VI(1)=VI(1)/(24.0*3600.0)
      VI(2)=VI(2)/(24.0*3600.0)
      VI(3)=VI(3)/(24.0*3600.0)
      VT(1)=VT(1)/(24.0*3600.0)
      VT(2)=VT(2)/(24.0*3600.0)
      VT(3)=VT(3)/(24.0*3600.0)
      WRITE(6,30) VI,VT
   30 FORMAT(//,'VI(1)=',E12.7,/,'VI(2)=',E12.7,/,'VI(3)=',E12.7,
     +//,'VT(1)=',E12.7,/,'VT(2)=',E12.7,/,'VT(3)=',E12.7)
C     COMPUTE THE DELTA-VEE AT DEPARTURE BETWEEN V-INFINITY
C     OF THE BARGE AND VI, LAMBERT VELOCITY
      DV1(1) = VINFI(1)-VI(1)
      DV1(2) = VINFI(2)-VI(2)
      DV1(3) = VINFI(3)-VI(3)
      WRITE(6,*) DV1
C     COMPUTE THE DELTA-VEE AT ARRIVAL BETWEEN MOON VELOCITY
C     AND VT, LAMBERT VELOCITY
C     MOON VELOCITY IS GIVEN BY GETORC AS THE ARRAY XDOT
      DV2(1) = XDOT(1)-VT(1)
      DV2(2) = XDOT(2)-VT(2)
      DV2(3) = XDOT(3)-VT(3)
      WRITE(6,*) DV2
      DVTOT1 = SQRT(DV1(1)**2+DV1(2)**2+DV1(3)**2)
      DVTOT2 = SQRT(DV2(1)**2+DV2(2)**2+DV2(3)**2)
      DVTOT = DVTOT1+DVTOT2
      WRITE(6,66) DVTOT
   66 FORMAT(//, ,'THE TOTAL DELTA-VEE IS ',F12.7,' KM/SEC')
   10 CONTINUE
      STOP
      END
```

(Fig. 3.4.18 Continued)

optimum time would be to send the probe.

Two methods of determining the final position vector have been considered. One method involves determining the rectangular components of Deimos relative to the center of Mars by inputting the orbital elements of Deimos into the subroutine OETORC. This mission library subroutine takes seven orbital elements and returns the rectangular components. The problem with this method is that the orbital elements of Deimos are not accurate for the time period in question. The second method involves finding the rectangular components by assuming Deimos orbit is circular about Mars. Given the orbital radius of Deimos, the final position vector is found at 30 degree increments around the orbit of Deimos using trigonometry, see Figure 3.4.19. Using this method, a locus of final position vectors can be calculated. The problem with this method is that the x and y components can be found but the z-component must be assumed to be zero.

After these two position vectors are calculated and input to SLMBRT, the subroutine will return the initial and final velocity vectors of both the barge and Deimos relative to Mars. To complete the analysis, the velocity of the moon must be subtracted vectorially from the final velocity vector. The initial velocity vector does not need to be modified because the original v-infinity vector was determined relative to the velocity of Mars. The vectorial difference of the modified final position vector and the initial position vector is the delta-v vector. Values of delta-v are then easily obtained.

The method of final position vector determination by use of orbital elements gave the lower values of delta-v ranging from 6.20 km/sec to 7.76 km/sec. Delta-v values obtained from the geometric method ranged from

ORBITAL ELEMENT METHOD

THIS IS FOR 1DAY(S)

THE TOTAL DELTA-VEE IS 6.8841540 KM/SEC

THIS IS FOR 7DAY(S)

THE TOTAL DELTA-VEE IS 6.9871454 KM/SEC

THIS IS FOR 1DAY(S)

THE TOTAL DELTA-VEE IS	10.2177759KM/SEC	30°
THE TOTAL DELTA-VEE IS	10.1173057KM/SEC	60°
THE TOTAL DELTA-VEE IS	10.0836178KM/SEC	90°
THE TOTAL DELTA-VEE IS	9.4349195KM/SEC	120°
THE TOTAL DELTA-VEE IS	7.8694737KM/SEC	150°

THIS IS FOR 7DAY(S)

THE TOTAL DELTA-VEE IS	8.5798838KM/SEC	30°
THE TOTAL DELTA-VEE IS	8.6262904KM/SEC	60°
THE TOTAL DELTA-VEE IS	8.3102238KM/SEC	180°
THE TOTAL DELTA-VEE IS	8.3416239KM/SEC	330°
THE TOTAL DELTA-VEE IS	8.4838210KM/SEC	360°

Figure 3.4.19 Lambert Delta-V Output

7.92 km/sec to 10.11 km/sec. As one would expect, the delta-v values decrease the further the barge is from Deimos. This would imply that it would be best to send the probe approximately seven days prior to Mars orbital insertion.

A study was completed to determine the effects of changing the inclination and eccentricity of the parking orbit on delta-v values to Phobos orbit. To effect this end, one of the orbit scenarios had to be chosen. The two-burn trajectory with the apsidal line perpendicular to the line of nodes was found to require the least delta-v and hence was utilized for this analysis. However, the four-burn trajectory should also be considered because phasing can then be used to simplify rendezvous maneuvers. It was not used in this analysis, however, to simplify the calculations.

A TK! Solver model, Fig. 3.4.20, was created in which eccentricity was varied from 0.0 to 0.5 for a given inclination. The inclinations varied from the current value of 64.12 degrees to 0.0 degrees with 36.0 degrees as an intermediate value. For each case, the original two-burn model was used to determine the delta-i lower, (ie.,the inclination to take out at first burn,) to minimize delta-v. After this lower inclination was determined, it was thereafter held fixed. The radius at periarian was also held fixed because at periarian the orbit reaches Phobos orbit. Since this is a desirable characteristic, it was left unchanged.

The two-burn trajectory was then modified such that delta-i lower was held fixed and eccentricity and the radius at apoarian were variable. As the eccentricity is changed, the radius at apoarian is also affected. A range of delta-v values was produced for twelve values of eccentricity. As expected, at 0.0 degrees inclination the delta-v values were the the

St	Input	Name	Output	Unit	Comment
		vc1		km/s	Lower orbit Velocity
	42828	mu		km^3/s^2	Graviational Parameter
		r1	5846.25	km	Lower Orbit Radius
		vtp	3.0085942	km/s	Perigee Transfer velocity
	9450	r2		km	Outer orbit radius
		dv1	.0316074	km/s	Delta v #1
		vta	1.8612692	km/s	Apogee transfer Velocity
		vc2	2.1288644	km/s	Higher Orbit Velocity
		dv2	1.2428599	km/s	Delta v #2
	36	dit		deg	Inclination between orbits
L		dvt	2.2211519	km/s	Total Delta v
	.5	dil		deg	Lower Delta Inclination
	35.5	dih		deg	Higher Delta Inclination
		vp1	3.0260787	km/s	velocity of park.orb.@ peria
L		ap		km	semi-major axis of park orb.
L	0	e			
	3897.5	rp		km	radius at periapsis
L		ra		km	radius at apoapsis of P.O.

```
* vp1 = sqrt(mu*(2/r1-1/ap))
* vtp = sqrt(2*mu*(1/r1-1/(r1+r2)))
* dv1 = sqrt(vtp^2+vp1^2-2*vtp*vp1*cos(dil))
* vta = sqrt(2*mu*(1/r2-1/(r1+r2)))
* vc2 = sqrt(mu/r2)
* dv2 = sqrt(vta^2+vc2^2-2*vta*vc2*cos(dih))
* dvt = dv1 + dv2
* dit = dil + dih
* r1  = ap*(1-e^2)
* rp  = ap*(1-e)
* ra  = ap*(1+e)
```

Figure 3.4.20 TK! Solver Model:
Delta-V Budget with Varying Eccentricity and Inclination

smallest and became even smaller with increasing eccentricity. These values ranged from .28 km/sec to 1.13 km/sec. A plot and an accompanying table appear as Fig. 3.4.21. A similar analysis completed at 36 degrees produced a range of delta-v values from 1.27 km/sec to 1.87 km/sec. A plot of delta-v vs. eccentricity and an accompanying table of the results were generated and appear as Fig. 3.5.22. Delta-v values shot up dramatically for the 64.12 degree inclination and the range of delta-v's was smaller than for the previous two cases. Values ranged from 2.16 km/sec to 2.65 km/sec. A plot generated of delta-v vs. eccentricity shows that beyond an eccentricity of approximately 0.47, the values of delta-v level off. This plot and an accompanying table appear as Fig. 3.5. 23.

The results of this study indicate that it would perhaps be worthwhile to modify the existing parking orbit to a lower inclination to accommodate the transfer missions to Phobos. From the energy requirement standpoint, an equatorial orbit would be highly desirable but would severely limit the attainable latitudes on Mars. The current parking orbit was chosen primarily to accommodate trans-Earth injection but considering all the possible traffic to and from Phobos, it would be well-advised to relax this constraint to save the energy needed to make such a large plane change time and time again.

We recommend that serious consideration be given to developing a new parking orbit. Additionally, proximity maneuvers should be investigated to rendezvous with a moon once moon orbit has been achieved. This entails studying the feasibilty of C-W targetting and equations. Initial calculations were made that imply that Mars is the dominant body for targetting maneuvers.

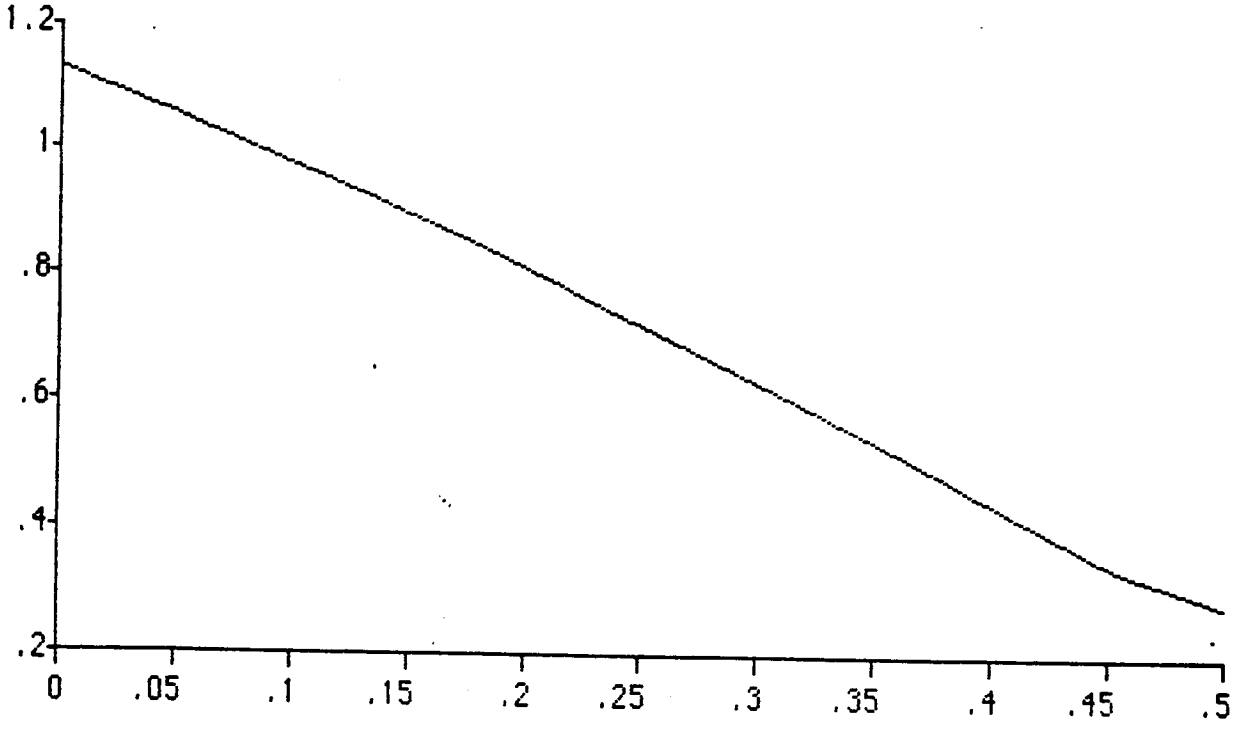

DELTA-V VS. ECCENTRICITY

DELTA-V WITH VARYING ECCENTRICITY: i= 0

ECCENTRICITY	SEMI-MAJ. AX	APOAP. RAD	DELTA-V
0	3897.5	3897.5	1.13166828
.04545454545455	4083.0952381	4268.69048	1.06349632
.09090909090909	4287.25	4677	.992395764
.13636363636364	4512.8947368	5128.28947	.918509263
.18181818181818	4763.6111111	5629.72222	.842003495
.22727272727273	5043.8235294	6190.14706	.76306486
.27272727272727	5359.0625	6820.625	.681894863
.31818181818182	5716.3333333	7535.16667	.598705431
.36363636363636	6124.6428571	8351.78571	.513714343
.40909090909091	6595.7692308	9294.03846	.427140985
.45454545454545	7145.4166667	10393.3333	.339202543
.5	7795	11692.5	.285079551

Figure 3.4.21 Delta-V vs. Eccentricity:
Inclination i=0°

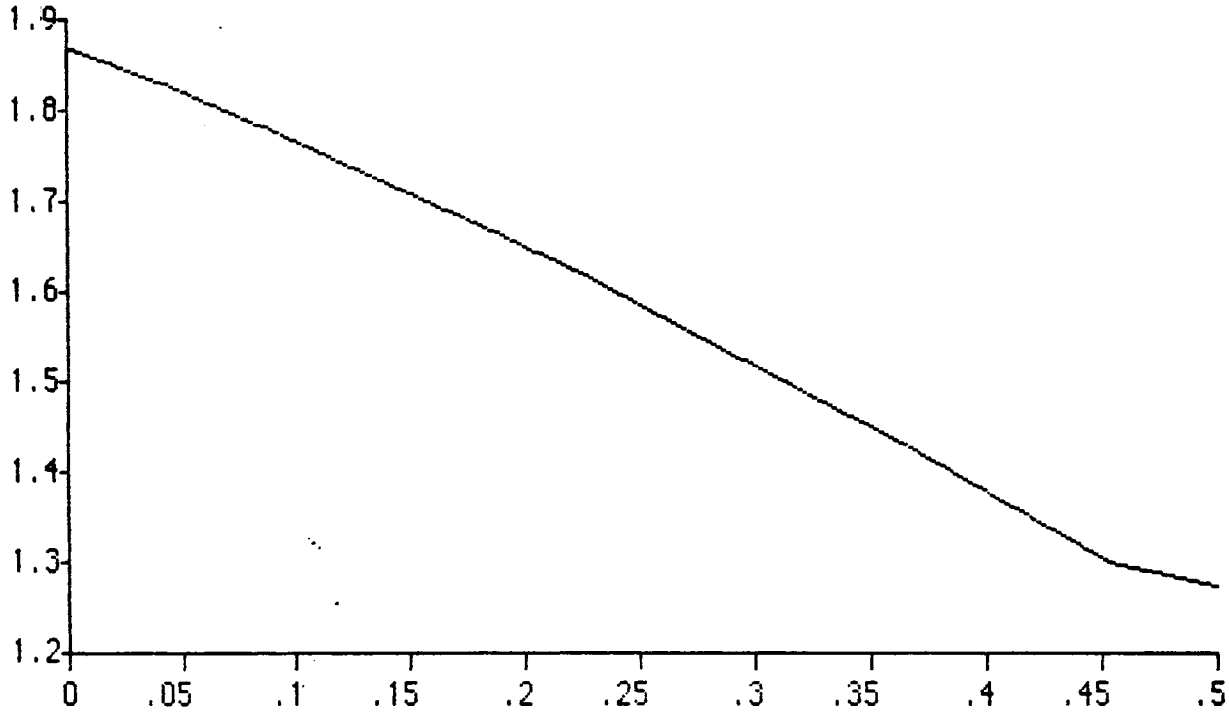

DELTA-V VS. ECCENTRICITY

DELTA-V WITH VARYING ECCENTRICITY: i=36

ECCENTRICITY	SEMI-MAJ. A	APOAP. RADI	DELTA-V
0	3897.5	3897.5	1.87127237
.04545454545455	4083.095238	4268.690476	1.82681746
.09090909090909	4287.25	4677	1.77898319
.13636363636364	4512.894737	5128.289474	1.72792339
.18181818181818	4763.611111	5629.722222	1.67381853
.22727272727273	5043.823529	6190.147059	1.61687351
.27272727272727	5359.0625	6820.625	1.55731765
.31818181818182	5716.333333	7535.166667	1.49541199
.36363636363636	6124.642857	8351.785714	1.43148248
.40909090909091	6595.769231	9294.038462	1.36607757
.45454545454545	7145.416667	10393.33333	1.30125398
.5	7795	11692.5	1.27446728

Figure 3.4.22 Delta-V vs. Eccentricity
Inclination i=36°

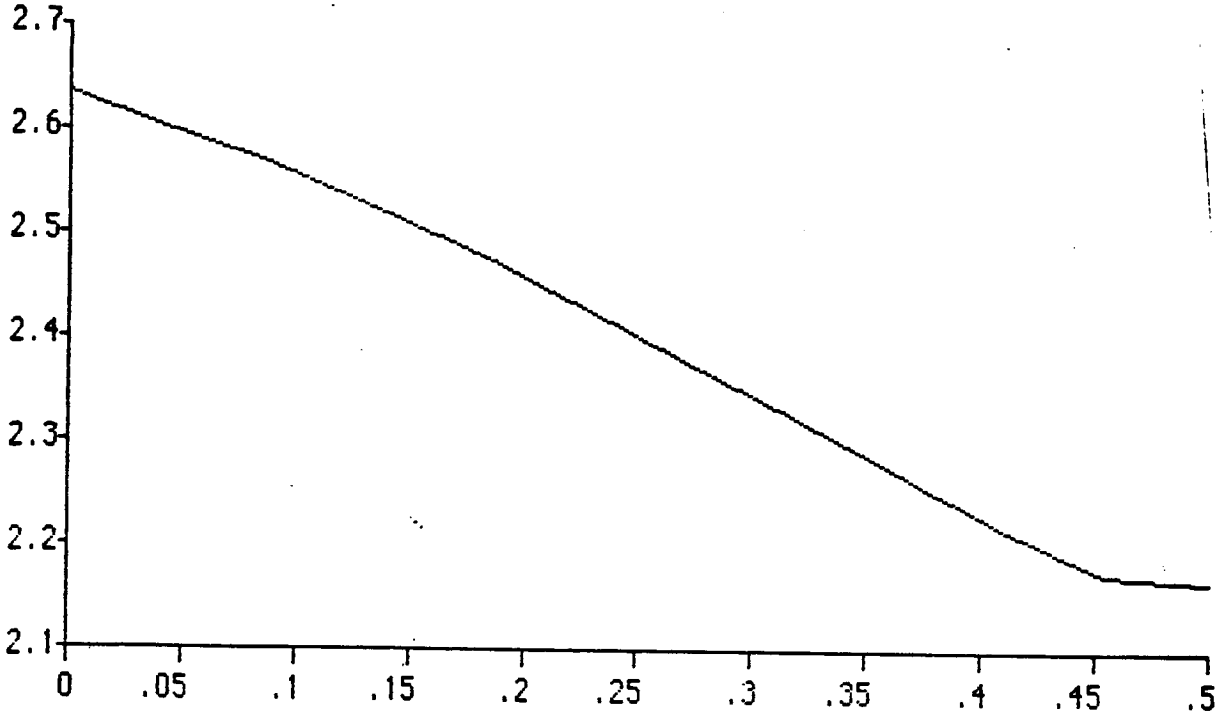

delta-v vs. eccentricity

DELTA-V WITH VARYING ECCENTRICITY; I=64.12

DEL-VTOT	ECCENTRICIT	APO. RADIUS	SEMI-MAJ. AXIS
2.635069846	0	3897.5	3897.5
2.60112627	.0454545455	4268.690476	4083.095238095
2.563268843	.0909090909	4677	4287.25
2.521728033	.1363636364	5128.289474	4512.894736842
2.476774937	.1818181818	5629.722222	4763.611111111
2.428734035	.2272727273	6190.147059	5043.823529412
2.378015426	.2727272727	6820.625	5359.0625
2.325200066	.3181818182	7535.166667	5716.333333333
2.271292415	.3636363636	8351.785714	6124.642857143
2.218625059	.4090909091	9294.038462	6595.769230769
2.174931334	.4545454545	10393.33333	7145.416666667
2.167014461	.5	H692.5	7795

Figure 3.4.23 Delta-V vs. Eccentricity
Inclination i=64.12°

3.5 MARS MOON ORBITAL TRANSFER AND RECONNAISSANCE VEHICLE

The projected use of the Mars Moon Orbital Transfer and Reconnaissance Vehicle (TRV) will be to ferry the exploration party from the Mar's Payload Transfer Vehicle (MPTV) to the moon Phobos. The TRV will also be upgradable for use in excursions to the moon Deimos and for deploying satellites about Mars.

A preliminary design study has been conducted on the basic configuration of the TRV. The study primarily concerned the logistics of module exchange and upgrading along with overall TRV upgrade capacity. Another key consideration of the study thus far has been the possibility that the vehicle may sink in a deep layer of moon dust.

3.5.1 VEHICLE CONFIGURATIONS UNDER CONSIDERATION

There are two basic design types under consideration, an excursion vehicle similar to the Apollo Lunar Module (LM) in shape and function (shown in Figure 3.5.1). The other type is a modular transport bus design. .

There are two basic subclasses of the modular transport vehicle: the closed truss system and the open truss system. A general closed truss system is shown in Figure 3.5.2. The external truss lends its rigidity and strength to the TRV and contains the various modules inside its structure. The open truss structure provides no containing walls to the TRV and consists primarily of a truss plane on which the components and mounted. A generalized open truss TRV is shown in Figure 3.5.3.

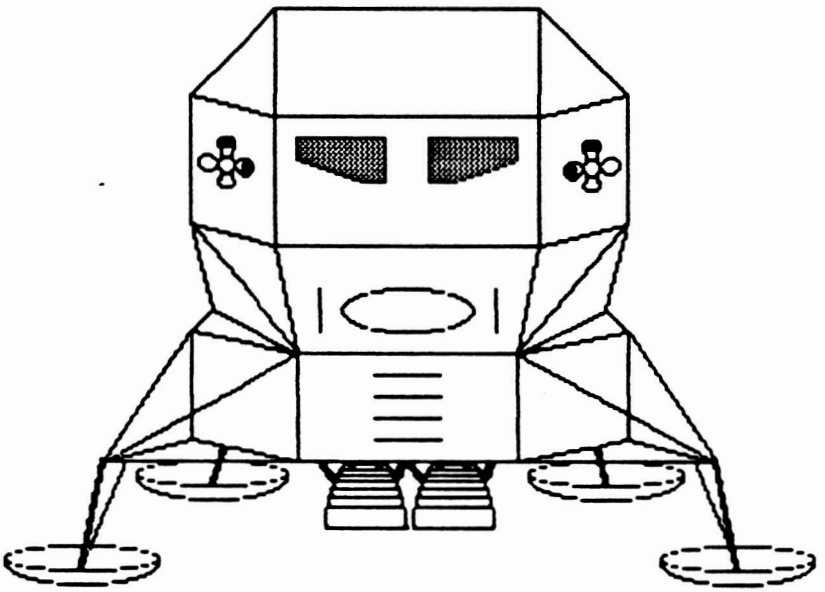

Figure 3.5.1 Generalized Lunar Module-Type
Transfer/Reconnaissance Vehicle

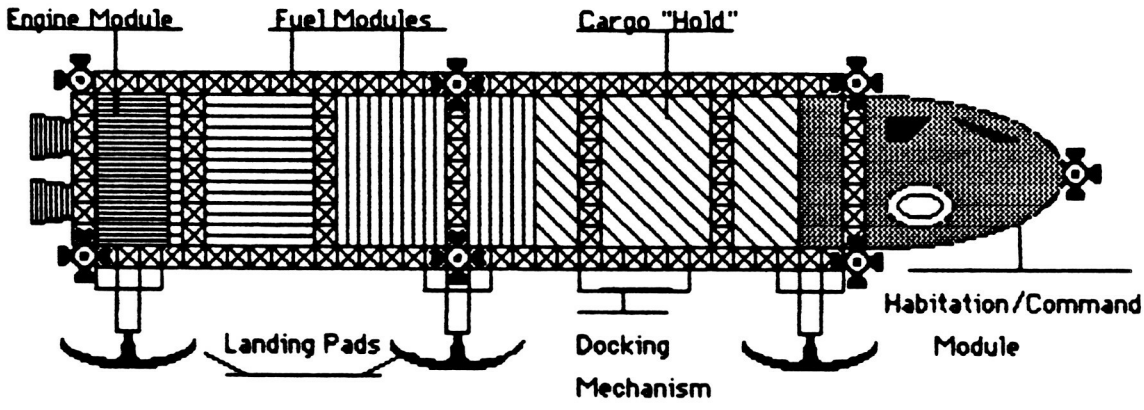

Figure 3.5.2 Generalized Closed Truss Bus

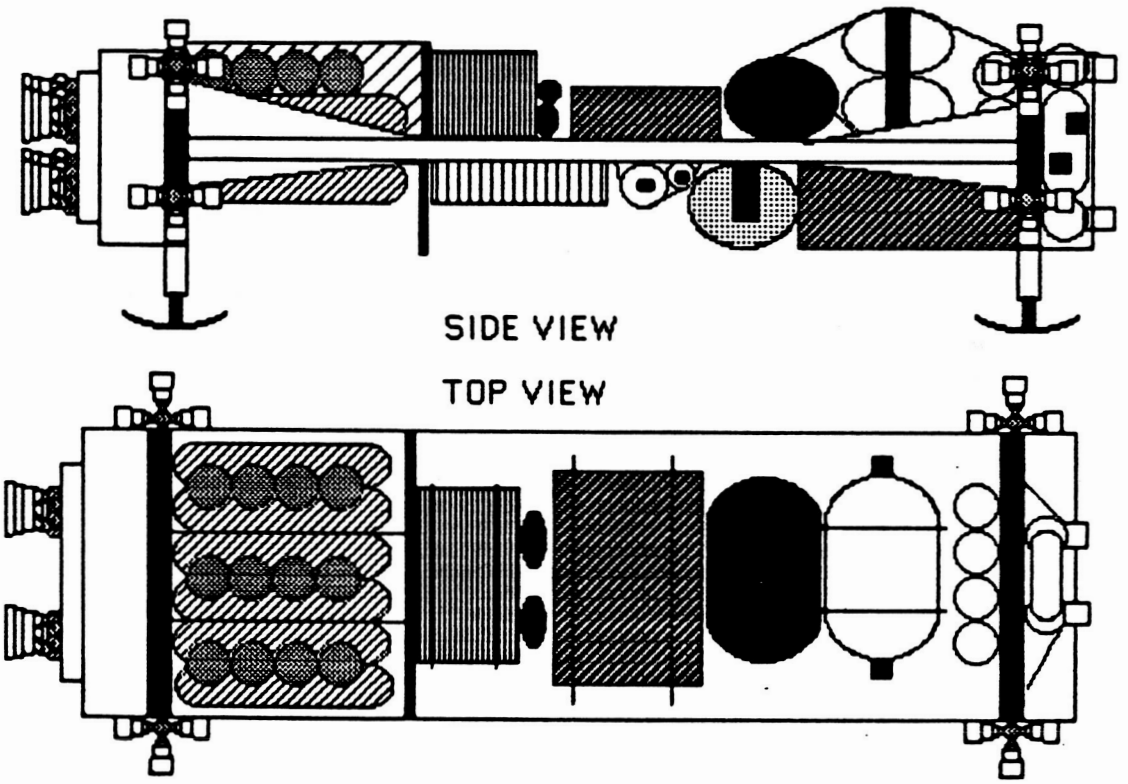

Figure 3.5.3 Generalized Open Truss Bus
(Flatbed TRV)

3.5.2 PRELIMINARY EVALUATION OF VEHICLE DESIGNS

3.5.2.1 EVALUATION CRITERIA

The preliminary design criteria were broadly stated so as to eliminate some ship designs with major shortcomings quickly. Table 3.5.1 shows the selection criteria chart and the results of the preliminary evaluation.

The ship must be able to land on the moon's surface and take off again. Due to the low gravity of the moons the structural limits of the TRV are not of major concern in this respect; the maximum sink depth of the vehicle in a loose soil enviroment is. To minimize the sink depth in the event that the landing gear is insufficient to support the vehicle above the surface, the base area of the vehicle must be reasonably large to allow the vehicle to "float" on the soil.

Modularity is a key feature of the design of the TRV. Because of the distance from Earth-based repair and manufacturing facilities, the vehicle must accommodate the capacity for repair and upgrade on site. To facilitate ease of repair and upgrade, the vehicle must be inherently modular. This will permit quick changeout of subsystems and remote repair and testing of subsystems as whole units.

Due to the isolation of the Mars system from the Earth the TRV must be able to perform a variety of missions. As all of the potential uses of the TRV have not been considered at this point, the capacity of the TRV for expansion must be included in the preliminary design. It is hoped that the TRV will eventually be upgradable into a vehicle that has the capacity to transport payload into the asteroid belt as future missions dictate. This expansibility will probably be implemented by the joining of the structures

of multiple TRV's together to form a larger vehicle or provision for additional modules on the baseline TRV as required for extended missions.

A final preliminary criterion was the ability of the TRV to handle a wide variety of cargos. Since the TRV is to provide orbital transport for the first mission to Mars and all the subsequent missions the varieties of cargos that the TRV is to carry can not be accurately modeled at this time. In response to this the TRV is being designed to accommodate as large a variety of shapes and sizes of payloads as possible.

3.5.2.2 EVALUATION RESULTS

As a result of our preliminary study of TRV's the following designs were dropped: the LM derived TRV (Figure 3.5.1) and the closed bus TRV (Figure 3.5.2). The general results of the study can be seen in Table 3.5.1.

The Apollo LM derived TRV provided a rigid, formed structure that limited the expansion capacity of the TRV and thus failed to meet the modularity criterion. The future expansion of the vehicle was limited by the same rigid structure that limited the modularity. The LM type TRV also failed to provide sufficent protection from the sink possiblility. As a result of sink the engines could become covered and/or clogged, possibly endangering the TRV, mission and crew. The cargo envelope is severely restricted due again to the rigid structure of the TRV. The cargo would have to go inside the main structure of the vehicle, thus taking up crew and fuel space. Access to the cargo required large doors in the structure, thus increasing the weight of the overall vehicle without providing any additional useful function. As a result of these failures to meet any of the criteria the LM type TRV design has been dropped from the analysis.

Table 3.5.1 Design Criteria Table

Criteria / TRV	Expansibility	Modularity	Large Base Area	Cargo Access
LM Design	Bad	Bad	Bad-Poor	Poor
Close Truss Bus	Fair-Poor	Fair-Good	Good	Poor
Open Truss Bus (flatbed)	Fair-Good	Good	Good	Good

Bad- Failed to meet Criterion completely
Poor- Barely acceptable in meeting Criterion
Fair - Sufficently meets Criterion
Good - Completely fullfills Criterion

The closed truss bus TRV failed to pass the criteria established for the preliminary study. The closed truss bus TRV ran into problems in its attendant modular exchange procedures. The removal and replacement of the fuel modules would require either the removal of the engines or a portion of the truss frame. To attach the fuel modules to the engines, accessing the propellant connections would have to be done in confined areas and the potential for dangerous conditions is thus increased. In addition to the module exchange problems this TRV design called for a special dedicated habitation/command module. This would restrict the potential growth of the vehicle and add additional weight to maintain the habitation and command areas in one vehicle. This last restriction could be overcome by replacing the dedicated module with the habitation modules from a space station. Therefore it is not one of the main reasons for dropping the design. The main

reasons for dropping this RTV are the lack of expansion capacity and the limited cargo envelope.

Expansion of this TRV would further restrict access to the inner modules and complicate the combination of two (or more) TRV's into a larger unit. The crucial failing of this TRV is the limited cargo envelope. The cargo is stored in a "hold" just aft of the habitation module. The cargo must be shaped and sized such that it will fit within this limited area. In addition to this shortcoming, the removal of the cargo is further complicated by the fact that if the cargo is large a truss member may have to be removed to provide sufficient clearance for cargo removal. This TRV failed to meet the standards set for the TRV to be used for exploration of Phobos, and consequently it has been dropped from further consideration.

The open truss TRV (or "flatbed") has the best rating against the established criteria. Figure 3.5.4 shows the generalized cross sections of the various flatbed designs that were under consideration. Figure 3.5.4a shows a double-sided flatbed. The advantage of this particular design lies in the area it provides for cargo and system modules. The problem with this design is that it would potentially trap cargo in the event of sinking into the soil. Other configurations studied were the inverted "T", the inverted "Y", and the "X" (Figures 3.5.4b ,3.5.4c , and 3.5.4d respectively).

The inverted "Y" and the "X" designs were found to have a problem due to the enclosing structures at their bases. This left the inverted "T" as the primary structure under consideration.

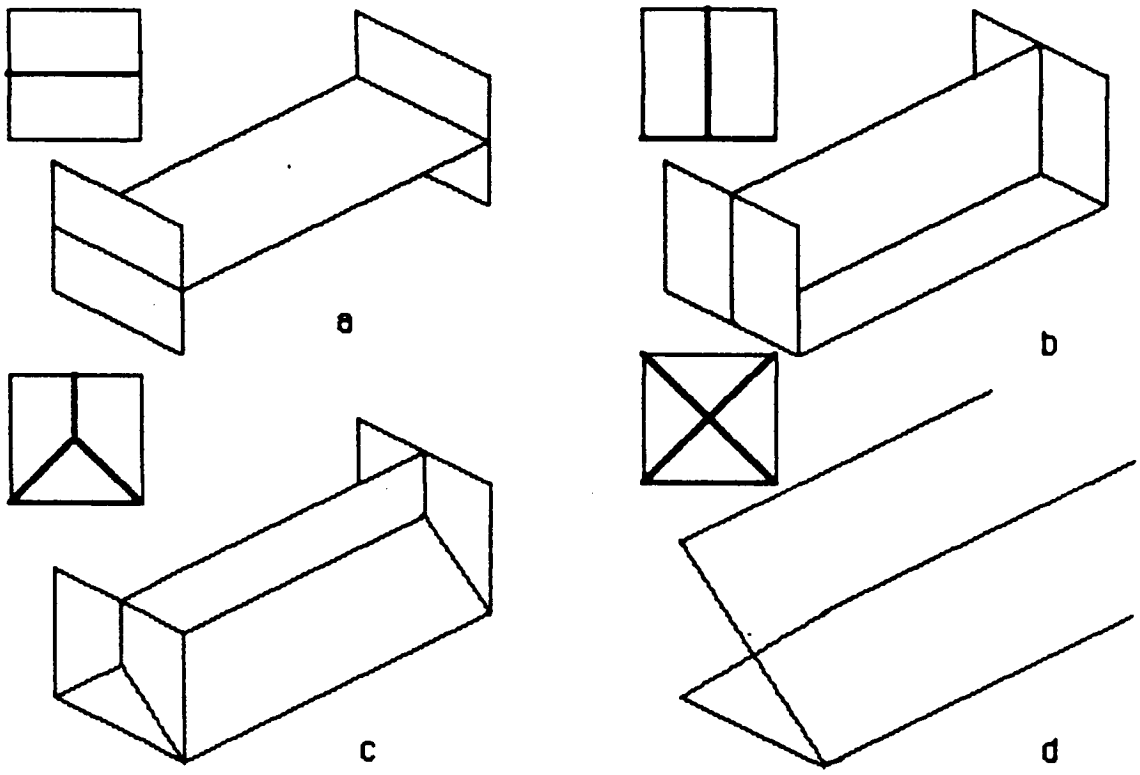

a Double-sided
b Inverted "T"
c Inverted "Y"
d "X"

Figure 3.5.4 Generalized Geometry of Open Truss Buses (Flatbeds)

3.5.3 VEHICLE CONFIGURATION

The TRV will consist of three inverted "T" segments on the transfer to Phobos and will consist of two on the return. The vehicle segment will be described in Section 3.5.3.1, and the specific configuration of the TRV elements will be described in Sections 3.5.3.2-3.5.3.4.

3.5.3.1 INVERTED "T" STRUCTURAL CONFIGURATION

The structure of the inverted "T" consists of two truss planes, one vertical and one horizontal, connected together to form the "T". The truss planes are composed of truss elements, similar to those proposed for the current space station design. The elements are cubes that measure three feet to a side and are composed of eighteen members. A simplified representation of one is presented in Figure 3.5.5.

The end of the segment is capped with a support plate that lends rigidity for the veritical members.

The main structure of the ship will be composed of segments of the "T" truss. This was chosen to establish a vehicle that was as modular as possible and to give as wide a range of uses for the vehicle and its components as possible. The truss segments measure 60 feet across the bottom of the inverted "T", 60 feet vertically, and have a length of 70 feet. The layout of the Inverted "T" segment is shown in Figure 3.5.6. The size of the segment was determined by the requirement that standardized habitation modules similar to those proposed for the space station be incorporated in the design. Further discussion of the habitation modules is in Section 3.5.3.2.

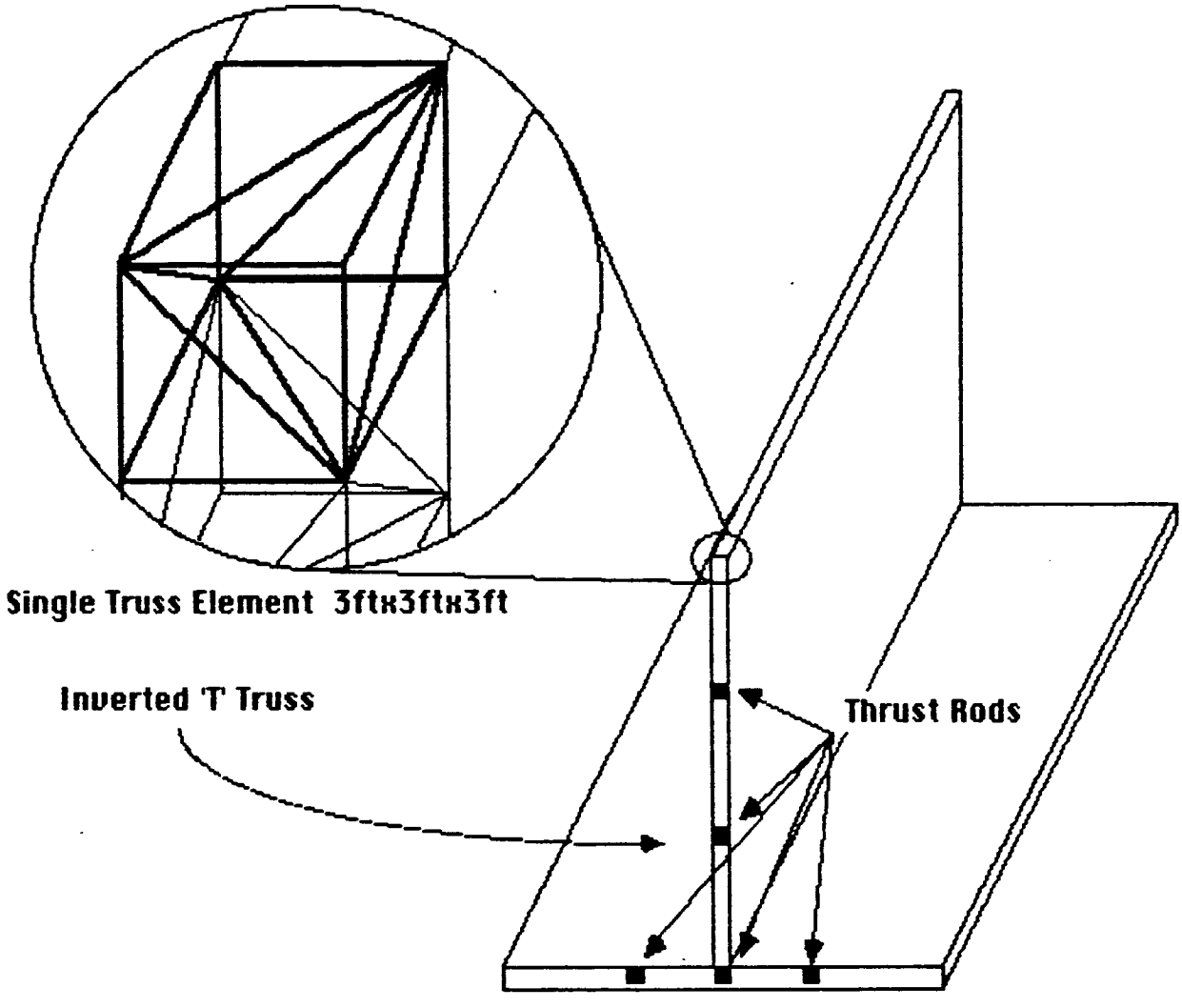

Figure 3.5.5 Inverted "T" Truss Segment
With Truss and Thrust Rods

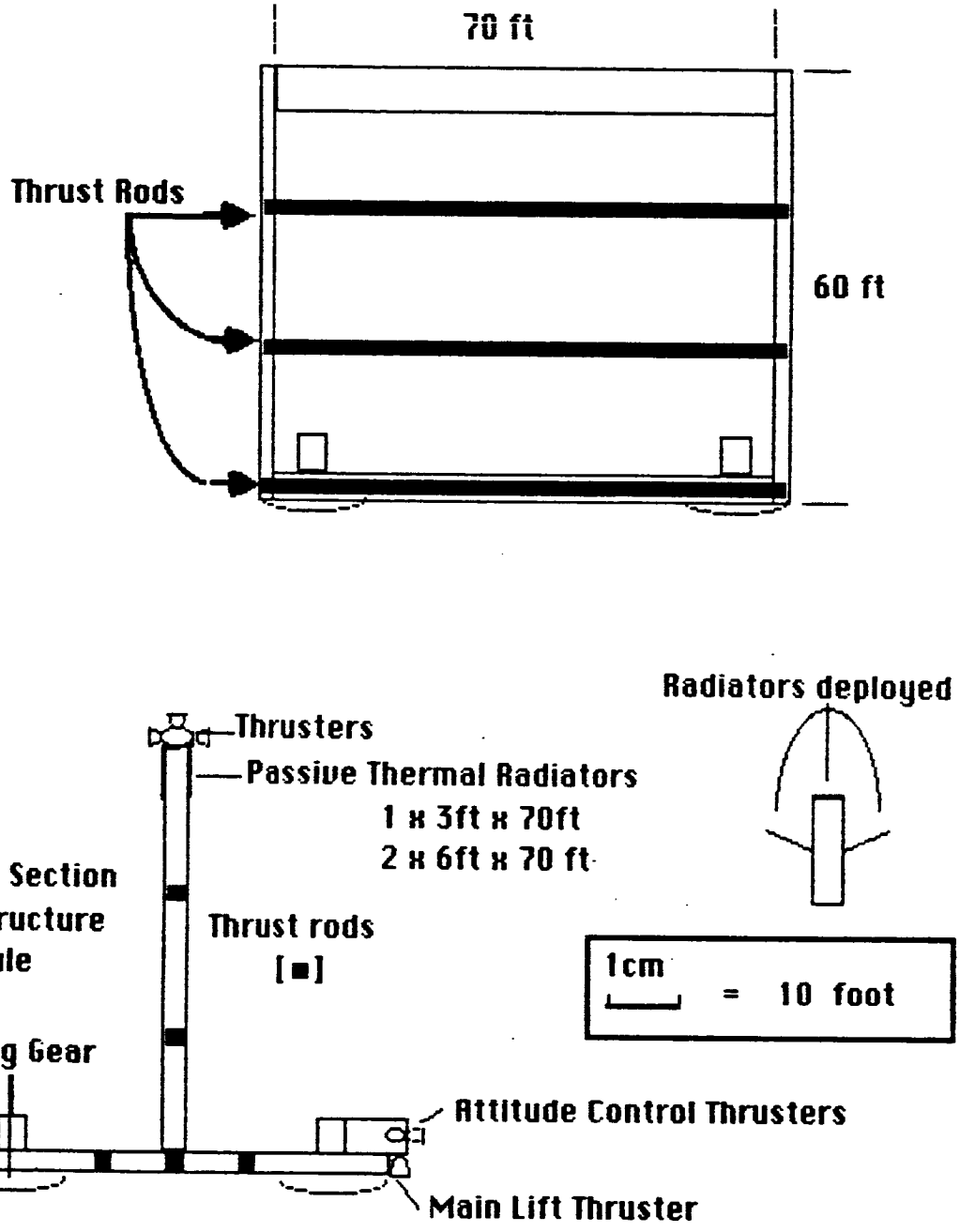

Figure 3.5.6 Structural Element Component Configuration

Table 3.5.2 : Structural Component Mass Table

Structural Component	Mass (kg)
Single Graphite-Epoxy Truss Element	.638831
Total Truss Component (697 Elements)	601.66294
Thrust Rods (5 Thrust Rods)	500.00 (approx)
Graphite-Epoxy Under Skin(.001533ft thick)	13.386
Landing Gear Assemblies	450.00 (approx.)
Thermal Panels & Auxillary	2700.00
Attitude Control Jets & Local Fuel & Tanks	750.00
Liftoff Thrusters & Local Fuel & Tanks	2400.00
End Plates	30.1
Additional Systems	2383.75
STRUCTURAL ELEMENT TOTAL MASS	9628

The structural segment was intended to maintain the loads of the components that were mounted to them but was not intended to maintain its integrity under full thrusting loads. To maintain the structural integrity during thrusting, thrust rods passing through the segment were proposed. The thrust rods are simply solid members that are able to transmit the thrust though the length of the ship and supply a mounting frame for the truss elements. The trusting rods are located along the center axis of the two truss planes, at the intervals of one-third of the length. The positioning of the thrust rods is shown in Figure 3.5.5 & 3.5.6. The thrust rods are connected together with the other segments of the vehicle in such a way that they can be easily engaged and disengaged manually.

Each segment of the Inverted "T" is equipped with landing gear in the vicinity of the four bottom corners, as well as a thin graphite-epoxy sheet covering the entire bottom of the structure. This graphite-epoxy sheet has

been included to prevent the possibility of sink into the potentially deep Phobian regolith. The possibility of using the bottom of the vehicle as a passive heat radiator has been suggested, but not explored in this study.

To meet the need for heat removal the top six feet of the inverted "T" has been reserved for radiator panels similar to those employed on the shuttle. The radiators will be placed along the top of the vertical truss (3 feet wide) and on the sides of the vertical truss (6 feet from top). The side panels have the ability of swinging out to double their effective radiating area. The area of the radiators is equivalent to that used by the shuttle (Reference 1). The radiated output should be improved by the fact that the increased distance from the sun reduces the amount of panel heating. The estimated heat rejection of a single structural segment is over 15.35 kWatts. The panel configurations are shown in Figure 3.5.6

The structural elements also have their own battery power backup, and the potential for chemical fuel cells, solar panels or nuclear power sources. As the primary design of the vehicle is for exploration of the Martian moon Phobos and like missions, a nuclear source will supply the needs for the vehicle and the batteries would be used as a back-up. This power source is similar in design to the SP-100 reactor and generates 50kW of electrical power. The mass of the reactor includes additional shielding for added protection for the crew.

The structural elements have their own propulsion units. The positioning of the units is shown in Figure 3.5.6. The attitude control of the entire vehicle is spread throughout the segments of the vehicle. This allows the segments, with the addition of a control unit, to be operated as a complete unit. This results in the fact that manipulators are not required

for construction of vehicle segments, and allows for the potential of using the segments as OTV's. The landing/liftoff thrusters , with additional fuel tanks, should also be capable of providing thrust for orbital maneuvers.

The segments have a trunk that conducts power along its length and also has provisions for carrying ECLSS materials. The ends of the trunk have easy connnect/disconnect capacity. The pipes that carry the fluids must be able to connect and disconnect without the loss or addition of material from or to the pipes. The trunk consists mainly of the pipes and cables required, plus a protective covering.

Every one of the components of the segment are removable for customization purposes. The landing gear requires that it be replaced with a truss element in the event of its removal. The control jets of the segment require tanks and supports that would have to be removed in addition to the control circuitry and the engines themselves.

3.5.3.2 HABITATION ELEMENT DESIGN

The foremost segment of the TRV is the Habitation Segment (see Figure 3.5.7). This segment contains all the neccessary components for the explorers to survive their trip (with the exclusion of the nuclear power source). The front of the vehicle is the location of the habitation modules. The size of the structural segments was dictated by the size of the standard habitation modules from the space station. The original space station modules had the capacity for maintaining the needs of four men for ninety days (Reference 2). The habitation modules chosen are identical in dimension to the ones chosen for the space station, but they are configured with sleeping arrangements for two in horizontal bunks. The horizontal

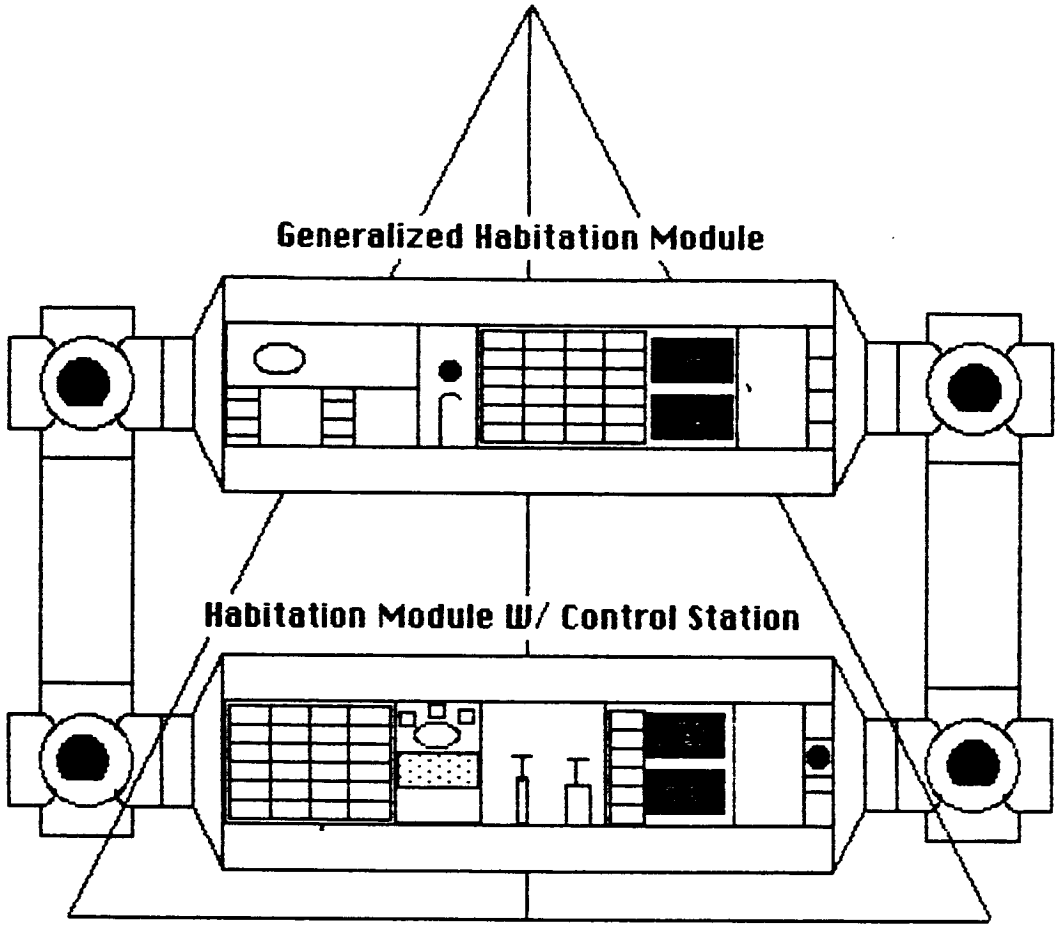

- Two Horizontal Sleepers per Habitation Module
- Control Console (forward) on Lower Module

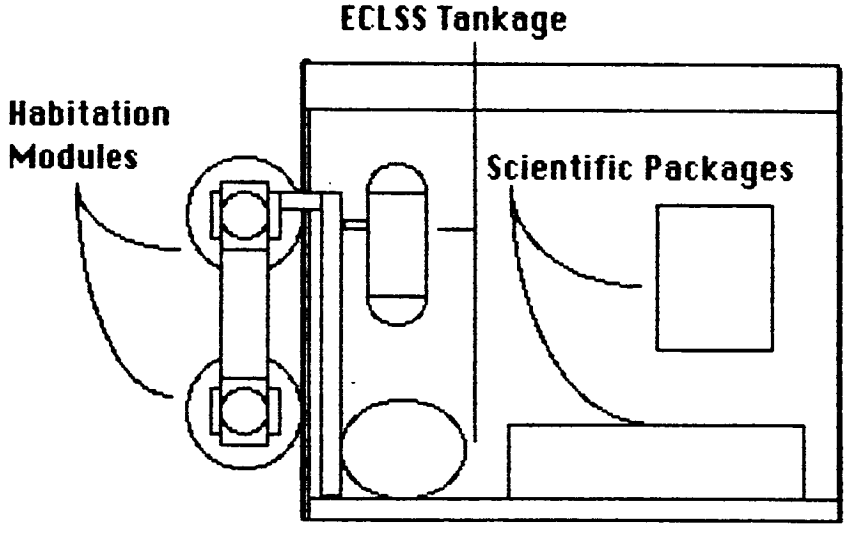

Figure 3.5.7 Habitation Segment of TRV

bunks are required because of the low gravity level of the moons. The low gravity would make vertical sleeping uncomfortable, and during thrust the back wall of the sleeping chamber would double as the acceleration couch. The floors of the habitation modules lie parallel to the cylindrical axis of the module. A representation of the modules and their size is shown in Figure 3.5.7. Due to the extended time that the crew members would have been in space it, was determined that the modules should provide as much space as possible.

The base width was determined by an approximation of the stability characteristics of the vehicle under loading by the habitation modules and other cargo. The height was determined by the separation of the habitation modules and the need for a working area for anchoring the habitation modules securely. The length of a single element was determined by the length of a habitation module with an interface module on each end. This was to allow for a variety of possible configurations for the habitation and laboratories aboard the vehicle.

The ECLSS supplies and the scientific cargo are stowed on the sides of the habitation segments. The location of the supplies is dictated only by the access required and weight balances.

3.5.3.3 ENGINE SEGMENT DESIGN

The engine segment is similar to the habitation segment in that it has a triangular truss piece on the end. Four engines that propel the vehicle during the transfer are mounted on the end piece. They are arranged such that in the event of a single, double or triple failure the engines will still balance the thrust along the vehicle's length. The engine segment and the

engine configuration are shown in Figure 3.5.8.

The sides of the structural element hold the fuel tanks and the nuclear plant (50kW). The fuel tanks are positioned to shield the area around the vehicle during excursion and the shielding on the nuclear generator itself is situated to provide maximum radiation protection for the crew in the habitation module. The variety of pumps and controls for the engines are situated opposite of the engines on the end plates, and the controlling circuitry is situated forward on the segment, as far from the nuclear reactor as possible to reduce the possibility of radiation damage to the circuits.

3.5.4 SAFE HAVEN / MOON DEPOT SEGMENT DESIGN

The middle segment is the save haven segment and is meant to be left behind on Phobos. On one side of the segment is a habitation module, configured with sleeping arrangements for four. Figure 3.5.9 shows a generalized layout of the components on the habitation module. The habitation module is meant to be buried on Phobos, so the need for a raised exit hatch dictated the need for two interface modules and a tunnel. Also on the Safe Haven segment are tanks for storage of fuel and ECLSS materials that can be accessed through a port that rises above the intended ground level. The Safe Haven is to be buried at a depth that has not yet been determined due to the lack of information about the composition and density of the Phobian regolith. This is one of the reasons that a precursory mission to the moons is advised. During this design phase ,the burial depth has been assumed to be less than fourty-five feet. This has been done to allow for the operation of the radiator panels after burial.

In addition to the components that are destined to be buried, there is

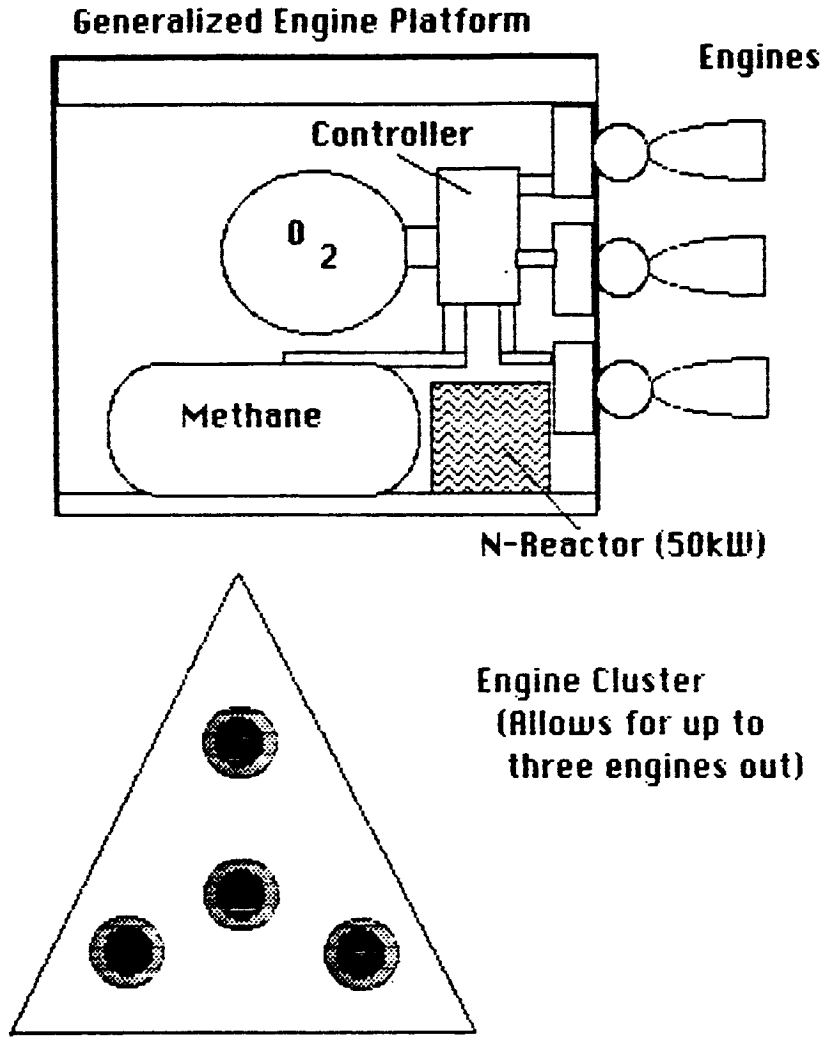

Figure 3.5.8 Engine Segment Configuration

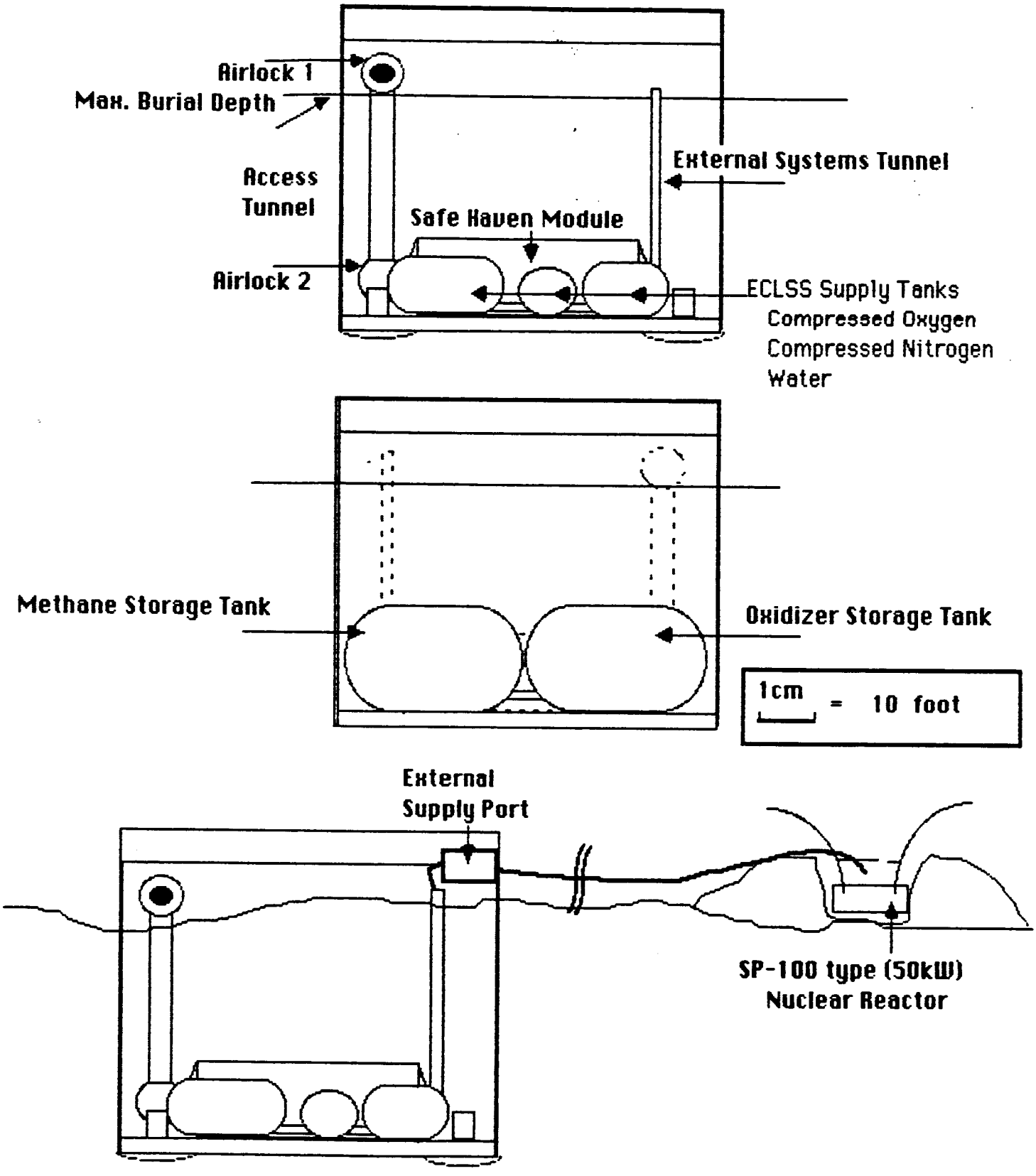

Figure 3.5.9 Safe Haven Segment Design and Burial Setup

also on the Safe Haven segment another nuclear power source (50kW). This power source is to be removed, set up and brought up to power a distance from the burial site. It should be encased in regolith and have its own independent radiator system.

3.5.5 VEHICLE SIZING

(The process of vehicle sizing was accomplished by using data from the space station design plans and current shuttle information. These sources are listed under references 3 through 5. Additional references will be presented in the text.)

The mass balancing and fuel/engine balancing was accomplished using two TK! Solver models. These are presented in Appedix E.1 and Appendix E.2. The model was the simulation of the mass and components of the structural segments. Trend approximation was used in determining the individual masses of many components when the actual masses could not be determined directly. Table 3.5.2 shows the mass list for the structural segment's components.

The truss structure of the system is composed of a Graphite-Epoxy composite, and is formed by elements that are three feet on a side. A density of this material has been calculated to be 2.079 g/cc. The underside and the endcaps of the truss segment are also composed of the Graphite-Epoxy composite. Using the masses of the systems, the TK! Solver models then iterated to calculate the fuel mass for a given Delta V for the transfer back from Phobos, less the system masses that were left or consumed on Phobos. This fuel mass was then entered as cargo mass for the trip to Phobos and the process repeated. In this manner the total launch

mass of the vehicle is obtained. The components of the vehicle and the masses involved are shown in Table 3.5.3. Table 3.5.4 shows the launch masses as a function of the Delta V for the one way transfer, Figure 3.5.10 graphically represents this data.

The data point for the 64° inclination barge orbit is sufficently high that it is advised that a lower inclination be used to lower fuel consumption, particularly if more than one mission to Phobos is desired.

3.5.6 VEHICLE USES FOR SUBSEQUENT MISSIONS

This vehicle design was developed to meet not only the needs of the initial manned survey of the Martian system, but to serve the orbital transfer needs for later missions. The TRV is highly modular, capable of expanding in length, by adding modules end to end, and in width ,by adding modules side to side. It is forseen that the first manned mission to an asteroid may be made using an expanded version of the TRV.

Table 3.5.3 Ship Mass Table

Ship Component	Mass (kg)
Structural Elements	9829.9
Habitation Module	23261.2
Tunnel	494.4
Interface Module w/ Airlock	5277.5
Engine (251757 N thrust)	1107.7
Nuclear Power Source (50kW)	3300.0
Power Backup Systems	200.0
ECLSS Supplies (O_2,N_2,H_2O,Food & tanks)	1293.36
Initial Cargo Mass	4000.0
EVA Equiptment	1117.26
EVA Fuel	500.0
Fuel	as per Mission

Table 3.5.4 : Fuel Mass

M_{fuel} kg	$\Delta V_{mission}$ m/s	M_{fuel} kg	$\Delta V_{mission}$ m/s
1000	31009.83	1676	58467.34
1026	31956.7	1702	59651.85
1052	32911.64	1728	60846.79
1078	33874.73	1754	62052.26
1104	34846.03	1780	63268.36
1130	35825.65	1806	64495.22
1156	36813.64	1832	65732.93
1182	37810.1	1858	66981.61
1208	38815.11	1884	68241.38
1234	39828.75	1910	69512.35
1260	40851.1	1936	70794.62
1286	41882.26	1962	72088.34
1312	42922.31	1988	73393.6
1338	43971.33	2014	74710.53
1364	45029.42	2040	76039.26
1390	46096.67	2066	77379.9
1416	47173.16	2092	78732.58
1442	48258.98	2118	80097.44
1468	49354.24	2144	81474.59
1494	50459.02	2170	82864.17
1520	51573.43	2196	84266.31
1546	52697.54	2222	85681.14
1572	53831.48	2248	87108.8
1598	54975.32	2274	88549.42
1624	56129.18	2300	90003.15
1650	57293.15		

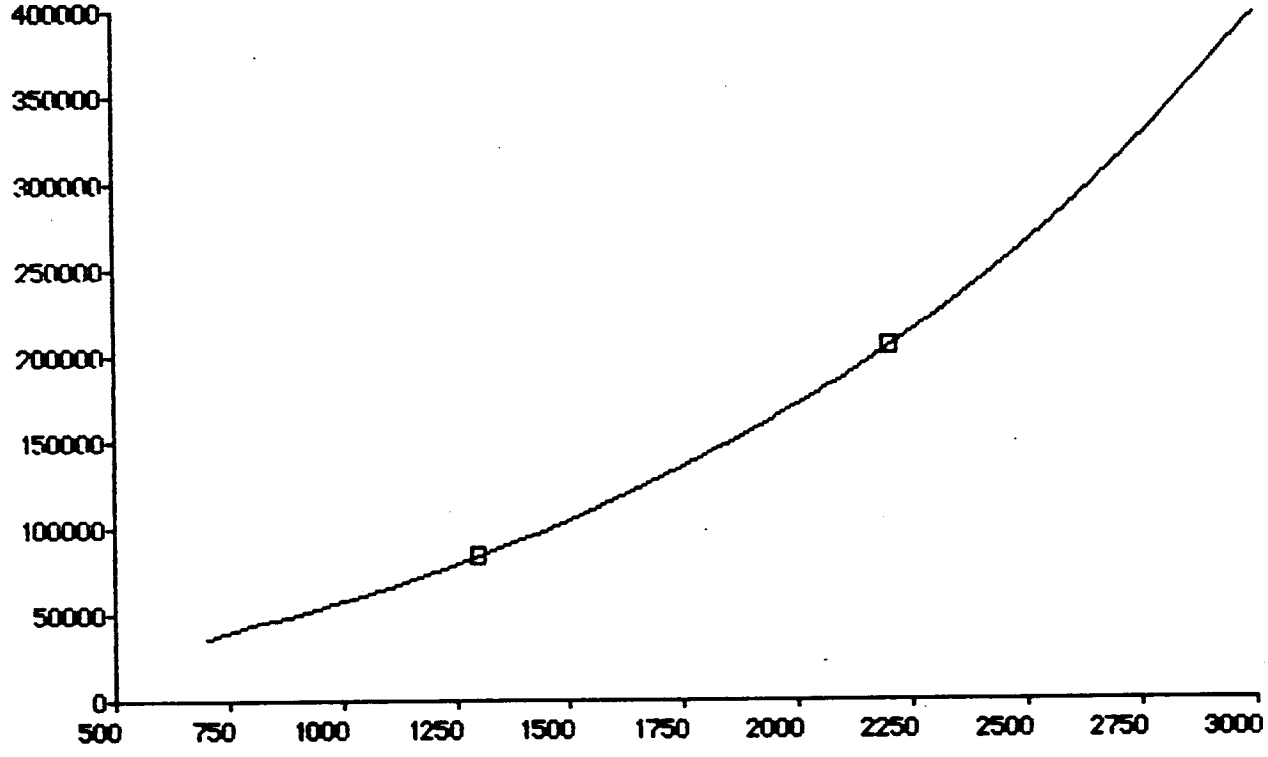

Figure 3.5.10 :

Delta V (M/S) for transfer vs. Fuel Mass (kg) required for Mission

REFERENCES

1. Rockwell International, "Shuttle Technical Information"

2. "Space Operations Center", Lyndon B. Johnson Space Center, Houston, November 29, 1979.

3. "Conceptual Design and Evaluation of Selected Space Station Concepts", Lyndon B. Johnson Space Center, Houston Texas, December 1983.

4. Mendell, W. ,"Lunar Bases and Space Activities of the 21st Century", Lunar and Planetary Institute, Houston, Texas, 1985

5. Gatland, Kenneth, "The Illustrated Encyclopedia of Space Technology", Harmony Books, New York, 1981.

3.6 SCENARIO FOR A MANNED RECONNAISSANCE OF PHOBOS

A preliminary scenario for a manned exploration of Phobos has been designed to accommodate the scientific and technical objectives outlined by the TSS Moon Science Group. This scenario consists of a mission timeline, initiated at transfer orbit insertion and concluding at barge rendevous, which details a preliminary crew activity plan which includes 11-15 EVAs covering 4-8 sites on Phobos. The timeline was estimated utilizing previous history (shuttle and Apollo) and a conservative approach whereby any major mission event (i.e, a rendevous, site change, or EVA) would require a dedicated mission day. The entire mission is currently 22 days in duration, but this value is dependent on the transfer trajectories which have not been selected as yet.

The timeline is shown in Table 3.6.1. Note that the term day refers to a 24 hour period. The backbone of the timeline is the requirement for two major EVAs at each primary site, with an option for an additional EVA at the second, third, and fourth primary sites. To maximize the efficiency of the mission time, a four-person crew was selected for the mission to permit back-to-back two-person EVAs at each site. In this way crew fatigue is minimized and no single crewmember conducts an EVA in two sequential days (unless the contingency days are utilized). The burial of the safe-haven on the third day after Phobian landing requires a three-person EVA, but the man-hours required for this operation has not been determined.

Tasks to be completed include a detailed estimation of man-hours required for safe-haven burial, testing, and systems initialization, EVA man-hours per sortie, and transit times. The detailed timeline resulting from these studies will be utilized to size the equipment and systems required for the overall reconnaissance mission.

TABLE 3.6.1 MISSION SCENARIO EVENT SCHEDULE

Event	Earth Days
PRE-LAUNCH SYSTEM CHECK	
ORBIT TRANSFER TO APPROXIMATE PHOBOS ORBIT	1
RENDEZVOUS WITH PHOBOS	
LANDING SITE SELECTION	
LANDING OPERATION SITE #1	
SHUT DOWN/ SAFING OF VEHICLE MAIN SYSTEMS	1
EVA #1 SITE #1	1
EVA #2 SITE #1	1
SAFE HAVEN BURIAL	4
TRANSIT TO SITE #2	1
EVA #1 SITE #2	1
EVA #2 SITE #2	1
(ONE DAY CONTINGENCY EVA FOR SITE #2)	1
TRANSIT TO SITE #3	1
EVA #1 SITE #3	1
EVA #2 SITE #3	1
(ONE DAY CONTINGENCY EVA FOR SITE #3)	1
TRANSIT TO SITE #4	1
EVA #1 SITE #4	1
EVA #2 SITE #4	1
(ONE DAY CONTINGENCY EVA FOR SITE #4)	1
RETURN TRIP PREPARATIONS	
LIFT OFF FROM PHOBOS	
TRANSFER 1	
RENDEZVOUS WITH BARGE/ SPACE STATION	
DOCKING OPERATION	
MAIN SYSTEM SHUTDOWN/ SAFING	1
	22 DAYS

3.6.1 EVA's : SCIENCE

The EVA's on Phobos involve all activities on Phobos in which the astronauts don space suits and life support systems and perform operations outside the pressurized habitation modules of the Transfer Reconnaissance Vehicle (TRV). Some possible EVA's include the removal or reinstallation of protective covers or tie downs, replacement and inspection of modular equipment and instrumentation on the payload or spacecraft, transfer of cargo, setting up surface experiments and collecting regolith and rock samples. The minimum crew requirement has been established to be four. This number provides for alternating two man teams during EVA periods.

EVA's on Phobos will be unlike any EVA's performed in the past. There will be surface activities, but with almost no surface gravity, these activities will almost resemble space walks. This presents a challenge to design new ways for surface exploration on sizeable objects with low gravity, such as the two moons of Mars or the vast number of asteroids in the Solar system.

Before any EVA's can be started, the space suits to be worn by the astronauts will have to be checked out. Once this has been accomplished the lengthy list of EVAs can begin. The first objective on the EVA schedule would be for the astronauts to become acquainted with the Phobos enviroment and to get a feel for working on the surface. Then, almost immediately, the placing of a safe haven on Phobos should commence. This safe haven would be needed in case any emergencies, such as solar flares or mechanical failures on the TRV, or unexpected problems occurred. An exact burial technique on a low-g body, such as Phobos, has not been worked out, and further study in this area is needed.

A few possible methods are suggested for the burial of the safe haven. One possiblity is the injection of water into the regolith. After the water freezes, an explosive charge would then blast the frozen mass out of the terrain. This would allieviate the problem of soil particles "clouding" the area about the work area , and the material loss to space would be greatly reduced. Machines to dig out the soil have been suggested but no coherent design has been developed. One final method that has been seriously considered is the use of the regolith stored in a crater's wall. Placing the safe haven next to a wall and crumbling the wall onto the safe haven would not require as much work as the other methods mentioned.

Once the astronauts are accustomed to the low-g enviroment of Phobos, and after the safe haven has been emplaced and tested, the extravehicular scientific experiments on the surface of Phobos could begin. The primary aim of these scientific experiments, and planetary geophysics in general, is to determine the structure, composition and state of a given body and the relationship between internal processes and surface tectonic features (Reference 1). Since Phobos is probably not much more than a large rock completely covered with regolith, the bulk of these scientific experiments will probably involve regolith materials and regolith characterization. However, the internal processes that created the many grooves on Phobos might be better understood as a result of the geophysical investigations.

One of the first experiments should include the placing of scientific packages, similar to the Apollo Lunar Scientific Experiment Packages (ALSEP's), on the surface of Phobos. These packages would have a central station to serve as a junction box for the cables linking all the scientific

equipment with a power supply, and as a transmitter/receiver for telemetry to and from the entire package. The Radioisotope Thermoelectric Nuclear Generator (RTG) used with the ALSEP's could also serve as a power supply for any packages left on Phobos. This generator provides approximately 70 W of power for up to several years at a time. Return missions to Phobos could replace these generators as they ran out of fuel. It is easily conceivable that more advanced power supplies will be designed by the time a manned mission to Mars and it moons is accomplished, but the RTG used in the Apollo program is a good baseline power supply. Solar wind spectrometers could be used to measure the velocity and direction of photons, electrons, and alpha particals in the solar wind. The amounts of solar and cosmic radiation reaching Phobos, and the interaction of this radiation with the surface of Phobos are critical factors in any considerations of long-term manned operations on the moons of Mars. Therefore, it would be convenient if one instrument could be incorporated to measure the velocity and direction of the solar wind as well as the radiation levels at the surface. Since the surface will most likely be radioactive, a gamma ray spectrometer could be added to identify and measure the radioactive elements. Active seismometers could be used to monitor impacts and measure surface vibrations, free oscillations or any tidal variations in surface tilt.

The scientific packages mentioned above could provide information on the gross internal structure of Phobos and possible mapping of the stratigraphy, a significant achievement for this first manned moon mission. Unfortunately, from an exploration standpoint, the very high rate of seismic energy dispersion that occurs in a regolith will very sharply decrease the

resolution and hence the usefulness of seismic waves in discerning shallow, subsurface structures (Reference 2). This establishes the rationale for possibly using other geophysical techniques to study the composition of Phobos.

The magnetic method for geophysical mapping is commonly used on Earth. With this technique, the detection of magnetic ores and various iron oxides could help establish lateral changes and boundaries in the regolith and could also give some information on the grain size distribution of metallic iron in the regolith (Reference 3). However, since Phobos probably has no magnetic field of its own, an artificial magnetic source would have to be used. This might take the form of a large coil placed on the surface to induce magnetization in the rocks (Refertence 4).

A better method for geophysical experiments might involve electromagnetics. There seems to be quite a bit of interest in this area, and improvements in this field could put electromagnetics ahead of seismics as the dominant technique for exploring near-surface features. Like the seismic and magnetic techniques, an active capacity would be needed to artificially generate and induce fields. Some active techniques include direct current (DC) resistivity, induced polarization (IP), conductive source electromagnetic (EM) depth sounding, inductive source EM depth sounding and displacement current techniques such as ground-penetrating radar (GPR) and very low frequency (VLF) soundings (Reference 5). Several of these techniques might be considered as preferable techniques. The IP technique, for example, is directly related to ground water. Since it is very possible that Phobos is similar to type 1 carbonaceous chondrites with approximately 20% water, this technique could possibly be used to find

areas of high water content or even concentrations of ice. GPR, though poor in penetration depth, provides high resolution for near-surface features.

Overall, these electromagnetic techniques could provide information on layering in the regolith and regolith thickness, and also on information on the regolith-rock interface. As mentioned earlier, electromagnetic techniques will be very useful for geophysical packages and could be used with the seismic experiments to provide a complete geophysical description of Phobos. These Phobos scientific packages, whatever their make-up, will be an important part of the scientific work done on Phobos.

Along with the placing of scientific packages on the surface of Phobos, another important aspect of the EVA schedule will be sample collection. Many of the sample collecting tools used by the Apollo astronauts could directly be used on Phobos. Hammers, chisels and long-handled tools such as scoops, rakes and tongs proved their value on Earth's moon. The long-handled tools proved especially useful because they eliminated the need to constantly bend over. Also, besides actual samples, the astronauts could obtain photographic samples by using small hand held cameras. Visual and photometric studies of groove and crater walls could reveal the strata and bedding of Phobos. The information gained, in conjuction with the information from samples taken from the rims of grooves and craters and from samples taken radially outward, would yield first-order insight into the mechanics of groove formation, impact cratering and regolith mixing (Reference 6).

Collecting subsurface samples would also be important. The value of drilling into a planet's surface has long been recognized as part of an exploration-exploitation strategy (Reference 7). However, drilling on

Phobos would be quite different from drilling on Earth or its moon because of the absence of gravity. This is an area where improvement in current technology is needed. Some sort of artificial gravity would have to be imposed on the drill. This might be accomplished by small thrusters pushing the drill into the surface as it spins. Cores could either be packed for Earth examination or examined on Phobos.

This brings up the point of what kind of scientific equipment and instruments should be included in the scientific section of the habitation modules. The astronauts will be busy enough designing and carrying out strategies for mapping and sample collecting that they need not be burdened with much sophisticated study 'in situ'. The hand lens and binocular microscope should suffice for most purposes, plus perhaps the ability to make some thin sections and examine them under a petrographic microscope (Reference 8). A mass spectrometer or other equipment for first-order chemical analysis and age-dating equipment could also be included. The above list of scientific instruments would provide a small but adequate laboratory on Phobos. This would allow for emphasis on scientific experiments in the areas of field observation, sample collection and initial characterization of samples.

REFERENCES

1. Hood,L.L., C.P. Sonett and C.T. Russell, "The Next Generation Geophysical Investigation of the Moon", Lunar Bases and Space Activities of the 21st Century, Lunar and Planetary Institute, Houston, Texas, 1985, p. 253.

2. Ander, Mark E., "Surface Electromagnetic Exploration, Geophysics Applied to the Moon", Lunar Bases and Space Activities of the 21st Century, Lunar and Planetary Institute, Houston, Texas, 1985, p. 273.

3. Strangway,D., "Geophysics and Lunar Resources", Lunar Bases and Space Activities of the 21st Century, Lunar and Planetary Institute, Houston, Texas 1985,p.267.

4. Ander, p. 272.

5. Ander, p. 274

6. Haskin, Larry A., Randy L. Korotev, David J. Lindstrom and Marilyn M. Lindstrom, " Geochemical and Petrological Sampling and Studies at the First Moon Base", Lunar Bases and Space Activities of the 21st Century, Lunar and Planetary Institute, Houston, Texas,1985,p. 204.

7. Oberg, James, Mission to Mars, The New American Library, Inc., New York, 1982, p. 135.

8. Haskin, p. 200.

3.6.2 EVA's : MARTIAN MOON SPACE SUIT

Since Phobos has no atmosphere of its own, the astronauts performing EVA's will have to be protected from the vacuum of space with space suits. Although there is no existing suit designed for exploring the Martian system, there are ideas on the "drawing board". There are many complex and important factors that contribute to the design of a space suit, especially since the ultimate purpose of the suit is to sustain human life in the hostile environment of space. This section suggests a few design factors for a space suit to be used on Phobos.

The Phobos space suit will most likely be a hard suit or semi-hard suit. A hard suit is one that has a hard outer shell, usually made out of metal or composite materials, as opposed to a soft fabric suit like the ones used for the Apollo lunar EVA's. There are several reasons why a hard suit is preferable over a soft suit. One reason is the protection against radiation and micrometeoroids. Hard suits can provide better protection against both of these potentially serious problems. The inherent nature of fabric suits lets more radiation pass through the fibers, whereas a hard suit is a solid, protective shield. Also, to reduce radiation problems, thermal-control coatings that exhibit properties of low solar absorptivity and low infrared emissivity could be applied to the hard suit (Reference 1). The strength of a hard outer shell would serve as a shield against micrometeoroids, whereas a fabric suit could be punctured or ripped open.

Another important reason that makes a hard suit the preferable choice is its ability to maintain a constant volume. A constant volume is very important because when an astronaut is performing some task on an

EVA, he will be moving all parts of his body. If a fabric suit was used, as one part of the body bent and compressed or creased a section of the suit, another section of the suit would "balloon" trying to keep the suit at a constant volume. With a hard suit, no "ballooning" occurs. This is because a hard suit would utilize joints that are true constant volume convolutes. Circular bearing joints could be used on hard suits and rolling convolute and toroidal convolute joints could be used on semi-hard suits. The term semi-hard is used because there are fabric sections in the rolling and toroidal convolutes.

The ability of an astronaut to move around inside the hard suit is also an added feature that the soft suit does not possess. It is conceivable that the astronaut could pull his arms out of the suit's arms and perform various tasks inside the suit. He could also conceivably twist or stretch in the case of fatigue during long or strenuous EVA's. Drinking and eating inside the suit would be possible, and pockets or bags for storage of small items or maps could also be available to the astronaut.

In the late 1960's, NASA developed a prototype hard suit for long term lunar exploration. This suit, the RX-5A (Figure 3.6.2.1), utilized a "sandwich structure" incorporating an inner sheet of thin aluminum faced with a fiberglass honeycomb and covered by a layer of fiberglass (Reference 2). This suit has an approximate weight of 90 lbs. and was designed for an operating pressure of 5 psid. A derivative of this suit would be a feasible option for a Phobos space suit.

There are several features that are either needed or that would enhance the capabilities of a hard suit. The first feature would be an anthropomorphic design of the suit. The suit and its joints should closely

Figure 3.6.2.1 RX-5A Prototype Hard Suit (NASA S-68-40472)

approximate the natural body and joint movements. By design, pressurized anthropomorphic garments require a force by the astronaut to overcome friction inherent in mobility joints. However, a feature similar to the Shuttle Extravehicular Mobility Unit (EMU) suit-joint neutral stability feature would alleviate this requirement to apply a counteracting force to maintain a desired position (Reference 3).

Also, it would be beneficial if the joints on the space suit were easily interchangeable. This way , broken or degraded joints could be replaced inside the habitation modules of the Transfer Reconnaissance Vehicle (TRV). Replacement modular suit parts could be part of a general maintenance inventory on-board the TRV.

Another key feature of the space suit would be its own portable life support system (PLSS). This system would have to supply the breathing air, remove and/or control the carbon dioxide and water vapor produced by the astronaut, provide temperature control of the space suit ventilation system and provide electrical power for all the systems in the suit. Again, it would be beneficial if the PLSS could be recharged or had easily replaceable systems. This would enable a large number of EVA's to be performed in a short time span. The ventilation system would have to be capable of removing 1500 to 2000 BTU/hr of heat. Testing has shown that a suited, pressurized astronaut generates 500-1000 BTU/hr of heat at low work levels and 1500-2000 BTU/hr when walking or working moderately hard (Reference 4). Since the astronauts will be working in the coldness of space, it has been suggested by some that maybe the metabolic heat output of an astronaut could be used for heating instead of removing it.

The pressure inside the space suit is a topic of controversy among

many designers. The only thing that everybody agrees on is a minimum pressure of 21.4 kN/m^2 (3.1 psid). This pressure is the minimum pressure needed to protect an astronaut from hypoxia. Values for suggested pressures range from the Shuttle's EMU value of 4.3 psid to 14.7 psid, or one atmosphere. Whatever value is selected, it would be beneficial if the space suit and the habitation modules worked at the same or close to the same pressure. This would alleviate the need for prebreathing to denitrogenatethe astronaut's blood to prevent "the bends" as he goes from a higher pressure to a lower pressure. Again,this would save time, and more EVA's and work inside the habitation modules could be accomplished.

Some other features might be :

- A "buddy system" attachment that would allow two astronauts to breathe off of one suit
- A two-gas breathing system
- A small airlock on the suit that would allow the passage of small packages containing food, medical supplies,etc. into and out of the suit
- A secondary pressure protection system in case the primary system fails
- Field maintainability
- Small lights on the helmet to illuminate the area in front of the astronaut
- A two-way UHF communication system
- The suit should be easy to get into and out of, and should be easily stowed

As mentioned earlier, there is not an existing suit that would be

feasible for use on Phobos, but the above ideas and many others could possibly be used in the design of a Phobos space suit.

REFERENCES

1. Hays, Edward L., "Space Suits", Manned Spacecraft: Engineering Design and Operation, Fairchild Publications, Inc., New York, 1964, p. 166.

2. Johnson Space Center Visitor Center, RX-5A Display, Houston, Texas.

3. Space Transportation System: EVA Description and Design Criteria, NASA-JSC, 1983, p.22.

4. Hays, p.165.

3.6.3 EVA's : MOBILITY

It would be advantageous if the lunar rover and EVA design from the Apollo program could be used on Phobos, but there is almost no gravity on Phobos, so the Apollo methods of mobility would not be feasible. Therefore, a completely new concept on the mobility on low gravity surfaces, such as Phobos, Deimos and the many asteroids, needs to be developed.

Three conceptual ideas for mobility units are proposed. The Ultimate Transporter (UT), the Transportation Augmentation Mobility Unit (TAMU) and the Phobos Vision : Automated Mobility Unit (PVAMU). The UT and TAMU are derivatives of the Manned Maneuvering Unit (MMU) used with the Space Shuttle. Since walking on Phobos could be a difficult task because of the low-g environment, and it could be potentially dangerous to the astronaut if a particularly strong step or leap sent the astronaut hundreds of meters in any direction (straight up could conceivably put the astronaut in orbit about Phobos), the idea of "jetting" around the surface of Phobos was developed. The UT would be a scaled down version of the present MMU and would be used for relatively long distance EVA's away from the Transfer Reconnaissance Vehicle (TRV). "Saddle bags" and tool racks would be attached to the UT to facilitate sample collection. The UT would also be used as the primary mobility unit for long duration, local EVA's that required any strenuous work. The TAMU would be a much smaller version of the UT, would be much less capable and used only for short, local, menial EVA's about the TRV.

The PVAMU (Figure 3.6.3.1) would be a remotely piloted vehicle that could be sent to areas that might be potentially dangerous to the astronauts.

1. Thrusters
2. Propellant Tank
3. Soil Sample Collecter
4. Light
5. Antenna
6. Television Camera (zoom)
7. Television Camera (wide-angle)
8. Landing Shock Absorber

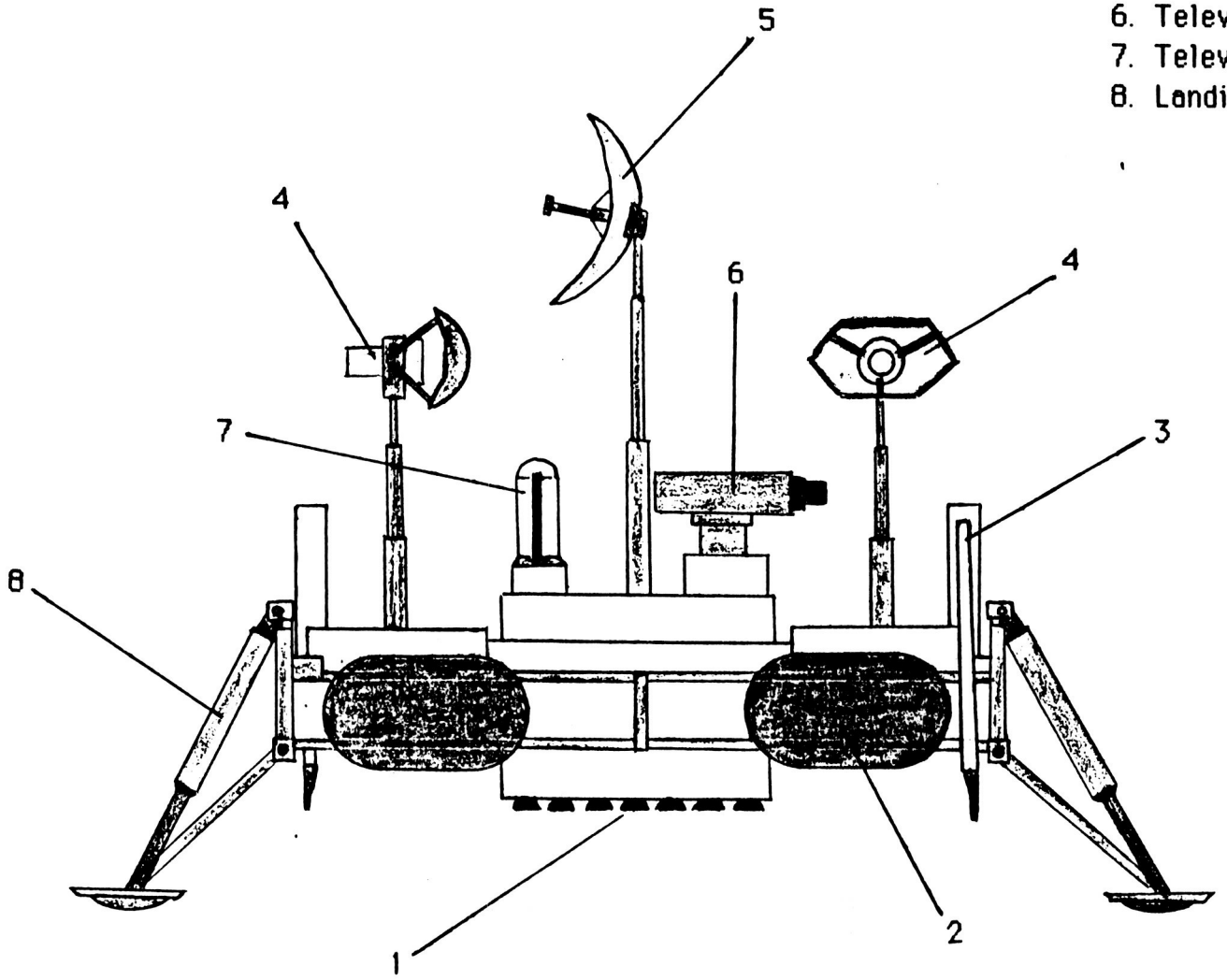

Figure 3.6.3.1 Phobos Vision : Automated Mobility Unit

It would move about the surface of Phobos in a hopping manner. Television cameras and automated sample collection devices would be used to collect samples from these dangerous areas. The PVAMU would also have large lights on the vehicle, so it could be used as a moveable light stand for the astronauts performing EVA's in darkness (since many EVA's on Phobos will be in darkness or partial darkness). All of the equipment on the PVAMU would be on telescoping mounts with 360° turning capabilities.

The three mobility units would allow the astronauts much freedom of movement about the surface of Phobos.

In areas of particular interest, such as the area around the TRV or at a scientifically interesting area, a grid system of pitons or short poles and guide wires would be set up on the surface. The pitons would be implanted into the surface and the guide wires would connect the pitons. This type of system would allow the astronaut to separate from either the UT or TAMU, tether the mobility unit and hook 'em onto the grid system to carry out scientific experiments, sample collection or any of a number of tasks. The astronaut would have a roll-up spool of safety tether attached to his space suit to hook 'em onto the grid system. The spool would unwind or wind-up as the astronaut moved about.

As mentioned in the beginning of this section, this is only a conceptual idea on how to perform EVA's on the surface of Phobos. Further study should be directed in this area.

3.7 PHOBOS LANDING SITES

From the results of the science study of the moons, landing sites have been selected for a manned landing on Phobos. Table 3.7.1 summarizes these locations, and a map of Phobos with the landing sites on it appears in figure 3.7.1. The landing sites were selected on a basis of usefulness and scientific value. The path from site to site was choosen because it represented the minimum distance path between the four primary sites.

Site #1 was selected primarily for its physical location. The first site is where the safe haven will be buried, and landing in the inner crater of Stickney might provide a crater wall which would facilitate the burial process. The depth of Stickney provides added protection from solar radiation. Also, this site is within close proximity of several ejecta blocks inside Stickney. This site is shown in figure 3.7.2.

Site #2 is in the area of the Stickney ejecta. This area could be either mantled ejecta blocks or a base-surge deposit, both scientifically interesting features. This site's close distance to site #1 will also be a good test for the TRV's ability to transfer from site to site. This site is shown in figure 3.7.3.

Site #3 may be the most interesting geologically. The data presented in the science study about the grooves supplies adequate evidence for this site. This location may provide significant clues to the origin of the grooves. This site is shown in figure 3.7.4.

Site #4 is in the area opposite of Stickney. This is where the grooves end , and the area could represent what the entire surface of Phobos looked like before the formation of Stickney. This site is also shown in figure 3.7.4.

The secondary sites were selected in the event that there were more

Primary Sites	SITE #1	Stickney Crater (inner crater/ejecta blocks) 50°-60° W , 10°-20° S
	SITE #2	Stickney Ejecta 10°-20° W , 0° N
	SITE #3	Major Groove Concentration 0°-20° W , 20°-30° N
	SITE #4	Antipodal of Stickney 270°-290° W , 0°-10° S
Secondary Sites	SITE #5	Southern Ridges 280°-300° W , 40°-60° S
	SITE #6	Hall Crater 210°-240° W , 60°-70° S
	SITE #7	Area West of Stickney 90°-120° W , 20° N-20° S
	SITE #8	Roche Crater 140°-170° W , 50°-70° N

Table 3.7.1 Phobos Landing Sites

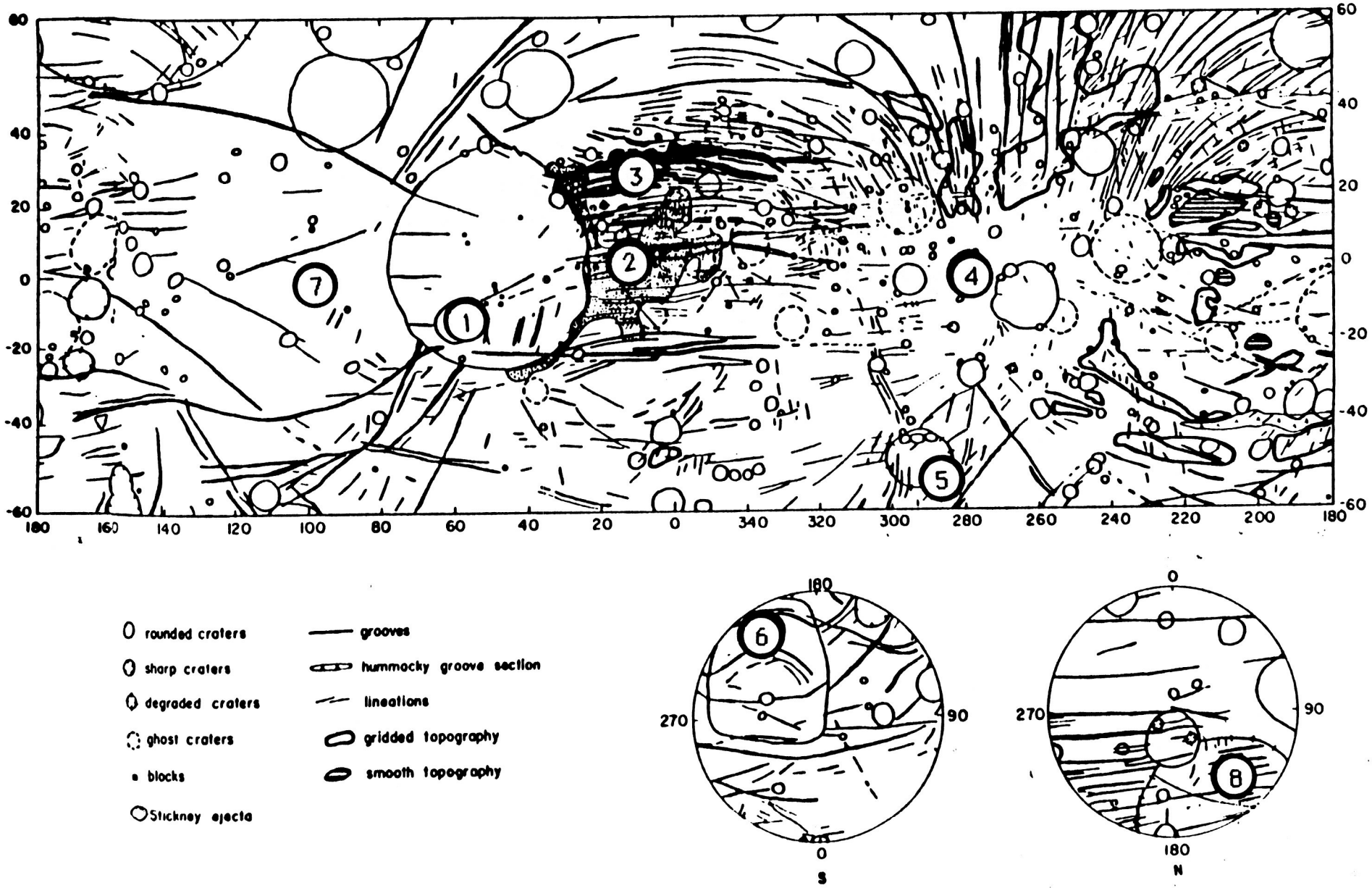

Figure 3.7.1 Landing Sites on Phobos (Reference 1)

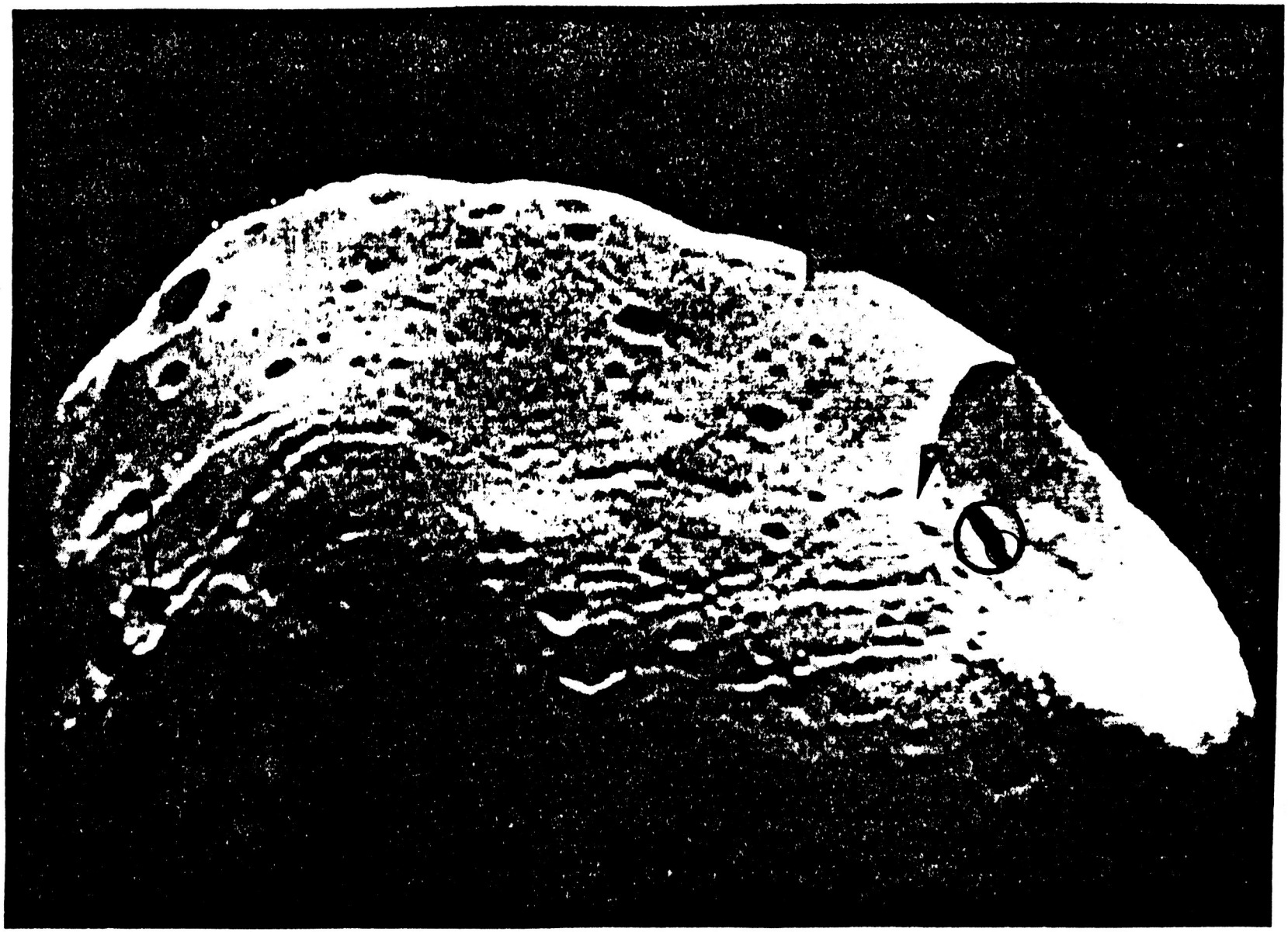

Figure 3.7.2 Phobos Site #1, Inner Stickney Crater

(Reference 2)

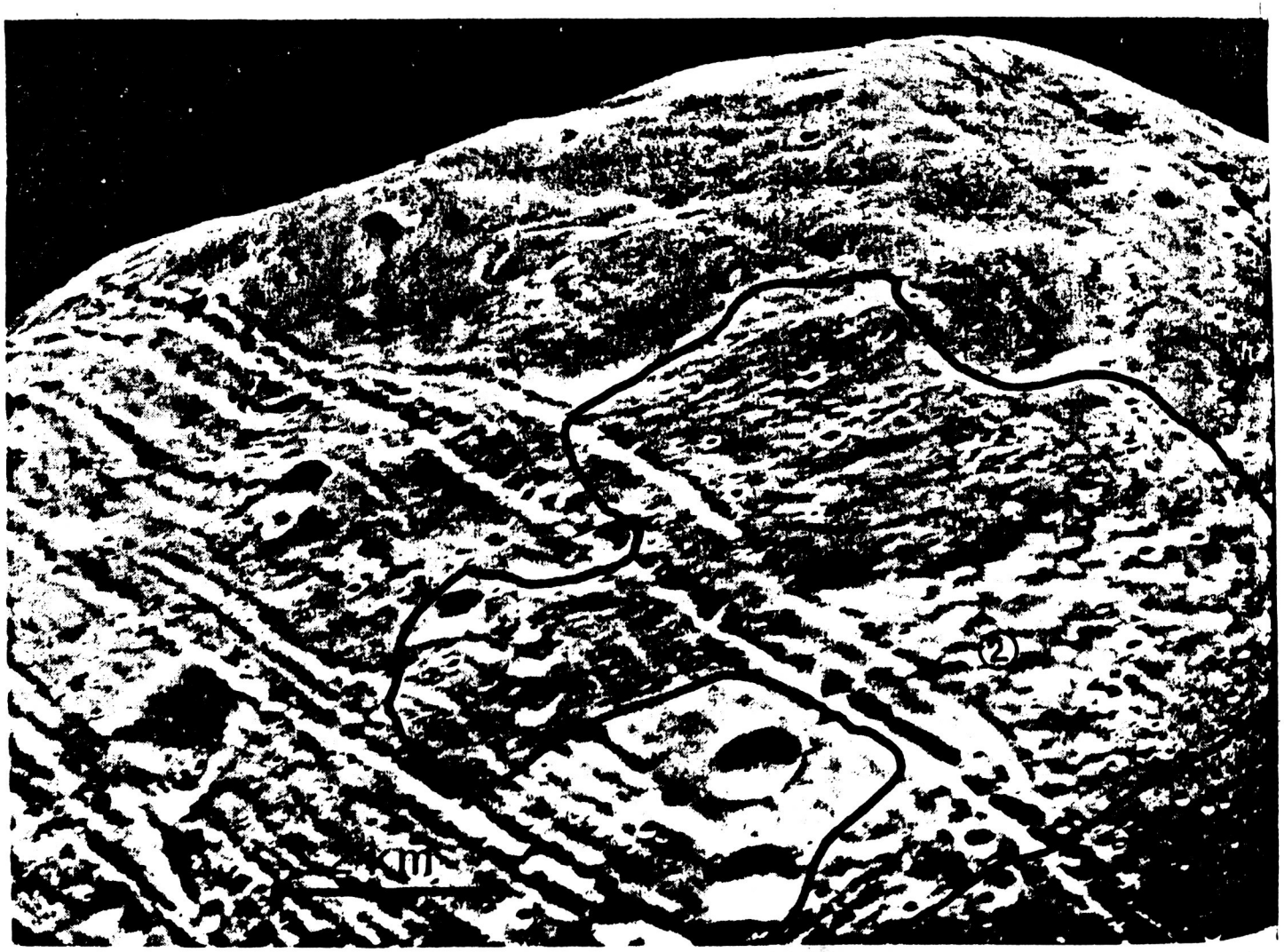

Figure 3.7.3 Phobos Site #2 , Stickney Ejecta (Reference 3)

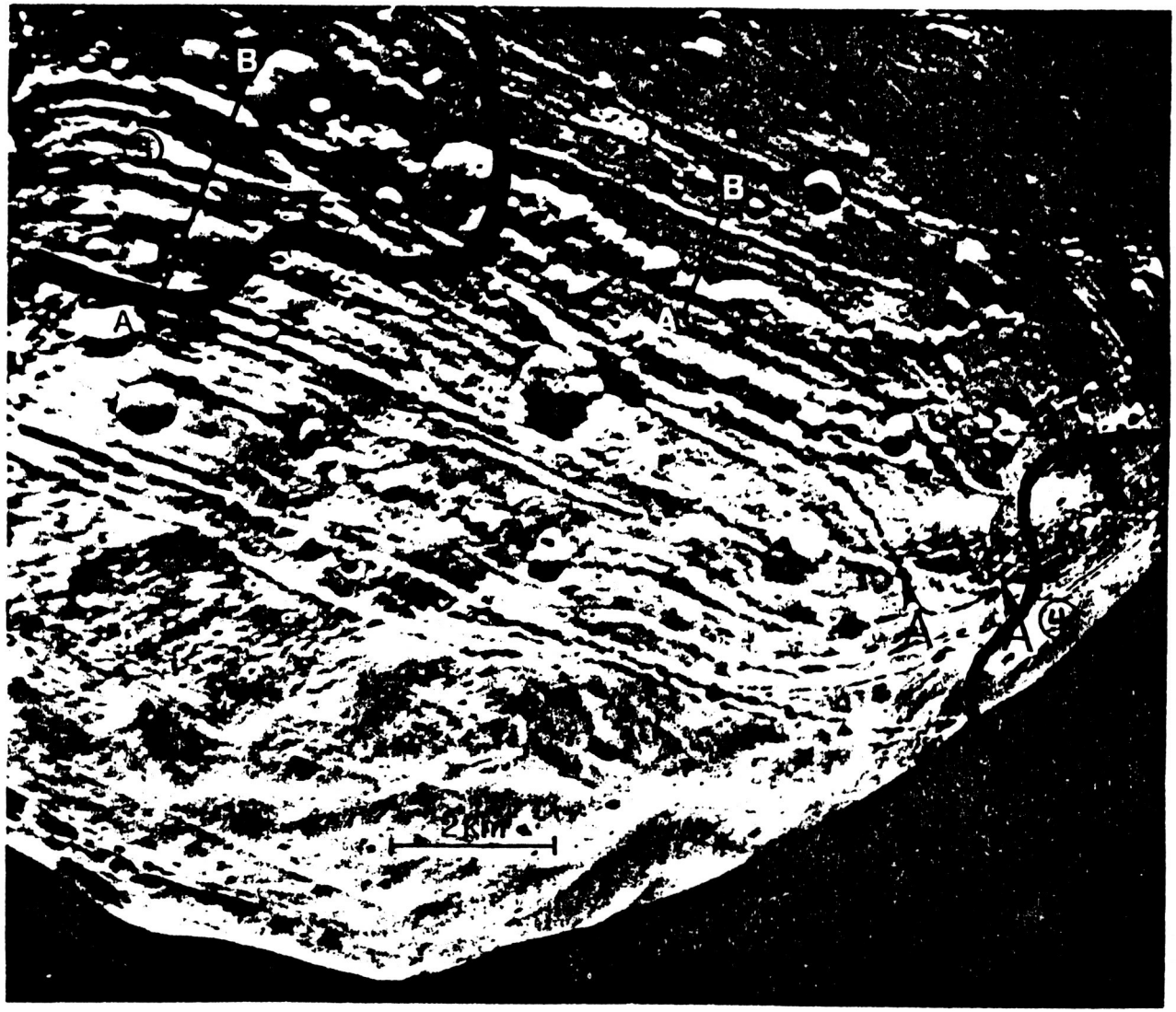

Figure 3.7.4 Phobos Sites #3 and #4 , Grooves and Stickney Antipodal (Reference 4)

available days to be spent on Phobos after visiting the four primary sites. Site #5 is along some of the ridges in the Southern hemispere. These ridges may be outcrops of material different from the regolith. Site #6 is inside Hall crater. Several layers of dark material has been observed in the crater walls. Site #7 is in the area west of Stickney. This area is void of many grooves and craters, and could represent a younger surface. Site #8 is inside Roche crater. This is a very interesting crater as far as surface morphology, and it would be the closest landing site to the north pole of Phobos.

REFERENCES

1. Thomas P., "Surface Features of Phobos and Deimos", Icarus, Vol. 40, No. 2, 1979, p. 225.

2. Thomas P. and J. Veverka, "Grooves on Asteroids: A Prediction", Icarus, Vol. 40, No. 3, 1979, p. 395.

3. Thomas, Icarus, No. 2, p. 230.

4. Thomas, P., J. Veverka, A. Bloom and T. Duxbury, "Grooves on Phobos: Their Distribution, Morphology and Possible Origin", Journal of Geophysical Research, Vol. 84, No. B14, 1979, p. 8460.

3.8 UNMANNED DEIMOS LANDER/ROVER

An unmanned Deimos lander/rover will be an integral part of the reconnaissance of the Martian moons. The design of a lander/rover should provide for adequate payload capability, flexibility of payload usage (i.e. 'in-situ' science packages or rover applications),minimum weight and the use or modification of existing systems. The use of existing, qualified systems and hardware, i.e. those of the Viking program, would greatly reduce the cost and simplify the design process of the vehicle. The lander/rover would be operated by astronauts on-board the barge orbiting Mars.

The payload on the lander would include scientific instruments and television cameras. The scientific instruments on the lander/rover will most likely be a minimal science package with the priority science measurements being geochemical and geochronological, emphasizing elemental composition and the age of Deimos respectively. Determining the presence of water, specifically the amount and availability, would definitely be a priority experiment. Like the Viking lander, a Radioisotope Thermoelectric Generator (RTG) would be used to power the Deimos lander/rover. Television cameras would provide high resolution pictures of the surface of Deimos.

By adding mobility to the lander/rover, access can be gained to virtually any point on the surface, making it possible to analyze both large and small surface variations. In addition to providing access to surface variations, mobility allows escape from landing site contamination and can be used to follow a path that will provide maximum communication windows.

There are several options on "the drawing boards" for the mobility of

unmanned probes (Reference 1). Some suggested mobility systems are: boom-deployed systems, flying (or "hopper") systems and wheeled systems. Furlable booms offer a practical means of getting short range mobility and could be considered for a stationary lander, but this system limits scientific data return significantly and can only be operated during limited communication windows. A flying rover system has the favorable characteristic of its ability to cross gross terrain obstacles that would require major detours by surface-constrained systems. However, the controllability of the vehicle and the protection of the scientific equipment during "hops" are problems with this system. Wheeled systems offer advantages over flying systems in the areas of weight, controllability and opportunity for adaptive science. The low gravity on Deimos would require the use of large diameter, light-weight wheels that provide enough traction to keep the vehicle on the surface. The uncertainity involved with a wheeled system on a low gravity surface leads us to believe that the "hopper" system would probably be the best option, but this is an area where a great deal of research and development should be conducted.

A sample return capability would also be a desired feature of the lander/rover. Small canisters could be filled with regolith or small surface rocks and ejected, with springs or small rocket motors, towards Mars for later rendezvous with the barge or TRV. The entire top half of the lander could possibly be designed for sample return, using lander separation similar to Apollo LEM separation on the moon. This system could also be utilized for the return of photographic film which would provide much greater imagery resolution than could television systems alone.

REFERENCE

1. Martin-Marietta Corp., " A Study of System Requirements for Phobos/Deimos", 1972.

3.9 DEIMOS LANDING SITES

Due to a lack of photo imagery on Deimos from the Mariner and Viking missions, it is not possible to go into as much depth on landing sites on Deimos as was done with Phobos. However, the scientifically interesting areas mentioned in Section 3.2 would be a logical place to start.

4.0 MANAGEMENT STATUS

To accomplish our project objectives, the TSS design team was divided into two technical groups, one management group, and a project manager, as depicted in Figure 4.1. The Ascent/Descent Group was responsible for developing preliminary designs for a two stage ascent/descent vehicle. The Mars Moon Reconnaissance Group was responsible for developing a reconnaissance mission to the Martion moons. The management group was composed of the technical directors of the two technical groups, and was responsible for assigning tasks, developing timelines, tracking progress, and supporting the project manager. The project manager was responsible for coordinating the efforts of the two technical groups and overseeing the entire design project. Program timelines and PERT/CPM charts leading to this report are shown in Figures 4.2-4.9. The time schedule was followed very well, however, the ascent/descent group was unable to complete the attitude control system analysis and the interior configuration of the vehicle, except for rudimentary placing of the tanks. Figure 4.10 depicts pie charts showing the percentage of hours that each group has worked and the percentage of personnel cost for each group. Figure 4.11 contains graphs showing the weekly proposed and actual manhours and costs.

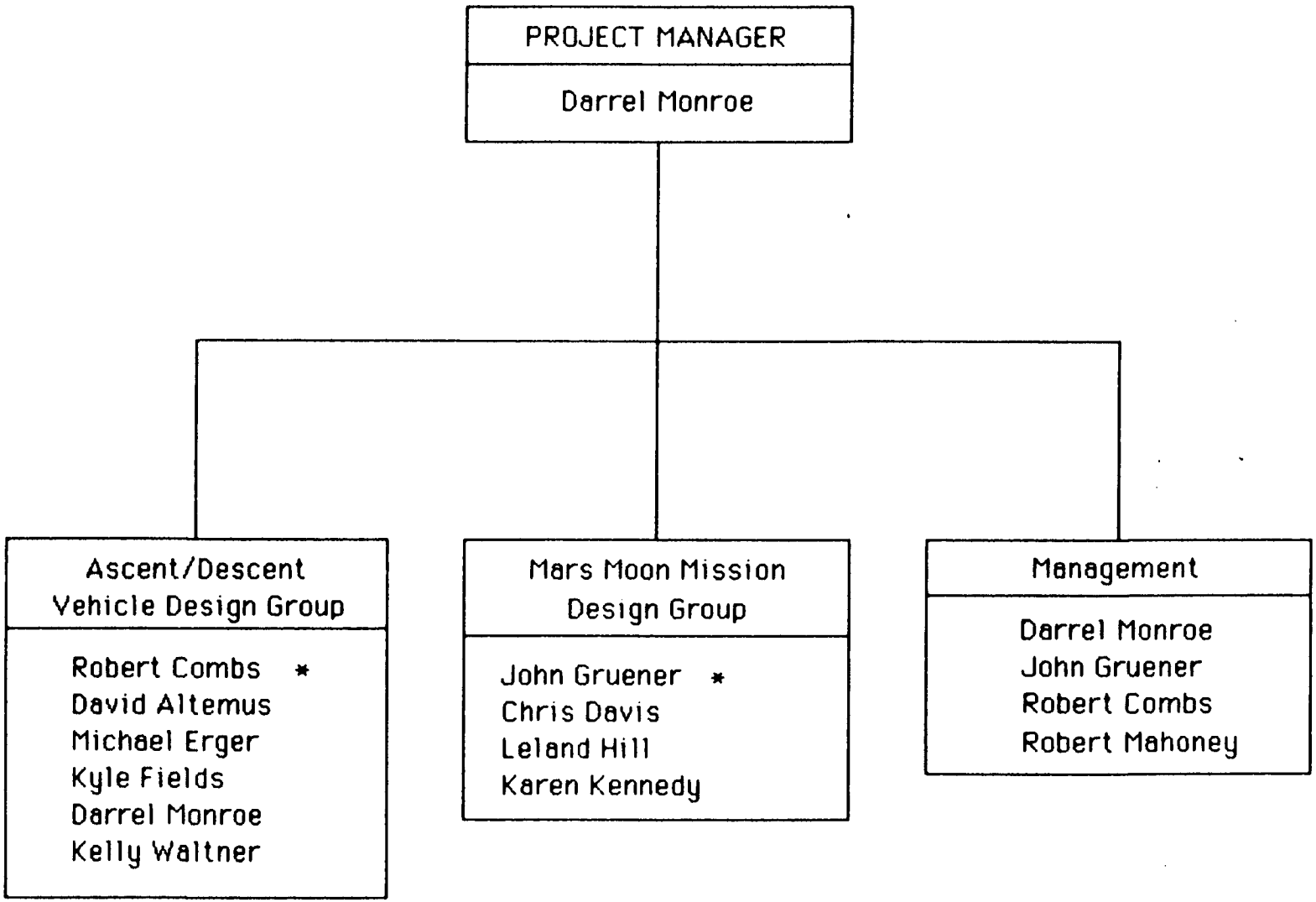

Figure 4.1 Organizational Structure

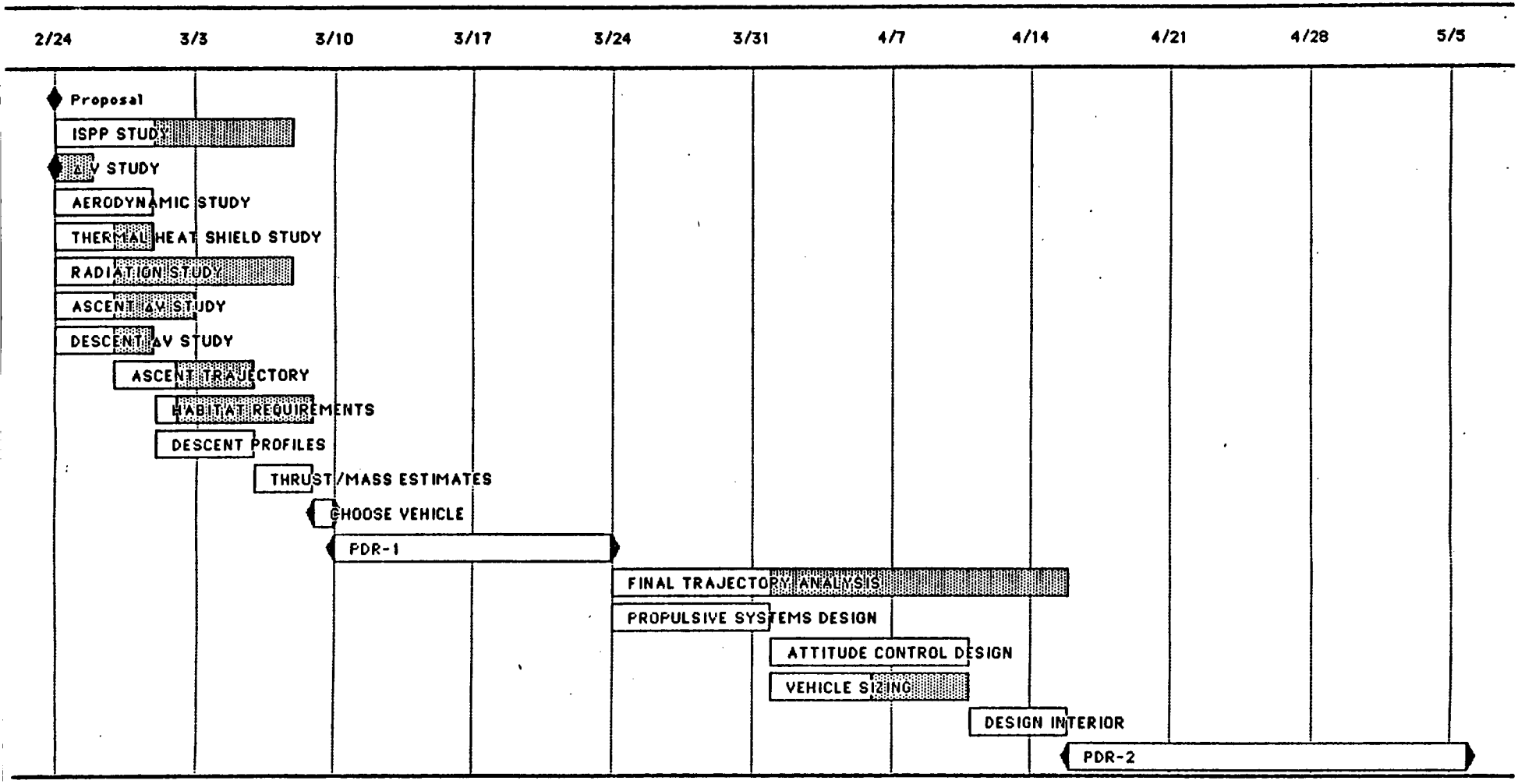

Figure 4.2 Ascent/Descent Timeline
Leading to PDR 1

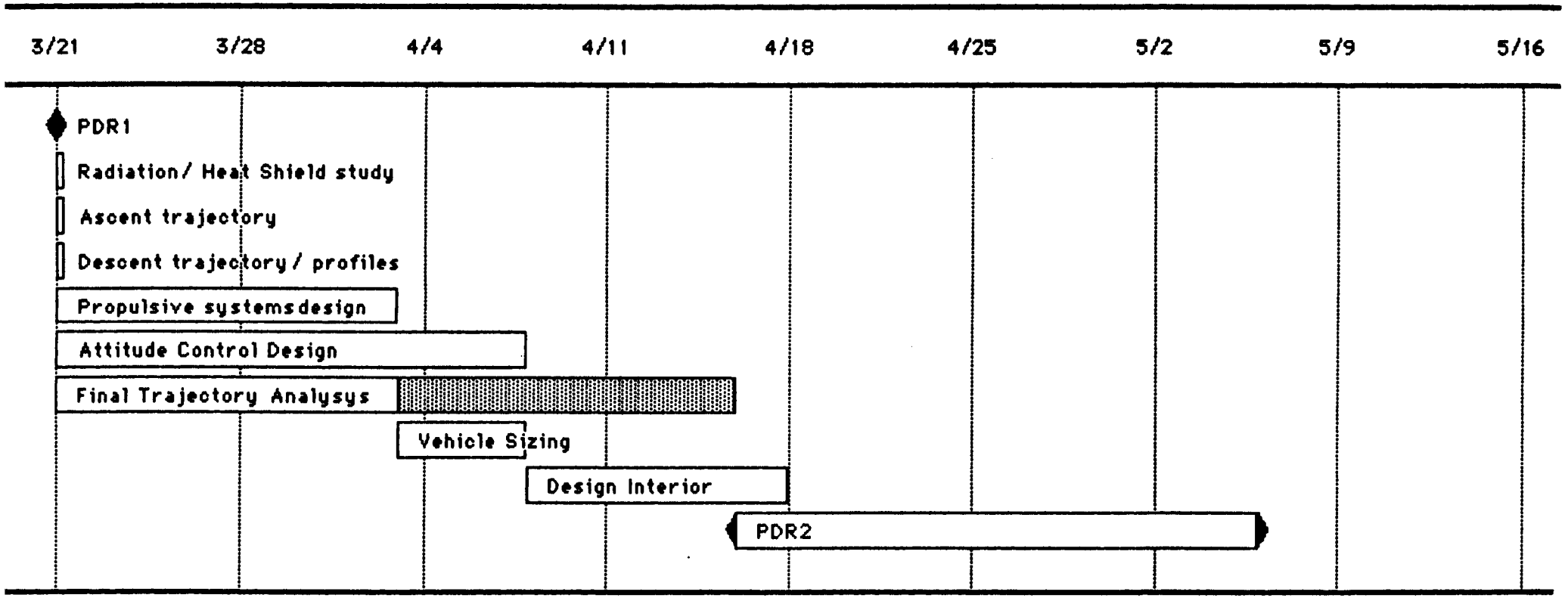

Figure 4.3 Ascent/Descent Timeline
Leading to PDR 2

Ascent /Descent Vehicle Group Schedule

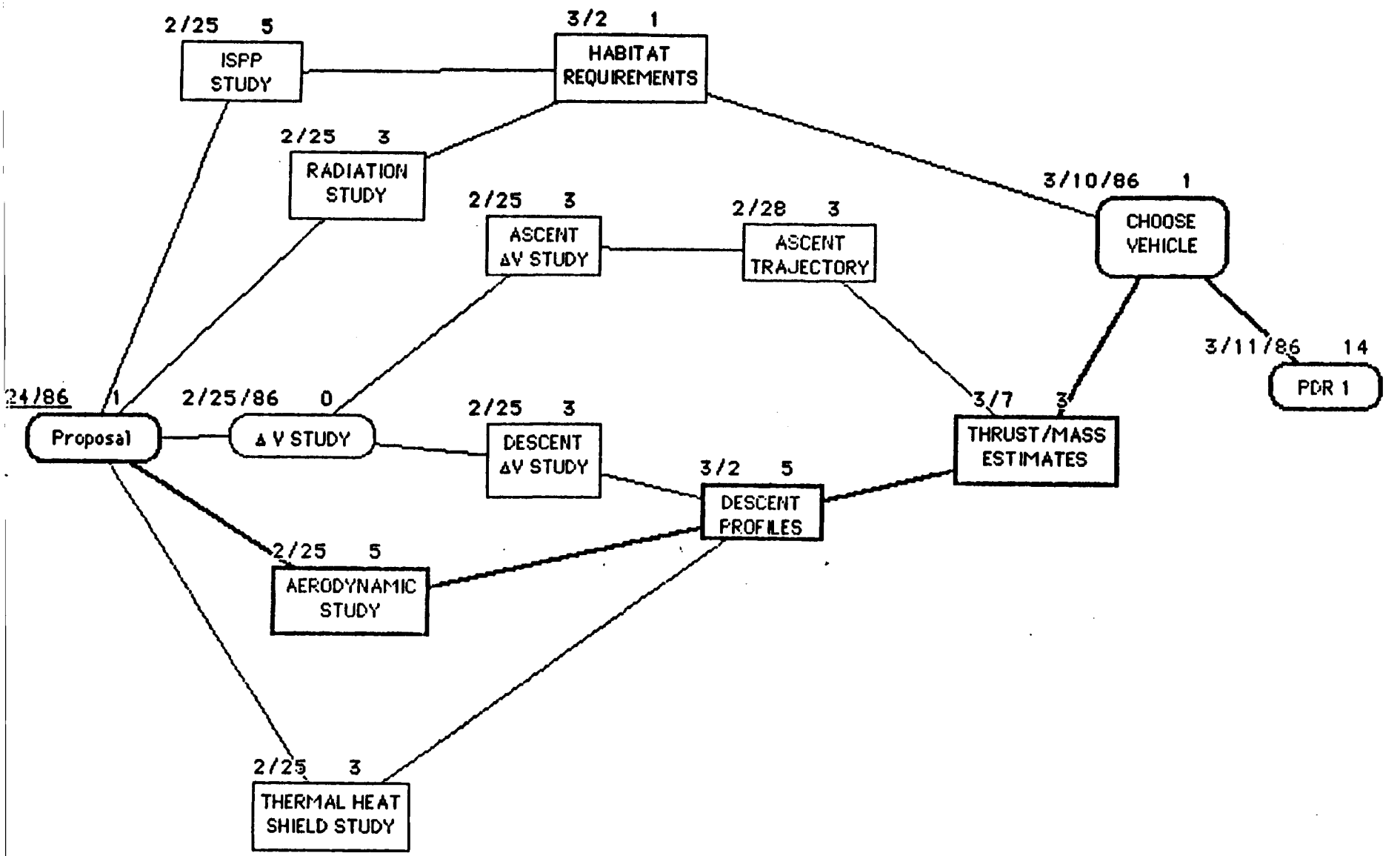

Figure 4.4 Ascent/Descent PERT/CPM Chart
Leading to PDR 1

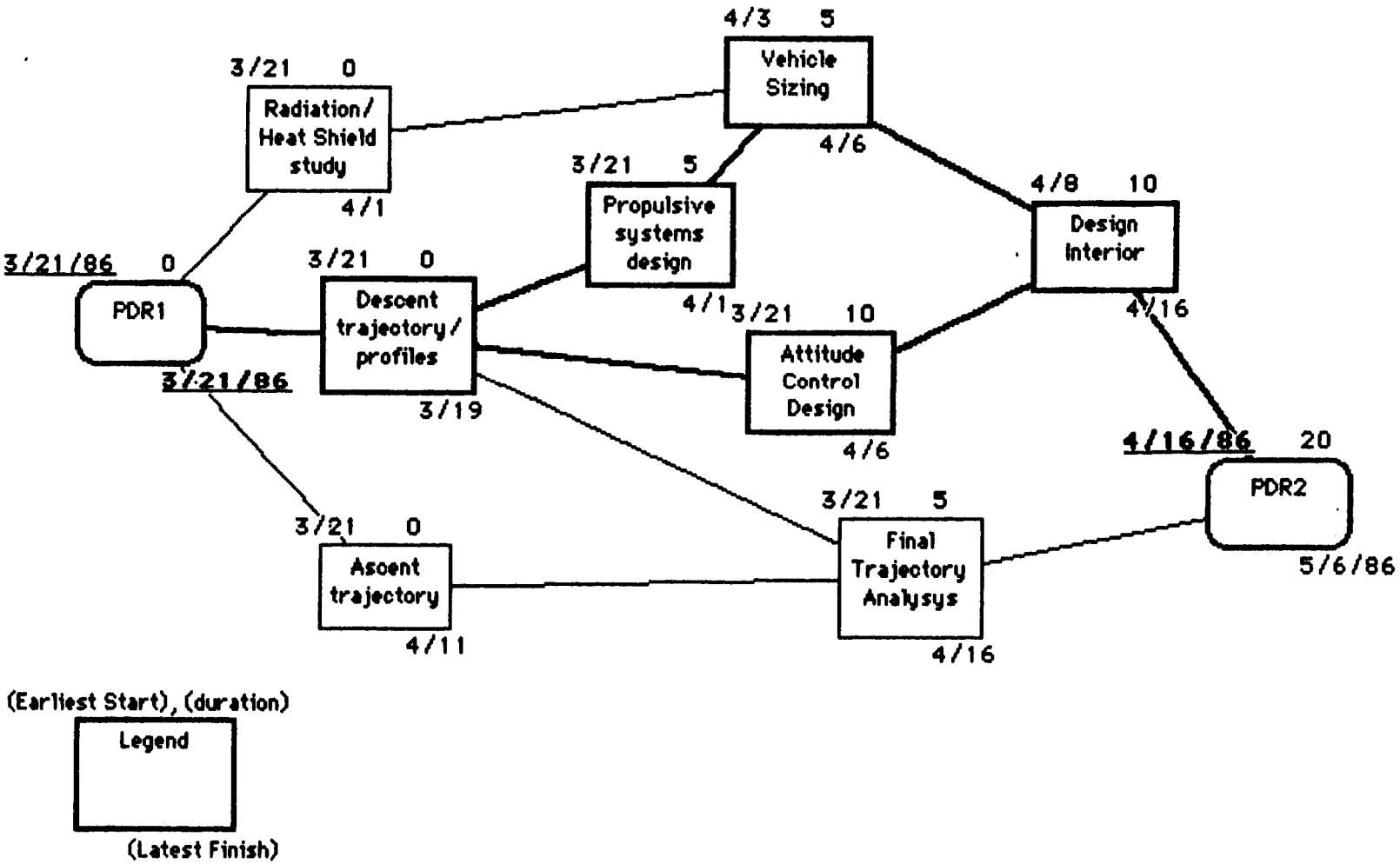

Figure 4.5 Ascent/Descent PERT/CPM Chart
Leading to PDR 2

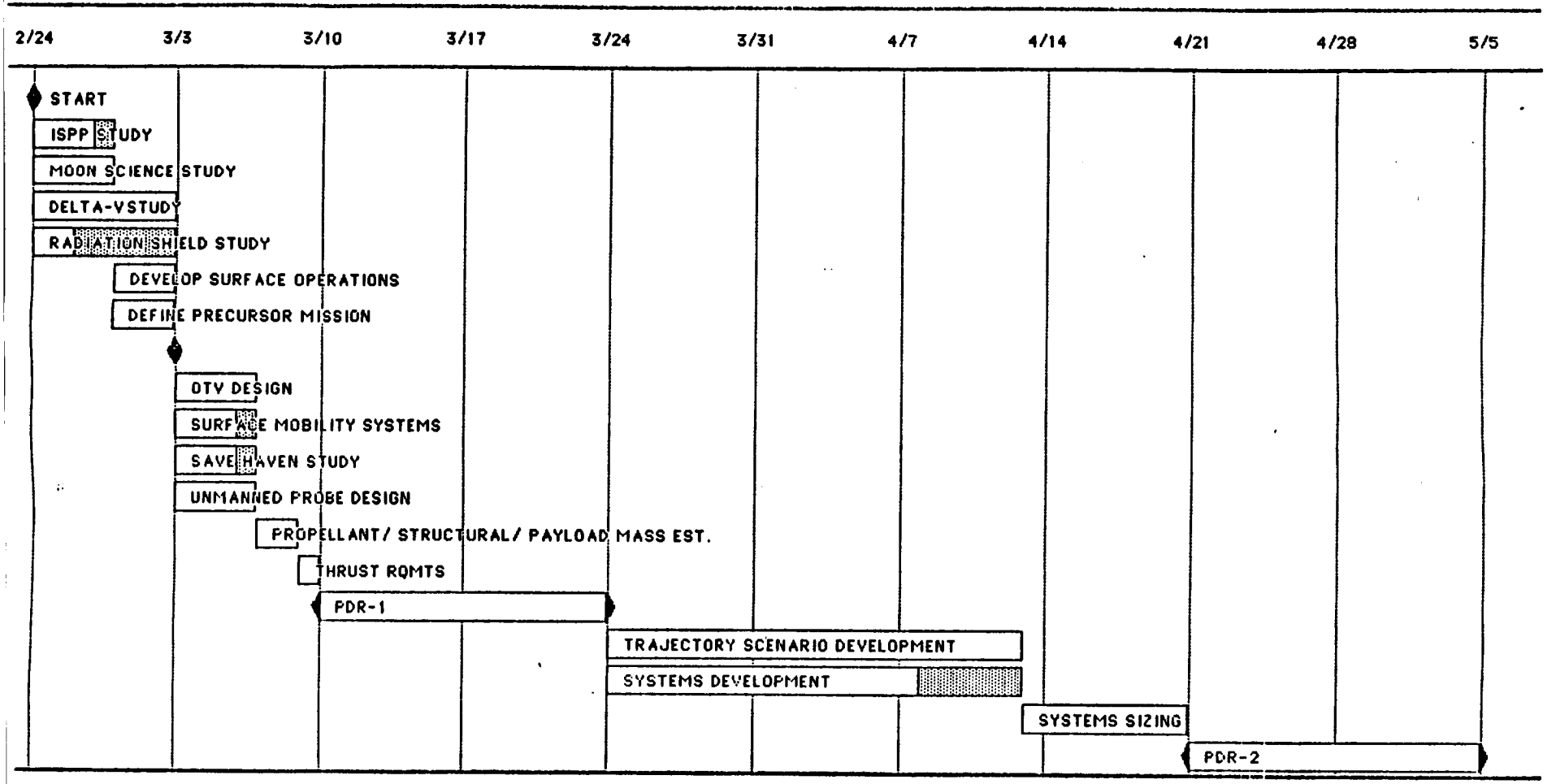

Figure 4.6 Moon Reconnaissance Timeline
Leading to PDR 1

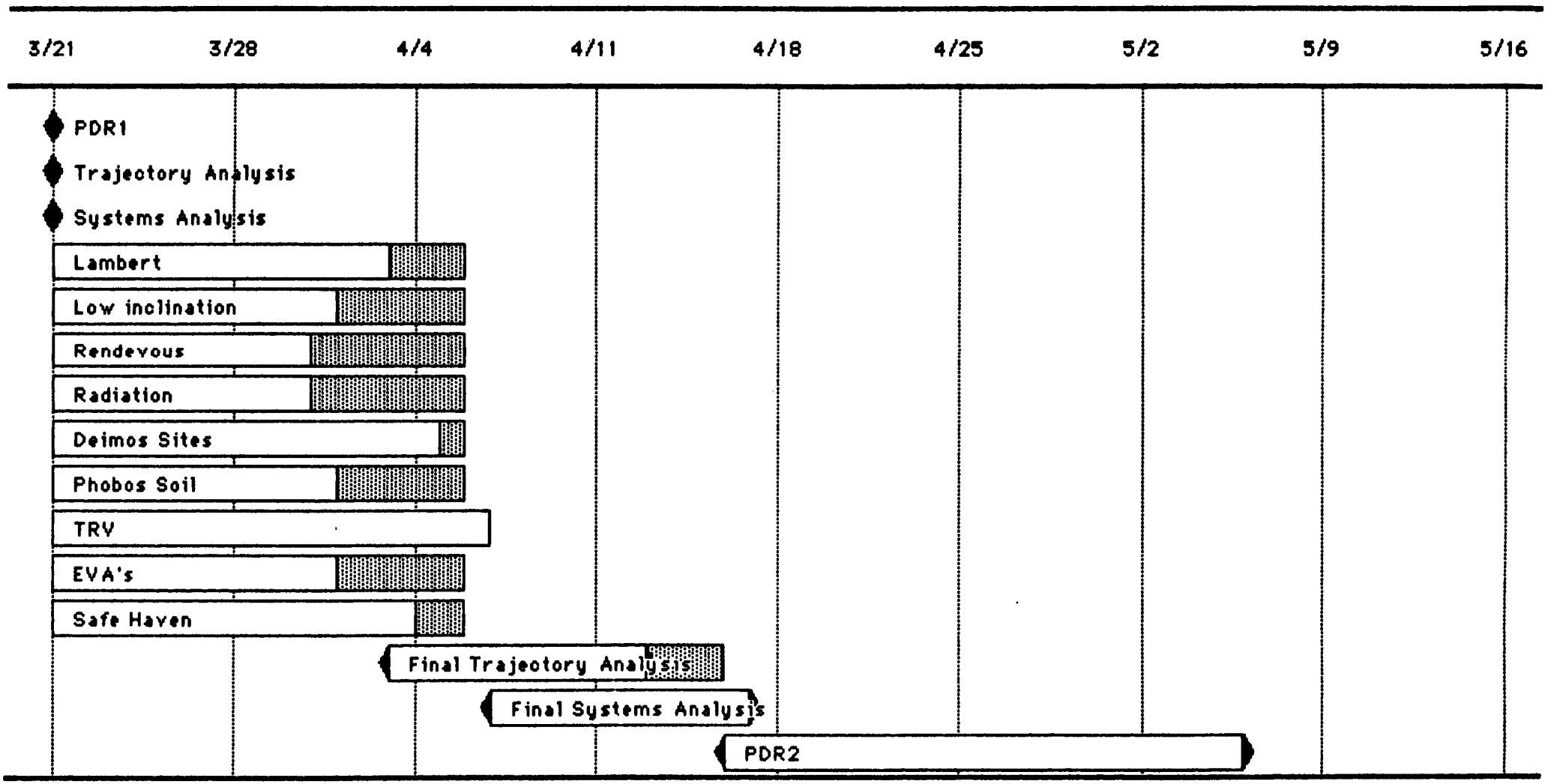

Figure 4.7 Moon Reconnaissance Timeline
Leading to PDR 2

Moon Reconaissance Group Schedule

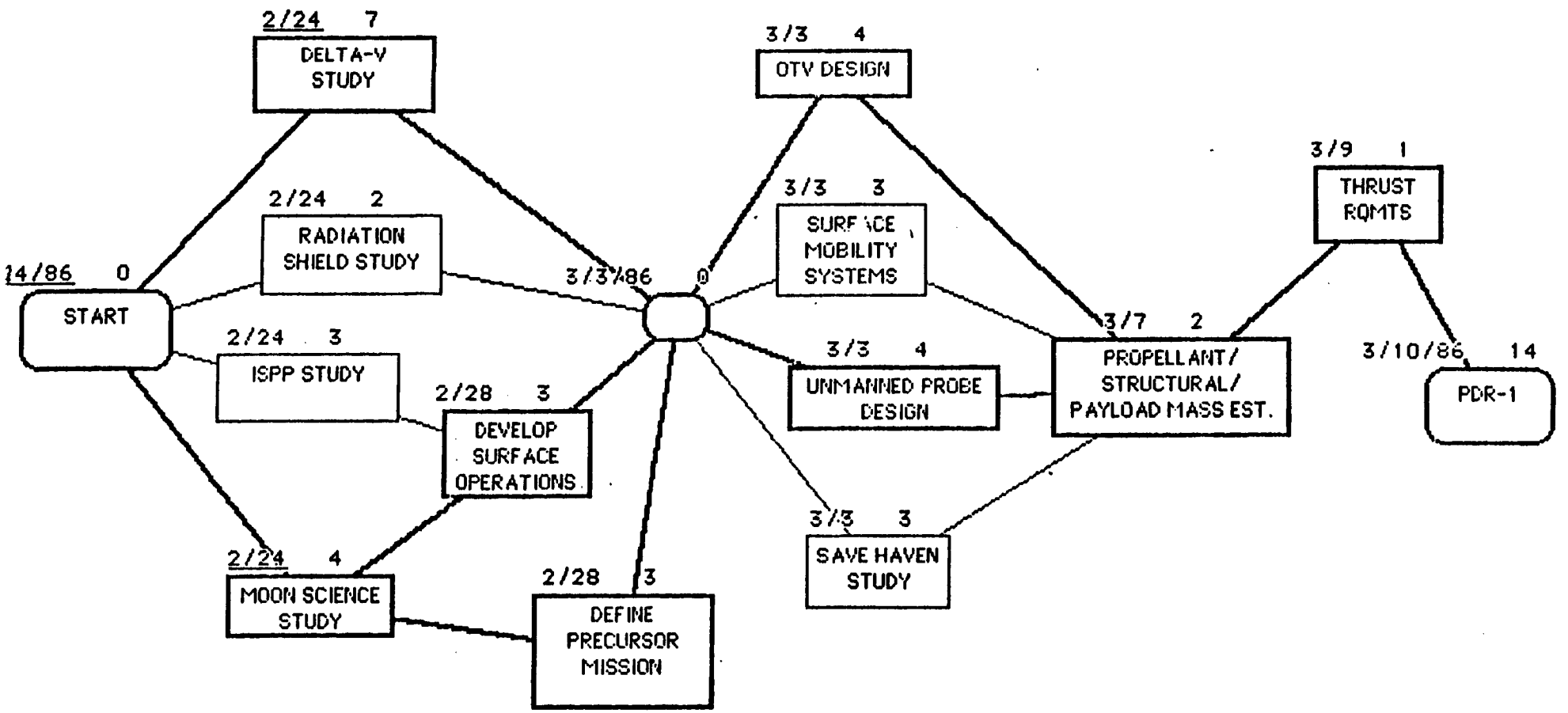

Figure 4.8 Moon Reconnaissance PERT/CPM Chart
Leading to PDR 1

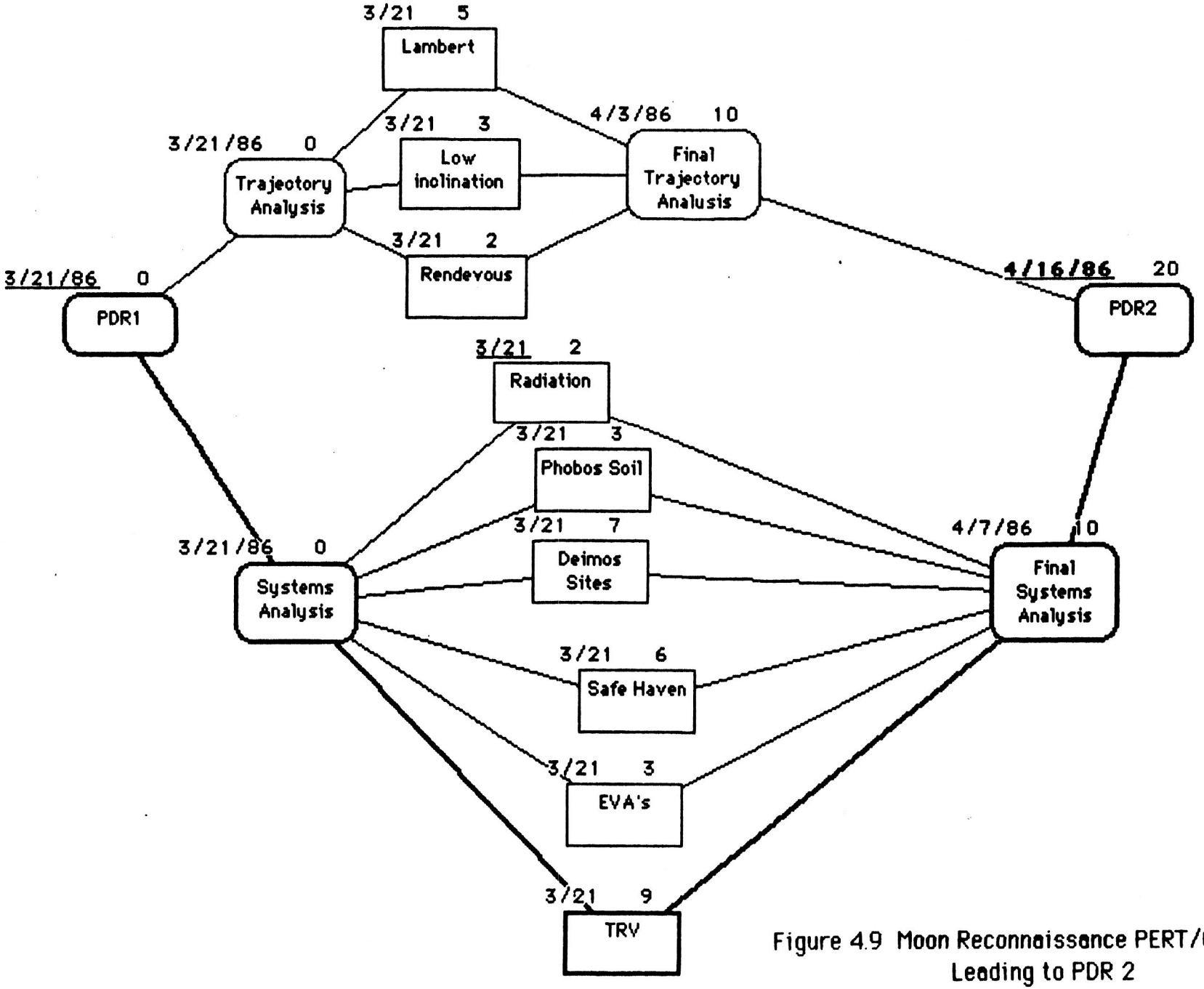

Figure 4.9 Moon Reconnaissance PERT/CPM Chart Leading to PDR 2

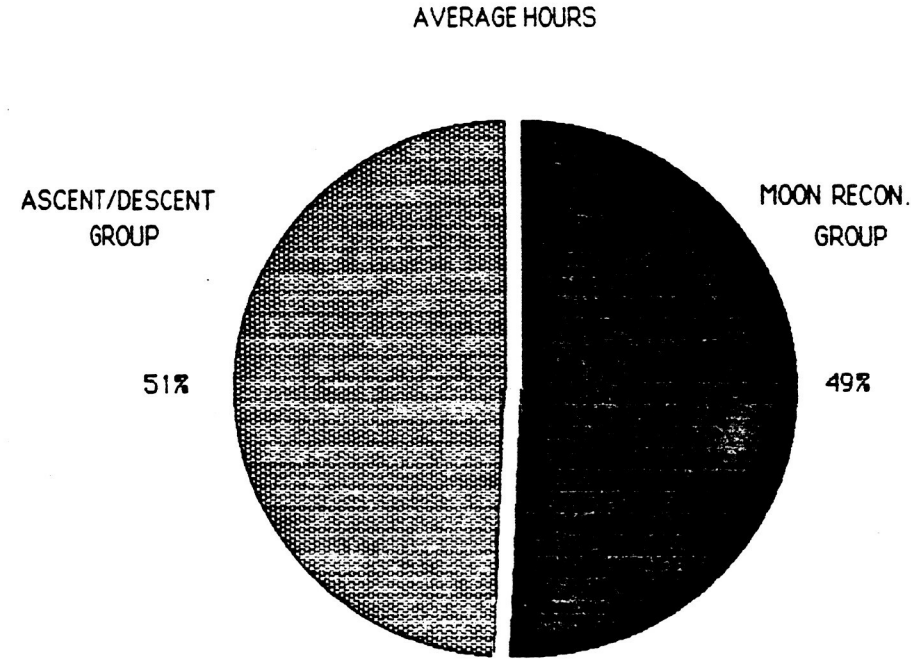

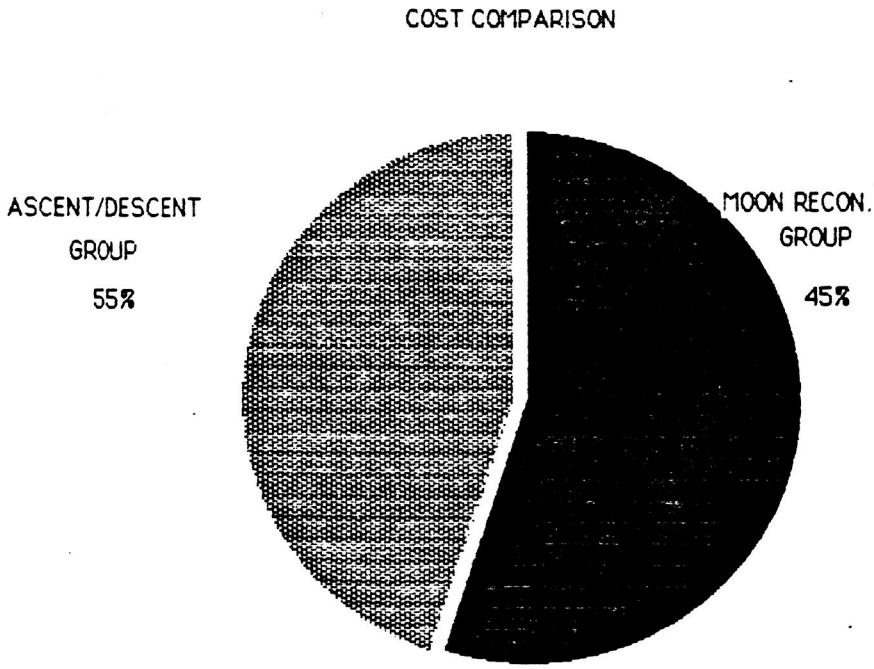

Figure 4.10 Pie Charts

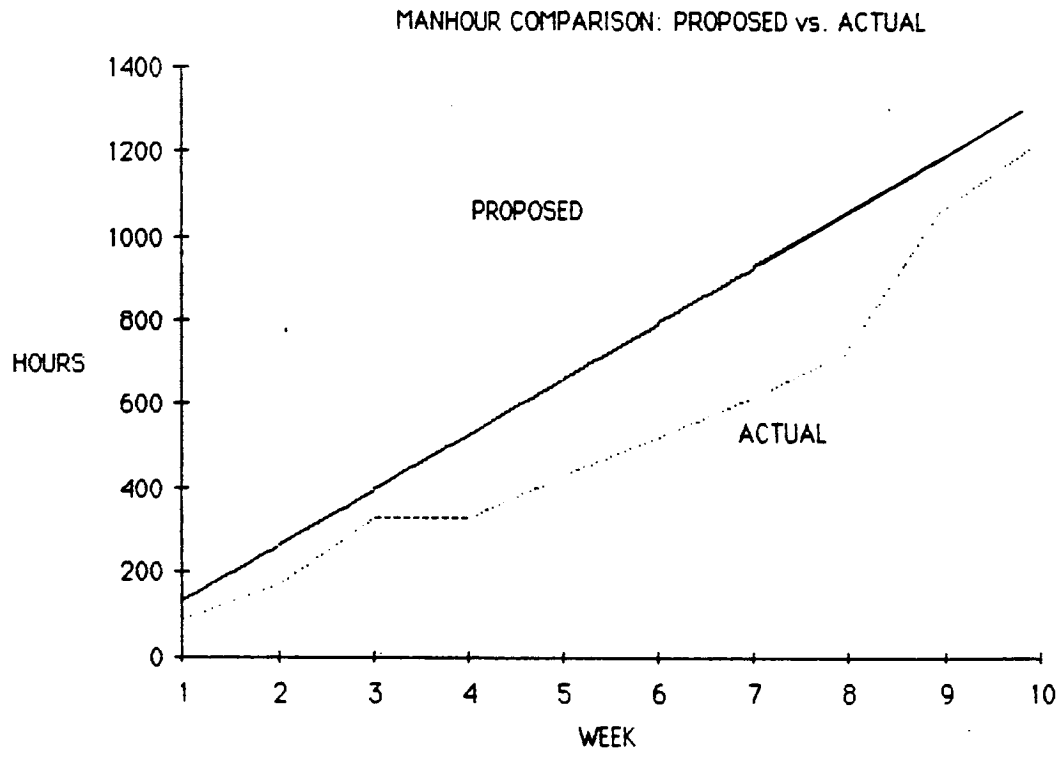

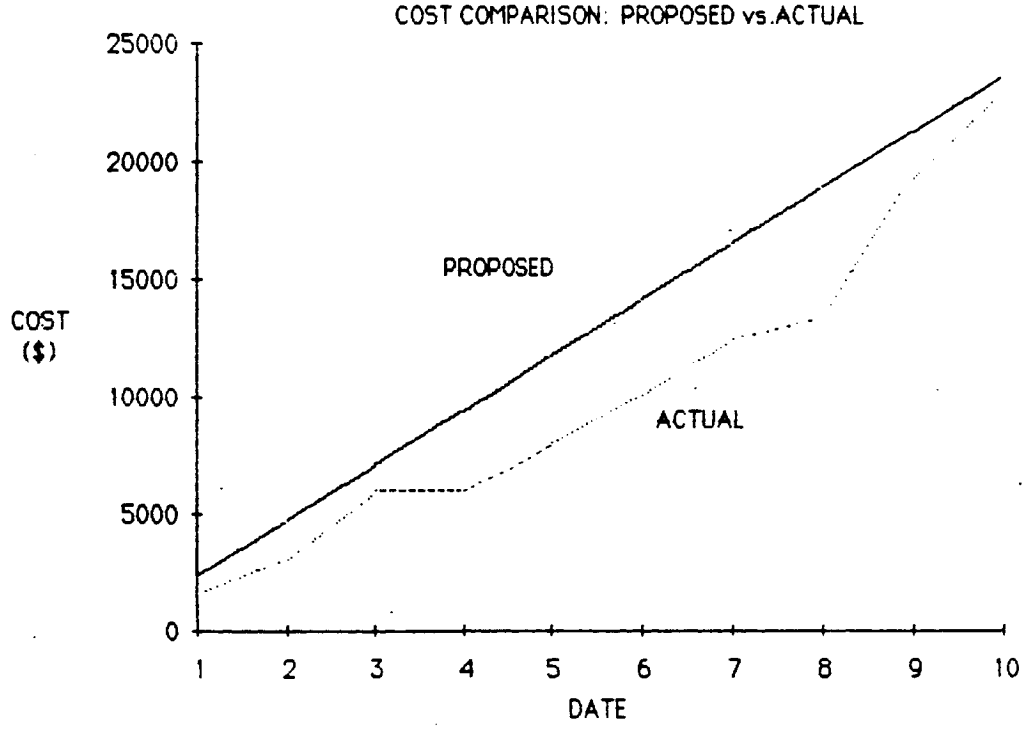

Figure 4.11 Manhour and Cost Comparison

4.1 RECOMMENDATIONS

During this contract period, *TSS* has considered both a two-stage ascent/descent vehicle and a reconnaissance mission to the two Martian moons. Work on the ascent/descent vehicle was based on developing worst case scenarios to prebuild a safety factor into the final chosen configuration. Moon reconnaissance work centered on developing an overall mission scenario which included trajectory analysis, system configuration, and EVA scenario development. In our estimation, we feel that overall, the final work done by both groups is well founded. The descent and ascent analysis are both strong in their use of worst case scenarios for vehicle sizing. The main propulsion system sizing is also strong, particularly in its implementation of the parabolic approximation of a bell shaped nozzle. The moon reconnaissance EVA scenarios developed are very thorough and have been well laid out. In a like manner, the trajectory analysis has also been well developed. The hardware systems proposed are very flexible in their expandibility and possible future uses. Though the TRV seems rather large for its mission to the moon Phobos, it must be remembered that the intent of the vehicle is not meerly to serve as a Phobos exploration vehicle, but also as a prototype asteroid exploration and mining vehicle. With the possible future use of the Martian system as a stepping stone to the asteroids and their natural resources, this is a logical, and farsighted suggestion.

However, there are some weaknesses and some areas which need further development. In the development on the mass and volume requirements of the ascent/descent vehicle, there is some question as to the validity of final requirements during descent. In our opinion, the fuel

requirement seems a bit on the low side for this vehicle. Although the vehicle does develop a large drag force on re-entry, this should not cut down on the fuel needed as drastically as it appears to in this analysis. In the ascent analysis, it would be desirable to rerun the Runge-Kutta integrator with real masses, as determined with the TKI sizing program. An effort should also be made to include in this model the effect of a rotating and spherical Mars. Also, work should be done in stability studies, attitude control system development, and descent trajectory analysis to include the ability of greater plane change capability. This would enable the development of a delta-v budget to evaluate the pros and cons of altering the parking orbit inclination. This delta-v budget should be developed in conjunction with moon reconnaissance trajectory analysis. Also in the area of the moon reconnaissance group trajectory analysis, future work should include the development of proximity operations using the CW equations. Time constraints prevented the detailed development of TRV propulsion systems, both main and attitude, and this should also be explored in the future. A logical area of future work would be to extend the TRV technology for use in an asteroid exploration vehicle, as mentioned previously.

5.0 COST STATUS

5.1 PERSONNEL COST

Pay scales were provided in the Request for Proposal as follows: Engineers, $15.00/hr; technical directors, $22.00/hr; and project manager, $25.00/hr. Table 5.1.1 below compares the proposed and actual personnel costs.

Table 5.1.1: EstimatedManhour Costs

Estimated weekly breakdown:	
1 project manager @ $25/hr, 16 hrs:	400.00
2 technical directors @ $22/hr, 16 hrs:	704.00
7 engineers @ $15/hr, 12 hrs:	1,260.00
total weekly personnel cost estimate:	$ 2,364.00
Projected cost for 10 weeks:	$ 23,640.00
plus 5th week total:	6,090.00
SUBTOTAL:	$ 29,730.00
plus 10% error estimate	$ 2,973.00
TOTAL ESTIMATE	$ 32,703.00

Actual costs

In section 4.0, a graph appeared depicting the actual costs compared to the projected costs. The actual manhour cost was $22,901.75, substantually less than predicted.

5.2 MATERIAL AND HARDWARE COST

The material and hardware cost estimates were based on expenses of previous design groups. Government furnished equipment (GFE) consisted of computer hardware, software, and mainframe time. A comparison of anticipated and actual costs follows in the table below.

Table 5.2.1 COMPARISON OF ANTICIPATED AND ACTUAL HARDWARE COSTS

	PROPOSED	ACTUAL
* Rental of Macintosh and peripherals:	$ 1,200	$ 1,200
* Rental of IBM PC-XT and peripherals:	2,780	2,780
software:	50	22
CDC computer mainframe time:	100	20
photocopies @ $0.05/each:	70	127.3
transparencies @ $0.70/each:	60	60.9
Purchase of Macintosh Plus/software	--	1,700
miscellaneous supplies	35	10
SUBTOTAL	$ 4,295	5,920.2
plus 10% estimated error	429.5	
TOTAL	$ 4,724.5	5,920.2

* Macintosh and IBM PC-XT rental rates based on current computer dealer rates.

5.3 TOTAL COST

	PROPOSED	ACTUAL
personnel cost:	$ 32,703.00	$ 22,901.75
material and hardware cost	4,724.5	5,920.20
GRAND TOTAL:	$ 37,427.5	$ 28,821.95

APPENDIX A

Program Volume Calculates Physical characteristics of ship

St	Input	Name	Output	Unit	Comment
		D	154.78565	M	Calculation constant
		B	-414.9534	M	Calculation constant
		E	161.5	M	Calculation constant
		A	2.6808257	M	Aspect ration
		C	162.5	M	Radius of curvature for shie
		H1	6.7143492	M	Height of upper module
L	1	H2		M	Height of lower module
	1800	V1		M^3	V/ upper module
	18	R		M	Radius of module
		V3	509.46161	M^3	V/ lower module, circle of c
					-- Kyle's radius=18M
L		Htot	7.7143492	M	Total height of vehicle
		Vtot	2309.4616	M^3	Total volume of vehicle
	100	Vasc		M^3	Total volume of ascentvehicl
L		Rasc	2.598449	M	Radius of Ascent vehicle
	16	R1		M	Radius of upper module

S Rule
* D=-B/A
* E-D=H1
* C-E=H2
* V1=PI()*R1^2*H1/3
* E^2+(A*E+B)^2=C^2
* A*E+B=R
* A=R/H1
* V3=PI()*(2*C^3-3*C^2*E+E^3)/3
* Htot=H1+H2
* Vtot=V1+V3
* Vasc=Pi()*(Htot-3)*Rasc^2

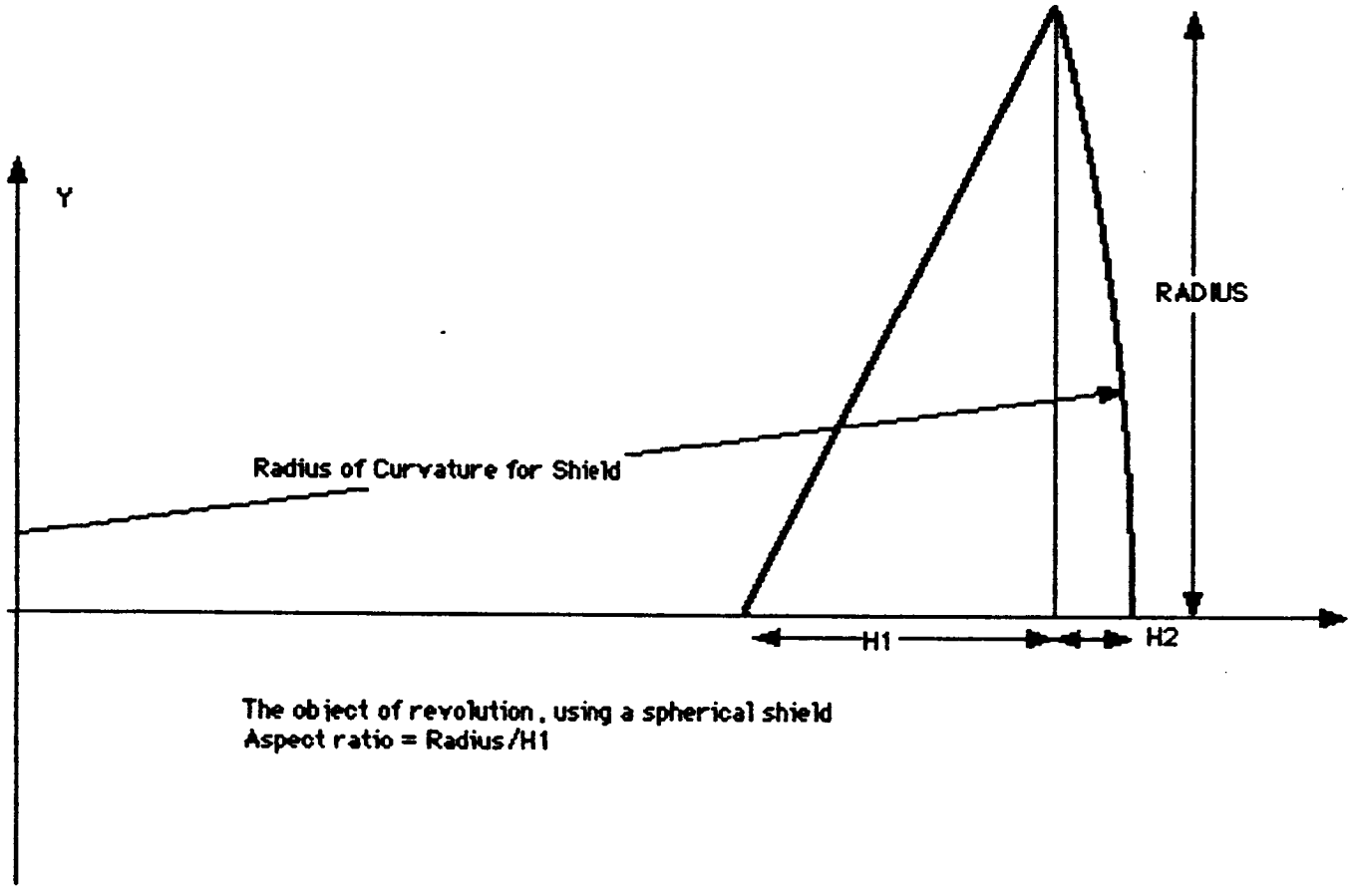

The object of revolution, using a spherical shield
Aspect ratio = Radius/H1

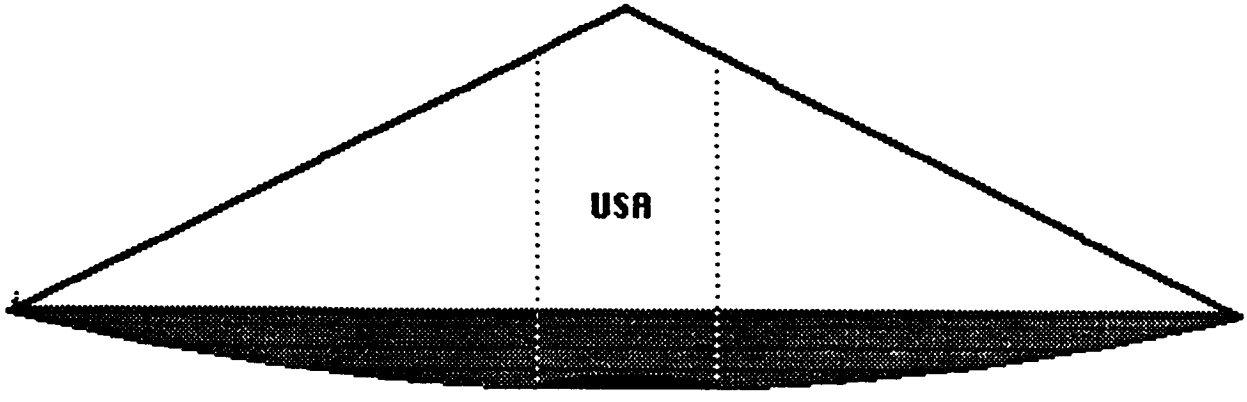

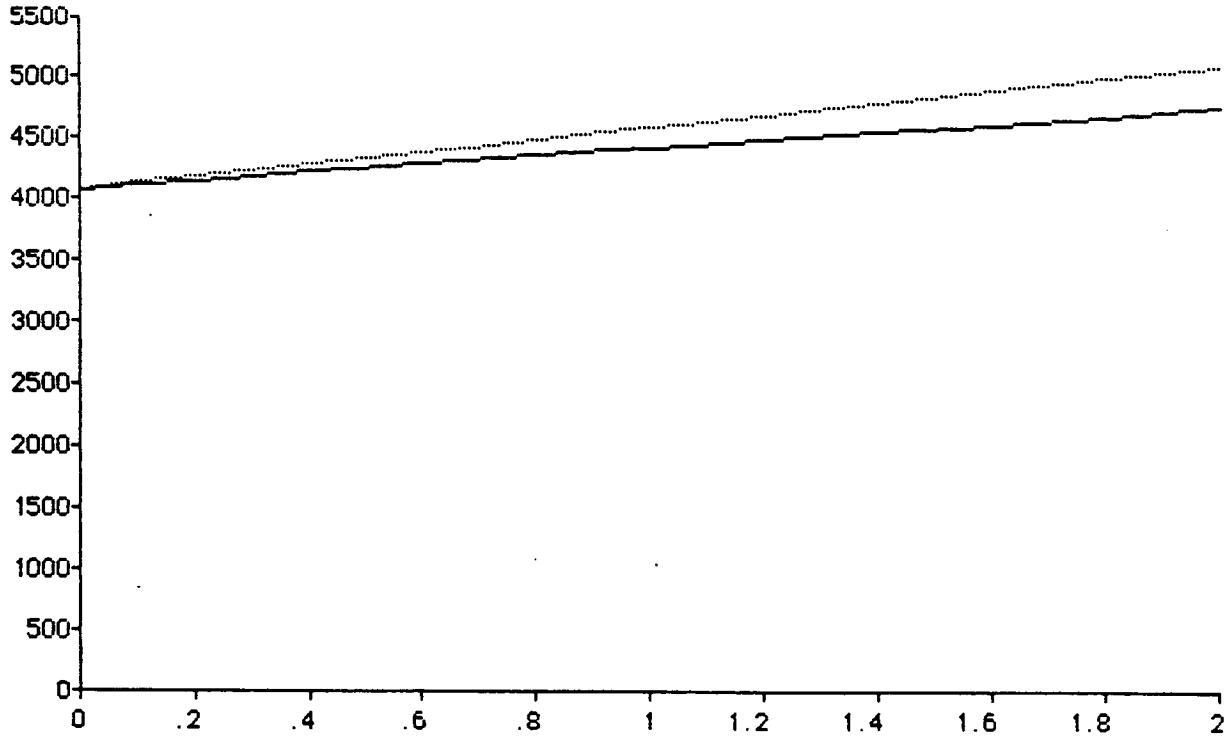

Volume of ship, m^3, two options

RADIUS = 18 m

H_1 = 12 m

H_2 = 1.6 m

APPENDIX B

DODV TKI Solver Program

Variable Sheet

	Input	Name	Output	Unit	Comment
	42828	mu		km^3/s^2	Grav. Paramater of planet
		r	9545	km	Radius at burn
	3895	Rp		km	Of parking orbit
		Ra	9545	km	Of parking orbit
	6720	a		km	Of parking orbit
		e	.4203869		Of parking orbit
		et	.515		Of transfer orbit
		ft	153.56194	deg	True anomaly of transfer orbit
		Vt	1.6898602	km/s	Velocity after burn
		Vi	1.6126682	km/s	Velocity before burn
		gamat	-23.0505	deg	Flight path angle after burn
		gamai	-2.34E-16	deg	Initial flight path angle at burn
		ftc	206.43806	deg	Corrected true anomaly after burn
L		Deltav	180.59345	m/s	Deltav of burn
		Rat	10605	km	Apoapsis of transfer orbit
		*** radius of Mars is 3395 km***			
	3395	Rpt		km	Perigee of transfer orbit
	3495	re		km	Radius at atmos entry
		fe	23.67615	deg	True anomaly at atmos entry
L		Ve	4233.1113	m/s	Velocity at atmos entry
L		dgama	-6.072074	deg	Change in flight path angle at deorbit burn.
L	6500	at		km	Of transfer orbit
L	180	f		deg	Of parking orbit
L		gamae	7.7944227	deg	flight path angle at entry

Rule Sheet

Rule

```
r = a*(1-e^2)/(1+e*cos(f))
Vi = sqrt(mu*(2/r-1/a))
tan(gamai) = e*sin(f)/(1+e*cos(f))
Rat = 2 *at - Rpt
et = (Rat-Rpt)/(2*at)
r = at*(1-et^2)/(1+et*cos(ft))
Vt = sqrt(mu*(2/r-1/at))
tan(gamat) = et*sin(ftc)/(1+et*cos(ftc))
ftc = 2*pi() - ft
Deltav = sqrt (Vi^2 + Vt^2 - 2*Vi*Vt*cos(gamat-gamai))
Ra = 2*a - Rp
e = (Ra-Rp)/(2*a)
Ve = sqrt(mu*(2/re-1/at))
re = at*(1-et^2)/(1+et*cos(fe))
dgama=gamat-gamai
tan(gamae) = et*sin(fe)/(1+et*cos(fe))
```

APPENDIX C

```
      PROGRAM MARSDES(TTY,OUTPUT,DATA,TP,TAPE3=OUTPUT,TAPE5=TTY,
     +TAPE6=TTY,TAPE7=TP,TAPE9=DATA)
C*****************************************************************
C  THIS IS THE MAIN PROGRAM OF THE MARS VEHICLE DESCENT SIMULATION
C  WRITTEN BY PRESTON CARTER.  MODIFICATIONS AND ADDITIONS TO THE
C  SIMULATION WERE WRITTEN BY KYLE FIELDS AND MICHAEL ERGER. THESE
C  ADDITIONS AND MODIFICATIONS INCLUDE THE PROPULSIVE DECELERATION
C  PHASE, AEROHEATING ROUTINE, AND G-LOADING INFORMATION.
C  THE CALCULATION UNITS OF THIS PROGRAM ARE METERS, KILOGRAMS,
C  AND SECONDS.
C*****************************************************************
      COMMON/RO/RO
      COMMON/RHOO/RHOO
      COMMON/HMAX/HMAX
      COMMON/E/E
      COMMON/BALLCL/BALLCL
      COMMON/BALLCD/BALLCD
      COMMON/G/G
      COMMON /AMO/AMO
      COMMON/HEQUIL/HEQUIL
      COMMON RB
      COMMON /PROP/FFR,DM,PALT,THRUST
      COMMON/TEMP/TEMP
C************* NECESSARY CHANGE ****************
      COMMON/ROLL/ROLL
C***********************************************
C
      DIMENSION X(7),DX(7)
      DIMENSION TEMP(101),PRESS(101)
      REAL LD
      CALL TPDATA(TEMP,PRESS)
C
      WRITE(9,*)'TEMP',TEMP(1),TEMP(100),TEMP(56)
C*************** NECESSARY CHANGE ***************
      ROLL = 0.0
      DX(4)=0.0
C***********************************************
      GMAX=0.0
      TWMAX=0.0
      G = 3.730
      RO = 3397500.0
      RHOO = 1.56E-2
C HMAX'S UNIT IS KILOMETERS INSTEAD OF METERS.
      HMAX = 100.0
      DT = 1.0
C PRINT OPENING STATEMENTS*
      CALL HOLA
      WRITE(6,*)'RADIUS OF VEHICLE (M)?'
      READ(5,*)RB
      WRITE(6,*)'MASS OF VEHICLE (KG)?'
      READ(5,*) AMO
      WRITE(6,*)'LIFT COEFFICIENT ?'
      READ(5,*)CL
      BALLCL=AMO/(CL*3.141592654*RB*RB)
      WRITE(6,*)'L/D ?'
      READ(5,*)LD
```

```
      BALLCD = BALLCL*LD
      WRITE(6,*)'INITIAL HEIGHT IS 100 KM'
      H=100000.0
      X(3) = H + RO
      WRITE(6,*)'INITIAL V (M/SEC)?'
      READ(5,*)X(4)
      WRITE(6,*)'INITIAL FLIGHT PATH ANGLE (DEG)?'
      READ(5,*)ANGLE
      X(5) = 0.017453 * ANGLE
      WRITE(6,*)'PULLOUT ALTITUDE (M)?'
      READ(5,*)HEQUIL
      WRITE(6,*)'EMMISIVITY OF ABLATIVE SURFACE?'
      READ(5,*)E
      WRITE(6,*)'OUTPUT TAPE NUMBER?'
      WRITE(6,*)'USE TAPE 6 FOR TTY OUTPUT'
      WRITE(6,*)'USE TAPE 9 FOR OUTPUT DIRECTED TO FILE CALLED DAT
A'
      WRITE(6,*)'OUTPUT TAPE NUMBER?'
      READ(5,*)IUNIT
C**PROPULSION INFO-----------------------------------------
      WRITE(6,*)'INITIAL PROPULSIVE DECELERATION ALTITUDE (KM)?'
      READ(5,*)PALT
      PALT=PALT*1000.0
      IF(PALT .EQ. 0.0)GO TO 333
      WRITE(6,*)'FUEL MASS FLOW RATE (KG/S)?'
      READ(5,*)FFR
      WRITE(6,*)'ENGINE THRUST (N)?'
      READ(5,*)THRUST
 333  CONTINUE
C-----------------------------------------------------------
      DX(7)=0.0
      X(1) = 0.0
      DX(4)=0.0
      X(2) = 0.0
      X(6) = 0.0
      X(7) = AMO
      TMAX = 5000.0
      TERMH = 0.0
      WRITE(6,*)'UPPER TRAJECTORY OUTPUT INTERVAL (S)'
      READ(5,*)NSTEPS
      WRITE(6,*)'SIMULATION IN PROGRESS...'
      TIME = 0.0
      WRITE(IUNIT,*)'      >>> MARS DESCENT SIMULATION <<< '
      WRITE(IUNIT,*)' '
      WRITE(IUNIT,*)'              DESCENT PROFILE      '
      WRITE(IUNIT,*)' '
      WRITE(IUNIT,*)'M/(CL*S) (KG/M**2) = ',BALLCL
      WRITE(IUNIT,*)'INITIAL MASS (KG) = ',AMO
      WRITE(IUNIT,*)'COEFFICIENT OF LIFT = ',CL
      WRITE(IUNIT,*)'RADIUS OF VEHICLE (M) =',RB
      WRITE(IUNIT,*)'L/D = ',LD
      WRITE(IUNIT,*)'H (M) = ',H
      WRITE(IUNIT,*)'V (M/SEC) = ',X(4)
      WRITE(IUNIT,*)'GAMA (DEG) = ',ANGLE
      WRITE(IUNIT,*)'THRUST (N) = ',THRUST
      WRITE(IUNIT,*)'INITIAL PROP. DEC. ALT. (KM) = ',PALT/1000.0
      WRITE(IUNIT,*)'FUEL FLOW RATE (KG/S) = ',FFR
```

```
      WRITE(IUNIT,*)'   '
      CALL OUTPUT(TIME,X,DX,TW,IUNIT)
      H = X(3) - RO
*************------ LOOP FOR DESCENT BEGINS -----************
  200 IF((TIME.LT.TMAX).AND.(H.GT.TERMH).AND.X(4).GT.0.0)THEN
      IF(X(3)-RO .LE. PALT+7000.)NSTEPS=5
      IF(X(3)-RO .LE. PALT+2000.)NSTEPS=1
      IF(X(3)-RO .LE. 100.)NSTEPS=1
      IF(X(3)-RO .LE. 100.)DT=.25
      DO 300 I=1,NSTEPS
          CALL RK(X,DX,DT,7)
          TIME = TIME + DT
      IF(DX(4) .LT. GMAX)GMAX=DX(4)
  300 CONTINUE
      CALL OUTPUT(TIME,X,DX,TW,IUNIT)
      IF(TW .GT. TWMAX)TWMAX=TW
          H = X(3) - RO
      ELSE
        GMAX=GMAX/9.81
        WRITE(6,*)' '
        WRITE(6,*)'TERMINATION TIME = ',TIME
        WRITE(6,*)'TERMINATION ALTITUDE = ',H
        WRITE(6,*)'MAXIMIMUM G-EARTH ACCELERATION=',GMAX
        WRITE(6,*)'MAXIMIMUM STAGNATION TEMPERATURE (K)=',TWMAX
        WRITE(6,*)'MASS OF FUEL USED (KG) = ',AMO-X(7)
        WRITE(6,*)' '
          IF(IUNIT .EQ. 6)GO TO 444
        WRITE(IUNIT,*)' '
        WRITE(IUNIT,*)' ------ FINAL AND MAXIMUM VALUES -------'
        WRITE(IUNIT,*)'TERMINATION TIME = ',TIME
        WRITE(IUNIT,*)'TERMINATION ALTITUDE = ',H
        WRITE(IUNIT,*)'MAXIMIMUM G-EARTH ACCELERATION=',GMAX
        WRITE(IUNIT,*)'MAXIMIMUM STAGNATION TEMPERATURE (K)=',TWMA
X
        WRITE(IUNIT,*)'MASS OF FUEL USED (KG) = ',AMO-X(7)
        WRITE(IUNIT,*)' '
C****************** CHANGE TO PRINT FINAL VALUES TO SCREEN **
  444   CALL OUTPUT(TIME,X,DX,TW,6)
C*************************************************************
        GO TO 999
      ENDIF
      GO TO 200
*************------ LOOP FOR DESCENT ENDS -----*********
C
 999  CONTINUE
      STOP
      END




C*************************************************************
C*************************************************************
      SUBROUTINE OUTPUT(TIME,X,DX,TW,IUNIT)
C*************************************************************
C  THIS IS AN OUTPUT ROUTINE FOR PRINTING AN EPHEMEROUS
```

```
C  OF THE DESCENT TRAJECTORY.
      COMMON/RO/RO
      COMMON/ROLL/ROLL
      COMMON/PROP/FFR,DM,PALT,THRUST
      COMMON/RHOO/RHOO
      DIMENSION X(7),DX(7)
      RADDEG = 57.29578
      THETA = ROLL*RADDEG
      DRG = X(1)/1000.0
      CRG = X(2)/1000.0
      H = (X(3) - RO)/1000.0
      V = X(4)
      GFORCE=DX(4)/9.81
      GAMA = X(5)*RADDEG
      AZE = X(6)*RADDEG
C     **THE AEROHEATING SUBROUTINE FRY IS CALLED FOR THE CURRENT
C       VALUE OF STAGNATION TEMPERATURE IN DEGREES K**
      RHOF=DENS(X(3))
      IF(H.LE.1.0 .OR. V.LE.1.0)RHOF=-9999.0
      CALL FRY(X,RHOF,TW)
      WRITE(IUNIT,*)' '
      WRITE(IUNIT,*)'TIME (SEC) = ',TIME,' ROLL (DEG) = ',THETA
      IF(DX(7) .NE. 0.0)THEN
           WRITE(IUNIT,*)'PROPULSION SYSTEMS ARE ON'
           WRITE(IUNIT,*)'MASS OF VEHICLE (KG) = ',X(7)
      ELSE
           WRITE(IUNIT,*)'PROPULSION SYSTEMS ARE OFF'
      ENDIF
      WRITE(IUNIT,*)'X DOWNRANGE (KM) = ',DRG
      WRITE(IUNIT,*)'Y CROSSRANGE (KM) = ',CRG
      WRITE(IUNIT,*)'H ALTITUDE (KM) = ',H
      WRITE(IUNIT,*)'V VELOCITY (M/SEC) = ',V
      WRITE(IUNIT,*)'GAMA FLT. PATH ANGLE (DEG) = ',GAMA
      WRITE(IUNIT,*)'AZE (DEG) = ',AZE
      WRITE(IUNIT,*)'ACCELERATION (G-EARTH) =',GFORCE
      WRITE(IUNIT,*)'STAGNATION TEMP (K) =',TW
C
      RETURN
      END




C*********************************************************
C*********************************************************
      SUBROUTINE RK(X,DX,DT,N)
C*********************************************************
C  THIS IS A RUNGE- KUTTA 4TH ORDER INTEGRATOR.  THIS
C  ROUTINE EXPECTS THE SUBROUTINE 'DERIV' TO BE SUPPLIED
C  BY THE USER.
C
      REAL X(7),U(7),F(7),D(7),DX(7)
C
      CALL DERIV(X,D)
      DO 1 I = 1,N
```

```
        D(I) = D(I)*DT
    1 U(I) = X(I) + 0.5*D(I)
        CALL DERIV(U,F)
        DO 2 I = 1,N
          F(I) = F(I)*DT
          D(I) = D(I) + 2.0*F(I)
    2 U(I) = X(I) + 0.5*F(I)
        CALL DERIV(U,F)
        DO 3 I = 1,N
          F(I) = F(I)*DT
          D(I) = D(I) + 2.0*F(I)
    3 U(I) = X(I) + F(I)
        CALL DERIV(U,F)
        DO 4 I = 1,N
    4 X(I) = X(I) + (D(I) + F(I)*DT)/6.0
C
        DX(4)=D(4)
        DX(7)=D(7)
        RETURN
        END



C*********************************************************
C*********************************************************
      SUBROUTINE DERIV(X,DX)
C*********************************************
C  THIS SUBROUTINE CONTAINS THE EQUATIONS OF MOTION.
C
      COMMON/BALLCL/BALLCL
      COMMON/BALLCD/BALLCD
      COMMON/G/G
      COMMON/RO/RO
      COMMON/AMO/AMO
      COMMON /PROP/FFR,DM,PALT,THRUST
      COMMON/ROLL/ROLL
C
      DIMENSION X(7),DX(7)
C
      Q = 0.5*DENS(X(3))*X(4)**2
      HDOT =  X(4)*SIN(X(5))
C
C  ---DX(7) IS THE MASS FUEL FLOW RATE---
C  ---X(7) IS THE MASS OF THE VEHICLE----
C
      IF(X(3)-RO .LE.PALT.AND.X(4).GT.30.0.AND.X(3)-RO.GT.40.)THEN
      DX(7)=-FFR
       PTHRUST=THRUST/X(7)
      ELSE
      DX(7)=0.0
      PTHRUST=0.0
      ENDIF
C
      CALL CMROLL(X(7),X(3),X(4),X(6),HDOT,Q,ROLL)
```

```
C
      DX(1) = X(4)*COS(X(6))*COS(X(5))
      DX(2) = X(4)*SIN(X(6))*COS(X(5))
      DX(3) =    HDOT
      DX(4) = -Q/(BALLCD*X(7)/AMO) + G*SIN(X(5)) - PTHRUST
      DX(5) = Q/(BALLCL*X(7)/AMO) / X(4)*COS(ROLL) - G/X(4)*COS(X(
5))
     &        + X(4)/X(3)* COS(X(5))
      DX(6) = Q/(BALLCL*X(7)/AMO)/X(4)/COS(X(5))*SIN(ROLL)

      RETURN
      END



C*************************************************************
C*************************************************************
      FUNCTION DENS(R)
C*************************************************************
C  THIS SUBROUTINE CONTAINS AN ANALYTICAL MODEL OF THE
C  MARTIAN ATMOSPHERE.  THIS MODEL WAS DEVELOPED AT JPL
C  FROM A BEST FIT OF THE VIKING I & II FLIGHT DATA.
C
      COMMON/RHOO/RHOO
      COMMON/HMAX/HMAX
      COMMON/RO/RO
C
      H = (R - RO)/1000.0
      IF (H.EQ.0.0) THEN
        DENS = RHOO
      ELSE IF ((H.GT.0.0).AND.(H.LE.50)) THEN
        DENS = RHOO*EXP(-(-0.5314+0.1083*H+2.188/H))
      ELSE IF ((H.GT.50.0).AND.(H.LE.HMAX)) THEN
        DENS = RHOO*EXP(-(-2.881+0.1396*H+42.55/H))
      ELSE IF (H.GT.HMAX) THEN
        DENS = 0.0
      ENDIF
      RETURN
      END



C*************************************************************
C*************************************************************
      SUBROUTINE CMROLL(W,R,V,AZE,HDOT,Q,ROLL)
C*************************************************
C  THIS SUBROUTINE CONTROLLS THE ROLL OF THE VEHICLE
C  DURING DESCENT.  FOR THIS SIMULATION, THE VEHICLE'S
C  LIFT IS MODULATED BY THE VEHICLE'S BANK ANGLE.  THIS
C  SIMULATION HAS ASSUMED CONSTANT L/D, AND
C  ANGLE OF ATTACK.  THIS SUBROUTINE IMPLEMENTS ALL OF
C  DESCENT TRAJECTORY PROFILE REQUIREMENTS.  SPECIFICALLY,
C  THIS ROUTINE CONTROLLS THE VEHICLE'S RATE OF DESCENT
C  AD FLIGHT AZIMUTH ACCORDING TO OUR SPECIFICATIONS.
C
```

```
C     NOTE: THE BALLISTIC CL NUMBER IS NO LONGER CONSTANT
C
      COMMON/BALLCL/BALLCL
      COMMON/G/G
      COMMON/RO/RO
      COMMON/HEQUIL/HEQUIL
      COMMON/AMO/AMO
C
      H = R - RO
      IF(ROLL.EQ.0.0) THEN
        SGN = 1.0
      ELSE
        SGN = ROLL/ABS(ROLL)
      ENDIF
C
      IF (Q.EQ.0.0) THEN
        ROLL = 0.0
      ELSEIF((H.LT.HEQUIL).AND.(HDOT.LT.0.0))THEN
        ROLL = 0.0
      ELSEIF(H.GT.HEQUIL) THEN
        ROLL = ACOS(0.0)
      ELSE
        COSEQG = ABS(G*(BALLCL*W/AMO)/Q*(1.0 - V**2/(G*R)))
        IF(COSEQG.GT.1.0) THEN
          ROLL = ACOS(0.0)
        ELSE
          ROLL = ACOS(COSEQG)
        ENDIF
      ENDIF
      IF(AZE.GT.1.57079) THEN
        ROLL = -1.0*ROLL*SGN
      ENDIF

      RETURN
      END



C*************************************************************
C*************************************************************
      SUBROUTINE FRY(X,RHOF,TW)
C*************************************************************
C THIS IS THE AEROHEATING SUBROUTINE WHICH USES AN EQUATION
C FOR CONVECTIVE HEATING TO CALCULATE THE STAGNATION TEMPERATURE
C THE EQUATION IS FROM CORNING'S AEROSPACE VEHICLE DESIGN.
C IT IS ASSUMED THAT RADIATIVE HEATING EFFECTS WILL BE NEGLIGIBLE
C SINCE THE VEHICLE WILL BE FLYING MUCH SLOWER THAN 10000 M/S
C
      COMMON RB
      COMMON/RO/RO
      COMMON/E/E
      COMMON/RHOO/RHOO
      COMMON/TEMP/TEMP
      DIMENSION TEMP(101)
      DIMENSION X(7)
```

```
C**** SEVERAL CONVERSIONS ARE NECESSARY SINCE EQUATION USES THE
C**** ARCHAIC SYSTEM OF UNITS.
      IF(RHOF .EQ. -9999.0)THEN
      TW=0.0
      GO TO 555
      ENDIF
      RBF=RB*3.2808
      VC=10831.5
      SBK=.48E-12
      ONE=17600./SQRT(RBF)
      TWO=SQRT(RHOF/RHOO)
      THREE=(X(4)/VC)**3.25
      TW4=ONE*TWO*THREE/(SBK*E)
      TW4=ABS(TW4)
      TW=SQRT(SQRT(TW4))
C**** TW IS CONVERTED FROM RANKINE TO KELVIN
      TW=TW/1.8
 555  CONTINUE
      IH=INT((X(3)-RO)/1000.)
      IF(IH .LT. 1)IH=1
      TT=TEMP(IH)
      TW=TW+TT
      RETURN
      END
C
      SUBROUTINE HOLA
      WRITE(6,*)' '
      WRITE(6,*)' '
      WRITE(6,*)'   >>>>     MARS DESCENT SIMULATION    <<<<  '
      WRITE(6,*)' '
      WRITE(6,*)'THIS PROGRAM INCORPORATES AERODYNAMIC DRAG'
      WRITE(6,*)'FOR BRAKING IN THE UPPER ATMOSPHERE AND   '
      WRITE(6,*)'PROPULSIVE DECELERATION FOR THE FINAL LANDING'
      WRITE(6,*)'PHASE.  IT IS SUGGESTED THAT THE PROPULSIVE'
      WRITE(6,*)'PHASE OF THE PROGRAM BE TURNED OFF FOR'
      WRITE(6,*)'INITIAL ANALYSES TO OBTAIN AERODYNAMIC '
      WRITE(6,*)'ENTRY DATA. THIS IS PERFORMED BY SETTING THE'
      WRITE(6,*)'INITIAL PROPULSIVE ALTITUDE EQUAL TO ZERO. '
      WRITE(6,*)'NOTE THAT THE PROPULSION SYSTEM WILL '
      WRITE(6,*)'AUTOMATICALLY SHUT OFF AT AN ALTITUDE OF '
```

```
C
      DX(1) = X(4)*COS(X(6))*COS(X(5))
      DX(2) = X(4)*SIN(X(6))*COS(X(5))
      DX(3) =    HDOT
      DX(4) = -Q/(BALLCD*X(7)/AMO) + G*SIN(X(5)) - PTHRUST
      DX(5) = Q/(BALLCL*X(7)/AMO) / X(4)*COS(ROLL) - G/X(4)*COS(X(
5))
     &        + X(4)/X(3)* COS(X(5))
      DX(6) = Q/(BALLCL*X(7)/AMO)/X(4)/COS(X(5))*SIN(ROLL)

      RETURN
      END



C*********************************************************
C*********************************************************
      FUNCTION DENS(R)
C*********************************************************
C  THIS SUBROUTINE CONTAINS AN ANALYTICAL MODEL OF THE
C  MARTIAN ATMOSPHERE.  THIS MODEL WAS DEVELOPED AT JPL
C  FROM A BEST FIT OF THE VIKING I & II FLIGHT DATA.
C
      COMMON/RHOO/RHOO
      COMMON/HMAX/HMAX
      COMMON/RO/RO
C
      H = (R - RO)/1000.0
      IF (H.EQ.0.0) THEN
        DENS = RHOO
      ELSE IF ((H.GT.0.0).AND.(H.LE.50)) THEN
        DENS = RHOO*EXP(-(-0.5314+0.1083*H+2.188/H))
      ELSE IF ((H.GT.50.0).AND.(H.LE.HMAX)) THEN
        DENS = RHOO*EXP(-(-2.881+0.1396*H+42.55/H))
      ELSE IF (H.GT.HMAX) THEN
        DENS = 0.0
      ENDIF
      RETURN
      END



C*********************************************************
C*********************************************************
      SUBROUTINE CMROLL(W,R,V,AZE,HDOT,Q,ROLL)
C*********************************************************
C  THIS SUBROUTINE CONTROLLS THE ROLL OF THE VEHICLE
C  DURING DESCENT.  FOR THIS SIMULATION, THE VEHICLE'S
C  LIFT IS MODULATED BY THE VEHICLE'S BANK ANGLE.  THIS
C  SIMULATION HAS ASSUMED CONSTANT L/D, AND
C  ANGLE OF ATTACK.  THIS SUBROUTINE IMPLEMENTS ALL OF
C  DESCENT TRAJECTORY PROFILE REQUIREMENTS.  SPECIFICALLY,
C  THIS ROUTINE CONTROLLS THE VEHICLE'S RATE OF DESCENT
C  AD FLIGHT AZIMUTH ACCORDING TO OUR SPECIFICATIONS.
C
C     NOTE: THE BALLISTIC CL NUMBER IS NO LONGER CONSTANT
```

```
C
      COMMON/BALLCL/BALLCL
      COMMON/G/G
      COMMON/RO/RO
      COMMON/HEQUIL/HEQUIL
      COMMON/AMO/AMO
C
      H = R - RO
      IF(ROLL.EQ.0.0) THEN
        SGN = 1.0
      ELSE
        SGN = ROLL/ABS(ROLL)
      ENDIF
C
      IF (Q.EQ.0.0) THEN
        ROLL = 0.0
      ELSEIF((H.LT.HEQUIL).AND.(HDOT.LT.0.0))THEN
        ROLL = 0.0
      ELSEIF(H.GT.HEQUIL) THEN
        ROLL = ACOS(0.0)
      ELSE
        COSEQG = ABS(G*(BALLCL*W/AMO)/Q*(1.0 - V**2/(G*R)))
        IF(COSEQG.GT.1.0) THEN
          ROLL = ACOS(0.0)
        ELSE
          ROLL = ACOS(COSEQG)
        ENDIF
      ENDIF
      IF(AZE.GT.1.57079) THEN
        ROLL = -1.0*ROLL*SGN
      ENDIF

      RETURN
      END



C*********************************************************
C*********************************************************
      SUBROUTINE FRY(X,RHOF,TW)
C*********************************************************
C THIS IS THE AEROHEATING SUBROUTINE WHICH USES AN EQUATION
C FOR CONVECTIVE HEATING TO CALCULATE THE STAGNATION TEMPERATURE
C THE EQUATION IS FROM CORNING'S AEROSPACE VEHICLE DESIGN.
C IT IS ASSUMED THAT RADIATIVE HEATING EFFECTS WILL BE NEGLIGIBLE
C SINCE THE VEHICLE WILL BE FLYING MUCH SLOWER THAN 10000 M/S
C
      COMMON RB
      COMMON/RO/RO
      COMMON/E/E
      COMMON/RHOO/RHOO
      COMMON/TEMP/TEMP
      DIMENSION TEMP(101)
      DIMENSION X(7)
C**** SEVERAL CONVERSIONS ARE NECESSARY SINCE EQUATION USES THE
```

```
C**** ARCHAIC SYSTEM OF UNITS.
      IF(RHOF .EQ. -9999.0)THEN
      TW=0.0
      GO TO 555
      ENDIF
      RBF=RB*3.2808
      VC=10831.5
      SBK=.48E-12
      ONE=17600./SQRT(RBF)
      TWO=SQRT(RHOF/RHOO)
      THREE=(X(4)/VC)**3.25
      TW4=ONE*TWO*THREE/(SBK*E)
      TW4=ABS(TW4)
      TW=SQRT(SQRT(TW4))
C**** TW IS CONVERTED FROM RANKINE TO KELVIN
      TW=TW/1.8
 555  CONTINUE
      IH=INT((X(3)-RO)/1000.)
      IF(IH .LT. 1)IH=1
      TT=TEMP(IH)
      TW=TW+TT
      RETURN
      END
C
      SUBROUTINE HOLA
      WRITE(6,*)' '
      WRITE(6,*)' '
      WRITE(6,*)'   >>>>     MARS DESCENT SIMULATION     <<<<  '
      WRITE(6,*)' '
      WRITE(6,*)'THIS PROGRAM INCORPORATES AERODYNAMIC DRAG'
      WRITE(6,*)'FOR BRAKING IN THE UPPER ATMOSPHERE AND    '
      WRITE(6,*)'PROPULSIVE DECELERATION FOR THE FINAL LANDING'
      WRITE(6,*)'PHASE.  IT IS SUGGESTED THAT THE PROPULSIVE'
      WRITE(6,*)'PHASE OF THE PROGRAM BE TURNED OFF FOR'
      WRITE(6,*)'INITIAL ANALYSES TO OBTAIN AERODYNAMIC '
      WRITE(6,*)'ENTRY DATA. THIS IS PERFORMED BY SETTING THE'
      WRITE(6,*)'INITIAL PROPULSIVE ALTITUDE EQUAL TO ZERO. '
      WRITE(6,*)'NOTE THAT THE PROPULSION SYSTEM WILL '
      WRITE(6,*)'AUTOMATICALLY SHUT OFF AT AN ALTITUDE OF '
      WRITE(6,*)'40 METERS AND A VELOCITY OF 30 METERS/SECOND.'
      WRITE(6,*)'ALSO NOTE THAT THE OUTPUT INTERVAL WILL  '
      WRITE(6,*)'BE RESET AS THE VEHICLE ENTERS THE PROPULSIVE'
      WRITE(6,*)'PHASE OF THE DESCENT. '
      WRITE(6,*)' '
      WRITE(6,*)' '
      RETURN
      END
C
      SUBROUTINE TPDATA(TEMP,PRESS)
C*********************************************************************
C     **READS TEMPERATURE AND PRESSURE DATA INTO THE TWO ARRAYS**
C     **TEMPERATURE IS IN DEGREES K**
C     **PRESSURE IS IN NEWTONS/SQUARE METER**
      DIMENSION TEMP(100),PRESS(100)
      IHI=100
    1 CONTINUE
```

```
      READ(7,*)J
      READ(7,*) BLIP
      READ(7,*)BLIPP
      TEMP(J)=BLIP
      PRESS(J)=BLIPP
      IF (J .EQ. IHI)GOTO 2
      GOTO 1
    2 CONTINUE
C     **INTERPOLATION OF ODD ALTITUDES**
      DO 5 I=0,98,2
      II=I+1
      III=I+2
      TEMP(II)=(TEMP(I)+TEMP(III))/2.0
      PRESS(II)=(PRESS(I)+PRESS(III))/2.0
    5 CONTINUE
      RETURN
      END
```

Program Hover- calculates amount of fuel and other parameters given burn time

St	Input	Name	Output	Unit	Comment
	6.672E-11	G		m^3/kg*s^	Universal Gravitational Cons
	6.374E23	Mmars		kg	Mass of Mars
	4.2828E13	MUmars		m^3/s^2	Mars Gravitational Parameter
	3387500	Rmars		m	Radius of Mars
	3540.2	ISP		m/s	Specific Impulse
L	180	TB		s	Burn Time
		TW	1.1268843		Thrust to Weight Ratio
		MDRY	157.39036	Mg	Final Dry Vehicle Mass
	.15	STFACT			Structural Factor
		MPROP	42.609644	Mg	Mass of Propellant
		MPAY	150.99891	Mg	Mass of Payload
L	200	MO		Mg	Initial Wet Vehicle Mass
	838037	THRUST		N	Thrust Required to Hover
		WEIGHT	743676.15	N	Weight of ADV on Mars
		g	3.7183807	m/s^2	Gravitational force on Mars
		Mdot	236.72024	kg/s	Mass flow rate of propellant
		MdotO	179.67922	kg/s	Mass flow rate of oxidizer
	3.15	OFRW			Oxidizer/Fuel Ratio by Weigh
		MdotF	57.041022	kg/s	Mass flow rate of Fuel
		DENSF	424	kg/m^3	Density of fuel
	1000	DENSH2O		kg/m^3	Density of Water
	.424	SGF			Specific Gravity of Fuel
		DENSO	1143	kg.m^3	Density of Oxidizer
	1.143	SGO			Specific Gravity of Oxidizer
		VdotF	.13453071	m^3/s	Volume flow rate of fuel
		VdotO	.15719967	m^3/s	Volume flow rate of oxidizer
		Vdot	.29173038	m^3/s	Volume flow rate of propella
		OFRV	1.1685039		Oxidizer/fuel ratio by volum
		MF	10.267384	Mg	Mass of Fuel
		MOx	32.34226	Mg	Mass of Oxidizer
		VOLP	52.511468	m^3	Volume of Propellant
		VOLO	28.29594	m^3	Volume of Oxidizer
		VOLF	24.215528	m^3	Volume of Fuel

S Rule
* MDRY=(STFACT*MPROP)+MPAY
* MO=MDRY+MPROP
* TW=THRUST/WEIGHT
* WEIGHT=MO*g
* Mdot=THRUST/ISP
* TB=MPROP/Mdot
* g=MUmars/(Rmars^2)
* MdotO=OFRW*Mdot/(1+OFRW)
* MdotF=Mdot/(1+OFRW)
* DENSF=DENSH2O*SGF
* DENSO=DENSH2O*SGO
* VdotF=MdotF/DENSF
* VdotO=MdotO/DENSO
* Vdot=VdotF+VdotO
* OFRV=VdotO/VdotF
* MF=MPROP/(1+OFRW)
* MOx=OFRW*MPROP/(1+OFRW)
* VOLP=VOLO+VOLF
* VOLF=MF/DENSF
* VOLO=MOx/DENSO

APPENDIX D

>>> MARS DESCENT SIMULATION <<<

DESCENT PROFILE

M/(CL*S) (KG/M**2) = 392.9751680768
INITIAL MASS (KG) = 200000.
COEFFICIENT OF LIFT = .5
RADIUS OF VEHICLE (M) =18.
L/D = .5
H (M) = 100000.
V (M/SEC) = 3500.
GAMA (DEG) = -.5
THRUST (N) = 800000.
INITIAL PROP. DEC. ALT. (KM) = 2.8
FUEL FLOW RATE (KG/S) = 387.

TIME (SEC) = 0. ROLL (DEG) = 0.
PROPULSION SYSTEMS ARE OFF
X DOWNRANGE (KM) = 0.
Y CROSSRANGE (KM) = 0.
H ALTITUDE (KM) = 100.
V VELOCITY (M/SEC) = 3500.
GAMA FLT. PATH ANGLE (DEG) = -.49999162417
AZE (DEG) = 0.
ACCELERATION (G-EARTH) =0.
STAGNATION TEMP (K) =601.8545208141

TIME (SEC) = 50. ROLL (DEG) = 90.00000076485
PROPULSION SYSTEMS ARE OFF
X DOWNRANGE (KM) = 174.938170108
Y CROSSRANGE (KM) = .003307905155276
H ALTITUDE (KM) = 98.18805012271
V VELOCITY (M/SEC) = 3497.792448878
GAMA FLT. PATH ANGLE (DEG) = -.687259617945
AZE (DEG) = .002259266436902
ACCELERATION (G-EARTH) =-.02590722713355
STAGNATION TEMP (K) =616.0098668292

TIME (SEC) = 100. ROLL (DEG) = 90.00000076485
PROPULSION SYSTEMS ARE OFF
X DOWNRANGE (KM) = 349.7417042925
Y CROSSRANGE (KM) = .01453611732843
H ALTITUDE (KM) = 95.80230819164
V VELOCITY (M/SEC) = 3494.880733898
GAMA FLT. PATH ANGLE (DEG) = -.8771245755442
AZE (DEG) = .005262826393812
ACCELERATION (G-EARTH) =-.03340275848797
STAGNATION TEMP (K) =635.2812351691

```
TIME (SEC) = 150. ROLL (DEG) = 90.00000076485
PROPULSION SYSTEMS ARE OFF
X DOWNRANGE (KM) = 524.3715804229
Y CROSSRANGE (KM) = .03671515250504
H ALTITUDE (KM) = 92.83519459587
V VELOCITY (M/SEC) = 3491.186181769
GAMA FLT. PATH ANGLE (DEG) = -1.070368493613
AZE (DEG) = .009578778203636
ACCELERATION (G-EARTH) =-.04194495006995
STAGNATION TEMP (K) =660.2788480041

TIME (SEC) = 200. ROLL (DEG) = 90.00000076485
PROPULSION SYSTEMS ARE OFF
X DOWNRANGE (KM) = 698.7832849322
Y CROSSRANGE (KM) = .0752691411579
H ALTITUDE (KM) = 89.27701943649
V VELOCITY (M/SEC) = 3486.565444017
GAMA FLT. PATH ANGLE (DEG) = -1.267952205025
AZE (DEG) = .01628624662477
ACCELERATION (G-EARTH) =-.05245380970073
STAGNATION TEMP (K) =691.8107766305

TIME (SEC) = 250. ROLL (DEG) = 90.00000076485
PROPULSION SYSTEMS ARE OFF
X DOWNRANGE (KM) = 872.9219672439
Y CROSSRANGE (KM) = .1403222471155
H ALTITUDE (KM) = 85.11543950637
V VELOCITY (M/SEC) = 3480.738203832
GAMA FLT. PATH ANGLE (DEG) = -1.471178887751
AZE (DEG) = .02756800383667
ACCELERATION (G-EARTH) =-.06692729497937
STAGNATION TEMP (K) =730.915196074

TIME (SEC) = 300. ROLL (DEG) = 90.00000076485
PROPULSION SYSTEMS ARE OFF
X DOWNRANGE (KM) = 1046.711853337
Y CROSSRANGE (KM) = .2518090499555
H ALTITUDE (KM) = 80.3344269826
V VELOCITY (M/SEC) = 3473.116265816
GAMA FLT. PATH ANGLE (DEG) = -1.682054247717
AZE (DEG) = .04811876315946
ACCELERATION (G-EARTH) =-.08997076303017
STAGNATION TEMP (K) =778.887244595

TIME (SEC) = 350. ROLL (DEG) = 90.00000076485
PROPULSION SYSTEMS ARE OFF
X DOWNRANGE (KM) = 1220.031648347
Y CROSSRANGE (KM) = .4514180187024
H ALTITUDE (KM) = 74.91220710632
V VELOCITY (M/SEC) = 3462.376697655
GAMA FLT. PATH ANGLE (DEG) = -1.904129152597
AZE (DEG) = .08868586932313
ACCELERATION (G-EARTH) =-.132849276202
STAGNATION TEMP (K) =837.2667832609
```

TIME (SEC) = 400. ROLL (DEG) = 0.
PROPULSION SYSTEMS ARE OFF
X DOWNRANGE (KM) = 1392.654050921
Y CROSSRANGE (KM) = .8262800116346
H ALTITUDE (KM) = 68.82272626688
V VELOCITY (M/SEC) = 3445.344028894
GAMA FLT. PATH ANGLE (DEG) = -2.123067231149
AZE (DEG) = .1539457248239
ACCELERATION (G-EARTH) =-.2239808429763
STAGNATION TEMP (K) =908.6023472139

TIME (SEC) = 450. ROLL (DEG) = 0.
PROPULSION SYSTEMS ARE OFF
X DOWNRANGE (KM) = 1564.111079123
Y CROSSRANGE (KM) = 1.286962107246
H ALTITUDE (KM) = 62.32186318812
V VELOCITY (M/SEC) = 3414.627404801
GAMA FLT. PATH ANGLE (DEG) = -2.20046306682
AZE (DEG) = .1539457248239
ACCELERATION (G-EARTH) =-.4235416791525
STAGNATION TEMP (K) =990.8266442494

TIME (SEC) = 500. ROLL (DEG) = 0.
PROPULSION SYSTEMS ARE OFF
X DOWNRANGE (KM) = 1733.386692729
Y CROSSRANGE (KM) = 1.741783033691
H ALTITUDE (KM) = 55.9069765529
V VELOCITY (M/SEC) = 3354.496585214
GAMA FLT. PATH ANGLE (DEG) = -2.097142042594
AZE (DEG) = .1539457248239
ACCELERATION (G-EARTH) =-.8365063542641
STAGNATION TEMP (K) =1073.499920796

TIME (SEC) = 550. ROLL (DEG) = 0.
PROPULSION SYSTEMS ARE OFF
X DOWNRANGE (KM) = 1898.452429952
Y CROSSRANGE (KM) = 2.18529258553
H ALTITUDE (KM) = 50.39443700032
V VELOCITY (M/SEC) = 3241.179217689
GAMA FLT. PATH ANGLE (DEG) = -1.659171369766
AZE (DEG) = .1539457248239
ACCELERATION (G-EARTH) =-1.481378841022
STAGNATION TEMP (K) =1132.887684848

TIME (SEC) = 600. ROLL (DEG) = 0.
PROPULSION SYSTEMS ARE OFF
X DOWNRANGE (KM) = 2056.301417526
Y CROSSRANGE (KM) = 2.60941169659
H ALTITUDE (KM) = 46.85258022487
V VELOCITY (M/SEC) = 3067.009417984
GAMA FLT. PATH ANGLE (DEG) = -.8738862155868
AZE (DEG) = .1539457248239
ACCELERATION (G-EARTH) =-1.959792192741
STAGNATION TEMP (K) =1142.829492387

```
TIME (SEC) = 650. ROLL (DEG) = 0.
PROPULSION SYSTEMS ARE OFF
X DOWNRANGE (KM) = 2204.757139845
Y CROSSRANGE (KM) = 3.008292360629
H ALTITUDE (KM) = 45.59383666666
V VELOCITY (M/SEC) = 2871.858273648
GAMA FLT. PATH ANGLE (DEG) = -.1353074301824
AZE (DEG) = .1539457248239
ACCELERATION (G-EARTH) =-1.947222024479
STAGNATION TEMP (K) =1108.423833247

TIME (SEC) = 700. ROLL (DEG) = 14.91699515198
PROPULSION SYSTEMS ARE OFF
X DOWNRANGE (KM) = 2343.767595241
Y CROSSRANGE (KM) = 4.022330743922
H ALTITUDE (KM) = 45.55072980355
V VELOCITY (M/SEC) = 2692.587197409
GAMA FLT. PATH ANGLE (DEG) = .0001884494586611
AZE (DEG) = .8026810962924
ACCELERATION (G-EARTH) =-1.716072080548
STAGNATION TEMP (K) =1060.400861556

TIME (SEC) = 750. ROLL (DEG) = 0.
PROPULSION SYSTEMS ARE OFF
X DOWNRANGE (KM) = 2474.33663899
Y CROSSRANGE (KM) = 5.967347308113
H ALTITUDE (KM) = 45.39584535925
V VELOCITY (M/SEC) = 2533.479895985
GAMA FLT. PATH ANGLE (DEG) = -.19847976169
AZE (DEG) = .8577372604279
ACCELERATION (G-EARTH) =-1.550181699259
STAGNATION TEMP (K) =1018.568286151

TIME (SEC) = 800. ROLL (DEG) = 0.
PROPULSION SYSTEMS ARE OFF
X DOWNRANGE (KM) = 2597.238708716
Y CROSSRANGE (KM) = 7.807370436921
H ALTITUDE (KM) = 44.42008509946
V VELOCITY (M/SEC) = 2383.468396564
GAMA FLT. PATH ANGLE (DEG) = -.7693814068265
AZE (DEG) = .8577372604279
ACCELERATION (G-EARTH) =-1.54014786348
STAGNATION TEMP (K) =988.6750674583

TIME (SEC) = 850. ROLL (DEG) = 0.
PROPULSION SYSTEMS ARE OFF
X DOWNRANGE (KM) = 2712.476555104
Y CROSSRANGE (KM) = 9.532648970817
H ALTITUDE (KM) = 42.11130266477
V VELOCITY (M/SEC) = 2224.247211302
GAMA FLT. PATH ANGLE (DEG) = -1.552150680211
AZE (DEG) = .8577372604279
ACCELERATION (G-EARTH) =-1.738122296088
STAGNATION TEMP (K) =969.9572612174
```

```
TIME (SEC) = 900. ROLL (DEG) = 0.
PROPULSION SYSTEMS ARE OFF
X DOWNRANGE (KM) = 2819.043311044
Y CROSSRANGE (KM) = 11.1281086415
H ALTITUDE (KM) = 38.49961361678
V VELOCITY (M/SEC) = 2034.549616614
GAMA FLT. PATH ANGLE (DEG) = -2.318019068644
AZE (DEG) = .8577372604279
ACCELERATION (G-EARTH) =-2.152011923014
STAGNATION TEMP (K) =955.4345949461

TIME (SEC) = 950. ROLL (DEG) = 0.
PROPULSION SYSTEMS ARE OFF
X DOWNRANGE (KM) = 2914.940035184
Y CROSSRANGE (KM) = 12.56382238324
H ALTITUDE (KM) = 34.13511055265
V VELOCITY (M/SEC) = 1797.099855022
GAMA FLT. PATH ANGLE (DEG) = -2.856092213989
AZE (DEG) = .8577372604279
ACCELERATION (G-EARTH) =-2.674905929797
STAGNATION TEMP (K) =927.6189554408

TIME (SEC) = 1000. ROLL (DEG) = 0.
PROPULSION SYSTEMS ARE OFF
X DOWNRANGE (KM) = 2997.747337341
Y CROSSRANGE (KM) = 13.80356839845
H ALTITUDE (KM) = 29.76241855121
V VELOCITY (M/SEC) = 1514.4605424
GAMA FLT. PATH ANGLE (DEG) = -3.190318251035
AZE (DEG) = .8577372604279
ACCELERATION (G-EARTH) =-3.025099873818
STAGNATION TEMP (K) =874.9125607552

TIME (SEC) = 1050. ROLL (DEG) = 0.
PROPULSION SYSTEMS ARE OFF
X DOWNRANGE (KM) = 3065.852777292
Y CROSSRANGE (KM) = 14.82320610664
H ALTITUDE (KM) = 25.66940095833
V VELOCITY (M/SEC) = 1215.123434488
GAMA FLT. PATH ANGLE (DEG) = -3.826904087589
AZE (DEG) = .8577372604279
ACCELERATION (G-EARTH) =-3.02415654693
STAGNATION TEMP (K) =797.8301117144

TIME (SEC) = 1100. ROLL (DEG) = 0.
PROPULSION SYSTEMS ARE OFF
X DOWNRANGE (KM) = 3119.168872844
Y CROSSRANGE (KM) = 15.62142577189
H ALTITUDE (KM) = 21.42412105489
V VELOCITY (M/SEC) = 928.0125285988
GAMA FLT. PATH ANGLE (DEG) = -5.632674988284
AZE (DEG) = .8577372604279
ACCELERATION (G-EARTH) =-2.819299502478
STAGNATION TEMP (K) =710.1981243574
```

```
TIME (SEC) = 1150. ROLL (DEG) = 0.
PROPULSION SYSTEMS ARE OFF
X DOWNRANGE (KM) = 3158.522757833
Y CROSSRANGE (KM) = 16.21061079333
H ALTITUDE (KM) = 16.37432025938
V VELOCITY (M/SEC) = 663.5344264782
GAMA FLT. PATH ANGLE (DEG) = -9.721083985811
AZE (DEG) = .8577372604279
ACCELERATION (G-EARTH) =-2.575187344649
STAGNATION TEMP (K) =619.7292434387

TIME (SEC) = 1200. ROLL (DEG) = 0.
PROPULSION SYSTEMS ARE OFF
X DOWNRANGE (KM) = 3184.879269669
Y CROSSRANGE (KM) = 16.60520619341
H ALTITUDE (KM) = 10.19906498276
V VELOCITY (M/SEC) = 425.3697570105
GAMA FLT. PATH ANGLE (DEG) = -18.37592270238
AZE (DEG) = .8577372604279
ACCELERATION (G-EARTH) =-2.269124357549
STAGNATION TEMP (K) =523.818579171

TIME (SEC) = 1250. ROLL (DEG) = 0.
PROPULSION SYSTEMS ARE OFF
X DOWNRANGE (KM) = 3199.263310063
Y CROSSRANGE (KM) = 16.82055624463
H ALTITUDE (KM) = 3.240567630902
V VELOCITY (M/SEC) = 224.3680181127
GAMA FLT. PATH ANGLE (DEG) = -38.09561019688
AZE (DEG) = .8577372604279
ACCELERATION (G-EARTH) =-1.801523758811
STAGNATION TEMP (K) =410.26611621

TIME (SEC) = 1251. ROLL (DEG) = 0.
PROPULSION SYSTEMS ARE OFF
X DOWNRANGE (KM) = 3199.4377686
Y CROSSRANGE (KM) = 16.82316814322
H ALTITUDE (KM) = 3.10231721805
V VELOCITY (M/SEC) = 220.8607226145
GAMA FLT. PATH ANGLE (DEG) = -38.69187780632
AZE (DEG) = .8577372604279
ACCELERATION (G-EARTH) =-1.788895897538
STAGNATION TEMP (K) =407.3980574477

TIME (SEC) = 1252. ROLL (DEG) = 0.
PROPULSION SYSTEMS ARE OFF
X DOWNRANGE (KM) = 3199.608050517
Y CROSSRANGE (KM) = 16.82571751172
H ALTITUDE (KM) = 2.964441727817
V VELOCITY (M/SEC) = 217.3787833639
GAMA FLT. PATH ANGLE (DEG) = -39.29868208091
AZE (DEG) = .8577372604279
ACCELERATION (G-EARTH) =-1.776000345115
STAGNATION TEMP (K) =404.6850669887
```

```
TIME (SEC) = 1253. ROLL (DEG) = 0.
PROPULSION SYSTEMS ARE OFF
X DOWNRANGE (KM) = 3199.774177478
Y CROSSRANGE (KM) = 16.82820467448
H ALTITUDE (KM) = 2.826966237038
V VELOCITY (M/SEC) = 213.9227633997
GAMA FLT. PATH ANGLE (DEG) = -39.91619735447
AZE (DEG) = .8577372604279
ACCELERATION (G-EARTH) =-1.762819604616
STAGNATION TEMP (K) =401.7215434961

TIME (SEC) = 1254. ROLL (DEG) = 0.
PROPULSION SYSTEMS ARE ON
MASS OF VEHICLE (KG) = 199677.5
X DOWNRANGE (KM) = 3199.935154996
Y CROSSRANGE (KM) = 16.83061474257
H ALTITUDE (KM) = 2.690774583891
V VELOCITY (M/SEC) = 207.1691823129
GAMA FLT. PATH ANGLE (DEG) = -40.5502856311
AZE (DEG) = .8577372604279
ACCELERATION (G-EARTH) =-3.377408598142
STAGNATION TEMP (K) =396.3286364699

TIME (SEC) = 1255. ROLL (DEG) = 0.
PROPULSION SYSTEMS ARE ON
MASS OF VEHICLE (KG) = 199290.5
X DOWNRANGE (KM) = 3200.088991814
Y CROSSRANGE (KM) = 16.83291790398
H ALTITUDE (KM) = 2.557609391689
V VELOCITY (M/SEC) = 199.8010332009
GAMA FLT. PATH ANGLE (DEG) = -41.21283299106
AZE (DEG) = .8577372604279
ACCELERATION (G-EARTH) =-3.757925419392
STAGNATION TEMP (K) =390.4188356219

TIME (SEC) = 1256. ROLL (DEG) = 0.
PROPULSION SYSTEMS ARE ON
MASS OF VEHICLE (KG) = 198903.5
X DOWNRANGE (KM) = 3200.235749368
Y CROSSRANGE (KM) = 16.83511507847
H ALTITUDE (KM) = 2.42750708431
V VELOCITY (M/SEC) = 192.4802706202
GAMA FLT. PATH ANGLE (DEG) = -41.9048243918
AZE (DEG) = .8577372604279
ACCELERATION (G-EARTH) =-3.733527079531
STAGNATION TEMP (K) =384.4636506796

TIME (SEC) = 1257. ROLL (DEG) = 0.
PROPULSION SYSTEMS ARE ON
MASS OF VEHICLE (KG) = 198516.5
X DOWNRANGE (KM) = 3200.375489238
Y CROSSRANGE (KM) = 16.83720718801
H ALTITUDE (KM) = 2.300512458906
V VELOCITY (M/SEC) = 185.2019964172
GAMA FLT. PATH ANGLE (DEG) = -42.62727959064
AZE (DEG) = .8577372604279
```

```
ACCELERATION (G-EARTH) =-3.711614919843
STAGNATION TEMP (K) =378.4587659112

TIME (SEC) = 1258. ROLL (DEG) = 0.
PROPULSION SYSTEMS ARE ON
MASS OF VEHICLE (KG) = 198129.5
X DOWNRANGE (KM) = 3200.508273572
Y CROSSRANGE (KM) = 16.83919516304
H ALTITUDE (KM) = 2.176679099351
V VELOCITY (M/SEC) = 177.9611104475
GAMA FLT. PATH ANGLE (DEG) = -43.38127719685
AZE (DEG) = .8577372604279
ACCELERATION (G-EARTH) =-3.692292015695
STAGNATION TEMP (K) =372.3997765882

TIME (SEC) = 1259. ROLL (DEG) = 0.
PROPULSION SYSTEMS ARE ON
MASS OF VEHICLE (KG) = 197742.5
X DOWNRANGE (KM) = 3200.634165436
Y CROSSRANGE (KM) = 16.84107994775
H ALTITUDE (KM) = 2.05606973803
V VELOCITY (M/SEC) = 170.7523138334
GAMA FLT. PATH ANGLE (DEG) = -44.16796540493
AZE (DEG) = .8577372604279
ACCELERATION (G-EARTH) =-3.675659917472
STAGNATION TEMP (K) =366.2822673932

TIME (SEC) = 1260. ROLL (DEG) = 0.
PROPULSION SYSTEMS ARE ON
MASS OF VEHICLE (KG) = 197355.5
X DOWNRANGE (KM) = 3200.753229222
Y CROSSRANGE (KM) = 16.84286250617
H ALTITUDE (KM) = 1.938756616577
V VELOCITY (M/SEC) = 163.5701152079
GAMA FLT. PATH ANGLE (DEG) = -44.98857564486
AZE (DEG) = .8577372604279
ACCELERATION (G-EARTH) =-3.661817180499
STAGNATION TEMP (K) =360.2019178615

TIME (SEC) = 1261. ROLL (DEG) = 0.
PROPULSION SYSTEMS ARE ON
MASS OF VEHICLE (KG) = 196968.5
X DOWNRANGE (KM) = 3200.86553112
Y CROSSRANGE (KM) = 16.84454382929
H ALTITUDE (KM) = 1.824821840927
V VELOCITY (M/SEC) = 156.408841014
GAMA FLT. PATH ANGLE (DEG) = -45.84444007534
AZE (DEG) = .8577372604279
ACCELERATION (G-EARTH) =-3.650857358452
STAGNATION TEMP (K) =353.9546423299
```

TIME (SEC) = 1262. ROLL (DEG) = 0.
PROPULSION SYSTEMS ARE ON
MASS OF VEHICLE (KG) = 196581.5
X DOWNRANGE (KM) = 3200.971139658
Y CROSSRANGE (KM) = 16.84612494304
H ALTITUDE (KM) = 1.714357724383
V VELOCITY (M/SEC) = 149.2626510943
GAMA FLT. PATH ANGLE (DEG) = -46.73701415489
AZE (DEG) = .8577372604279
ACCELERATION (G-EARTH) =-3.642866374622
STAGNATION TEMP (K) =347.6367733706

TIME (SEC) = 1263. ROLL (DEG) = 0.
PROPULSION SYSTEMS ARE ON
MASS OF VEHICLE (KG) = 196194.5
X DOWNRANGE (KM) = 3201.070126318
Y CROSSRANGE (KM) = 16.84760691763
H ALTITUDE (KM) = 1.607467111185
V VELOCITY (M/SEC) = 142.1255609438
GAMA FLT. PATH ANGLE (DEG) = -47.66790594255
AZE (DEG) = .8577372604279
ACCELERATION (G-EARTH) =-3.637919199615
STAGNATION TEMP (K) =341.2452991753

TIME (SEC) = 1264. ROLL (DEG) = 0.
PROPULSION SYSTEMS ARE ON
MASS OF VEHICLE (KG) = 195807.5
X DOWNRANGE (KM) = 3201.162566242
Y CROSSRANGE (KM) = 16.84899087802
H ALTITUDE (KM) = 1.50426367116
V VELOCITY (M/SEC) = 134.991472057
GAMA FLT. PATH ANGLE (DEG) = -48.63891434447
AZE (DEG) = .8577372604279
ACCELERATION (G-EARTH) =-3.636075797445
STAGNATION TEMP (K) =334.7781665292

TIME (SEC) = 1265. ROLL (DEG) = 0.
PROPULSION SYSTEMS ARE ON
MASS OF VEHICLE (KG) = 195420.5
X DOWNRANGE (KM) = 3201.248539031
Y CROSSRANGE (KM) = 16.85027801599
H ALTITUDE (KM) = 1.404872154579
V VELOCITY (M/SEC) = 127.8542117454
GAMA FLT. PATH ANGLE (DEG) = -49.65207929508
AZE (DEG) = .8577372604279
ACCELERATION (G-EARTH) =-3.637376362941
STAGNATION TEMP (K) =328.2346613813

```
TIME (SEC) = 1266. ROLL (DEG) = 0.
PROPULSION SYSTEMS ARE ON
MASS OF VEHICLE (KG) = 195033.5
X DOWNRANGE (KM) = 3201.328129659
Y CROSSRANGE (KM) = 16.85146960371
H ALTITUDE (KM) = 1.309428594828
V VELOCITY (M/SEC) = 120.7075835312
GAMA FLT. PATH ANGLE (DEG) = -50.70974793054
AZE (DEG) = .8577372604279
ACCELERATION (G-EARTH) =-3.641835971417
STAGNATION TEMP (K) =321.6158776838

TIME (SEC) = 1267. ROLL (DEG) = 0.
PROPULSION SYSTEMS ARE ON
MASS OF VEHICLE (KG) = 194646.5
X DOWNRANGE (KM) = 3201.401429505
Y CROSSRANGE (KM) = 16.85256700925
H ALTITUDE (KM) = 1.218080446005
V VELOCITY (M/SEC) = 113.5454286768
GAMA FLT. PATH ANGLE (DEG) = -51.81466232213
AZE (DEG) = .8577372604279
ACCELERATION (G-EARTH) =-3.649438904266
STAGNATION TEMP (K) =314.9252807281

TIME (SEC) = 1268. ROLL (DEG) = 0.
PROPULSION SYSTEMS ARE ON
MASS OF VEHICLE (KG) = 194259.5
X DOWNRANGE (KM) = 3201.468537525
Y CROSSRANGE (KM) = 16.85357171413
H ALTITUDE (KM) = 1.13098664248
V VELOCITY (M/SEC) = 106.3616984729
GAMA FLT. PATH ANGLE (DEG) = -52.97007652144
AZE (DEG) = .8577372604279
ACCELERATION (G-EARTH) =-3.660133103785
STAGNATION TEMP (K) =308.1693614257

TIME (SEC) = 1269. ROLL (DEG) = 0.
PROPULSION SYSTEMS ARE ON
MASS OF VEHICLE (KG) = 193872.5
X DOWNRANGE (KM) = 3201.529561583
Y CROSSRANGE (KM) = 16.85448533322
H ALTITUDE (KM) = 1.04831756942
V VELOCITY (M/SEC) = 99.15053553283
GAMA FLT. PATH ANGLE (DEG) = -54.17991393924
AZE (DEG) = .8577372604279
ACCELERATION (G-EARTH) =-3.673825435932
STAGNATION TEMP (K) =301.3583596279
```

```
TIME (SEC) = 1270. ROLL (DEG) = 0.
PROPULSION SYSTEMS ARE ON
MASS OF VEHICLE (KG) = 193485.5
X DOWNRANGE (KM) = 3201.584619967
Y CROSSRANGE (KM) = 16.85530963749
H ALTITUDE (KM) = .9702549369931
V VELOCITY (M/SEC) = 91.90636052241
GAMA FLT. PATH ANGLE (DEG) = -55.44898117091
AZE (DEG) = .8577372604279
ACCELERATION (G-EARTH) =-3.690378668444
STAGNATION TEMP (K) =213.9

TIME (SEC) = 1271. ROLL (DEG) = 0.
PROPULSION SYSTEMS ARE ON
MASS OF VEHICLE (KG) = 193098.5
X DOWNRANGE (KM) = 3201.633843126
Y CROSSRANGE (KM) = 16.85604657992
H ALTITUDE (KM) = .8969915576279
V VELOCITY (M/SEC) = 84.62395863336
GAMA FLT. PATH ANGLE (DEG) = -56.78326267188
AZE (DEG) = .8577372604279
ACCELERATION (G-EARTH) =-3.709611239877
STAGNATION TEMP (K) =213.9

TIME (SEC) = 1272. ROLL (DEG) = 0.
PROPULSION SYSTEMS ARE ON
MASS OF VEHICLE (KG) = 192711.5
X DOWNRANGE (KM) = 3201.677375673
Y CROSSRANGE (KM) = 16.85669832561
H ALTITUDE (KM) = .8287310346663
V VELOCITY (M/SEC) = 77.29855801198
GAMA FLT. PATH ANGLE (DEG) = -58.19033483997
AZE (DEG) = .8577372604279
ACCELERATION (G-EARTH) =-3.731300906432
STAGNATION TEMP (K) =213.9

TIME (SEC) = 1273. ROLL (DEG) = 0.
PROPULSION SYSTEMS ARE ON
MASS OF VEHICLE (KG) = 192324.5
X DOWNRANGE (KM) = 3201.715378737
Y CROSSRANGE (KM) = 16.85726728687
H ALTITUDE (KM) = .7656873830408
V VELOCITY (M/SEC) = 69.92589083827
GAMA FLT. PATH ANGLE (DEG) = -59.67996341849
AZE (DEG) = .8577372604279
ACCELERATION (G-EARTH) =-3.755193094485
STAGNATION TEMP (K) =213.9
```

```
TIME (SEC) = 1274. ROLL (DEG) = 0.
PROPULSION SYSTEMS ARE ON
MASS OF VEHICLE (KG) = 191937.5
X DOWNRANGE (KM) = 3201.748032773
Y CROSSRANGE (KM) = 16.85775616538
H ALTITUDE (KM) = .7080846158564
V VELOCITY (M/SEC) = 62.50222750733
GAMA FLT. PATH ANGLE (DEG) = -61.26499590063
AZE (DEG) = .8577372604279
ACCELERATION (G-EARTH) =-3.781014173657
STAGNATION TEMP (K) =213.9

TIME (SEC) = 1275. ROLL (DEG) = 0.
PROPULSION SYSTEMS ARE ON
MASS OF VEHICLE (KG) = 191550.5
X DOWNRANGE (KM) = 3201.775541011
Y CROSSRANGE (KM) = 16.85816800381
H ALTITUDE (KM) = .6561563444287
V VELOCITY (M/SEC) = 55.02437601363
GAMA FLT. PATH ANGLE (DEG) = -62.96275573139
AZE (DEG) = .8577372604279
ACCELERATION (G-EARTH) =-3.808488923948
STAGNATION TEMP (K) =213.9

TIME (SEC) = 1276. ROLL (DEG) = 0.
PROPULSION SYSTEMS ARE ON
MASS OF VEHICLE (KG) = 191163.5
X DOWNRANGE (KM) = 3201.798133855
Y CROSSRANGE (KM) = 16.85850625162
H ALTITUDE (KM) = .6101454513073
V VELOCITY (M/SEC) = 47.48964230024
GAMA FLT. PATH ANGLE (DEG) = -64.79734754055
AZE (DEG) = .8577372604279
ACCELERATION (G-EARTH) =-3.837360430688
STAGNATION TEMP (K) =213.9

TIME (SEC) = 1277. ROLL (DEG) = 0.
PROPULSION SYSTEMS ARE ON
MASS OF VEHICLE (KG) = 190776.5
X DOWNRANGE (KM) = 3201.816074723
Y CROSSRANGE (KM) = 16.85877485256
H ALTITUDE (KM) = .5703039051145
V VELOCITY (M/SEC) = 39.89575215942
GAMA FLT. PATH ANGLE (DEG) = -66.803751786
AZE (DEG) = .8577372604279
ACCELERATION (G-EARTH) =-3.867409988134
STAGNATION TEMP (K) =213.9
```

```
TIME (SEC) = 1278. ROLL (DEG) = 0.
PROPULSION SYSTEMS ARE ON
MASS OF VEHICLE (KG) = 190389.5
X DOWNRANGE (KM) = 3201.829668255
Y CROSSRANGE (KM) = 16.85897836754
H ALTITUDE (KM) = .5368927963376
V VELOCITY (M/SEC) = 32.24073907194
GAMA FLT. PATH ANGLE (DEG) = -69.03580506597
AZE (DEG) = .8577372604279
ACCELERATION (G-EARTH) =-3.898475039228
STAGNATION TEMP (K) =213.9

TIME (SEC) = 1279. ROLL (DEG) = 0.
PROPULSION SYSTEMS ARE ON
MASS OF VEHICLE (KG) = 190196.
X DOWNRANGE (KM) = 3201.839520934
Y CROSSRANGE (KM) = 16.85912587652
H ALTITUDE (KM) = .5095259702653
V VELOCITY (M/SEC) = 26.62859661347
GAMA FLT. PATH ANGLE (DEG) = -71.52962619662
AZE (DEG) = .8577372604279
ACCELERATION (G-EARTH) =-3.072089381603
STAGNATION TEMP (K) =213.9

TIME (SEC) = 1280. ROLL (DEG) = 0.
PROPULSION SYSTEMS ARE OFF
X DOWNRANGE (KM) = 3201.846880467
Y CROSSRANGE (KM) = 16.85923605945
H ALTITUDE (KM) = .4857921685278
V VELOCITY (M/SEC) = 23.06517425719
GAMA FLT. PATH ANGLE (DEG) = -74.07164775624
AZE (DEG) = .8577372604279
ACCELERATION (G-EARTH) =-1.813795759578
STAGNATION TEMP (K) =213.9

TIME (SEC) = 1281. ROLL (DEG) = 0.
PROPULSION SYSTEMS ARE OFF
X DOWNRANGE (KM) = 3201.852272958
Y CROSSRANGE (KM) = 16.8593167929
H ALTITUDE (KM) = .46522489959
V VELOCITY (M/SEC) = 19.45654737329
GAMA FLT. PATH ANGLE (DEG) = -76.61401761117
AZE (DEG) = .8577372604279
ACCELERATION (G-EARTH) =-1.83719201606
STAGNATION TEMP (K) =213.9

TIME (SEC) = 1282. ROLL (DEG) = 0.
PROPULSION SYSTEMS ARE OFF
X DOWNRANGE (KM) = 3201.855986683
Y CROSSRANGE (KM) = 16.85937239278
H ALTITUDE (KM) = .4479858785868
V VELOCITY (M/SEC) = 15.80973994279
GAMA FLT. PATH ANGLE (DEG) = -79.15665293417
AZE (DEG) = .8577372604279
ACCELERATION (G-EARTH) =-1.857013894375
STAGNATION TEMP (K) =213.9
```

```
TIME (SEC) = 1283. ROLL (DEG) = 0.
PROPULSION SYSTEMS ARE OFF
X DOWNRANGE (KM) = 3201.858323174
Y CROSSRANGE (KM) = 16.85940737345
H ALTITUDE (KM) = .4342107125968
V VELOCITY (M/SEC) = 12.13187885919
GAMA FLT. PATH ANGLE (DEG) = -81.69948955435
AZE (DEG) = .8577372604279
ACCELERATION (G-EARTH) =-1.87320780025
STAGNATION TEMP (K) =213.9

TIME (SEC) = 1284. ROLL (DEG) = 0.
PROPULSION SYSTEMS ARE OFF
X DOWNRANGE (KM) = 3201.859594835
Y CROSSRANGE (KM) = 16.85942641207
H ALTITUDE (KM) = .4240077971071
V VELOCITY (M/SEC) = 8.430171962258
GAMA FLT. PATH ANGLE (DEG) = -84.2424769011
AZE (DEG) = .8577372604279
ACCELERATION (G-EARTH) =-1.885731402086
STAGNATION TEMP (K) =213.9

TIME (SEC) = 1285. ROLL (DEG) = 0.
PROPULSION SYSTEMS ARE OFF
X DOWNRANGE (KM) = 3201.860122484
Y CROSSRANGE (KM) = 16.85943431174
H ALTITUDE (KM) = .4174574371576
V VELOCITY (M/SEC) = 4.711887421494
GAMA FLT. PATH ANGLE (DEG) = -86.78556372134
AZE (DEG) = .8577372604279
ACCELERATION (G-EARTH) =-1.894552948572
STAGNATION TEMP (K) =213.9

TIME (SEC) = 1286. ROLL (DEG) = 0.
PROPULSION SYSTEMS ARE OFF
X DOWNRANGE (KM) = 3201.86023282
Y CROSSRANGE (KM) = 16.85943596363
H ALTITUDE (KM) = .4151111978292
V VELOCITY (M/SEC) = .2843344783388
GAMA FLT. PATH ANGLE (DEG) = -89.32825722747
AZE (DEG) = .8577372604279
ACCELERATION (G-EARTH) =-1.899650584888
STAGNATION TEMP (K) =213.9


 ------ FINAL AND MAXIMUM VALUES -------
TERMINATION TIME = 1287.
TERMINATION ALTITUDE = 415.4914865196
MAXIMIMUM G-EARTH ACCELERATION=-3.898475039228
MAXIMIMUM STAGNATION TEMPERATURE (K)=1142.829492387
MASS OF FUEL USED (KG) = 9804.
```

APPENDIX E

```
      PROGRAM MAIN
C
C     ************************************************************************
C     *                                                                      *
C     *     THIS PROGRAM DETERMINES THE ASCENT FLIGHT HISTORY OF A           *
C     *     LAUNCH VEHICLE BY RUNGE-KUTTA ITEGRATION OF THE EQUATIONS        *
C     *     OF MOTION.  THE EQUATIONS ARE INTEGRATED FROM FINAL              *
C     *     CONDITIONS TO DETERMINE OPTIMUM INITIAL CONDITIONS.              *
C     *                                                                      *
C     ************************************************************************
C
      DIMENSION X(5),DX(5)
      REAL MF, ISP, MU
      COMMON /SPECS/ ISP, BETA, MU, RMARS
      OPEN(6, FILE='ASCENT.OUT', STATUS='NEW')
C
C     ***** INITIALIZE CONSTANTS *****
C     SEA LEVEL ACCELERATION DUE TO GRAVITY ON EARTH (FT/SEC^2)
      GEARTH = 32.174
C
C     GRAVITATIONAL PARAMETER AND RADIUS OF MARS
C          (FT^3/SEC^2)                    (FT)
C
      MU = 1.513220398156+15
      RMARS = 10859448.
C
C     ***** ENTER DATA INTERACTIVELY *****
C
      WRITE(*,100)
      READ(*,*)ISP
      WRITE(*,202)
      READ(*,*)HF
      WRITE(*,204)
      READ(*,*)DELTA
      WRITE(*,205)
      READ(*,*)FACTOR
C
C     ***** FINAL CONDITIONS *****
C
      XF = 0.
      A  = RMARS + ((HF + 1640419.948) / 2)
      VF = SQRT(MU * ((2/(HF + RMARS)) - (1/A)))
      GAMMAF = 0.
      MF = 1.
C
C     ***** SET MASS RATIO USING IDEAL DELTA-V FORMULA *****
C
      RATIO = EXP(FACTOR*VF / ISP / GEARTH)
C
C     ***** ECHO PRINT DATA *****
C
      WRITE(6,400) ISP, MF, RATIO, HF, VF, DELTA
C
      DELTA = -DELTA
      DO 10 I=100.600,10
         TF = REAL(I)
```

```
C
C           ***** SET PROPELLANT FLOW RATE *****
C
            BETA = MF * (RATIO - 1) / TF
C           WRITE(7,600)
            X(1) = XF
            X(2) = HF
            X(3) = VF
            X(4) = GAMMAF
            X(5) = 1.
            T    = TF
            CALL ASCENT(T,X,DELTA)
            WRITE(6,800) TF,X(1),X(2),X(3),X(4),DX(5)
C            IF (X(3).LT.0.OR.X(4).GT.1.6)GOTO 20
   10 CONTINUE
   20 CONTINUE
  100 FORMAT(///,' ENTER SPECIFIC IMPULSE (SECONDS)')
  202 FORMAT(///,' ENTER ALTITUDE OF ORBIT AFTER GRAVITY TURN (FT)')
  204 FORMAT(///,' ENTER INTEGRATION STEP SIZE IN SECONDS')
  205 FORMAT(///,' ENTER DELVA-V CORRECTION FACTOR')
  400 FORMAT('1',///,15X,'MARS ASCENT',/
     2        15X,11('='),//,
     3        15X,'ISP = ',F9.4/
     4        15X,'MF  = ',G15.8/
     5        15X,'MO  = ',G15.8/
     6        15X,'HF  = ',G15.8/
     7        15X,'VF  = ',G15.8/
     8        15X,'INTEGRATION STEP SIZE = ',F7.3//
     9        11X,'TOF',4X,'XO (FEET)',4X,'HO (FEET)',4X,
     9           'VO (FT/S)',6X,'GAMMAO','H (FT/S**2)',/,11X,'(SEC)',/
     C        10X,5('='),5(2X,11('=')))
  800 FORMAT(/10X,F4.0,5(2X,G11.4))
      STOP
      END

      SUBROUTINE ASCENT(T,X,DELTA)
      DIMENSION X(5),DX(5)
      LIMIT = INT(T / (-DELTA))
      DO 10 N = 1, LIMIT, 1
           CALL RUNGE (T,X,DELTA,5,DX)
   10 CONTINUE
      RETURN
      END
```

```
      SUBROUTINE DERIV(T,X,DX)
C
C     ****************************************************************
C     *                                                              *
C     *     THIS SUBROUTINE CONTAINS THE EQUATIONS OF MOTION FOR AN  *
C     *     ASCENT TRAJECTORY.  ASSUMPTIONS IMPLICIT                 *
C     *          i.   FLAT PLANET MODEL IS USED, NON-ROTATING        *
C     *          ii.  STATIONARY ATMOSPHERE                          *
C     *          iii. POINT MASS REPRESENTATION, ALL FORCES ACT      *
C     *               THROUGH THE CENTER OF GRAVITY.                 *
C     *                                                              *
C     *     INPUTS TO THE SUBROUTINE (IN CALL PARAMETERS)            *
C     *          T       ≡ TIME                                      *
C     *          X(1)    ≡ RANGE                (X)                  *
C     *          X(2)    ≡ ALTITUDE             (H)                  *
C     *          X(3)    ≡ VELOCITY             (V)                  *
C     *          X(4)    ≡ FLIGHT PATH ANGLE (GAMMA IN RADIANS)      *
C     *          X(5)    ≡ WEIGHT               (W)                  *
C     *                                                              *
C     *     INPUTS TO THE SUBROUTINE THROUGH COMMON BLOCKS           *
C     *          VARIABLE                        BLOCK NAME          *
C     *          ========                        ==========          *
C     *          RATIO   ≡ MASS RATIO              /SPECS/           *
C     *          ISP     ≡ SPECIFIC IMPULSE        /SPECS/           *
C     *          BETA    ≡ PROPELLANT FLOW                           *
C     *            .       RATE                    /SPECS/           *
C     *          MU      ≡ GRAVITATIONAL                             *
C     *                    PARAMETER               /SPECS/           *
C     *          RMARS   ≡ RADIUS OF PLANET        /SPECS/           *
C     *          GEARTH  ≡ ACCELERATION DUE                          *
C     *                    TO GRAVITY              /SPECS/           *
C     *                                                              *
C     *     OUTPUT FROM SUBROUTINE                                   *
C     *          DX(1)   ≡ RANGE COMPONENT OF VELOCITY               *
C     *          DX(2)   ≡ VERTICAL COMPONENT OF VELOCITY            *
C     *          DX(3)   ≡ ACCELERATION                              *
C     *          DX(4)   ≡ TIME RATE OF CHANGE OF FLIGHT PATH ANGLE  *
C     *          DX(5)   ≡ TIME RATE OF CHANGE OF MASS (-PROPELLANT  *
C     *                    FLOW RATE)                                *
C     *                                                              *
C     ****************************************************************
C
      DIMENSION X(5), DX(5)
      REAL MF, ISP, MU
      COMMON /SPECS/ ISP, BETA, MU, RMARS
C
C     ***** GRAVITY AS FUNCTION OF ALTITUDE *****
C
      G(H) = MU / ((H + RMARS)**2)
C
C     ***** EFFECTIVE VELOCITY (C) AND THRUST *****
C
      THRUST= BETA * ISP
C
C     ***** DERIVATIVES *****
C
      DX(1) = X(3) * COS(X(4))
      DX(2) = X(3) * SIN(X(4))
      DX(3) = (THRUST / X(5)) - (G(X(2)) * SIN(X(4)))
      DX(4) = -G(X(2)) * COS(X(4)) / X(3)
      DX(5) = -BETA
      RETURN
      END
```

```
      SUBROUTINE RUNGE(T,X,DELT,N,DX)
C
C     ***************************************************************
C     *                                                             *
C     *     THIS SUBROUTINE INTEGRATES N FIRST ORDER ORDINARY DIF-  *
C     *     FERENTIAL EQUATIONS BY THE RUNGE-KUTTA METHOD.          *
C     *                                                             *
C     ***************************************************************
C
      DIMENSION X(6), DX(6), DELX(6,3), XV(6)
      T2 = T + DELT/2.0
      CALL DERIV(T,X,DX)
      DO 10 I=1, N
           DELX(I,1) = DX(I) * DELT
           XV(I) = X(I) + DELX(I,1) / 2.0
   10 CONTINUE
      CALL DERIV(T2,XV,DX)
      DO 20 I=1,N
           DELX(I,2) = DX(I) * DELT
           XV(I) = X(I) + DELX(I,2) / 2.0
   20 CONTINUE
      CALL DERIV(T2,XV,DX)
      DO 30 I=1,N
           DELX(I,3) = DX(I) * DELT
           XV(I) = X(I) + DELX(I,3)
   30 CONTINUE
      T = T + DELT
      CALL DERIV(T,XV,DX)
      DO 40 I=1,N
           X(I) = X(I) + (DELX(I,1) + DX(I) * DELT + 2.0 * (DELX(I,2) +
     C          DELX(I,3))) / 6.0
   40 CONTINUE
      RETURN
      END
```

```
      PROGRAM MAIN
C
C     ******************************************************************
C     *                                                                *
C     *     THIS PROGRAM DETERMINES THE ASCENT FLIGHT HISTORY OF A     *
C     *     LAUNCH VEHICLE BY RUNGE-KUTTA ITEGRATION OF THE EQUATIONS  *
C     *     OF MOTION.                                                 *
C     *                                                                *
C     ******************************************************************
C
      DIMENSION X(5)
      REAL MF, ISP, MU
      COMMON /SPECS/ RATIO, ISP, BETA, MU, RMARS, GEARTH
      OPEN(6, FILE='ASCENT.OUT', STATUS='NEW')
C      OPEN(7, FILE='ASCENT.HIS', STATUS='NEW')
C
C     ***** ENTER DATA INTERACTIVELY *****
C
      WRITE(*,100)
      READ(*,*)ISP
      WRITE(*,202)
      READ(*,*)HF
      WRITE(*,203)
      READ(*,*)TF
      WRITE(*,204)
      READ(*,*)DELTA
C
C     ***** INITIALIZE VARIABLES *****
C
C     SEA LEVEL ACCELERATION DUE TO GRAVITY ON EARTH (FT/SEC^2)
      GEARTH = 32.174
C
C     GRAVITATIONAL PARAMETER AND RADIUS OF MARS
C          (FT^3/SEC^2)                    (FT)
C
      MU = 1.513220398152E+15
      RMARS = 10859448.
C
      T = TF
      X1F = 0.
      RF = (RMARS + HF)
      VF = SQRT(MU / RF)
      GAMMAF = 0.
      MF = 1.
C
C     ***** ECHO PRINT DATA *****
C
      WRITE(6,500) ISP, TF, MF, HF, VF, DELTA
C
      DELTA = -DELTA
      DO 10 I=20,100
C
C          ***** SET MASS RATIO AND PROPELLANT FLOW RATE *****
C
           RATIO = .1 * REAL(I)
           BETA = MF * (RATIO - 1) / TF
C          WRITE(7,600)
```

```
            X(1) = X1F
            X(2) = RF
            X(3) = VF
            X(4) = GAMMAF
            X(5) = 1.
            T    = TF
            CALL ASCENT(T,X,DELTA)
            WRITE(6,800) X
            IF (X(3).LT.0.OR.X(4).GT.1.6)GOTO 20
   10 CONTINUE
   20 CONTINUE
  100 FORMAT(///,' ENTER SPECIFIC IMPULSE (SECONDS)')
  202 FORMAT(///,' ENTER ALTITUDE OF ORBIT AFTER GRAVITY TURN (FT)')
  203 FORMAT(///,' ENTER TIME OF FLIGHT (SECONDS)')
  204 FORMAT(///,' ENTER INTEGRATION STEP SIZE IN SECONDS')
  500 FORMAT('1',///,15X,'MARS ASCENT',/
     2        15X,11('='),//,
     3        15X,'ISP = ',F9.4/
     4        15X,'TOF = ',G15.8/
     5        15X,'MF  = ',G15.8/
     6        15X,'HF  = ',G15.8/
     7        15X,'VF  = ',G15.8/
     8        15X,'INTEGRATION STEP SIZE = ',F7.3//
     9        13X,'XO (FEET)',4X,'HO (FEET)',4X,
     9           'VO (FT/S)',6X,'GAMMAO',7X,'MASS',/,
     0        10X,5(2X,11('=')))
  800 FORMAT(/10X,5(2X,G11.4))
      STOP
      END

      SUBROUTINE ASCENT(T,X,DELTA)
      DIMENSION X(5)
      LIMIT = INT(T / (-DELTA))
      DO 10 N = 1, LIMIT, 1
           CALL RUNGE (T,X,DELTA,5)
C          WRITE (7,700)T,X
   10 CONTINUE
C 600 FORMAT('1',14X,'HISTORY',/,15X,7('='),//
C    2        16X,'TIME',3X,'X ( FEET )',3X,'H (FEET)',5X,
C    2           'V FT/S ',7X,'GAMMA',8X,'MASS',/)
C 700 FORMAT(15X,F6.2,5(2X,G11.4))
      RETURN
      END
```

```
C
C     ****************************************************************
C     *                                                              *
C     *     THIS SUBROUTINE CONTAINS THE EQUATIONS OF MOTION FOR AN  *
C     *     ASCENT TRAJECTORY.  ASSUMPTIONS IMPLICIT                 *
C     *          i.   FLAT PLANET MODEL IS USED, NON-ROTATING        *
C     *          ii.  STATIONARY ATMOSPHERE                          *
C     *          iii. POINT MASS REPRESENTATION, ALL FORCES ACT      *
C     *               THROUGH THE CENTER OF GRAVITY.                 *
C     *                                                              *
C     *     INPUTS TO THE SUBROUTINE (IN CALL PARAMETERS)            *
C     *          T       ≡ TIME                                      *
C     *          X(1)    ≡ ANGLE IN FLIGHT    (X)                    *
C     *          X(2)    ≡ RADIUS OF FLIGHT   (H)                    *
C     *          X(3)    ≡ VELOCITY           (V)                    *
C     *          X(4)    ≡ FLIGHT PATH ANGLE (GAMMA IN RADIANS)      *
C     *          X(5)    ≡ WEIGHT             (W)                    *
C     *                                                              *
C     *     INPUTS TO THE SUBROUTINE THROUGH COMMON BLOCKS           *
C     *          VARIABLE                          BLOCK NAME        *
C     *          ========                          ==========        *
C     *          RATIO   ≡ MASS RATIO                /SPECS/         *
C     *          ISP     ≡ SPECIFIC IMPULSE          /SPECS/         *
C     *          BETA    ≡ PROPELLANT FLOW                           *
C     *                    RATE                      /SPECS/         *
C     *          MU      ≡ GRAVITATIONAL                             *
C     *                    PARAMETER                 /SPECS/         *
C     *          RMARS   ≡ RADIUS OF PLANET          /SPECS/         *
C     *          GEARTH  ≡ ACCELERATION DUE                          *
C     *                    TO GRAVITY                /SPECS/         *
C     *                                                              *
C     *     OUTPUT FROM SUBROUTINE                                   *
C     *          DX(1)   ≡ ANGULAR RATE ABOUT PLANET                 *
C     *          DX(2)   ≡ RADIAL COMPONENT OF VELOCITY              *
C     *          DX(3)   ≡ ACCELERATION                              *
C     *          DX(4)   ≡ TIME RATE OF CHANGE OF FLIGHT PATH ANGLE  *
C     *          DX(5)   ≡ TIME RATE OF CHANGE OF MASS (-PROPELLANT  *
C     *                    FLOW RATE)                                *
C     *                                                              *
C     ****************************************************************
C
      DIMENSION X(5), DX(5)
      REAL MF, ISP, MU
      COMMON /SPECS/ RATIO, ISP, BETA, MU, RMARS, GEARTH
C
C     ***** GRAVITY AS FUNCTION OF ALTITUDE *****
C
      G(R) = MU / ((R)**2)
C
C     ***** EFFECTIVE VELOCITY (C) AND THRUST *****
C
      C      = ISP * GEARTH
      THRUST= BETA * C
C
C     ***** DERIVATIVES *****
C
      DX(1) = (X(3) * COS(X(4))) / X(2)
      DX(2) = X(3) * SIN(X(4))
      DX(3) = (THRUST / X(5)) - (G(X(2)) * SIN(X(4)))
      DX(4) = DX(1) - G(X(2)) * COS(X(4)) / X(3)
      DX(5) = -BETA
      RETURN
      END
```

```
      SUBROUTINE RUNGE(T,X,DELT,N)
C
C     ****************************************************************
C     *                                                              *
C     *     THIS SUBROUTINE INTEGRATES N FIRST ORDER ORDINARY DIF-   *
C     *     FERENTIAL EQUATIONS BY THE RUNGE-KUTTA METHOD.           *
C     *                                                              *
C     ****************************************************************
C
      DIMENSION X(6), DX(6), DELX(6,3), XV(6)
      T2 = T + DELT/2.0
      CALL DERIV(T,X,DX)
      DO 10 I=1, N
           DELX(I,1) = DX(I) * DELT
           XV(I) = X(I) + DELX(I,1) / 2.0
   10 CONTINUE
      CALL DERIV(T2,XV,DX)
      DO 20 I=1,N
           DELX(I,2) = DX(I) * DELT
           XV(I) = X(I) + DELX(I,2) / 2.0
   20 CONTINUE
      CALL DERIV(T2,XV,DX)
      DO 30 I=1,N
           DELX(I,3) = DX(I) * DELT
           XV(I) = X(I) + DELX(I,3)
   30 CONTINUE
      T = T + DELT
      CALL DERIV(T,XV,DX)
      DO 40 I=1,N
           X(I) = X(I) + (DELX(I,1) + DX(I) * DELT + 2.0 * (DELX(I,2) +
     C          DELX(I,3))) / 6.0
   40 CONTINUE
      RETURN
      END
```

MARS ASCENT

ISP = 310.0000
TOF = 642.00000
MF = 1.0000000
HF = 1640400.0
VF = 11002.690
INTEGRATION STEP SIZE = 2.000

XO (FEET)	HO (FEET)	VO (FT/S)	GAMMAO	MASS
-.4676E+07	.3436E+05	6603.	.7964	2.000
-.4493E+07	.7925E+05	6169.	.8235	2.100
-.4317E+07	.1237E+06	5758.	.8515	2.200
-.4148E+07	.1679E+06	5369.	.8804	2.300
-.3985E+07	.2119E+06	5000.	.9105	2.400
-.3829E+07	.2559E+06	4649.	.9415	2.500
-.3678E+07	.2998E+06	4316.	.9737	2.600
-.3532E+07	.3438E+06	3998.	1.007	2.700
.3392E+07	.3880E+06	3694.	1.041	2.800
-.3257E+07	.4324E+06	3404.	1.077	2.900
.3127E+07	.4771E+06	3127.	1.113	3.000
.3002E+07	.5222E+06	2861.	1.151	3.100
-.2881E+07	.5677E+06	2606.	1.189	3.200
-.2766E+07	.6138E+06	2361.	1.229	3.300
.2655E+07	.6603E+06	2125.	1.269	3.400
-.2548E+07	.7074E+06	1898.	1.309	3.500
-.2447E+07	.7552E+06	1677.	1.349	3.600
-.2350E+07	.8035E+06	1464.	1.389	3.700
-.2258E+07	.8525E+06	1256.	1.428	3.800
-.2170E+07	.9021E+06	1053.	1.466	3.900
-.2088E+07	.9523E+06	855.0	1.500	4.000
.2011E+07	.1003E+07	660.3	1.529	4.100
-.1938E+07	.1054E+07	468.8	1.552	4.200
-.1871E+07	.1106E+07	280.0	1.566	4.300
.1809E+07	.1158E+07	93.76	1.571	4.400
-.1756E+07	.1193E+07	-875.5	4.446	4.500

123

MARS ASCENT

ISP = 310.0000
TOF = 640.00000
MF = 1.0000000
HF = 1640400.0
VF = 11002.690
INTEGRATION STEP SIZE = 2.000

XO (FEET)	HO (FEET)	VO (FT/S)	GAMMAO	MASS
-.4661E+07	.4519E+05	6587.	.7945	2.000
-.4479E+07	.8981E+05	6152.	.8216	2.100
-.4303E+07	.1340E+06	5741.	.8497	2.200
-.4135E+07	.1780E+06	5352.	.8787	2.300
-.3972E+07	.2217E+06	4983.	.9088	2.400
-.3816E+07	.2654E+06	4632.	.9399	2.500
-.3665E+07	.3091E+06	4298.	.9721	2.600
-.3520E+07	.3529E+06	3980.	1.005	2.700
.3381E+07	.3968E+06	3677.	1.040	2.800
.3246E+07	.4410E+06	3387.	1.076	2.900
-.3116E+07	.4855E+06	3110.	1.112	3.000
.2991E+07	.5304E+06	2844.	1.150	3.100
-.2871E+07	.5757E+06	2589.	1.189	3.200
.2756E+07	.6215E+06	2344.	1.228	3.300
-.2645E+07	.6678E+06	2108.	1.268	3.400
-.2539E+07	.7148E+06	1881.	1.309	3.500
-.2438E+07	.7623E+06	1660.	1.350	3.600
-.2341E+07	.8105E+06	1447.	1.390	3.700
-.2249E+07	.8593E+06	1239.	1.429	3.800
-.2162E+07	.9087E+06	1037.	1.467	3.900
-.2080E+07	.9587E+06	838.4	1.501	4.000
.2003E+07	.1009E+07	643.7	1.531	4.100
-.1931E+07	.1060E+07	452.2	1.553	4.200
.1864E+07	.1112E+07	263.5	1.567	4.300
-.1802E+07	.1164E+07	77.20	1.571	4.400
-.1751E+07	.1190E+07	1048.	4.505	4.500

ISP = 310.0000
TOF = 644.00000
MF = 1.0000000
HF = 1640400.0
VF = 11002.690
INTEGRATION STEP SIZE = 2.000

XO (FEET)	HO (FEET)	VO (FT/S)	GAMMAO	MASS
-.4691E+07	.2349E+05	6620.	.7983	2.000
-.4508E+07	.6865E+05	6186.	.8253	2.100
-.4331E+07	.1134E+06	5775.	.8533	2.200
-.4162E+07	.1578E+06	5386.	.8822	2.300
-.3998E+07	.2021E+06	5017.	.9122	2.400
-.3841E+07	.2463E+06	4666.	.9431	2.500
-.3690E+07	.2904E+06	4333.	.9752	2.600
-.3544E+07	.3347E+06	4015.	1.008	2.700
-.3403E+07	.3791E+06	3712.	1.043	2.800
-.3268E+07	.4237E+06	3422.	1.078	2.900
-.3138E+07	.4687E+06	3144.	1.114	3.000
-.3012E+07	.5140E+06	2879.	1.152	3.100
-.2891E+07	.5597E+06	2624.	1.190	3.200
-.2775E+07	.6060E+06	2379.	1.229	3.300
-.2664E+07	.6527E+06	2143.	1.269	3.400
-.2557E+07	.7001E+06	1915.	1.309	3.500
-.2455E+07	.7480E+06	1695.	1.349	3.600
-.2358E+07	.7965E+06	1481.	1.389	3.700
-.2266E+07	.8457E+06	1273.	1.428	3.800
-.2178E+07	.8955E+06	1070.	1.465	3.900
.2096E+07	.9459E+06	871.7	1.499	4.000
-.2018E+07	.9968E+06	677.0	1.528	4.100
-.1945E+07	.1048E+07	485.5	1.551	4.200
-.1878E+07	.1100E+07	296.6	1.566	4.300
-.1815E+07	.1153E+07	110.3	1.571	4.400
-.1758E+07	.1188E+07	-841.8	4.666	4.500

MARS ASCENT

ISP = 310.0000
TOF = 646.00000
MF = 1.0000000
HF = 1640400.0
VF = 11002.690
INTEGRATION STEP SIZE = 2.000

XO (FEET)	HO (FEET)	VO (FT/S)	GAMMAO	MASS
-.4706E+07	.1257E+05	6637.	.8001	2.000
-.4522E+07	.5800E+05	6203.	.8271	2.100
-.4345E+07	.1030E+06	5792.	.8551	2.200
-.4175E+07	.1477E+06	5403.	.8840	2.300
-.4012E+07	.1922E+06	5034.	.9138	2.400
-.3854E+07	.2366E+06	4684.	.9448	2.500
-.3702E+07	.2810E+06	4350.	.9767	2.600
-.3556E+07	.3255E+06	4032.	1.010	2.700
-.3415E+07	.3701E+06	3729.	1.044	2.800
-.3279E+07	.4150E+06	3439.	1.079	2.900
.3148E+07	.4602E+06	3162.	1.115	3.000
-.3022E+07	.5057E+06	2896.	1.153	3.100
-.2901E+07	.5517E+06	2641.	1.191	3.200
-.2785E+07	.5981E+06	2396.	1.230	3.300
-.2673E+07	.6451E+06	2160.	1.269	3.400
-.2566E+07	.6926E+06	1932.	1.309	3.500
-.2464E+07	.7408E+06	1712.	1.349	3.600
-.2367E+07	.7895E+06	1498.	1.388	3.700
.2274E+07	.8388E+06	1290.	1.427	3.800
.2186E+07	.8888E+06	1087.	1.464	3.900
-.2103E+07	.9394E+06	888.5	1.497	4.000
-.2025E+07	.9905E+06	693.7	1.527	4.100
-.1952E+07	.1042E+07	502.1	1.550	4.200
-.1884E+07	.1094E+07	313.2	1.565	4.300
.1821E+07	.1147E+07	126.9	1.571	4.400
-.1765E+07	.1190E+07	-631.6	4.507	4.500

MARS ASCENT

ISP = 310.0000
TOF = 650.00000
MF = 1.0000000
HF = 1640400.0
VF = 11002.690
INTEGRATION STEP SIZE = 2.000

XO (FEET)	HO (FEET)	VO (FT/S)	GAMMAO	MASS
.4736E+07	-9392.	6671.	.8039	2.000

MARS ASCENT

ISP = 310.0000
TOF = 690.00000
MF = 1.0000000
HF = 1640400.0
VF = 11002.690
INTEGRATION STEP SIZE = 2.000

XO (FEET)	HO (FEET)	VO (FT/S)	GAMMAO	MASS
-.5039E+07	-.2393E+06	7024.	.8404	2.000
-.4843E+07	-.1877E+06	6591.	.8667	2.100
-.4656E+07	-.1368E+06	6183.	.8937	2.200
-.4475E+07	-.8625E+05	5796.	.9214	2.300
-.4301E+07	-.3605E+05	5429.	.9499	2.400
-.4134E+07	.1394E+05	5079.	.9792	2.500
-.3973E+07	.6381E+05	4747.	1.009	2.600
-.3818E+07	.1137E+06	4429.	1.040	2.700
-.3669E+07	.1635E+06	4126.	1.072	2.800
-.3525E+07	.2136E+06	3836.	1.104	2.900
-.3386E+07	.2638E+06	3559.	1.137	3.000
-.3253E+07	.3143E+06	3292.	1.171	3.100
-.3124E+07	.3651E+06	3036.	1.205	3.200
.3001E+07	.4163E+06	2790.	1.239	3.300
.2882E+07	.4679E+06	2552.	1.274	3.400
.2768E+07	.5199E+06	2322.	1.309	3.500
.2660E+07	.5725E+06	2100.	1.344	3.600
-.2556E+07	.6255E+06	1884.	1.378	3.700
-.2456E+07	.6791E+06	1674.	1.412	3.800
-.2362E+07	.7332E+06	1469.	1.444	3.900
-.2273E+07	.7878E+06	1268.	1.475	4.000
.2188E+07	.8429E+06	1072.	1.503	4.100
-.2109E+07	.8984E+06	878.9	1.527	4.200
.2034E+07	.9544E+06	688.9	1.547	4.300

-.1965E+07	.1011E+07	501.7	1.561	4.400
-.1900E+07	.1067E+07	316.9	1.569	4.500
-.1840E+07	.1124E+07	134.5	1.571	4.600
-.1786E+07	.1166E+07	-797.4	4.564	4.700

MARS ASCENT
==========

ISP = 310.0000
TOF = 700.00000
MF = 1.0000000
HF = 1640400.0
VF = 11002.690
INTEGRATION STEP SIZE = .500

XO (FEET)	HO (FEET)	VO (FT/S)	GAMMAO	MASS
-.5115E+07	-.2997E+06	7117.	.8494	2.000
-.4917E+07	-.2467E+06	6685.	.8755	2.100
-.4726E+07	-.1944E+06	6277.	.9022	2.200
-.4543E+07	-.1425E+06	5890.	.9297	2.300
-.4368E+07	-.9095E+05	5523.	.9579	2.400
-.4198E+07	-.3964E+05	5174.	.9868	2.500
-.4035E+07	.1153E+05	4841.	1.016	2.600
-.3878E+07	.6263E+05	4524.	1.047	2.700
-.3727E+07	.1138E+06	4221.	1.078	2.800
-.3581E+07	.1650E+06	3931.	1.109	2.900
-.3440E+07	.2164E+06	3653.	1.142	3.000
-.3305E+07	.2680E+06	3386.	1.175	3.100
.3175E+07	.3200E+06	3130.	1.208	3.200
-.3050E+07	.3723E+06	2883.	1.242	3.300
-.2930E+07	.4250E+06	2645.	1.276	3.400
-.2815E+07	.4780E+06	2415.	1.310	3.500
-.2704E+07	.5316E+06	2191.	1.343	3.600
-.2599E+07	.5857E+06	1975.	1.377	3.700
-.2498E+07	.6402E+06	1764.	1.410	3.800
-.2403E+07	.6953E+06	1559.	1.441	3.900
-.2312E+07	.7508E+06	1358.	1.471	4.000
-.2226E+07	.8069E+06	1161.	1.498	4.100
-.2145E+07	.8633E+06	967.5	1.523	4.200
-.2069E+07	.9202E+06	777.2	1.543	4.300

-.1998E+07	.9775E+06	589.4	1.558	4.400
-.1932E+07	.1035E+07	404.6	1.567	4.500
-.1870E+07	.1093E+07	221.8	1.570	4.600
-.1813E+07	.1151E+07	41.44	1.571	4.700
-.1750E+07	.1112E+07	-2001.	-1.493	4.800

```
S Rule
- ----
$ Mdot=(At$Pc/sqrt(R$Tc))$sqrt(gamma$((2/(gamma+1))^((gamma+1)/(gamma-1))))
$ Me=sqrt((2/gm1)$(((Pc/Pe)^(gm1/gamma))-1))
$ Ae/At=(1/Me)$((2/(gamma+1))$(1+((gamma-1)/2)$Me^2))^((gamma+1)/2/(gamma-1))
$ Aratio=Ae/At
$ Rt=sqrt(At/pi())
$ Re=sqrt(Ae/pi())
$ R1=1.5$Rt
$ R2=.382$Rt
$ Ln=Lf$(Rt$(sqrt(Aratio)-1)+R1$((1/tan(alpha))-1))/tan(alpha)
$ gp1=gamma + 1
$ gm1=gamma - 1
$ nu=(sqrt(gp1/gm1)$atan(sqrt(gm1$(Me^2-1)/gp1)))-(atan(sqrt(Me^2-1)))
$ theta1=nu/2
$ Na=.382$Rt$sin(theta1)
$ Nt=Rt$(1+.382$(1-cos(theta1)))
$ Ln=a$((Re+b)^2)+c
$ Na=a$((Nt+b)^2)+c
$ a=tan(phi1)/(2$(Nt+b))
$ phi2=atan(2$a$(Re+b))
$ phi1=(pi()/2)-theta1
$ phi2=(pi()/2)-theta2
$ thrust=Mdot$Ue
$ SOS=sqrt(gamma$R$Te)
$ Te=Tc/(1+(gm1$Me^2/2))
$ Ue=Me$SOS
$ RICIRC=HICIRC+Rmars
$ VICIRC=SQRT(MUmars/RICIRC)
$ RPOA=HPOA+Rmars
$ RPOP=HPOP+Rmars
$ APO =(RPOA+RPOP)/2
$ VPOP=SQRT(MUmars$((2/RPOP)-(1/APO)))
$ DVPOI=VPOP-VICIRC
$ MRPOI=EXP(DVPOI/ISP)
$ RCOA=HCOA+Rmars
$ RCOP=HCOP+Rmars
$ ACO =(RCOA+RCOP)/2
$ VCOA=SQRT(MUmars$((2/RCOA)-(1/ACO)))
$ DVCIRC=VICIRC-VCOA
$ MRCIRC=EXP(DVCIRC/ISP)
$ VCOP=SQRT(MUmars$((2/RCOP)-(1/ACO)))
$ DVCOI=sqrt((VCOP^2)+(2$g$HCOP))
$ DVT=DVCOI+DVCIRC+DVPOI+DVGRAV
$ MRCOI=EXP(DVCOI/ISP)
$ MRTOTAL=MRCOI$MRCIRC$MRPOI$MRGRAV
$ MDRY=(STFACT$MPROP)+MPAY
$ MO=MDRY+MPROP
$ RICIRC=RCOA
$ RICIRC=RPOP
$ DVGRAV=g$TB
$ TWRATIO=THRUST/WEIGHT
$ WEIGHT=MO$g
$ Mdot=THRUST/ISP
$ TB=(MO$(1-(1/(MRCOI$MRGRAV))))/Mdot
$ MRGRAV=EXP(DVGRAV/ISP)
$ g=MUmars/(Rmars^2)
$ MRTOTAL=MO/MDRY
$ Gmax=THRUST/(MO/(MRCOI$MRGRAV))/9.8066
$ MdotO=OFRW$Mdot/(1+OFRW)
$ MdotF=Mdot/(1+OFRW)
$ DensF=DensH2O$SpGrF
$ DensO=DensH2O$SpGrO
$ VdotF=MdotF/DensF
$ VdotO=MdotO/DensO
$ Vdot =VdotF+VdotO
$ OFRV =VdotO/VdotF
$ MF=MPROP/(1+OFRW)
$ MOx=OFRW$MPROP/(1+OFRW)
$ VolProp = VolO + VolF
$ VolF=MF/DensF
$ VolO=MOx/DensO
$ ISP=sqrt(2$gamma$R$Tc$(1-((Pe/Pc)^(gm1/gamma)))/gm1)
```

APPENDIX E.1

St	Input	Name	Output	Unit	Comment
		TM	178659.02	kg	total mass
					CONSTANTS
	9.81	ge		m/s^2	Earth gravity
	4	nCREW			# crew
	24	nDAYS		day	# days of mission
	.79	O2pcd		kg/day	oxygen/crew/day
	3.49	O2loss		kg/day	Oxygen loss to space/day
	4	N2loss		kg/day	Nitrogen loss to space/day & crew/cabin
	5	WUF		kg/day	water use/man/day for food
	5	WUH		kg/day	water use/man/day for hygiene
	.81	FMR		kg/day	food mass/crew/day
	1.95	CO2P		kg/day	CO2 production/man/day
	500	CM		kg	cargo mass
	0	CargoFu		kg	Cargo Fuel Mass
	500	EVAfuel		kg	fuel for eva systems
	2	nScMuni			Number of Structural modules
	9829	ScM		kg	Mass of structural module
		SSM	19658	kg	Structural System mass
		PSM	3500	kg	power supply mass nuclear+batteries
	1117.26	EVM		kg	EVA Support mass
L		FM	79413.482	kg	Fuel mass (input guess)
	2	NoHabit			#Number of Habitation Mod.+cargo Mod
	23261.2	MHabit			Mass of habitation module
	2	NoTunne			Number of tunnels*includes cargo
	494.2	MTunnel			Mass of tunnel
	4	NoIFM			Number of Interface modules w/airlock+ca
	5277.5	MIFM			Mass of interface module w/airlock
		HABM	68620.8		Mass of Habitation elements
					ENGINES
	4	nE		#	number of engines
		MEng	1039.2978		Mass of engines
	1	pT		%	percent maximum during normal use
	365	Isp		sec	specific thrust of engine
		c	3580.65	m/s	exit velocity
L	2105	deltav		m/s	delta v required to obtain transfer
		Mo	178659.02	kg	total mass of vessel
		T	236959.9	N	thrust of one engine
		Me	79413.482	kg	Mass expelled by engines (actual as per
		TTT	947839.61	N	TOTAL THRUST OF ALL ENGINES
		TT	236959.9	N	Maximum thrust of one engine
	300	TOB		sec	time of burn
					ECLSS SYSTEM
		O2M1	159.6	kg	Mass of Oxygen needed by crew/cabin
		N2M1	96	kg	Mass of Nitrogen needed by crew/cabin
		WaterM1	960	kg	mass of water needed for crew support
		foodM1	77.76	kg	Mass of food required
		CO2M1	187.2	kg	mass carbon dioxide produced
	1	noREACT		#	number of sp-100 type reactors
	50	kWATTpR		kW	power of the nuclear reactor
	66	PwR		kg/kW	power per kg of the reactor system
	200	BACKUP		kg	power back up system Batteries
		TankMas	1178.9883		Approximaste mass of tanks
		ENGINEM	4170.4943		Mass of engines total
	.0044	TF		kg/N	mass of engine per unit thrust
L		Mratio	.55550255		ratio of masses for transit one way.

```
S Rule
  " ECLSS SYSTEM
* O2M1= nCREW*nDAYS*O2pcd  +  O2loss*nDAYS
* O2M1= nCREW*nDAYS*O2pcd  +  O2loss*nDAYS
* N2M1= nDAYS*N2loss
* WaterM1=nCREW*nDAYS*(WUH+WUF)
* foodM1= nCREW * nDAYS * FMR
* CO2M1 = nCREW * nDAYS * CO2P
  "  END ECLSS PRIMARY

* TankMass=(O2M1+N2M1)/2.9+(FM/107)+WaterM1*1.5/4.13


  "Mass of system
* SSM=ScM*nScMunits
* HABM=NoHabit*MHabit+NoTunnel*MTunnel+NoIFM*MIFM
* TM=PSM+SSM+EUM+CM+FM+EVAfuel+HABM+TankMass+ENGINEMASS+CargoFuel
  " POWER SYSTEM MASS
* PSM=noREACTORS*kWATTpR*PwR+BACKUP
  "engine section
* TM=Mo
* ENGINEMASS=nE*T*TF
* c=Isp*ge
* Mratio=1/(Mo/(Mo-Me))
* deltav= c * ln(Mo/(Mo-Me))
* TT=Me/TOB/nE*c
* T=TT/pT
* TTT=TT*nE
  "   now establish the sizing criteria for iterative solving
* Me=FM
* MEng=T/220
```

APPENDIX E.2

St	Input	Name	Output	Unit	Comment
		notm	897	*	number of truss elements
	437	ntt		*	number of truss elements verically
	460	ntb		*	number of truss elements horizontally
		mtm	.63883096	kg	total mass of single truss element
	18	nm		*	number of members in truss element
	3.4142	avlm		m	average length of truss element members
	.1	crsec		cm 2	cross sectional area of truss element me
	2.079	densmat		g/cc	density of material used GRAPHITE EPOXY
		MASSTRU	601.68294	kg	total mass of truss system
		MassCOM	9828.917		Mass of total structural component
		MASSEND	30.084147		mass of end plates
	5	noTHRUS			number of thrust rods used
	100	mTHRUST			mass of thrust rods used
		MASSBOT	1.4115248	kg	Mass of the Understructure
	70	LENGTH		ft	Length of vehicle module structure
	60	WIDTH		ft	Width of vehicle module structure
	.001533	DEPTH		ft	thickness of the underskin
		MASSLan	450	kg	total mass of landing gear subsystem
	112.5	massLan		kg	mass of single landing gear subsystem
		MASSthe	4860	kg	total mass of thermal rejection system
	9	noPANEL		*	number of thermal panels
	450	massPan		kg	mass of each of 70'x3' panels
	1.2	AUXFN		*	add subsystem mass
		WATTrem	17.356211	KW	energy disapated
		MASSrts	750	kg	control jet mass
	6	noRTS		*	number of control jets
	50	unitMAS		kg	mass of one control jet
	75	rtsFUEL		kg	mass of rts fuel&tank on site
	4	HiTr		*	High Thrust Engines for lift off
	100	HiMAS		kg	Mass of High THrust Engine
	500	HiF		kg	Mass of High Thrust Fuel (local, feed fr
		MHiTH	2400		Mass System

```
S Rule
* notm=ntt+ntb
* mtm=nm*avlm*crsec*densmater*.05
* MASSTRUSS=notm*mtm*1.05     "note correction for additional securing mass
* MASSEND=.05*MASSTRUSS
* MASSBOT=LENGTH*WIDTH*DEPTH*densmater/1000
* MASSLanding=4*massLanding
* MASSthermal=noPANELS*massPanels*AUXFN
* WATTremoved=noPANELS*.17143*1.2*LENGTH/100*WIDTH/100"using the rated output of
* MASSrts= noRTS*unitMASSrts+noRTS*rtsFUEL
* MHiTH=HiTr*(HiMAS+HiF)
* MassCOMP=(MASSBOT+MASSTRUSS+MHiTH+MASSEND+MASSthermal+MASSrts+noTHRUSTRODS*mTHR
```